Stable isotope mass balance of the North American Laurentian Great Lakes

by

Scott Jasechko

A thesis
presented to the University of Waterloo
in fulfilment of the
thesis requirement for the degree of
Master of Science
in
Earth Sciences

Waterloo, Ontario, Canada, 2011

Author's Declaration

I hereby declare that I am the sole author of this thesis. This is a true copy of the thesis, including any required final revisions, as accepted by my examiners. I understand that my thesis may be made electronically available to the public.

Abstract

This thesis describes a method for calculating lake evaporation as a proportion of water inputs (E/I) for large surface water bodies, using stable isotope ratios of oxygen ($^{18}O/^{16}O$) and hydrogen ($^{2}H/^{1}H$) in water. Evaporation as a proportion of inflow (E/I) is calculated for each Laurentian Great Lake using a new dataset of 516 analyses of $\delta^{18}O$ and $\delta^{2}H$ in waters sampled from 75 offshore stations during spring and summer of 2007. This work builds on previous approaches by accounting for lake effects on the overlying atmosphere and assuming conservation of both mass and isotopes (^{18}O and ^{2}H) to better constrain evaporation outputs.

Results show that E/I ratios are greatest for headwater Lakes Superior and Michigan and lowest for Lakes Erie and Ontario, controlled largely by the magnitude of hydrologic inputs from upstream chain lakes. For Lake Superior, stable isotopes incorporate evaporation over the past century, providing long-term insights to the lake's hydrology that may be compared to potential changes under a future – expectedly warmer – climate. Uncertainties in isotopically derived E/I are comparable to conventional energy and mass balance uncertainties. Isotope-derived E/I values are lower than conventional energy and mass balance estimates for Lakes Superior and Michigan. The difference between conventional and isotope estimates may be explained by moisture recycling effects. The isotope-based estimates include only evaporated moisture that is also advected from the lake surface, thereby discounting moisture that evaporates and subsequently reprecipitates on the lake surface downwind as recycled precipitation. This shows an advantage of applying an isotope approach in conjunction with conventional evaporation estimates to quantify both moisture recycling and net losses by evaporation.

Depth profiles of $^{18}O/^{16}O$ and $^{2}H/^{1}H$ in the Great Lakes show a lack of isotopic stratification in summer months despite an established thermocline. These results are indicative of very low over-lake evaporation during warm summer months, with the bulk of evaporation occurring during the fall and winter. This seasonality in evaporation losses is supported by energy balance studies. For Lakes Michigan and Huron, the isotope mass balance approach provides a new perspective into water exchange and evaporation from these lakes. This isotope investigation shows that Lake Michigan and Lake Huron waters are distinct, despite sharing a common lake level. This finding advocates for the separate consideration of Lake Michigan and Lake Huron in future hydrologic studies.

Acknowledgements

John Gibson,
John, you have provided me with one of the greatest gifts I have been granted in my lifetime thus far: the opportunity to prove myself with a considerable research project. The confidence you've placed in me, your enthusiasm throughout this and research project and the leadership you provide to our Alberta Innovates research group have each surpassed all reasonable expectations for a supervisor. Throughout our work you have challenged me, while simultaneously showing me how to succeed. You have helped me enormously to meet my immediate M.Sc. graduation goals - the test of an excellent supervisor - and I am in the position I am today largely because of your support and encouragement. Thank you John.

Jean Birks and Yi Yi,
I have benefitted so much from working with each of you since 2009. You have devoted a great deal of time toward bettering my understanding of stable isotope geochemistry, and consistently did so in a patient, understanding and cheering mannerism. Thank you so much for your support Jean and Yi.

Tom Edwards,
Tom, since meeting, you have shown all the traits I believe a graduate student should value most in a supervisor. You have remained supportive - even from thousands of kilometres away! - throughout my entire program. I am so pleased to have joined you on an enlivening adventure to the Yukon, Alaska, and northern B.C.. This trip will be a memory I will hold dear when recalling graduate studies at the University of Waterloo. Thank you so much for your continued support Tom.

Dioni Cendón, Carly Delavau, Paul Eby, Jason Fisher, Sanjeev Kumar, Andres Marandi, Mike Moncur, Kent Richardson, Christophe Sturm, Martina Svabova, and Kevin Tattrie,
Working with you has benefitted both my education and my overall enjoyment of my work with Alberta Innovates. I approached each of you with expertise requests on numerous occasions; these conversations were matched in every occasion with respect, affability and helpfulness.

Brent Wolfe and Roland Hall,
The research group you have constructed in Waterloo, Ontario is scientifically unique and should be a source of great pride to you both. This group is distinguished not only in its scientific merit, but also in its exceptionally welcoming and supportive atmosphere. My immediate integration into this research group is one of my happiest memories of the spring 2010 semester.

To numerous other supporters of this project and to my education including (but certainly not limited to): Alain Pietroniro (Water Survey of Canada), Jeffrey Welker (University of Alaska, Anchorage), Thomas Johengen and Tim Hunter (National Oceanic and Atmospheric Administration), Tom Gleeson (McGill University), Jacqueline Adams (Environmental Protection Agency), Miranda Bilotta and Susan Fisher (University of Waterloo), and to the members of the Canadian Water Network that have provided me with exceptional travel, networking and learning opportunities during my studies.

This work was supported by the Natural Sciences and Research Council of Canada's (NSERC) Industrial Postgraduate Scholarship (IPS) and Undergraduate Student Research Award (USRA) programs, with sponsorship by Alberta Innovates – Technology Futures. Project funding was provided by Environment Canada's Water Survey of Canada (WSC).

Dedication

To Gordon, Jennifer and Glenn for their love and encouragement.

Table of Contents

List of Figures

List of Tables

Chapter 1
Introduction and Background

This thesis describes the hydrology of the Great Lakes and uses stable isotopes of oxygen and hydrogen in water to calculate the average evaporation flux as a proportion of total inputs (E/I) of each lake within the residence time of each body. An approach to calculating E/I is developed with new modifications that account for the incorporation of evaporated moisture into the atmosphere above a surface water body.

The motivation for this work is to better the knowledge of the Great Lakes' water cycle. Large uncertainties are associated with prior "conventional" estimates of precipitation and evaporation losses over the Great Lakes (~40%). Stable isotopes provide a yet untested approach to estimating the average evaporation losses from each Great Lake as a proportion of inflow within the Lake's residence time. A stable isotope technique provides new insights to Lake Superior's long term hydrologic operation over the last 100 years, extending well beyond satellite and physical climate monitoring records. These estimates provide a baseline estimate for Lake Superior evaporation losses; this may be a useful to assessing changes to Lake Superior's hydrologic cycling under a changing climate.

Chapter one introduces the purpose of this study and describes the relevance of evaporation to the Laurentian Great Lakes and significance to ecosystems in the region. The broad applicability of stable isotopes of oxygen and hydrogen to hydrology is discussed. This section then reviews the history of isotopic studies in hydrology dating back to the first uses in the 1950s. The applications of isotope mass balances to surface water bodies are reviewed, specifically highlighting advancements in the study of lake water balances. The chapter concludes by introducing the Laurentian Great Lakes basin. The bedrock geology and Quaternary formation of the Great Lakes are presented. Finally, Great Lakes hydrology is reviewed with estimated fluxes and uncertainties from previous approaches to the water balance of the Lakes.

Chapter two describes sources of isotopic, climatic and physical datasets applied to this project. The steps taken to develop input parameters for each lake's stable isotope mass balance are described in addition to a derivation of the isotopic mass balance. Finally, the development of a model for quantifying the contribution of recycled moisture to atmospheric vapour in the Great Lakes region is described.

Calculation results are presented and discussed in chapter three. This includes calculations for evaporation as a proportion of inflow for each of the North American Great Lakes and calculation sensitivity analysis. The thesis concludes by summarizing major findings and discussing implications and potential use of results in chapter four.

Delta notation is used in this thesis to refer to stable isotope ratios of oxygen and hydrogen. This is the most common reporting method in the field of isotope geochemistry. Delta values are calculated following: $\delta = (R_x/R_{STANDARD} - 1)\cdot 1000$ where R refers to the ratio of either $^{18}O/^{16}O$ or $^{2}H/^{1}H$ and the subscripts *x* and *STANDARD* refer to these ratios in the sample and international standard, respectively (standard mean ocean water - SMOW - used here). The ratios of $^{2}H/^{1}H$ and $^{18}O/^{16}O$ in SMOW are $0.00015575 \pm 0.00000008$ and $0.00200520 \pm 0.00000043$, respectively (de Wit et al. 1980; Baertschi 1976).

In other works, the isotope standard for oxygen and hydrogen stable isotopes is often reported as V-SMOW ("Vienna" Standard Mean Ocean Water). This is meant to show the reader that the isotope analysis was calibrated against both ocean water and SLAP (Standard Light Antarctic Precipitation). But as Z.D. Sharp draws attention to, this rigorous approach is not completed by all laboratories and adding the "V" to SMOW may simply complicate matters (Sharp 2007).

Isotopes of oxygen and hydrogen are incorporated directly into the water molecule, producing various isotopologues of water. Although any combination of the three naturally occurring hydrogen isotopes and three oxygen isotopes may combine to form an isotopologue only three will be considered here: $^{1}H^{1}H^{16}O$, $^{1}H^{1}H^{18}O$ and $^{2}H^{1}H^{16}O$. Figure 1-1a shows a schematic of the naturally occurring isotopes of hydrogen and oxygen. Figure 1-1b shows the H_2O isotopologues considered in this thesis: $^{1}H^{1}H^{16}O$, $^{1}H^{1}H^{18}O$ and $^{2}H^{1}H^{16}O$.

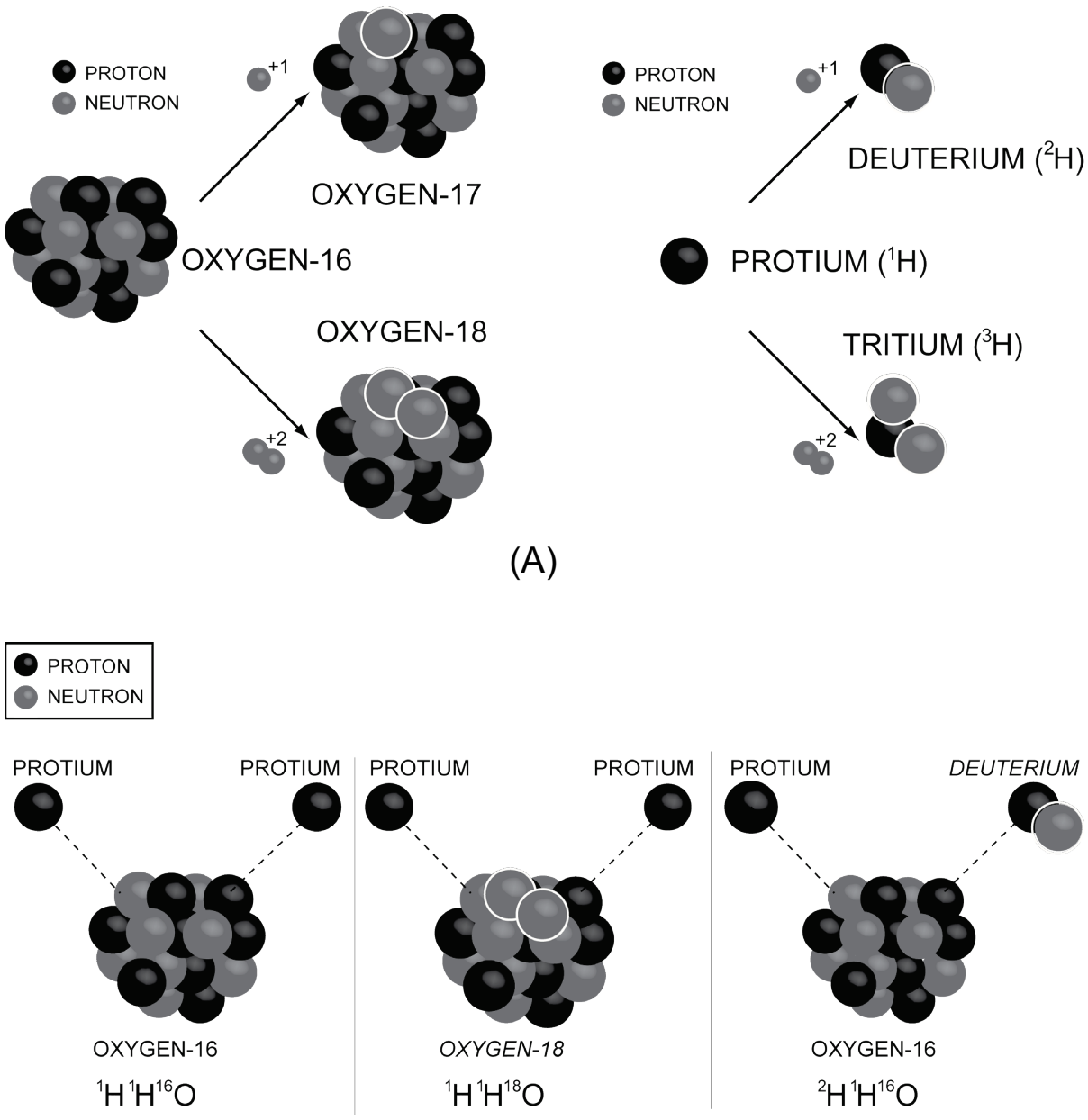

Figure 1-1. Schematic of naturally occurring isotopes of oxygen and hydrogen. In the above figures, black spheres represent protons and grey spheres represent neutrons; white circles highlight additional neutrons that make the particular nuclide unique (an isotope!). (a) Naturally occurring isotopes of oxygen (left) and hydrogen (right). All shown here are stable with the exception of tritium (^{3}H; half life of). (b) The three most common isotopologues of H_2O used in stable isotope geochemistry. From left to right: $^1H^1H^{16}O$ (18 a.m.u.), $^1H^1H^{18}O$ (20 a.m.u.) and $^2H^1H^{16}O$ (19 a.m.u.). Designed using Adobe Illustrator.

1.1 Literature Review: Isotopes of oxygen and hydrogen in hydrology

The following section provides the necessary background for chapters two and three of this thesis. First, advancements leading to the identification of the existence of isotopes of oxygen and hydrogen in nature are discussed. Next, an overview of studies in the last 60 years that have led to the quantification of lake evaporation rates applying a stable isotope mass balance are presented. Still, a knowledge gap exists: how does the build-up of evaporated moisture over large surface waters influence downwind isotope effects during evaporation? The requirement for a new approach for large systems that influence their own climate is evident in many of the works reviewed in this section; this thesis describes such an approach.

This section describes the discovery of the elements of interest in this thesis - oxygen and hydrogen - and their isotopes and introduces a selection of early works in the field of isotope hydrology.

The two elements oxygen and hydrogen were discovered in the eighteenth century. However, the classical elements of earth, air, fire, and water were first proposed by the Greek philosopher Empedocles (492 BC to 432 BC). Empedocles' elements - despite being incorrect - were perhaps the first attempt to describe the composition of matter on earth in terms of a select number of entities with differing properties. Today, matter is described in terms of interaction between nuclides (a particle defined by its nucleons - proton or neutron) of various chemical elements. *Atomos* were first proposed by the Greek scientist Democritus (460 BC to 370 BC), who postulated that materials could only be divided to a certain small size, after which point the particle would be indivisible. Unfortunately, the Greek philosopher Aristotle (384 to 322 BC) discounted Democritus' remarkable and largely correct theorization that matter consisted of indivisible *atomos* (atoms.) However, Aristotle did contribute to the field of earth science. Aristotle proposed a new approach to describing natural systems in terms of both change and stability, the primary components of modern thermodynamics. These very early theories were the first attempts to describe the composition of natural materials and lead to the discovery of the elements as we know them today.

The discovery of the element oxygen occurred in the late 18th century when English historian and scientist, Joseph Priestly, conducted an experiment by heating red mercury calx (HgO). This produced a liquid metal (mercury: Hg) and also a gas that Priestly attributed to the prevailing notion of phlogiston, a combustible substance that essentially combined two of the classic Greek elements of fire and air. Priestly correctly identified the original reactants as a compound, describing the reactant as "a metallic earth united to phlogiston" (Priestly 1775). Priestly shared his work with a French scientist, Antoine-Laurent Lavoisier, at a meeting in Paris. Lavoisier set out to repeat the experiment of Priestly; however, Lavoisier added the important step of weighing his reactants and products. Lavoisier showed that by burning sulphur or phosphorus, the product weighed more than the original sulphur or phosphorus that Lavoisier burned. From the law of conservation of mass - which Lavoisier is credited as discovering - Lavoisier proposed that a constituent in air is added to certain materials under combustion. The term "oxygen" was developed by combining the terms acid (*oxys*) and forming (*gen*). The early discoveries made by Lavoisier when he burnt sulphur and phosphorus and created an acid are now known to be sulphuric and phosphoric acids formed by SO_4^{2-} and PO_4^{2-} molecules instead of oxygen alone. Lavoisier correctly acknowledged that the addition of oxygen to the elements of phosphorous and sulphur produced an acidic solute; although the production of acidic conditions is not a universal outcome for all dissolved

products of combustion that contain the element oxygen, the title of *oxygen* persisted. It should be added that Carl Scheele discovered oxygen prior to Joseph Priestly; however, Scheele did not publish his work before Priestly and does not receive (perhaps due) credit for his discovery (Bryson 2003).

Lavoisier also named the element Hydrogen. From earlier works described by British scientist Henry Cavendish, Lavoisier understood that the reaction of metals with strong acids produced an inflammable substance. Both Cavendish and Lavoisier demonstrated that the combination of this inflammable substance with oxygen produced water. Lavoisier is credited with coining the title hydrogen which is the Greek translation of the word *hudor* for "water maker".

Although the discovery of the elements of oxygen and hydrogen occurred in the 18th century, it would take another 150 years until the existence of the isotopes of oxygen and hydrogen were discovered. The discovery of the stable isotopes of oxygen and hydrogen begins, as do all accounts of the evolution of stable isotopes in science, with the discovery of isotopes (thorium and uranium; McCoy and Ross 1907) and first scientific acknowledgement of isotopes (Soddy 1912; early history reviewed at a Nobel Lecture delivered in 1922 - Soddy 1966). The term "isotopes" was first used by Soddy to distinguish radionuclides with different decay rates and different atomic masses but identical chemical character. In his Nobel Prize address, Soddy (1922) describes the current understanding of isotopes from his radioactive perspective: "Put colloquially, their atoms have identical outsides but difference insides... These elements which are identical in their whole chemical character and are not separable by any method of chemical analysis are now called isotopes." The small mass differences between isotopes have since been demonstrated to produce differences in physiochemical behaviour, so that the assumption of identical physiochemical properties is no longer entirely correct. Separation techniques for many isotopes are now well established and also occur during some natural processes. Soddy's definition of an isotope is refined to now describe nuclides that have an identical number of protons (Z) but a different number of neutrons (N) within the atomic nucleus. The isotopes reviewed here are those that are incorporated into the water molecule: oxygen and hydrogen.

The natural occurrence of stable isotopes of oxygen and hydrogen (^{16}O, ^{17}O, ^{18}O and ^{1}H, ^{2}H) was not confirmed for nearly two decades following the initial discoveries of Soddy and others. The formation of an isotope of oxygen with mass 17 a.m.u. (^{17}O) was first documented by Blackett (1925) who photographed alpha particle (He^{2+}; two protons, two neutrons) capture by a ^{14}N atom and coincident proton emission, essentially documenting the production of an oxygen atom with nine neutrons ($^{17}_{8}O$) - instead of the much more abundant form with eight neutrons ($^{16}_{8}O$) - from a common nitrogen atom ($^{14}_{7}N$). This isotope was later confirmed to occur naturally in the atmosphere as discovered through infrared absorbance spectrum measurements by Giauque and Johnson (1929a). Oxygen of atomic mass 18 a.m.u. (^{18}O) was reported in the same year (Giauque and Johnson 1929b).

Hydrogen of atomic mass 2 a.m.u. (^{2}H, "deuterium;" Urey et al. 1932) was discovered in 1932, despite its occurrence in nature being questioned by early advancements in mass spectrometry. Until this point, the majority of hundreds of isotopes had been discovered with Aston's mass spectrograph. However, as Urey states in his Nobel Prize address (at the young age of 41), none of these isotopes were as rare on a percentage basis as the maximum abundance suspected for hydrogen of mass two (maximum deuterium abundance of $^{1}H:^{2}H \approx 1:4500$; Birge and Menzel 1931; this review for studies reporting prior to 2011 finds natural lake waters range in $^{1}H:^{2}H$ between 1:5950 and 1:7500). Urey and his co-authors reported

on a lengthy electrolysis process that concentrated ^{2}H from water as a residue, and thus proved the existence of ^{2}H in nature (Urey et al. 1932).

The Second World War slowed progress in the study of variability of isotopes in nature; attention turned to advancing separation techniques of isotopes for induced fission of ^{235}Ur. Following the war, Harmon Craig analyzed samples of water from rivers, lakes and precipitation for $\delta^{2}H$ and $\delta^{18}O$ values. Craig described a linear correlation between the values of $\delta^{2}H$ and $\delta^{18}O$ measured in these samples (Craig 1961a). The trend follows a regression of $\delta^{2}H = 8 \cdot \delta^{18}O + 10$ (Craig's meteoric water line). Updated $\delta^{2}H$-$\delta^{18}O$ regressions for monthly samples from over 500 meteorological stations around the world agree with the trend produced by Craig in 1961 with only tiny modifications ($\delta^{2}H = 8.13 \cdot \delta^{18}O + 10.8$; Rozanski et al. 1993). However, it should be mentioned that Craig was not the first to report a correlation between oxygen and hydrogen isotopes in water. Irving Friedman (Friedman 1953) should be credited as first determining the correlation of $\delta^{18}O$ and $\delta^{2}H$. A slope of ~8 is shown for results of waters (Figure 6 in Friedman 1953). Friedman (1953) also suggests that evaporation to be an important process to explain particularly high $\delta^{18}O$ values of the Rio Grande (south-central United States) and Apalachicola (Florida) Rivers.

The $\delta^{18}O$-$\delta^{2}H$ regression is explained by an equilibrium fractionation process. Since the mass difference between oxygen-18 and oxygen-16 is roughly 12.5%, and the mass difference between deuterium (^{2}H) and protium (^{1}H) is roughly 100%, it follows that a slope of eight is entirely reasonable based on equilibrium isotope effects resulting from mass differences alone (12.5/100 = 8). However, not all samples followed the observed regression. As Craig (1961a) describes, "The straight line… represents the relationship $\delta D = 8 \cdot \delta^{18}O + 10$… and is seen to be an adequate fit to the data, except for waters from closed basins in which evaporation is a dominant factor governing the isotopic relationship." These closed basins fall to the right of the $\delta^{2}H$-$\delta^{18}O$ regression line, with lower $\delta^{2}H$ values than the empirical relationship of meteoric waters predicts as a function of $\delta^{18}O$. The $\delta^{2}H/\delta^{18}O$ slope of the closed basins is closer to a value of four or five, as opposed to eight as is the case for precipitation. Craig proposed that precipitation follows a Rayleigh distillation process at liquid-vapour equilibrium, but that evaporation is controlled by kinetic isotope effects and atmospheric exchange, an observation described much more quantitatively four years later. Moreover, if Rayleigh processes alone controlled evaporating systems then closed basins would be expected to have extremely high $\delta^{18}O$ and $\delta^{2}H$ in the heavy isotope species of hydrogen and oxygen; however, the East African rift lakes, and other closed basins analyzed by Craig, are not significantly different from those of meteoric waters, with the exception of lower $\delta^{2}H/\delta^{18}O$ slopes. Finally, the $\delta^{2}H$ intercept of the regression line is ten (greater than zero). This implies that evaporating moisture from the oceans, which is the ultimate source for precipitation, is not an equilibrium process; otherwise, the intercept for meteoric waters (ten) would be identical to that of the oceans (zero) and that is not observed. These observations demanded a closer evaluation of the processes governing the stable isotope composition of the residual water in evaporating surface waters.

It should be mentioned that due to the advancements in the past century, the tracers of oxygen-18 and deuterium are perhaps the most commonly measured isotopes in water cycle studies. Further, the isotopes' capability to trace water sources and quantify a selection of governing process such as evaporation, water-rock interaction, recharge conditions, water parcel mixing, and many others has propelled stable water isotopes to become a conventional analyte in hydrogeology. The ability to use $\delta^{18}O$

and δ^2H measurements to quantify the extent of surface water evaporation is the focus of this thesis; works leading to the formulation of the existing approach are discussed next.

The ocean, being the largest reservoir of water on the earth's surface, was chosen as the standard reference for oxygen and hydrogen isotope measurements (Craig 1961b). Standard Mean Ocean Water - SMOW - is the standard for measurements of stable oxygen and hydrogen isotopes in hydrology. However, even the values of $\delta^{18}O$ and δ^2H vary regionally within the oceans due to elevated evaporation in semi-enclosed basins (Mediterranean Sea; Gat et al. 1996) or freshwater inputs to regions of the oceans with relatively short residence times (<1000 years for the Arctic Ocean; Bauch et al. 1995). The same water balance processes - freshwater inputs and evaporation - control the isotopic composition of water within lakes.

The identification of lakes that fall below the meteoric water line by Craig (1961) demands an isotopic composition for the outgoing evaporate that falls above the meteoric water line. Craig discovered that instead of the slope of eight in δ^2H-$\delta^{18}O$ space, evaporating waters followed a slope closer to a value of four or five. To produce these lower slopes, a relatively greater isotope effect must influence $^{18}O/^{16}O$ than $^2H/^1H$. To estimate the isotope values for δ^2H and $\delta^{18}O$ of outgoing evaporate (δ_E), a model developed by Craig and Gordon (1965) is utilized. The model uses three general assumptions to calculate the values of δ^2H and $\delta^{18}O$ for δ_E (Gat 1996): (1) equilibrium conditions persist at the air-water interface (relative humidity of 100%; isotope composition of vapour is in isotopic equilibrium with the surface of the liquid); (2) the vertical flux of water is constant; and (3) no isotopic fractionation occurs during the turbulent transportation of water. This model continues to be the basis for calculations of evaporating moisture although some of the notation in the original publication is no longer used in the same manner. Nearly five decades after its formulation, the model is still widely applied. Gonfiantini (1986) described the approach as "subdividing the evaporation process into steps," and clearly demonstrates the wide acceptance of the model "firstly proposed by Craig and Gordon (1965) and subsequently adopted by everybody."

The Craig and Gordon (1965) model (C-G model) follows a Langmuir-type linear resistance model coupled to an assumption of equilibrium (saturated) conditions at the liquid-air interface. Four atmospheric layers are used to describe the boundary conditions of the atmosphere: (i) a saturated layer (h=1) at equilibrium with the liquid, (ii) a diffusive sub-layer at the liquid-air interface, (iii) a turbulent sub-layer beneath (iv) a free atmosphere. The vapour flux from the liquid-air interface is assumed to be proportional to the humidity gradient and transport resistance terms for both the diffusive (ϱ_M) and turbulent (ϱ_T) sub-layers. The resistance terms, under natural conditions, are proportional to the molecular diffusion of a water isotopologue. As the diffusivity of $^1H^1H^{16}O$ is higher (faster) than that for the heavier isotopologues of water $^1H^1H^{18}O$ and $^1H^2H^{16}O$, transport (kinetic) isotope effects influence the isotope composition of evaporate (diffusivity ratios for $D(^1H^1H^{18}O)/D(^1H^1H^{16}O)$ and $D(^2H^1H^{16}O)/D(^1H^1H^{16}O)$ are 0.9723 and 0.9755. This work is reviewed in several publications. J.R. Gat has provided both a thorough review of the model (Gat 1996) and a review of the history of the development of the model (Gat 2008). Both are excellent publications, and use updated notation from the original 1965 publication (Craig and Gordon 1965). Another comprehensive review of the Craig and Gordon (1965) model, in addition to other discussion of stable isotopes in surface waters is available free of charge on the International Atomic Energy Agency's website (International Atomic Energy Agency

2011;
http://www-naweb.iaea.org/napc/ih/IHS_resources_publication_hydroCycle_en.html).

The work by Craig and Gordon (1965) provided a basis for calculating the isotope composition of evaporating moisture. Friedman et al. (1964) was the first study to apply stable isotopes to a lake water balance; however, this work did not take atmospheric exchange into account. The first consideration of isotope effects imparted during atmosphere-lake interaction was by Gat (1970). However, a major obstruction impeded the wider use of the Craig and Gordon (1965) model: uncertainties in the kinetic and equilibrium fractionation factors for $^{18}O/^{16}O$ and $^{2}H/^{1}H$ under different climatic conditions (humidity, wind speed, temperature). By 1971, the fractionation factors for equilibrium conditions were reported (Bottinga and Craig 1969; Majoube 1971) and kinetic fractionation factors were developed experimentally by 1976 (Vogt 1976). With these values now available, lake evaporation studies applying the Craig and Gordon (1965) evaporate model could be formulated.

By this point, the governing processes for precipitation were also beginning to be described. This is an important conceptual step for lake evaporation studies, since the isotope composition of precipitation is a calculation input useful for estimating the isotope composition of the atmosphere (input into the calculation of δ_E). Of further importance to lake evaporation, an estimate of the isotope composition of hydrologic inputs to a lake is required for evaporation estimates. Precipitation is a direct lake input and often controls the isotopic composition of overland runoff and groundwater inputs to a lake as well. Dansgaard (1964) developed a conceptual model that described four processes governing the isotopic composition of precipitation. The first two are essentially temperature-dependent effects: altitude and latitude. At higher altitudes and latitudes, temperature generally decreases. At lower temperatures, the equilibrium isotope effects during evaporation and condensation are greater, producing larger isotopic separations to $\delta^{18}O$ and $\delta^{2}H$ values between water-ice and vapour during phase transitions. This produces lower values for $\delta^{18}O$ and $\delta^{2}H$ in precipitation at high latitudes and altitudes. The third concept described a continental effect whereby regions distant from the coast receive precipitation with lower isotopic values for $\delta^{18}O$ and $\delta^{2}H$. This effect is better described as an air-mass trajectory effect where an air mass contains relatively greater amounts of the lighter isotopes of oxygen and hydrogen as it proceeds inland ($^{18}O/^{16}O$ of the air mass decreases). This effect is produced as the air mass rains out, favouring incorporation of the isotopically-heavy isotopologues of water ($^{1}H^{1}H^{18}O$, $^{1}H^{2}H^{16}O$) into the liquid phase, preferentially retaining more of the isotopically-light water isotopologue ($^{1}H^{1}H^{16}O$). This process manufactures an isotopically lighter residual vapour. Subsequent precipitation events from the same air mass will produce precipitation that is isotopically heavy compared to the air mass, but isotopically light relative to the initial rainout event from the same air mass. This process continues to isotopically lighten as the air mass moves inland and cools to temperatures below the dew point of the air mass (relative humidity of 100%). This rainout effect is described quantitatively by a Rayleigh-distillation process (Rayleigh 1896). A distillation process may also contribute to the latitude effects observed, since the majority of Earth's atmospheric moisture originates in the tropics and rains out as convection drives the air mass poleward.

The first calculation of evaporation from lakes using stable isotopes applying a modern approach (in this case, as a proportion of outflow) was presented by Zuber (1983). This work re-examined previous datasets (Dinçer 1968; Fontes et al. 1979; Zimmerman 1979) applying experimentally derived equilibrium and kinetic fractionation factors (Majoube 1971; Vogt 1976). However, the approach described by Zuber

finds large discrepancies for the deuterium balance resulting from uncertainties in the kinetic fractionation factor of deuterium-protium under evaporation. Further, the Zuber (1983) study applies long-term average values for humidity and the isotope composition of precipitation as input values, now proposed to be weighted to periods when evaporation occurs (Gibson 2002a). Zuber (1983) also studies lakes that are large enough for steady state to be assumed (with the exception of Lake Waidsee). For smaller lakes with large seasonal isotopic variability - or extremely large surface waters with residence times in excess of 100 years that are in disequilibrium with current climate (Lake Baikal, Seal and Shanks 1998; Lake Superior, this thesis) - this is not an entirely valid assumption. A non-steady approach is examined for lakes with considerable intra-annual variation in isotopic composition, such as small arctic lakes that receive a significant quantity of snowmelt each spring (Gibson et al. 1996; 1998; Gibson 1996; 2002b). Further contributions by this group report evaporation estimates for both heavy isotope tracers in the water molecule (^{18}O, ^{2}H), and show agreement between the tracers as would be expected under conservative behaviour (Gibson et al. 2002; Gibson and Edwards 2002). The values for evaporation as a proportion of inflow (E/I) obtained for the two tracers generally agree within 10% (Gibson et al. 2002).

A discussion of isotope studies for large lakes and inland seas is presented below. A selection of important contributions leading to the formulation of the modern approach to estimating evaporation using stable isotopes in water is shown in Table 1–1).

Table 1–1. Selected advancements in contemporary lake water balance studies using stable isotope tracers

Citation	Contributions
Emiliani 1955; Dansgaard et al. 1993; Bond et al. 1993; Edwards et al. 1996; Hoffman et al. 1998; Zachos et al. 2001; Wolfe et al. 2005; Clementz and Sewall 2011	Interest in paleo-climatology and paleo-oceanography continues to drive contemporary isotope hydrology, since a comprehensive understanding of the modern operation of hydrologic systems is required to interpret past variations in isotopic signatures. For example, roughly 50% of lakes >1000km^2 with isotope data compiled in this study originate from paleolimnology studies rather than contemporary hydrologic investigations.
Craig 1961a	Development of global meteoric water line Recognizes lower slopes for evaporating surface waters
Dansgaard 1964	Describes factors governing isotope composition of precipitation: altitude, distance from coast, latitude, "amount effect." d-excess parameter is defined by fitting a slope of eight through values of $\delta^{18}O$ and $\delta^{2}H$ and calculating the y-intercept: d-excess = $\delta^{2}H - 8 \cdot \delta^{18}O$
Friedman et al. 1964	First proposal of the use of stable isotopes to estimate evaporation. Applies a deuterium balance to estimate evaporation (Lake Tahoe), but does not account for molecular exchange with atmosphere.
Craig and Gordon 1965	Models isotope composition of evaporating water as a function of humidity, temperature, isotope composition of surface water and ambient moisture
Dinçer 1968	Applies stable isotopes to calculate the water balance of lakes, assuming isotopic and hydrologic steady state. δ_E calculated from Lake Burdur - which has a known water balance - then used to calculate water balance for Lakes Egridir and Beysehir applying the Craig and Gordon (1965) model to estimate the isotope composition of evaporated moisture
Gat 1970	Applies stable isotopes of oxygen ($\delta^{18}O$) to water balance of lake (Tiberias). Also, isotope values for an evaporation pan experiment are attempted for use in calculating kinetic isotope effects during evaporation.
Bottinga and Craig 1969; Majoube 1971	Equilibrium fractionation factors for water-vapour are developed experimentally
Sofar and Gat 1975; Gat 1979; 1984	Shows that for high salinity waters an activity correction for $\delta^{2}H$ and $\delta^{18}O$ values is required; Dead Sea waters used as an example
Vogt 1976	Experimental kinetic fractionation factors for water-vapour developed by wind tunnel experiments

Table 1–1 (continued).

Citation	Contributions
Zuber 1983	Utilizes fractionation factors from Majoube (1971) and Vogt (1976) to calculate δ_E and estimate outflow as a proportion of evaporation (O/E) for lakes: Chala (Tanzania); Titicaca (Bolivia; data from Fontes et al. 1979); Burdur, Beysehir and Egridir (Turkey; data from Dinçer 1968); Lake Waidsee (Germany; data from Zimmerman 1979)
Gonfiantini 1986	Describes a step-wise approach for water balance estimates of small lakes using stable isotopes where each time step is sufficiently short for steady-state to be assumed.
Edwards and Fritz 1986	Examine multiple tracers (^{18}O and ^{2}H) in modeling leaf water evaporative enrichment.
Gat and Bowser 1991	Introduces necessary modifications to input isotope composition for string of lake systems. For example, a headwater lake receives only runoff, groundwater input, and direct precipitation; whereas a lake downstream of another lake receives a connecting channel input that has already undergone potentially significant evaporation and heavy isotope enrichment.
Benson and White 1994	Assumption of equilibrium between turbulent-zone vapour (δ_A) and precipitation shown to be invalid for arid areas (example from Nevada). This assumption produces δ_A values that are too ^{18}O- and ^{2}H-depleted relative to actual measured (~2 to 4 per mille in $\delta^{18}O$ values).
Horita and Weslowski 1994	Updates Majoube 1971 equilibrium fractionation factors. The equations presented here are those currently in use for water-vapour phase transitions
Gibson 1996	Develops non-steady state equations for estimating lake evaporation as a proportion of inflow (E/I) using a stable isotope mass balance.
Gibson and Edwards 2002	Use of interpolation to map regional variability in small lake evaporation rates using a stable isotope mass balance and two isotopic tracers
Gibson 2002a	Highlights importance of weighting climate and isotope input parameters to the calculation of δ_E to time periods when evaporation is occurring. In previous publications, long-term averages were used (Zimmerman 1979; Zuber 1983)
Yi et al. 2008	Mass and isotope conservation applied for the first time to simultaneously match E/I outputs for ^{2}H and ^{18}O tracers

As this study concerns the very large Great Lakes of North America, it is important that existing studies for large surface waters utilizing isotopes are discussed. Isotope investigations for lakes on the order of 10^3 - 10^4 km^2 in area are reviewed here. The lakes reviewed here include Lake Tanganyika (Craig 1975), Lake Malawi (Gonfiantini 1979), Lake Chad (Fontes et al. 1970), Lake Turkana (Ricketts and Johnson 1996), Lake Titicaca (Fontes et al. 1979; Zuber 1983), Lake Baikal (Seal and Shanks 1998), and saline bodies such as the Mediterranean Sea (Gat et al. 1996), Red Sea (Craig 1966) and the Caspian Sea (Froehlich 2000). Finally, previous works for the North American Great Lakes region will be reviewed (Gat et al. 1994; Machavaram and Krishnamurthy 1995; Yang et al. 1996; Karim et al. 2008).

Lake Tanganyika (32,900 km^2), one of the Great African lakes, was sampled for stable isotope ratios of oxygen and hydrogen in its waters (Craig 1975). Craig reported that the lake was "isotopically upside down," referring to the higher δ^2H and δ^{18}O values below the mixed layer (~100m). The difference in δ^{18}O values between the surface and hypolimnion is roughly 0.4‰ (+3.6 at depth, +3.2 at the surface). Craig noted that the concentration gradient of ^{18}O between Lake Tanganyika and its largest input - the Ruzizi River - was the greatest concentration gradient of any of the measured conservative analytes. The large isotopic offset highlighted the potential use of isotope ratios of oxygen and hydrogen as tracers of water parcels during transport and mixing. Relative to the epilimnion, deep waters have lower temperatures, more apparent kinetic fractionation effects in δ^{18}O-δ^2H space, and higher chloride concentrations. This is interpreted as the signal of colder and drier conditions that prevailed within the flushing time of Lake Tanganyika (volume divided by liquid inputs, ~2000 years; Craig 1975). Finally, an important statement was made for Lake Tanganyika that has implications for the treatment of data for other large poorly mixed lakes. Craig stated that: "In many ways Lake Tanganyika resembles the oceans, especially in the long "residence time" of deep water relative to replacement by mixing with surface water." The "residence time" referred to here should be referred to as a lake's flushing time, which is distinct from residence time as it only examines liquid fluxes (evaporation flux is not considered). This is an important distinction since the residence time of Lake Tanganyika is closer to 400 years (Bootsma and Hecky 1993).

Isotopic datasets for a third Great African Lake, Malawi (28,800 km^2) were presented by Gonfiantini et al. (1979). Tanganyika and Malawi are geographically and geologically similar lakes. Both are meromictic (perennially stratified) and both were formed by tectonic processes within the east African Rift Valley. The lakes lie within a complex of normal faults producing half-grabens that have filled with water. The heavy isotope enrichment observed at depth for Malawi is not as apparent as in Lake Tanganyika. This is attributed to a greater degree of mixing between the epilimnion and hypolimnion in Malawi, supported by the presence of radioactive hydrogen (^{3}H; half life 12.3 years) in the hypolimnion of Lake Malawi (at depths exceeding 600m; Gonfiantini et al. 1979). Using a box model representing the geometry of Lake Malawi as an upside-down triangle, the mixing rate between the epilimnion, metalimnion and hypolimnion was calculated. Gonfiantini et al. (1979) calculated that twenty-five percent of the metalimnion and twenty percent of the hypolimnion mixes into the epilimnion annually.

Isotope data for Lake Chad (20,000 km^2) were examined by Fontes et al. (1970). Lake Chad is a closed basin (no surface water outflow) unlike lakes Malawi and Tanganyika that lose six and 17 percent, respectively of total water through surface outflows (Gonfiantini et al. 1979). Lake Chad is separated by sand bars; the degree of horizontal mixing between the basins was unknown. Results showed an immense scatter ranging in δ^{18}O values from ~0‰ to 15‰. δ^{18}O was positively correlated with electrical

conductivity in the water in all cases. However, this trend followed distinct trajectories for each of the northern and southern basins, leading the authors to conclude mixing between the basins is negligible (Gonfiantini 1986).

The study of Lake Turkana (6500 km^2) - one of the smaller lakes in the African Rift valley - by Ricketts and Johnson (1996) took advantage of the known water balance of this closed lake to estimate the amount of advected moisture entering the basin following the method of Benson and White (1994). This method applies a two point mixing for moisture sources between (1) calculated lake-derived evaporate and (2) advected moisture measured from outside the basin. For Lake Turkana, the fraction of water vapour entering the basin was calculated to be roughly 40% applying a stable isotope mass balance to atmospheric moisture. This study is particularly interesting, as it highlighted a driving force of isotope hydrology. The study examined the contemporary isotopes in the lake to better understand observed fluctuations in the $\delta^{18}O$ of authigenic calcite ($CaCO_3$) obtained from a lake sediment core. As in multiple cases, use of stable isotopes in paleolimnology and paleoclimatology required an understanding of contemporary processes. The study of Ricketts and Johnson (1996) yields important contemporary isotope hydrology information largely as a by-product of an interest in the paleolimnology of a lake.

Missing from this discussion is the largest of the east African rift lakes, Lake Victoria (69,000 km^2). The contemporary $\delta^{18}O$ value for Lake Victoria water is reported as +3.5‰ from a paleolimnology study (Beuning et al. 2002); no thorough evaluation of the distribution of $\delta^{18}O$ or $\delta^{2}H$ is readily available in published literature for this lake. Isotope values for several smaller African lakes were reported by Cerling et al. (1988).

Isotope data for Lake Titicaca waters were first presented in Fontes et al. (1979) and its water balance was evaluated by applying stable isotopes in Zuber (1983). Only two percent of water loss was estimated to occur as surface outflow, making Titicaca's basin nearly endorheic (internally drained). Assuming $\delta^{18}O$ of precipitation was represented by local groundwater samples (Fontes et al. 1979), Zuber calculated outflow as a proportion of evaporation (O/E) to be two percent (E/I = 1/[(O/E)+1] = 98 percent), but only used the ^{18}O tracer and neglected to discuss deuterium. Further, Zuber (1983) described a sensitivity analysis whereby a small shift (1 per mille) in $\delta^{18}O$ values can lead to an O/E value of either 10 percent (E/I = 91 percent) or a negative value for evaporation losses.

The volume of Lake Baikal is roughly 20 percent of all lake water on Earth (Figure 1-13). The oxygen and stable isotope composition of the waters of Lake Baikal are roughly 20 per mille less than those in the Great African Lakes, highlighting rainout and latitude effects on the precipitation at Lake Baikal's inland and northern setting. Data for Lake Baikal were reported by Seal and Shanks (1998). An E/I calculation for Baikal was not completed by the authors, likely due to complications from the large residence time of the lake (330 years; Falkner et al. 1991) and isotopic disequilibrium with the current climate. The authors estimated climate and isotopic input stability must have persisted for roughly one millennium before an isotopic steady state assumption could be made. Natural climate fluctuations often occur on time scales much less than 1000 years, such as the Little Ice Age (-1°C temperature anomaly: ~16th to ~19th centuries) and the Medieval Warm Period (+1°C anomaly ~10th to the ~13th centuries: anomaly relative to temperature proxies for the ~1st to ~9th centuries). However, for Lake Baikal, the most important fluctuations to the isotope composition are changes in precipitation distribution within the basin and subsequent changes to the importance of major inflows to the lake's isotope composition.

Stable isotope ratios of oxygen (n = 147) and hydrogen (n = 149) in the eastern Mediterranean Sea (2,500,000 km^2) waters were reported by Gat et al. (1996). The trajectory observed in $\delta^{18}O$-δ^2H space for waters is unlike that of other evaporating systems that commonly plot along a slope of ~4-5. The Mediterranean Sea waters demonstrate evaporative enrichment in ^{18}O, but this is not matched by a corresponding enrichment of deuterium (i.e. δ^2H-$\delta^{18}O$ slope approaching zero). This is unprecedented; for most other evaporating systems, the two elements enrich in their respective heavy isotope species in similar fashion. Even in the case of other enclosed seas, such as the Red Sea, δ^2H-$\delta^{18}O$ cross plots reveal a seawater trajectory with a slope of six (Craig 1966). An explanation for this was proposed by Gat et al. (1996). To explain the deficiency of an increase in δ^2H as $\delta^{18}O$, the authors proposed that a combination of deviations to local meteoric water lines over the Mediterranean and surface water evaporation explained the δ^2H-$\delta^{18}O$ trajectory. The authors proposed that the δ^2H-$\delta^{18}O$ trajectory of the Mediterranean Sea is controlled by a dominant wintertime evaporation as a result of depleted and dry continental air mass advection over the Sea surface. Also, when discussing the input parameterization for humidity and the isotope composition of the overlying atmosphere, the authors stressed the importance of evaporated moisture build-up down-fetch. The authors advocated a two part mixing model to formulate "downwind" conditions, assuming any relative humidity build-up was the result of added evaporate. This is not strictly correct since saturation vapour pressure is a function of temperature and air mass warming/cooling - depending on season - occurs over the Sea due to thermal conduction and latent heat effects of the Mediterranean Sea on the overlying atmosphere. Nevertheless, the discussion of isotope modifications of a water body on the overlying atmosphere is an important consideration and is one that is rarely considered in stable isotope mass balance evaporation calculations.

Isotopes of oxygen and hydrogen in the waters of the Red Sea (Persian Gulf) and Salton Sea (California, south-western North American continent) were presented by Harmon Craig (1966). The paper's focus is more on the origin of the water in brines found in the region that, in the case of one brine, were determined to be meteoric in origin (Salton Sea, California) and oceanic for another (Red Sea). Meteoric brine is determined from an ^{18}O-enriched trajectory at a constant δ^2H value. This is the result of incorporation of ^{18}O-enriched oxygen sources such as carbonates and silicates. However, since most rocks contain negligible amounts of available hydrogen in comparison to leachable oxygen, deuterium content does not vary, producing a slope of zero in $\delta^{18}O$-δ^2H space. Isotope composition for the brine of oceanic source (Red Sea brine) is intermediate to waters from the northern Red Sea and the Gulf of Aden, located between the Red Sea and the Indian Ocean. Craig concluded that the brine originated from mixing waters of the Red Sea and the Gulf of Aden, recharging at a sill between the two water bodies.

Further discussion of large saline water bodies focuses attention on the largest inland water body on Earth - the Caspian Sea (400,000 km^2) - which contains nearly as much water as the combination of all surface fresh waters on Earth (78k km^3 in Caspian Sea, ~110k km^3 of surface fresh water on Earth). $\delta^{18}O$ values for the Caspian are lowest at the surface and increase with depth (down to depths >1000m). Surface waters plot near -1.9 per mille, increasing to -1.4 per mille at 700m depth (Froehlich 2000). This study of the Caspian Sea promoted the use of an evaporating pan as a means of calculating the isotope composition of the ambient atmosphere. Humidity build-up over the Caspian is significant, with relative humidity of advecting air masses increasing from <50% to ~75% from near land to the centre of the sea. The range in ambient moisture conditions advocates the use of a model that simultaneously accounts for

isotopic, humidity and temperature modifications to atmospheric moisture by the evaporating Sea. Finally, it should be mentioned that the authors in the study advocated the use of isotopic measurements of evaporation pans (over lake) to help constrain atmospheric parameters such as humidity and temperature, but also the isotope composition of atmospheric moisture. Unfortunately, physical barriers placed over drying evaporation pans to block input of precipitation likely modifies the natural atmospheric conditions and may not represent over lake conditions. Furthermore, as the pan evaporates, a build-up of evaporate in air overlying the pan significantly modifies the air's isotope composition, similar in some ways to effects over large water bodies. The study proposed drying a sample of lake water in an evaporation pan and applying the δ^2H-$\delta^{18}O$ enrichment trajectory of the residual pan water over a short time period to simulate the atmospheric conditions and isotope effects during evaporation. However, this may not be a helpful approach. The use of a pan for a short duration only provides a small snapshot of the isotope effects over the duration the pan evaporates. This does not capture the conditions of the atmosphere for systems that have residence times greater than the period that the pan is evaporating (Caspian Sea residence time is >200 years). The short time span of an evaporating pan becomes a severe drawback for seasonally evaporating lakes where flux-weighting of atmospheric parameters to periods when evaporation is greatest is a requirement.

For the North American Great Lakes, several studies have examined isotope ratios in regional precipitation (Gat et al. 1994; Machavaram and Krishnamurthy 1995) and Great Lake waters (Yang et al. 1996; Karim et al. 2008). The precipitation studies utilize the systematic offset of evaporating waters from the global meteoric water line (Craig 1961) produced by disequilibrium (kinetic) isotope effects to assess the contribution of evaporate to the downwind atmosphere (Gat et al. 1994; Machavaram and Krishnamurthy 1995). The contribution of Great Lakes evaporate has been assessed semi-quantitatively (Gat et al. 1994; Machavaram and Krishnamurthy 1995) capitalizing on the increase in the deuterium excess parameter as evaporated waters are incorporated into the atmosphere. Gat et al. (1994) estimated that roughly 8% of leeward atmospheric moisture is derived from Great Lakes evaporate. For each of the previously discussed water bodies, values presented in each paper are extracted and compiled in a new database of isotope values for large lakes and inland seas (Table 1–2). Results are presented in a δ^2H-$\delta^{18}O$ cross plot (Figures 1-2a) and by geographic distribution (Figure 1-3; 1-4). For water samples from the largest African Lakes (Malawi, Tanganyika, Victoria), $\delta^{18}O$ values are generally greater than zero per mille relative to standard mean ocean water (SMOW), contrasting Lake Baikal's mean value near -16 per mille (Figure 1-6). The most ^{18}O-poor natural lake in the world is Lake Vostok, a subglacial lake located beneath roughly four kilometres of the eastern Antarctic ice sheet (-58 per mille, SMOW); although this "lake" is not exposed to the atmosphere. It should also be noted that the greatest range in $\delta^{18}O$ and δ^2H occurs for the lakes with short residence times (Lake Chad) or fluctuating storage volumes (Aral Sea, Great Salt Lake; Figure 1-2a) whereas lakes that have a large groundwater input component, or are well mixed and have long residence times, show less variance in their stable isotopes of oxygen and hydrogen (Lake Superior and Lake Baikal). The same argument might be used to describe Lake Tanganyika; however, the waters at depth are relict because the lake is meromictic.

Yang et al. (1996) produced an estimate for evaporative losses as a proportion of inflow (E/I) of seven percent applying a stable isotope method. The authors proposed that seven percent corresponds to a value of 10.5 km^3 per year for the entire Great Lakes basin. Multiplying their value for E/I of seven percent by the mean annual precipitation for the Great Lakes basin of 850mm (650 km^3/yr), a value of 45

km^3/yr is obtained, roughly four times the value reported by Yang et al. (1996). Therefore, Yang et al.'s (1996) evaporation flux of 10.5km^3/yr is a miscalculation. This value is an order of magnitude lower than a value obtained from mass balance estimates (159±71 km^3/yr evaporating from Great Lakes; Neff and Nicholas 2005). The authors quote Gonfiantini (1986) as the source of the equations applied. However, a recalculation of E/I using the exact inputs outlined in Yang et al. (1996) using the equations quoted from Gonfiantini (1986) produces an E/I value of 22% (146 km^3/yr), which is a similar value to that obtained through physical hydrology approaches (24%±11%; Neff and Nicholas 2005). One the authors from Yang et al. (1996) attempted to quantify evaporation losses applying a stable isotope mass balance for the Great Lakes basin again in 2008 (Karim et al. 2008). This time, the authors obtained values more consistent with lower-end estimates of physical hydrology models for the Great Lakes (Neff and Nicholas 2005). Karim et al. (2008) report an E/P value of 14% and effectively changing the estimate in Yang et al. (1996) of 10km^3/y to 96km^3/y. The approach of Karim et al. (2008) does not account for internal recycling of moisture, does not weight parameters seasonally as shown to be necessary in Gibson (2002a), does not make use of measurements of δ^2H, and effectively ignores that the E/I output for deuterium following their approach does not match that obtained from an ^{18}O mass balance. Furthermore, despite collecting samples distributed amongst four of the five Great Lakes, the authors opted to not use this extensive set of cruise sample results and resorted to using the flux weighted output for the entire basin instead of evaluating each lake individually. The authors used their evaporation result to calculate total transpiration on the basis of a mass balance and apply estimates of total basin interception. The authors coupled the transpiration value to water use efficiency ratios from area weighted vegetation indices, and calculated the total CO_2 storage annually. Applying their values, the authors postulated that uptake within the Great Lakes basin could account for the suggested missing North American carbon sink. These final steps are an innovative use of stable isotope mass balance results; however, the authors' E/I calculation requires additional considerations (as discussed above).

For interest, the dataset compiled in this literature review of large lakes encompasses more than 75% of the estimated 110 thousand cubic kilometres of lake water on Earth. Averaging each of the δ^{18}O values of the compiled lakes, and volume-weighting the averaged δ^{18}O values, I calculate a volume-weighted δ^{18}O value of roughly -6 per mille for the ~20 most voluminous lakes on earth. If the remaining lake water on Earth 25k km^3 of lake waters on Earth that have not been measured are assumed to have an average δ^{18}O of -5 to -20 per mille the volume-weighted δ^{18}O value of Earth's surface fresh water reservoir can be constrained to be -7.6±1.7 per mille (Figure 1-6). Lake Vostok is not included in this calculation as it is not exposed at the surface. If the Caspian Sea (saline water) is included in this calculation the volume weighted δ^{18}O of surface waters is modified to -5.6±1.5 per mille; this point is shown in Figure 1-2b. The volume weighted isotope composition of Earth's lakes is ^{18}O-depleted relative to the oceans, showcasing processes that act to deplete oceanic-evaporate prior its redeposition on the land surface (and integration into lakes). Further, the offset from the meteoric water line of the volume-weighted isotope composition of lake waters shows that evaporation plays an important role in governing this reservoir (Figure 1-2b).

Hydrologic balance calculations have been completed for roughly half of the world's ~100 largest lakes. For water balances derived from stable isotopes of oxygen and hydrogen in lake waters, this figure is much less. Closer to 15 percent of the world's largest lakes have reported values for ^{18}O/^{16}O and ^{2}H/^{1}H, and less than 5 percent of these use isotopic techniques to quantitatively evaluate the lake water

balance. There is an abundance of data available for isotope ratios of precipitation from worldwide monitoring stations; values for isotopes in precipitation are available from stepwise regression models for areas without monitoring stations (Bowen and Revenaugh 2003; grids made available for download by Bowen 2009). For small lake systems, it has been shown that a simple set of analyses of 30 mL grab samples of lake water can successfully map variability in E/I ratios (Gibson and Edwards 2002). Perhaps a new approach using large lakes with well established water balances can be applied to estimate the evaporation as a proportion of inflow for the world's largest lakes, many of which are surprisingly poorly known (for example, Lake Tanganyika's water balance is poorly quantified). Additionally, changes to the isotope composition of atmospheric moisture may be a useful tracer of an expectedly faster global water cycle under a warmed global climate as has been shown to be the case during the Eocene (60Ma to 34Ma, global temperatures up to 12 degrees warmer than present during Eocene climatic optimum; Clementz and Sewall 2011). Moisture sources to the atmospheric reservoir - which has a short residence time of ~10 days and a total volume of ~10^4 km^3 of water - are either inland or oceanic. The isotope composition of the oceans is well established and readily available (Schmidt et al. 1999), but that of inland sources is not. This new lakes database could help to evaluate the global contribution of evaporation from large inland surface waters to the overlying atmospheric water budget. The compiled dataset contains lake name, lake basin endorheic/exhorheic status, lake area, catchment area, lake age, lake volume, lake residence time, sample location, sample depth, sample date, original reference, $\delta^{18}O$, $\delta^{2}H$, temperature, salinity, physical water budget data and water balance uncertainties.

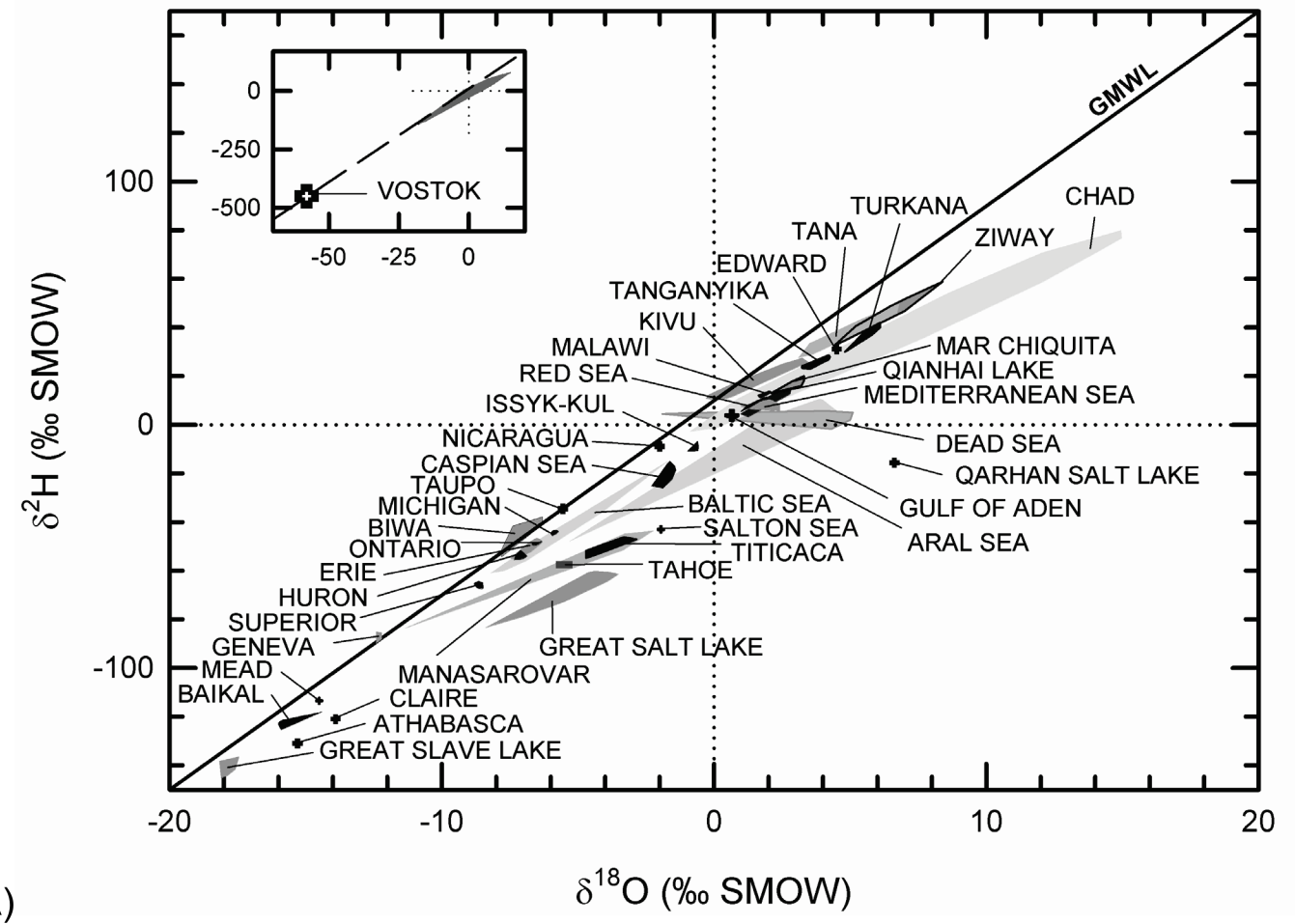

Figure 1-2. (A) δ^2H-$\delta^{18}O$ cross plot of a selection of major lakes and inland or semi-enclosed seas from previous works (labelled in figure). A convex hull (area connection outermost points) derived from results for each water body is plotted instead of point-data in order to simplify the plot. A regression of meteoric waters (GMWL; $\delta^2H = 8 \cdot \delta^{18}O + 10$; Craig 1961) is plotted for reference.

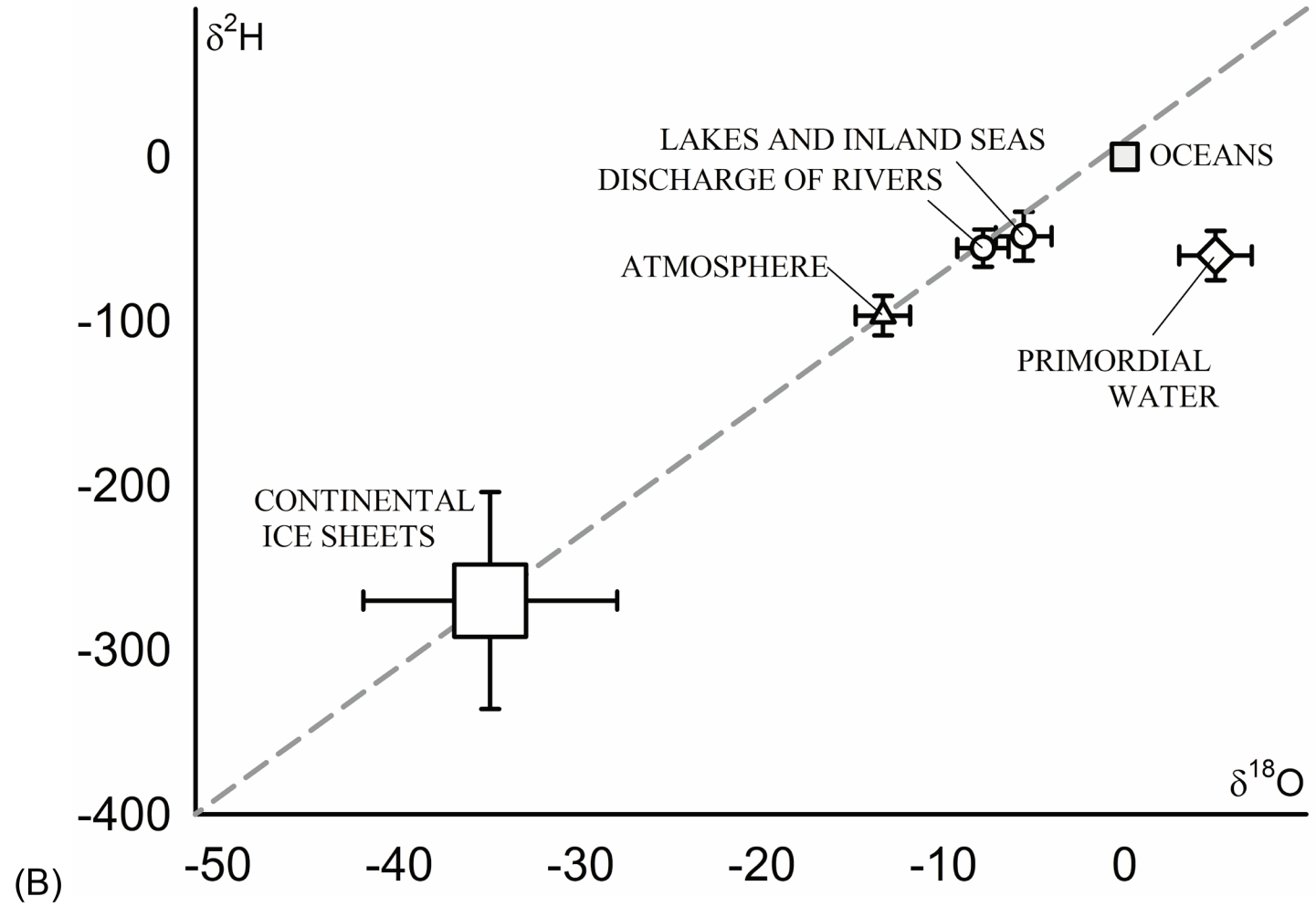

Figure 1-2. (B) Volume- or discharge- weighted isotope composition of Earth's surface water reservoirs: ice sheets, oceans, lakes and inland seas, and rivers. The isotope composition of Earth's primordial (original) waters are shown as a black diamond.

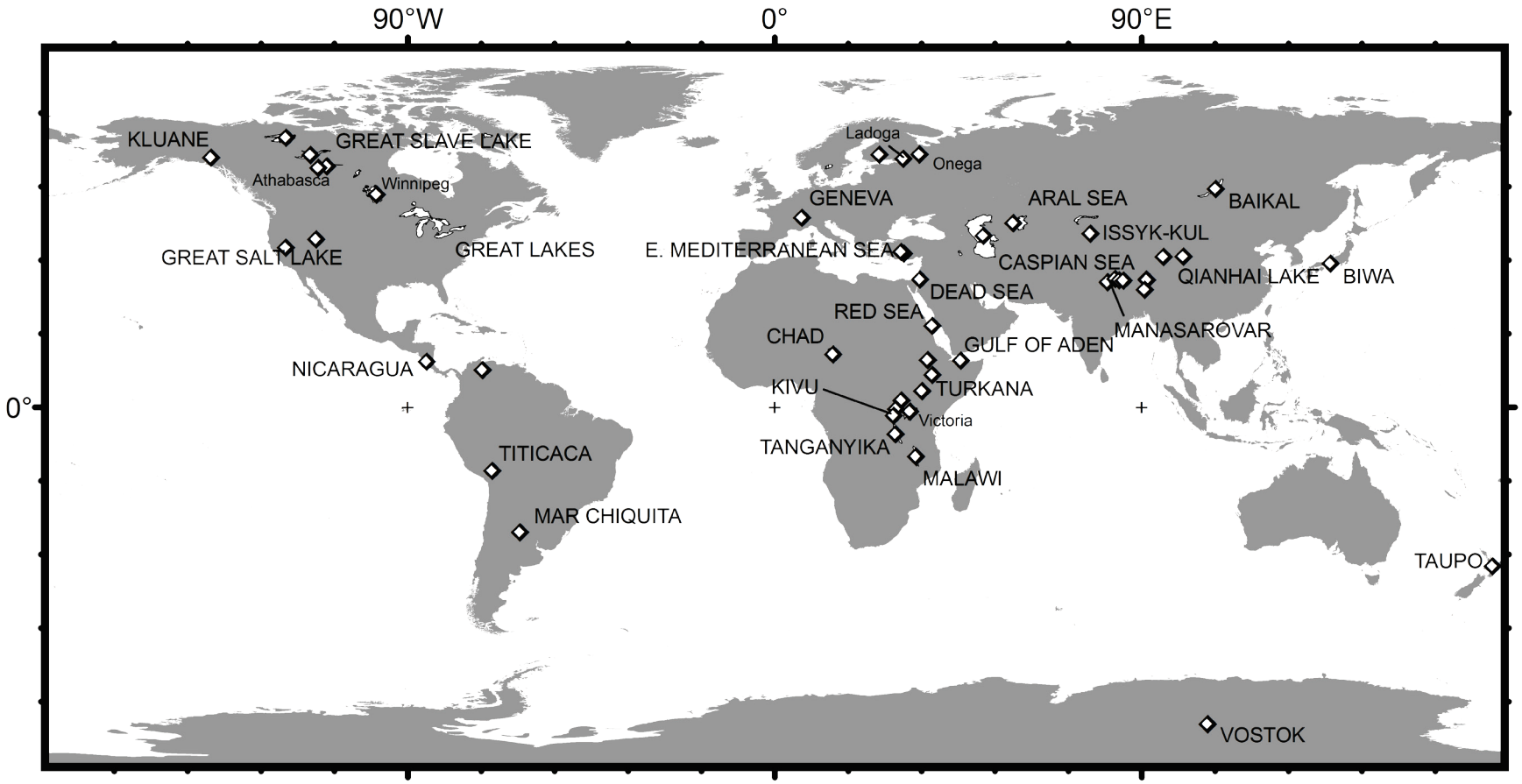

Figure 1-3. Map of available $\delta^{18}O$ and $\delta^{2}H$ data for selected large lakes and inland seas (white diamonds and upper case labels; lakes selected are over ~400 km^2). Stable isotope data for lakes only reporting $\delta^{18}O$ values (but not $\delta^{2}H$) are labelled in lower case letters.

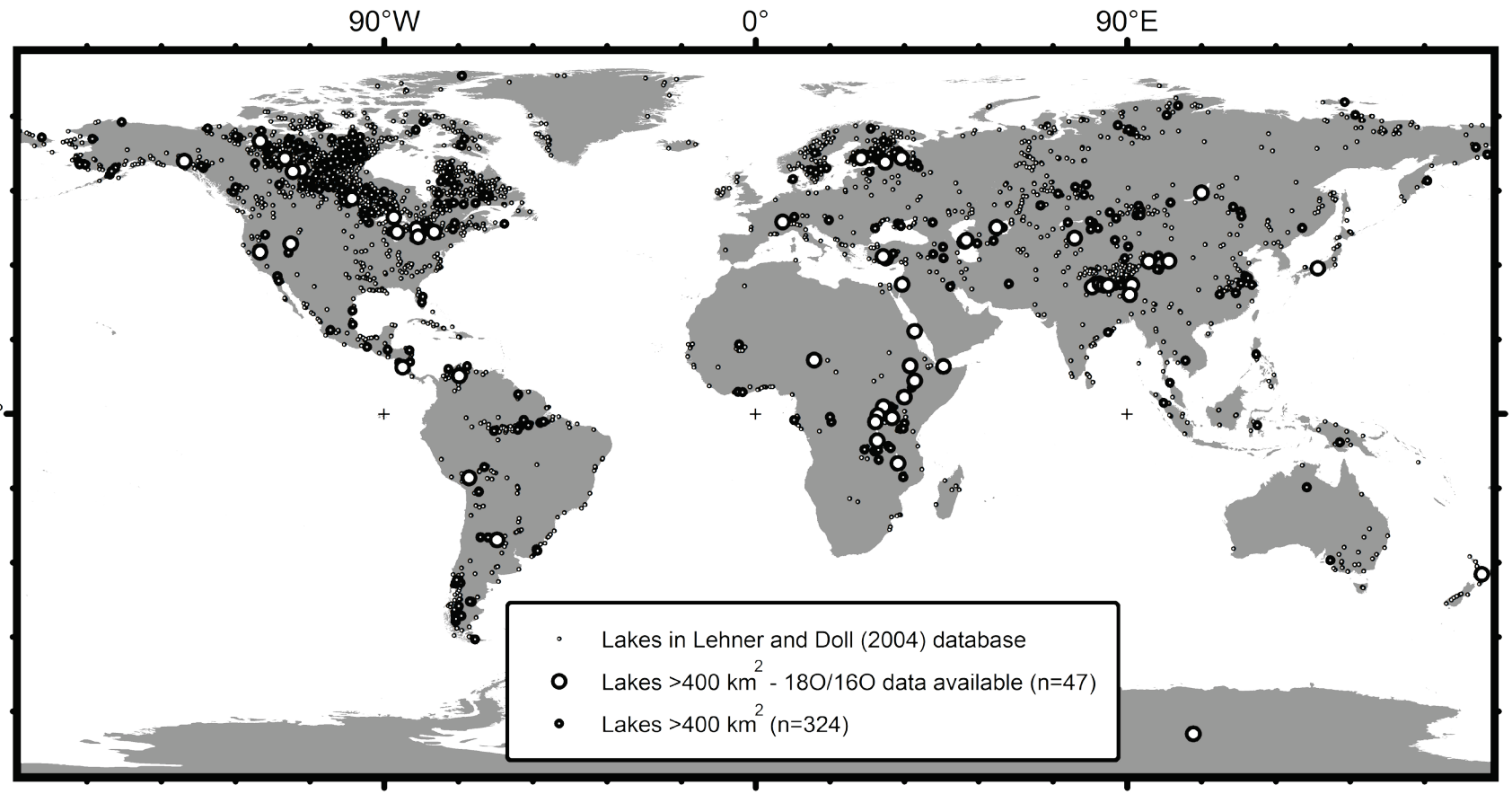

Figure 1-4. A map of large lakes and inland seas (area exceeding 400 km^2) on Earth (GIS data based upon Lehner and Doll 2004). Surface waters with an areal extent exceeding 500 km^2 are represented by black dots (n = 255); those with $\delta^{18}O$ data available in are represented by white circles. Large surface waters are concentrated in the mid-high latitudes, particularly on the Canadian and Fennoscandinavian shields. An estimated 15 percent of Earth's large surface water bodies have reports of $^{18}O/^{16}O$ data available. Lakes <400km^2 are shown as small points. Note that 23% of lakes with surface areas >400km^2 are located within Canada. 41% of all lakes in the Lehner and Doll (2004) database are Canadian.

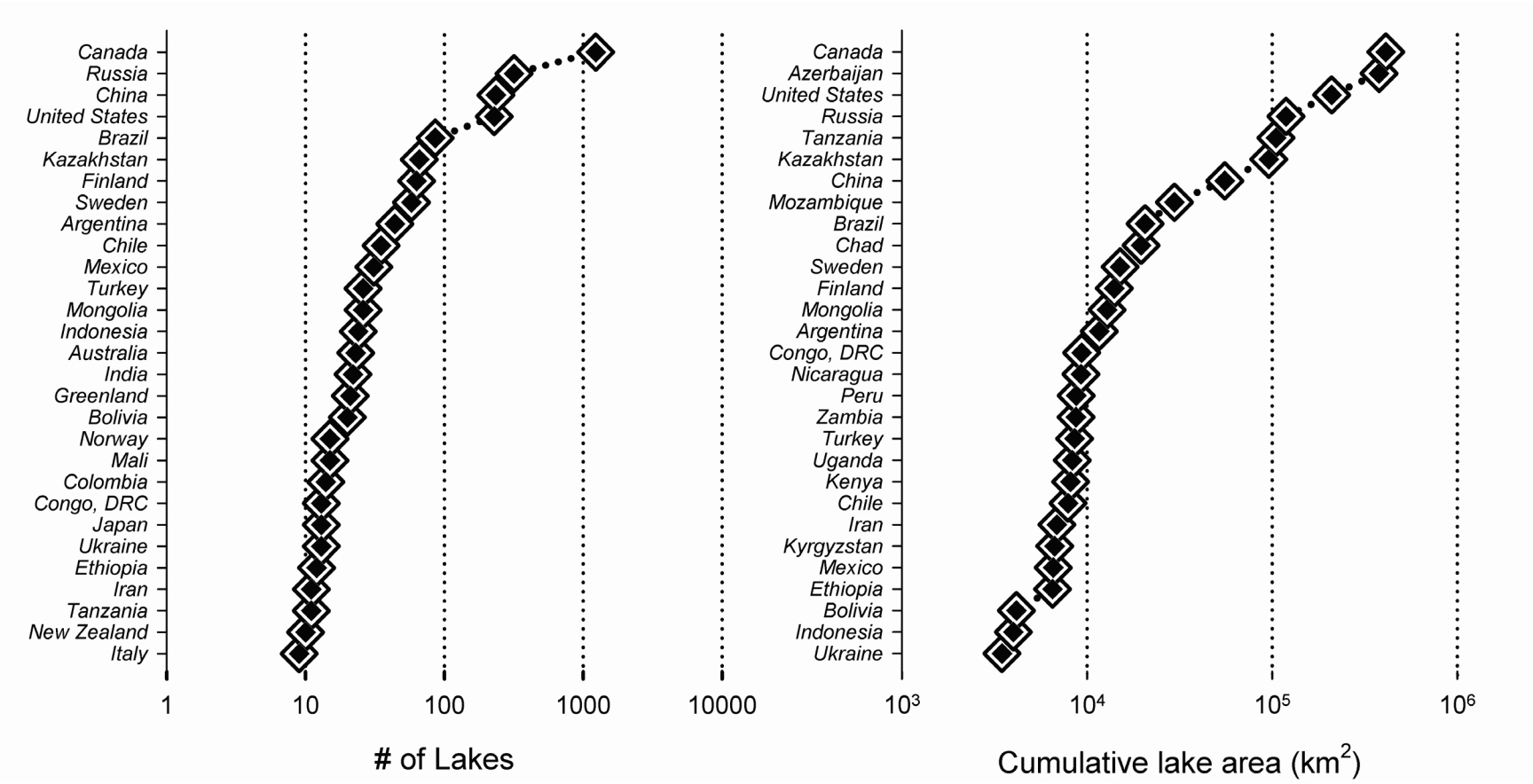

Figure 1-5. Lakes by nation using data from Lehner and Doll (2004). The left plot shows the number of point data (lakes) within each country, whereas the right plot shows this by country (note high value for Azerbaijan influenced by using point locations resulting in a uni-national Caspian Sea at 371,000 km² in area). Canada has the largest number of lakes both in quantity (~40% of world's lakes) and by surface area. Note that this database vastly underestimates the number of total lakes in the world (estimated at 300 million covering $4.2 \cdot 10^6$ km²; Downing et al. 2006). This diagram shows the heterogeneity in the geographical distribution of Earth's lakes.

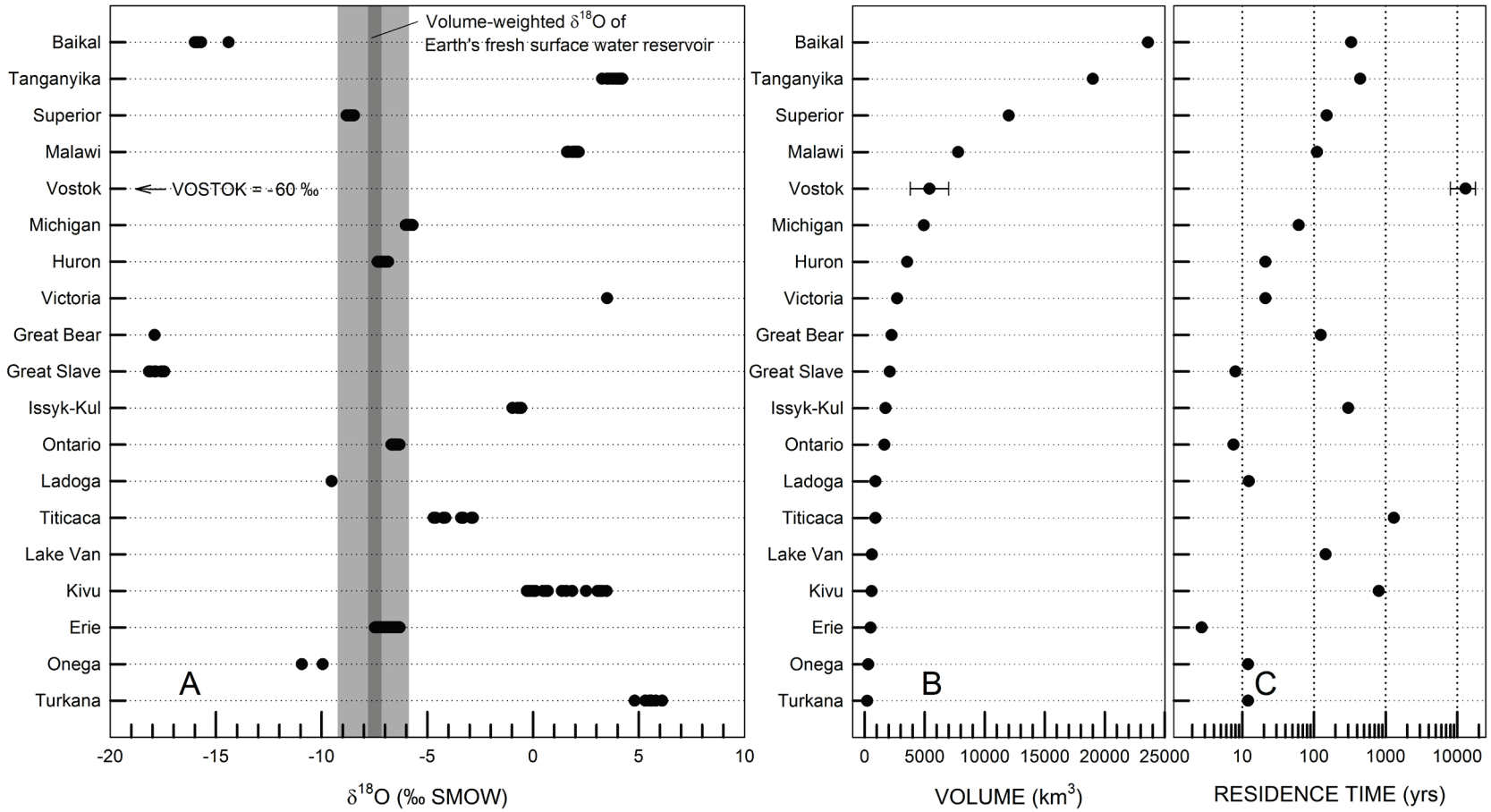

Figure 1-6. (A) $\delta^{18}O$ of samples collected from large surface waters. Grey shading represents the volume weighted $\delta^{18}O$ for Earth's surface freshwaters. The volume in cubic kilometres of a selection of large lakes is presented in (B) and estimated residence times for the large lakes are presented in (C). The lakes here account for over 85k km^3 of the estimated ~110k km^3 of lake water on earth (>75%). Estimating that the remaining ~25k km^3 has a $\delta^{18}O$ value between -20‰ to -5‰, the volume weighted $\delta^{18}O$ value for freshwater lakes on the surface of planet Earth is between -6‰ and -9‰ (grey shading in A). Individual sample points are shown instead of ranges to reflect small sampling density of some lakes (only one sample for Lake Victoria).

Table 1–2. Number of isotope results (n_{18O}, n_{2H}) reported for some large lakes and semi-enclosed seas. Residence time is represented by τ.

Name	Latitude (deg)	Longitude (deg)	Altitude (m)	Area (km^2)	Catchment (km^2)	Volume (km^3)	Origin	Age (yr)	τ (yr)	Reference	n_{18O}	n_{2H}
Chad	13.0	14.2	244	20000	1035000	>50	Tectonic	-	1	Fontes et al. 1970	95	95
Dead Sea	31.3	35.5	-420	900	42000	140	Tectonic	12k - 70k	100	Gat 1984	27	26
Turkana	4.0	36.0	360	6500	130000	200	Tectonic	>3M	12	Cerling et al. 1988; Ricketts and Johnson 1996	9	9
Titicaca	-15.5	-69.4	3827	8400	58000	900	Tectonic	2M - 20M	1300	Fontes et al. 1979	12	12
Victoria	1.0	33.0	1133	69000	200000	2750	Tectonic	10k - 100k	21	Beuning et al. 2002	1	0
Malawi	-12.0	34.5	471	29500	100500	7780	Tectonic	2M - 20M	110	Gonfiantini et al. 1979	21	21
Tanganyika	-6.5	29.5	773	32600	220000	19000	Tectonic	2M - 20M	440	Craig 1975	29	29
Baikal	53.5	108.0	450	31700	560000	23600	Tectonic	2M - 20M	330	Seal and Shanks 1998	32	32
Caspian Sea	42.0	51.0	-28	400000	1400000	78000	Tectonic	2M - 20M	250	Froehlich 2000	25	25
Red Sea	20.0	38.5	0	440000	-	230000	Tectonic	~35M	-	Craig 1966	16	16
Gulf of Aden	11.5	45.5	0	530000	-	250000	Tectonic	~35M	-	Craig 1966	4	4

1.2 The North American Laurentian Great Lakes

The Great Lakes hydrologic basin is 750,000 km² in area, roughly three percent of the North American land mass. Despite its relatively small landmass on a continental scale, the basin supports a population density roughly twice that of the North American average and a world class economy. For example, if the two Canadian provinces of Quebec and Ontario and the eight United States surrounding the Great Lakes were considered as one nation, their gross domestic product per capita would be within the top ten nations in the world (45k USD per citizen; World Business Chicago 2011), surpassed only by China, Japan and the entire United States. The large population surrounding the Great Lakes and its burgeoning economy supports functions such as trade, transportation, tourism, finance, education, and scientific and technical innovation. The North American Great Lakes form the foundation of the basic needs for many of these sectors. For example, each year over 200 million tonnes of grain, base metals and ore, hydrocarbons, and other agricultural products are shipped annually along the St. Lawrence Seaway and within the Great Lakes. Ships frequently operate with minimal under-keel clearance to the sediment water interface; maximum loads are restricted, particularly when lake levels are lowered. Evaporation plays an important role on the water level of the Great Lakes, however, evaporation-magnitude are large. Therefore, an improved calculation of the evaporation flux from each Great Lake within each lake's residence time is needed, particularly if changes in evaporation rates are to be evaluated under a changing climate.

1.2.1 Geology, Natural Ecosystems and Human Geography

The Laurentian Great Lakes and surrounding hydrologic basin support a dense population in a variety of ecoregions that cover Quaternary drift and much older bedrock. This section focuses on the geography of the region and begins by introducing the earth materials and the formation of the Great Lakes (1.3.1.1.). Next, the importance of the Great Lakes basin to the Canadian and United States economies is discussed in relation to industry, agriculture, water resources and the surrounding ecozones of the Great Lakes basin (1.3.1.2.).

1.2.1.1 Geology and ecosystems of the Great Lakes

The Great Lakes basin is a geologically young area; however, the oldest bedrock within the basin first crystallized when the Earth was relatively young. The "young" landscape is the product of the most recent glaciation known as the Wisconsinan. Most studies generally refer to a glaciation reaching maximum extent roughly 30ka and culminating roughly 10ka (other names used include Weichsel - British Isles, Weichsel-Devensian - Europe, and Fraser - Pacific Cordillera). The Wisconsinan ice sheets covered the current location of the Great Lakes. The most recent glaciation's ice did not extend as far as the two preceding glaciations: the Illinoisan and Kansan (Pre-Illinoian A, Anglian or Elster). The development of the Great Lakes is complex. Its history is made up a series of glacial retreats and advances that formed extensive proglacial lakes and produced a dissimilar drainage pattern to present conditions. The late-Pleistocene regional hydrology of the present Great Lakes region is summarized next.

Prior to the Wisconsinan glaciation, the Great Lakes had already developed the modern discharge course to the Atlantic with one major difference- the present day Lake Huron did not drain southward into Lake Erie via the St. Claire River as it does today. Instead, waters drained into present day Georgian Bay and continued to flow into present day Lake Ontario, effectively excluding Paleo-Lake Erie (Farrand 1988). Paleo-Lake Erie flowed into Lake Ontario independently, much as it does today. Here, the inflow from the upper lake waters and those of Lake Erie assembled in Paleo-Lake Ontario before flowing eastward.

During the Wisconsinan, the vast majority of the Great Lakes catchment area was covered by the Laurentide ice-sheet. This ice sheet's margins were located in the southern Great Lakes basin and the ice was divided into a series of lobes that covered and carved the present day locations of the Great Lakes. The ice sheet extended sufficiently far south to empty its melt waters into the Mississippi system, which drains south to the Gulf of Mexico. It was not until the most recent (Wisconsinan) ice sheet retreat began that the present-day Great Lakes began to take shape (~14.5ka). Roughly 14ka, proglacial lakes Chicago and Maumee covered present day locations of eastern Lake Michigan and Lake Erie respectively. Both proglacial lakes were bounded by the southern extent of the Laurentide ice sheet and both lakes drained southward into the Mississippi system. A series of glacial retreats and advances occurred between 14ka and 13ka. By 13ka, the lake overlying present day Lake Erie drained westward between present day Lakes Huron and Michigan, discharging into Lake Chicago (located in the southern half of present day Lake Michigan). Lake Chicago drained south to the Gulf of Mexico.

A series of advances and retreats between 13ka and 11ka occurred; the history of these events is recorded by glacial moraines throughout the Great Lakes basin. By 11ka, the Laurentide ice sheet was removed from present-day locations of Lake Erie and Lake Ontario and the early forms of these two lakes had taken shape. However, the remaining three Great Lakes (Superior, Huron and Michigan) were an amalgamated body known as glacial Lake Algonquin, a proglacial lake. Glacial Lake Algonquin drained southward 11ka. By 9.5ka, the ice sheet had uncovered the majority of the areas covered by the present day Great Lakes. However, the ice sheet's retreat also opened a new outlet for glacial Lake Algonquin to directly discharge to the Atlantic. Two chain lake systems were established at this stage. One where Lake Erie feeds Lake Ontario before draining into the Atlantic. Another, where paleo-Lake Michigan (Lake Chippewa) and paleo-Lake Superior (Lake Minong) drained into paleo-Lake Huron (Lake Stanley) before discharging directly into the Atlantic along a channel north of present day Lake Ontario.

The Laurentide ice sheet continued its retreat between 9.5ka and ~5ka. Isostatic depression induced by the weight of the overlying ice sheet on the bedrock below depressed the land surface hundreds of metres below today's elevations in the present day northern extent of the Great Lakes basin. As isostatic rebound continued, the drainage along the northern corridor for the upper paleo-Great Lakes slowed, and eventually diverted to the pattern of present day by ~4ka (Farrand 1988). Even today, the northern portion of the Great Lakes basin continues to uplift a metre every 200 to 1000 years (greater rebound rate in the north basin).

The principle geologic role of the Pleistocene ice-sheets was the erosion of Earth's landscape. Erosion of millions of years of strata in the Great Lakes region has drastically diminished geologists' ability to speculate on the region's conditions for certain periods. The Pleistocene glaciations have provided a

benefit for today's geologists. Much of the Canadian landscape is made up of immensely old geologic strata that are now either exposed or covered by a relatively thin veneer of overburden.

The bedrock exposed by ice within the Great Lakes basin today varies over immense geologic time scales. The exposed rock also varies greatly amongst the three broad forms of bedrock: igneous, metamorphic, and sedimentary. Broadly, endogenous rocks of Precambrian age (550Ma to ~3.5Ba) underlie the northern ~25% of the Great Lakes basin, whereas younger Mesozoic-aged clastic and chemical sedimentary strata underlie the southern portion (Figure 1-7; 1-8).

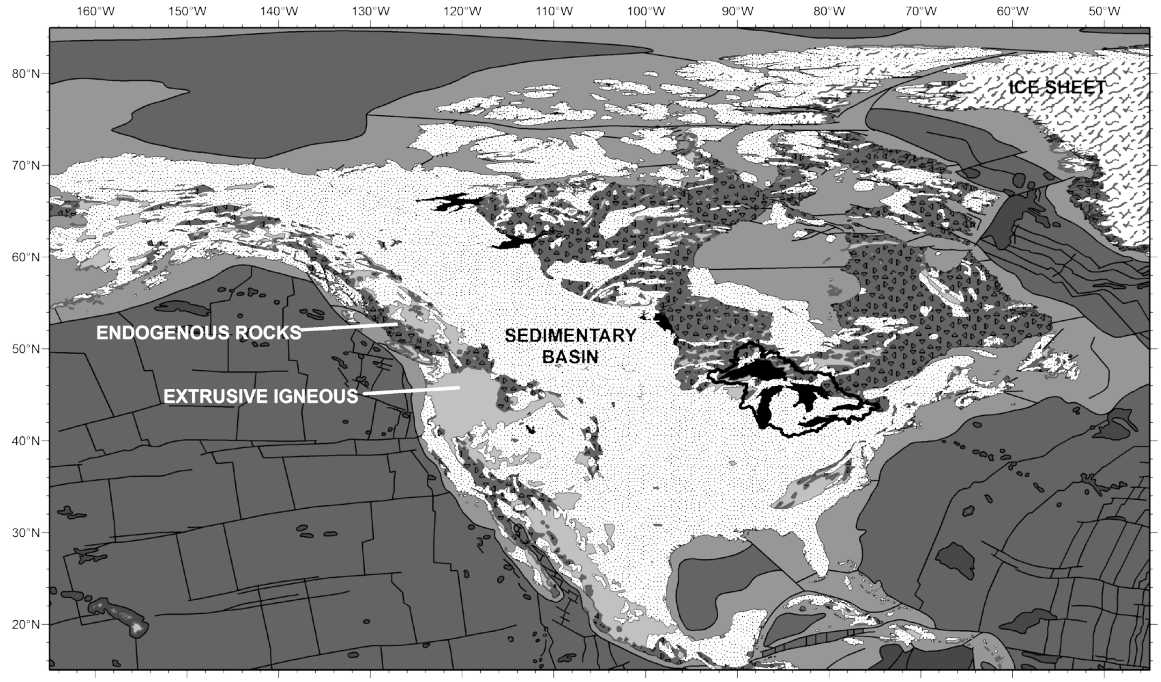

Figure 1-7. Broad geological features for the North American continent. Geographic dataset made available by OneGeology 2011. The Great Lakes basin is delineated with a thick black line. Sedimentary rocks are represented by a light stipple. Endogenous rocks are represented by dark grey with triangles (metamorphic, or crystalline igneous) or by light grey (extrusive).

Slightly more specifically, chemical-type sedimentary rocks make up the bedrock of much of the Great Lakes basin (brick pattern; Figure 1-8). The Michigan basin is perhaps the most recognized set of sedimentary rocks in the Great Lakes basin (Figure 1-8). These rocks are dolostones ($CaMgCO_3$), limestones ($CaCO_3$), or evaporite group minerals such as halite, sylvite, carnallite, and gypsum group (anhydrite, gypsum). The Devonian- and Silurian-aged evaporites are of particular interest as some are commercial grade despite being a considerable depth below the surface (>300m for some operating mine sites). Certain shales within the Michigan basin contain commercial hydrocarbon reservoirs.

Igneous and metamorphic rocks make up much of the basin north of the shorelines of the Great Lakes and almost the entire Lake Superior basin. In a very broad sense, the lithologies here are massive and foliated granites and granodiorites, syenites, quartzites, migmatitic gneisses and various mafic to

ultramafic lithologies (gabbros, diabase dykes, greenstones). The dominant igneous rock texture is phaneritic; however, some aphanitic volcanic deposits are present. Some of these lithologies contain concentrations of precious and base metals at extractable levels (Figure 1-9).

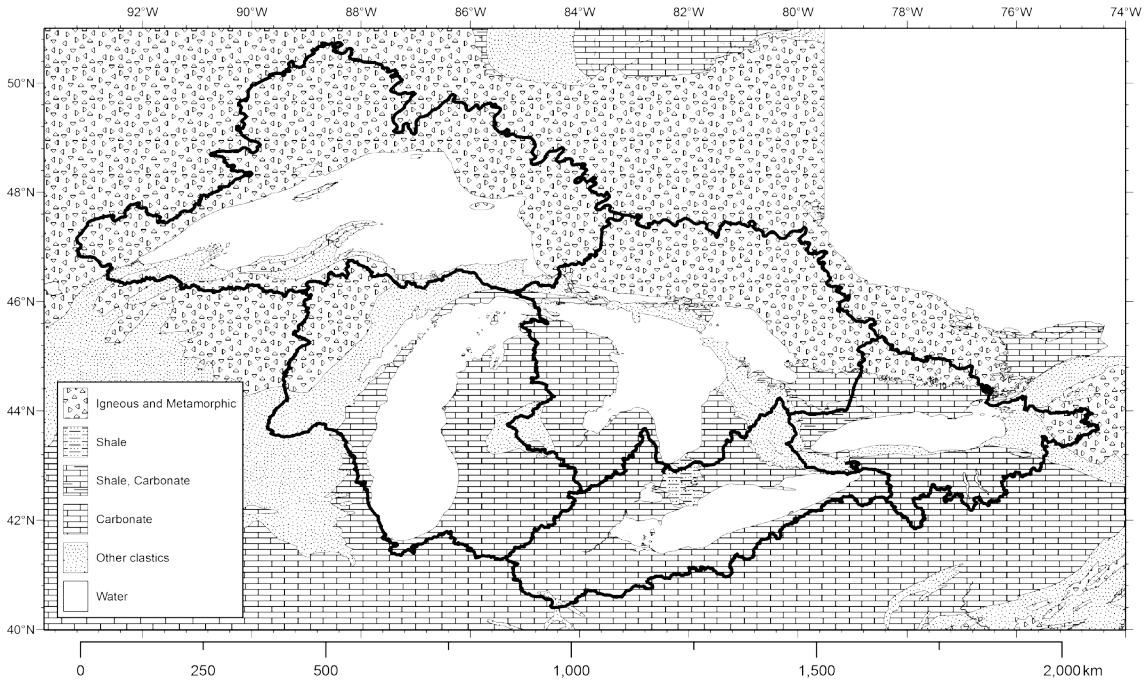

Figure 1-8. Bedrock geology of the Great Lakes basin. Chemical sedimentary rocks (carbonates: dolostone, limestone; lesser evaporites) are marked by a brick pattern. Crystalline gneiss and granites are represented by triangles. Clastic sedimentary rocks are represented by stipple and shales interbedded with carbonates are presented as a brick with additional dashes.

Over 75 mine sites are active within the basin, extracting resources ranging from base metals such as iron, zinc, nickel and copper, to precious metals such as gold, platinum and cobalt. One of the greatest mineral resources in Canada is located in Sudbury, Ontario. Here, an immense bolide (250 km^2) struck the Earth in the Proterozoic (aged 1.85±0.03Ba), excavating a massive pseudo-hemispherical crater (second largest known bolide impact in post-Archean; review by Grieve et al. 1991). The Sudbury bolide is similar in size to the Chicxulub asteroid (~170 km^2; Earth Impact Database 2011) that impacted the Earth at the present day northern coastline of the Yucatan Peninsula (now directly attributed to one of Earth's five mass extinction events that occurred at the Cretaceous-Paleogene boundary by a cohort of scientists: Schultz et al. 2010; although, a volcanogenic role of large igneous province eruptions ~65Ma - the Deccan basalts - is not extinguished by this work). The Sudbury impact could well have influenced Proterozoic single-celled life on Earth. Following impact, magmatic differentiation during a slow cooling process created a spectacular mineral resource concentrated in sublayers beneath the city of Sudbury, Ontario (Figure 1-9). Sudbury sublayers are mined today as a world class precious metal (gold, platinum) and base metal (nickel, copper) resource.

Other mineral resources in the Great Lakes region include iron ore deposits of the Lake Superior basin. These were, historically extracted in great quantities so the highest grade deposits were diminished

by the middle of the 1900s. Evaporite mineral (halite, gypsum group) extraction is ongoing in the southern portion of the Great Lakes basin in the Detroit-Windsor area midway between Lake Huron and Lake Erie (Figure 1-9). Immense shallow seas covered the present day southern Great Lakes basin during the Silurian-Devonian periods. In fact, the majority of interior North American continent was - at some point - covered by oceanic waters between the Ordovician and the Paleogene. Salt deposits found today in the southern Great Lakes basin could only have formed if these seas had desiccated in regions. At this time the Great Lakes were located in a much warmer "tropical" type climate. Under this paleo-climate the biogenic carbonate platforms that underlie much of southern Ontario and the north-eastern United States were formed. These geological features are consistent with a near-equatorial paleo-geographical setting for Laurentia (North American lithosphere; Scotese and McKerrow 1990).

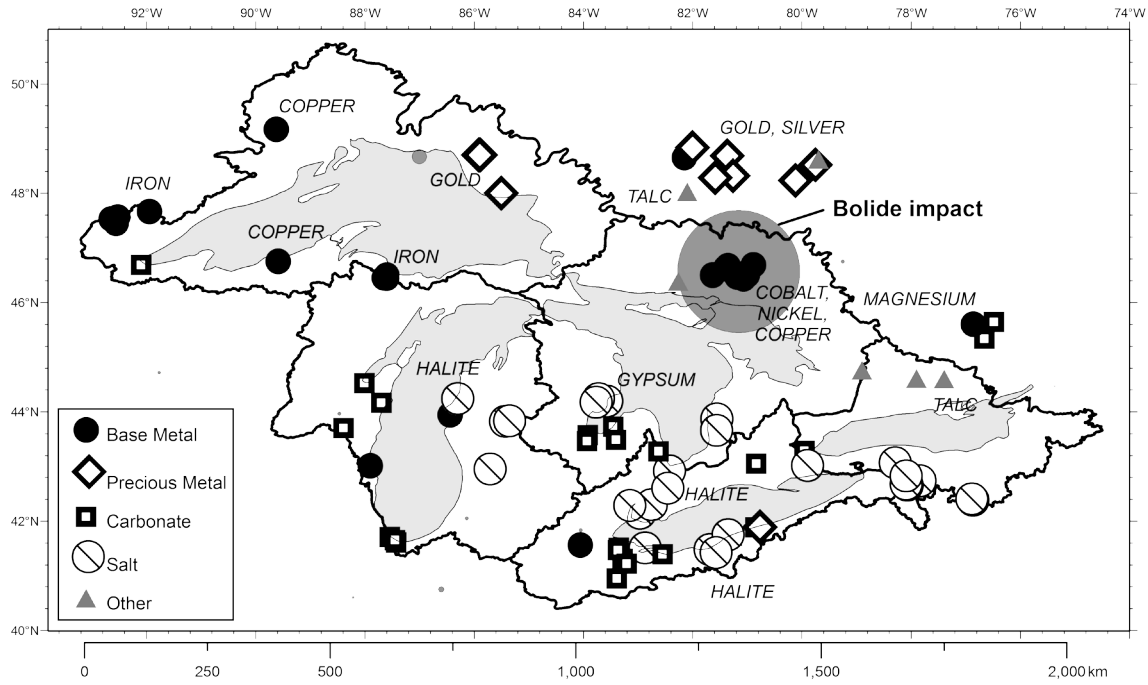

Figure 1-9. Mines in the Great Lakes basin and surrounding region (USGS 2011). Black circles identify sites extracting metals such as copper, magnesium, iron, nickel, zinc, and cobalt. White diamonds identify precious metal mines (gold, titanium). White squares identify mines extracting carbonates (lime, dolomite). Mines extracting salts are represented by white circles crosscut by a diagonal line (mostly halite extraction operations, some gypsum mines and one site extracting sylvite). Other mines - grey triangles - include extraction sites for bromine, talc, serpentinite and vermeculite. Meteorite impact crater sites are presented as dark grey circles. Circle size is proportional to estimates of the diameter of the asteroid (Earth Impact Database 2011). The Sudbury impact is the largest bolide impact shown (1.85±0.03Ga).

1.2.1.2 Human Geography and natural ecosystems of the Great Lakes

The Great Lakes basin is home to nine million Canadians and 24 million Americans. The population densities of Canada (3.4 persons/km^2) and the United States (32 persons/km^2) have comparably low

values compared to the European continent (~70 persons/km²). However, within the Great Lakes basin the population density approaches that of European nations (~40 persons/km²). The lower two Great Lakes - Erie and Ontario - are the most densely populated basins on average (greater than 150 persons/km²; Table 1–3 and Figure 1-10). The greatest population densities within the Great Lakes basin are along the southern Lake Michigan shores at the cities of Chicago and Milwaukee. Other densely populated areas include southern Ontario and central Michigan between Lakes Huron and Erie (Windsor, ON; Detroit, MI.) and along the north shore of Lake Ontario (Toronto, ON.; Figure 1-10).

Table 1–3. Population densities for 2010 within the Great Lakes basin (population density data from Center for International Earth Science Information Network 2005). Values presented are approximate.

Region/Country	Population density (person per km²)		
	Mean	1σ	Max
Superior	5	30	1010
Huron	25	90	2360
Michigan	70	70	10750
Erie	170	400	3860
Ontario	175	615	7540

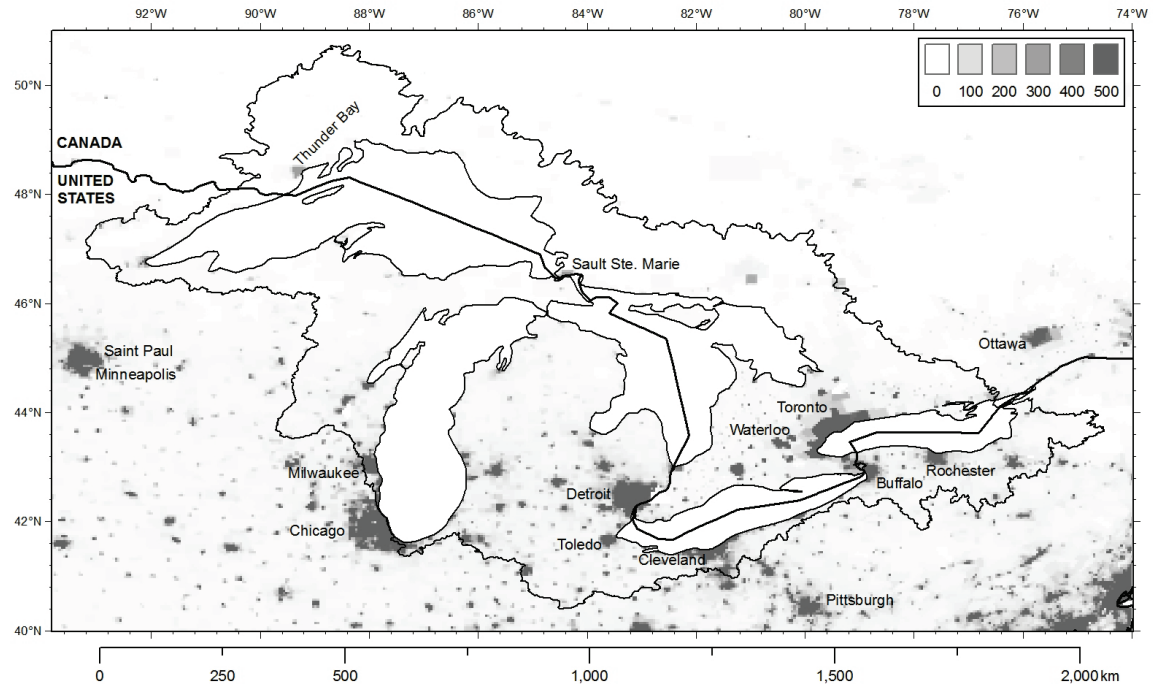

Figure 1-10. Population distribution in the Great Lakes basin, estimated for 2010. Units for population density are persons per square kilometre. Gridded data is from the Center for International Earth Science Information Network (2005). The lower lakes and southern lake Michigan are the most populated in the Great Lakes basin (outlined in black).

A significant portion of the Canadian (30%) and United States (10%) population lives within the Great Lakes basin (Environmental Protection Agency 2011). The success of the Canadian and United States economies is highly dependent on the Great Lakes region. These waterways provide a shipping corridor for roughly 200 million tonnes of raw and refined products such as limestone, sand, gravel, raw and refined ores, hydrocarbons, salt and agricultural products annually. The Great Lakes also support a lucrative recreational and commercial fishing industry for both the United States and Canada. Furthermore, the waters of the Great Lakes supply drinking water for shoreline cities; inland settlements commonly draw groundwater for municipal and agricultural use.

Natural ecosystems in the Great Lakes region fall broadly into one of two categories. In the northern (Canadian) Lake Superior drainage basin, land cover is part of the boreal forest ecozone. This region is characterized by poorly drained wetlands spotted with white spruce (*Picea glauca*), black spruce (*Picea mariana*) and tamarack (*Larix*). The majority of the southern Lake Superior basin and the vast majority of each of the southern Great Lake basins are categorized as a temperate broadleaf forest ecozone (Figure 1-11). Trees within this ecozone are generally dominated by deciduous species, especially in comparison to the boreal ecozone to the north (Figure 1-11). Agricultural land now makes up a large areal extent of today's Great Lakes basin. Figure 1-11 shows the natural ecozones; these may not exist today.

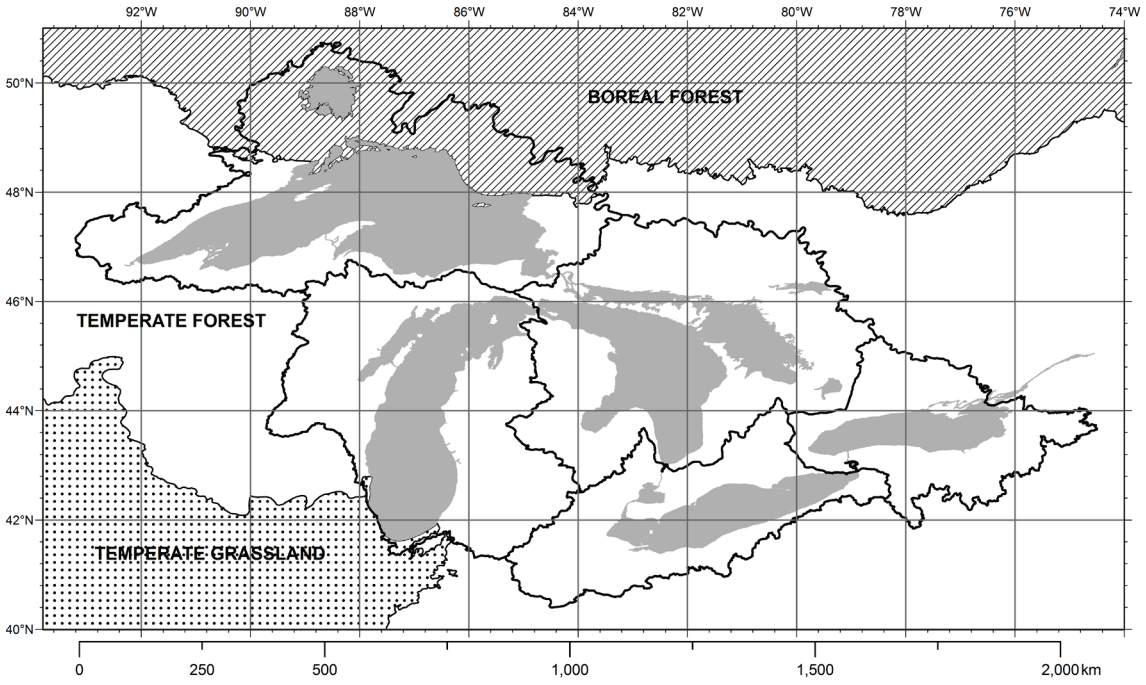

Figure 1-11. Broad ecoregions in the Great Lakes basin. Temperate broadleaf and mixed forests dominate the Great Lakes basin. Boreal forest is present throughout the northern portion of Lake Superior's catchment; the boreal ecozone does not make up a significant area for any of the remaining four Great Lakes. Temperate grasslands border the southwest of Lake Michigan's catchment, becoming the dominant ecozone in the north-eastern extent of the Mississippi drainage basin.

1.2.2 Hydrology

The transport and distribution of water in the Great Lakes basin is discussed in this section. The section is divided into four sections. First, a semi-quantitative overview of hydrologic reservoirs and transport modes in the Great Lakes basin is presented (section 1.3.2.1). Next, physical data pertinent to hydrology (1.3.2.2) such as reservoir volumes, topography/bathymetry and catchment areas is presented for each Great Lake and catchment and for general physical characteristics of the entire Great Lakes basin. Next, climate and limnology for the Great Lakes and region are discussed, highlighting spatial variability within the basin (1.3.2.3.). To conclude, quantitative estimates for the water balance of the lakes from existing studies are compiled and compared (section 1.4.2.3). Volumes are reported in km^3 and areas in km^2. Fluxes are reported in km^3/yr, distances are reported in km, depths and elevations are reported in metres or metres above sea level.

1.2.2.1 Hydrologic circulation in the Great Lakes

Two features of the Great Lakes water cycle are explored in this section. First, the input of water to the Great Lakes basin in the form of precipitation is discussed. Secondly, the processes and fluxes that operate on the waters as they advance toward the Gulf of St. Lawrence and the Atlantic Ocean are reviewed.

The majority of precipitation in the Great Lakes region is derived from four moisture sources: (1) the Arctic Ocean (2) the Gulf of Mexico, (3) the Pacific Ocean and (4) the Atlantic Ocean (Gat et al. 1994). Moisture input from the Arctic is expected to be less than that of the three other moisture sources. Waters evaporated from the Great Lakes themselves and recycled into precipitation in the Great Lakes basin contribute an estimated five to 16 percent (Gat et al. 1994) or nine to 21 percent of precipitation (Machavaram and Krishnamurthy 1995) for western Lake Michigan. These sources replenish the waters of the basin in the form of snow and rainfall. Precipitation in the basin is divided between over lake precipitation (direct precipitation) and precipitation falling on the surrounding over-land area within the catchment boundary (catchment precipitation). Direct precipitation is incorporated into the lakes either upon deposition (rain) or upon melting of seasonal ice on the lake surface. However, catchment precipitation is subject to several processes prior to entering a Great Lake.

Catchment precipitation falling on a vegetated land surface must first pass through the terrestrial biosphere prior to becoming surface water. Precipitation that passes through this layer is known as throughfall, whereas precipitation that is retained on the surface of plants and wholly returned to the atmosphere by evaporation is referred to as interception. An estimated 20 percent of incident precipitation is intercepted and returned to the atmosphere for a southern Great Lakes forest (Carlyle-Moses and Price 1999), although as mentioned earlier, the area of Great Lakes forests has been reduced for agriculture. Precipitation stored in a vegetative canopy becomes surface water either by falling to the ground before it can evaporate (throughfall) or by transferring through the interior of the plant to the forest floor (stemflow). A review of estimates of these fluxes relative to incident precipitation found stemflow to range from five to >10 percent and throughfall to range from 70 to 90 percent for a temperate forested catchment (Levia and Frost 2003).

Once a surface water reservoir has developed in a forested catchment, water may (1) evaporate or sublimate, (2) transpire, (3) runoff, or (4) infiltrate into the subsurface. Waters that evaporate recycle back into the atmosphere and are redeposited as precipitation at a location controlled by atmospheric advection, convection and climate. Vegetation uptakes water from the shallow subsurface and releases it to the atmosphere from stomata in an exchange process for atmospheric $CO_{2(g)}$ uptake for photosynthesis (at an averaged ratio of 1 mol of CO_2 acquired, to roughly 850 mol H_2O released to the atmosphere for the Great Lakes basin; Karim et al. 2008). Some surface waters are directly incorporated as runoff in channels such as rills, streams and rivers. These surface waters flow down gradient according to topography, eventually discharging into a Great Lake. During their transport, a portion of surface waters infiltrate pore spaces in the subsurface. These reservoirs may be either subsaturated (vadose - near ground surface) or saturated (phreatic - below vadose zone) with respect to a fluid. Migration of subsurface waters is controlled by advection, dispersion, and chemical reactions. Subsurface waters may recharge underlying aquifers or enter streams by interflow (vadose zone) or discharge at seeps (phreatic zone). These fluxes are summarized schematically in Figure 1-12.

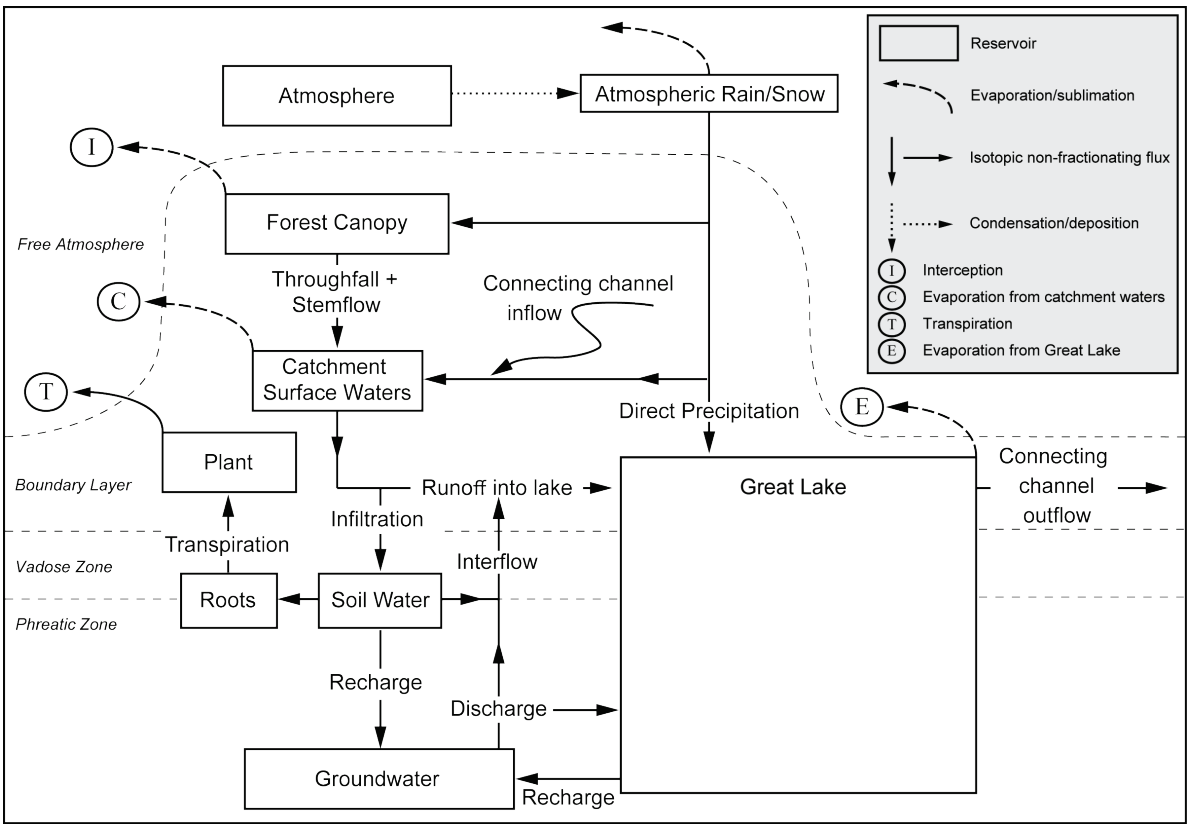

Figure 1-12. Qualitative schematic of major natural hydrologic fluxes for a Great Lake basin; general structure based upon figures in Gat and Airey (2006).

In summary, the two major intra-basin supplies of water to a Great Lake are inflows into the lake as runoff and direct over lake precipitation. To provide a comprehensive examination of the water balance to a Great Lake, the interaction of the Great Lakes with regional aquifers must be discussed.

The Great Lakes region has three types of general bedrock aquifers controlled by geology: (1) Precambrian igneous rocks, (2) permeable carbonates and sandstones, and (3) impermeable rocks dominated by shales. Quaternary overburden aquifers also host groundwaters in the basin. The Superior, western Michigan, and northern Huron and Ontario drainage basins contain Archean to Proterozoic aged granite and gneiss (Figure 1-8), which act as a moderate to poor aquifer (Grannemann et al. 2000). The remaining aquifers in the Great Lakes basin are Phanerozoic-aged sedimentary deposits. Carbonate aquifers are present on the western shores of Lake Michigan and the northern and eastern peripheries of Lake Huron. The basins of Lakes Ontario and Erie are dominated by carbonate based aquifers often mixed with clastic fragments. Low permeability shales and carbonate-shale combinations are present in some areas in the Lake Erie and Ontario catchments.

With respect to the water budget of the Great Lakes, direct groundwater-lake interaction has been neglected in most hydrologic water balance studies for the Great Lakes. Grannemann and Weaver (1998) reviewed estimated direct groundwater discharge rates to the Great Lakes from a suite of prior studies. Estimates of the groundwater discharge into Lake Michigan, which is expected to have the greatest groundwater discharge rate of all Great Lakes, is only 2.4 km^3 per year (Grannemann et al. 2000). If the highest estimated value for groundwater discharge to the each of the Great Lakes listed in Neff et al. (2004) is used - 3.1, 5.8, 1.4 and 1.1 cubic kilometres for Lakes Superior, Michigan-Huron, Erie and Ontario, respectively - groundwater discharge is less than 10 percent of over lake precipitation for all lakes (9.4 7.4, 7.2, and 6.5 percent for Lakes Superior, Michigan-Huron, Erie and Ontario). As this value is considerably less than the range of uncertainties for runoff, precipitation, and evaporation (10% to 45%; Neff et al. 2004), natural groundwater input is disregarded in hydrologic balance analyses for the Great Lakes. However, groundwater withdrawals for human and industrial purposes add an additional indirect input of groundwater to the Great Lakes as return flow. An estimated 2.1 km^3 of water per year is withdrawn from the entire Great Lakes basin (Solley et al. 1998). Roughly 95 percent of this extracted water is returned to streams which enter the Great Lakes, while the remaining 5 percent is consumed by evaporation and enters the atmospheric reservoir (Grannemann et al. 2000). Even with this anthropogenic groundwater modification, the flux of groundwater to the Great Lakes is small compared to estimates for runoff, direct precipitation, and connecting channel inflows.

1.2.2.2 The Great Lakes reservoir: Physical hydrologic data

This section is divided into three categories describing the Great Lakes system in the context of world water. Lake volumes (1.3.2.2.1), lake and catchment areas (1.3.2.2.2) and topography and bathymetry (1.3.2.2.3) are reviewed for the Great Lakes catchment.

1.2.2.2.1 Lake volumes

Globally, the amount of water contained in the Great Lakes represents 0.0015 percent of all water contained within Earth's outermost layers. Over 94 percent of the 1.4 billion cubic kilometres of water on Earth is held by the Pacific, Atlantic, Indian and Southern Oceans combined. Three percent is contained

within the remaining saline water bodies including the Arctic Ocean (1.2%) and inland or partially enclosed saline water bodies (1.8%) including (in decreasing volume) the Caribbean Sea (0.54%), Mediterranean Sea (0.32%), South China Sea (0.29%), Bering Sea (0.27%), Gulf of Mexico (0.18%), Japan Sea (0.10%), Okhotsk Sea (0.10%), Andaman Sea (0.05%), East China Sea (0.02%), Red Sea (0.02%), Hudson Bay (0.01%) and the world's largest inland water body, the Caspian Sea (0.01%). Therefore, less than three percent of water on earth is freshwater, classified as containing less than one-thousand mg L^{-1} total dissolved solids. Of this remaining freshwater, over two-thirds is perennially frozen in glaciers and ice caps, permafrost or multi-year snow and ice. Another 30 percent is contained within the pore spaces of soils and rocks (vadose and phreatic zones) as soil moisture and groundwater or is chemically bound to hydrated minerals. A relatively small amount of water is in circulation in the atmosphere. Of all freshwater on Earth, only 0.3 percent is liquid and exposed on Earth's surface (Figure 1-13).

Of the world's fresh surface water, 20.6 percent is contained within the five North American Laurentian Great Lakes reservoir, amounting to roughly 22,700 cubic kilometres of water. When combined, the Great Lakes rank as a world class fresh surface water resource, second only to Lake Baikal (21.5%) and narrowly exceeding Lake Tanganyika containing 17.2% of the planet's surface fresh water. These three lake systems represent over half (59%) of the unfrozen fresh water on Earth's surface (Figure 1-13).

Water in the five Great Lakes is unevenly distributed. Lake Superior contains more than all the other four Great Lakes combined (~53% of total Great Lakes waters). It is ranked as the third largest freshwater lake by volume, following lakes Baikal (23,000 km^3) and Tanganyika (17,800 km^3; Herdendorf 1982). Lakes Michigan and Huron contain 21.7 and 15.6 percent of the water in the Great Lakes, respectively. Lake Erie is the shallowest of all the Great Lakes and contains only 2.1 percent of the water in the Great Lakes system. Despite covering an area smaller than that of Lake Erie, Lake Ontario contains 7.2 percent of the water in the Great Lakes system because its mean depth (86.5m) is four times greater than that of Lake Erie (18.8m).

It should be noted that water contained within Earth's deep interior below the crust has been exempted from the preceding discussion of Earth's hydrologic reservoirs. Estimates of water contained within the lower mantle range from 50 percent (Bolfan-Casanova et al. 2002) up to 500 percent (Murakami et al. 2002) of the oceanic H_2O reservoir, a discrepancy controlled by the large range in estimates for the solubility of water in the lower mantle (reviewed by Hirschmann 2006). Seismic data suggest that the distribution of this water is heterogeneous, concentrated along active margins associated with Earth's major tectonic plates such as eastern Asia and western North America where the Pacific plate subducts (Lawrence and Wysession 2005). Earth's deep water cycle and reservoir is not well understood and possible transport pathways such as subducting oceanic slabs into lower mantle (Lawrence and Wyession 2005) are disputed (Green II et al. 2010). Current estimates suggest that the volume of water in Earth's deep interior reservoirs is comparable in volume to the total water in the uppermost crust and troposphere.

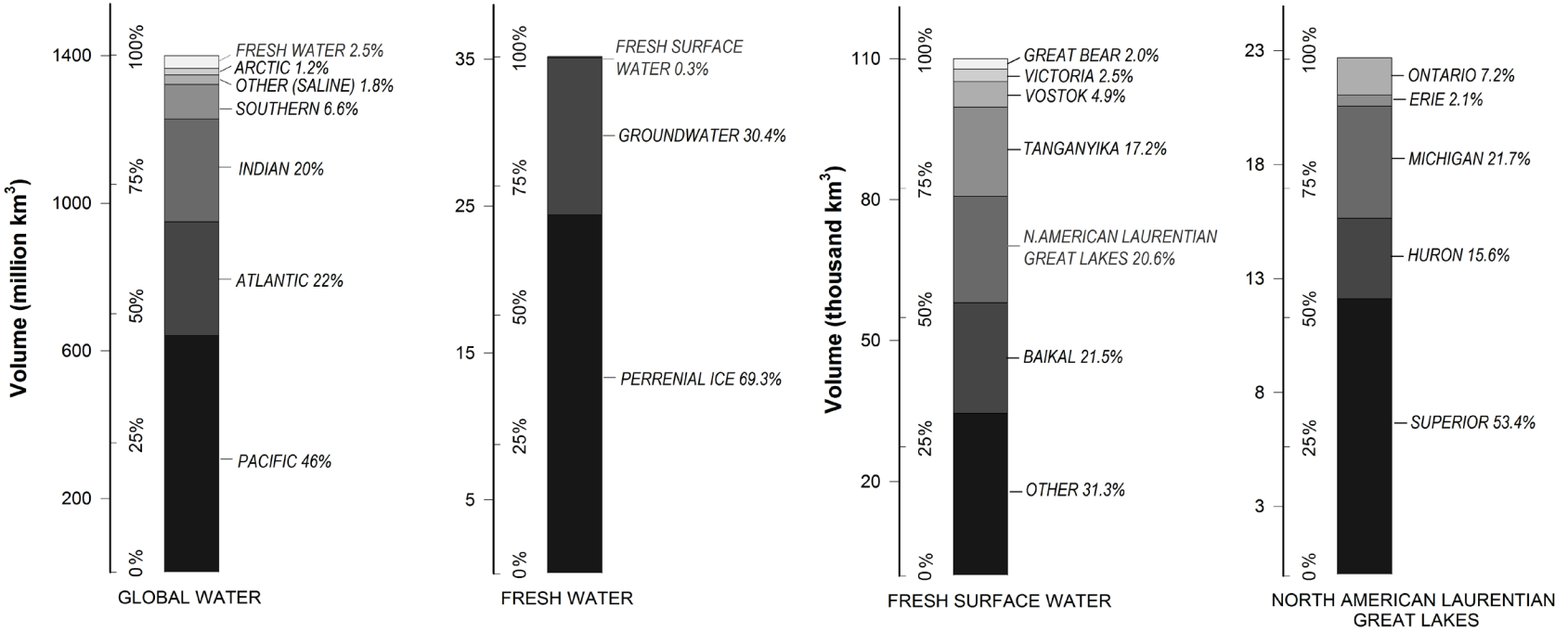

Figure 1-13. The distribution of water along the lithosphere-atmosphere boundary divided by volume and related to the North American Laurentian Great Lakes.

1.2.2.2.2 Lake and catchment area

The five Great Lakes and their surrounding drainage basins cover an area of 768 thousand square kilometres. When combined with the St. Lawrence drainage basin to the east, the system covers an area over one million square kilometres. The five lakes themselves cover an area of 245 thousand square kilometres, together forming the largest surface area of connected fresh water lakes on Earth.

Lake Superior is the largest lake in the world by area at 82 thousand square kilometres. The lake is bounded by latitudes 46.4ºN to 49.1ºN; however, the catchment basin extends as far north as 50.7ºN. Lake Superior is the most northerly and farthest inland from the Atlantic Ocean of the lakes. The lake surface represents 39 percent of the total catchment area with a drainage basin to lake ratio of 1.5. Lake Superior's area makes up the largest percent of its own catchment of all of the lakes. The area draining into Lake Superior is covered by a large amount of lake area. Excluding the five Great Lakes, Lake Nipigon is the largest lake in the Great Lakes-St. Lawrence catchment, covering over 4,800 km^{2}s, a quarter of the area of Lake Ontario. The Superior catchment is enlarged by two artificial divergences (Figure 1-14). Water that would otherwise flow into Hudson Bay from the headwaters of the Ogoki River is diverted into Lake Nipigon and the Great Lakes catchment. The Ogoki diversion dam was completed in the early 1940s and adds 14 thousand square kilometres of area to the Lake Superior catchment basin (Neff and Nicholas 2004). The Long Lac divergence is located north of Lake Superior and diverts an additional 4300 km^2 into the basin. The two divergences combined represent an added area of 14 percent of the natural Lake Superior on-land catchment. The added area is estimated to divert five cubic kilometres of water into the Lake Superior basin each year (Neff and Nicholas 2004), water that would otherwise enter the Hudson Bay catchment.

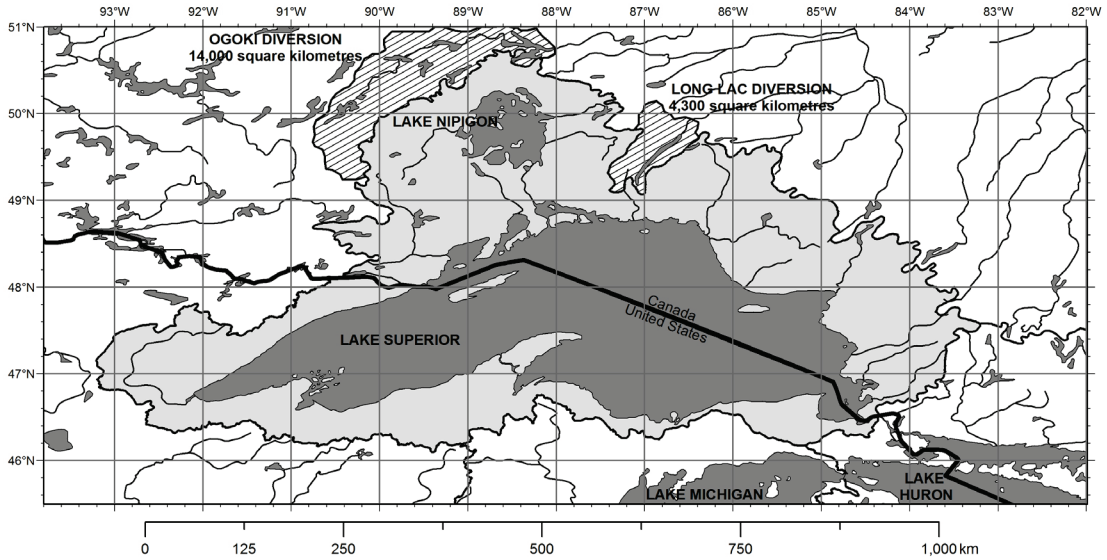

Figure 1-14. Artificially diverted drainage area into the Lake Superior basin in the 1940s. The Ogoki (northeast) and Long Lac (north) divergences combined cover over 18,000 km^{2}equal to 14% of the natural on-land Lake Superior catchment (light grey).

The Hudson Bay drainage basin collects water north of Lake Superior and drains it to the north. A major river system - the Nelson - borders the north-western Lake Superior catchment. At the western extent of Lake Superior, a triple point occurs where the Atlantic (Great Lakes - St. Lawrence system; drains eastward), Hudson Bay (Nelson River; drains northward) and Gulf of Mexico (Mississippi; drains southward to the Gulf of Mexico) catchments meet. Figure 1-11 presents the major drainage patterns in the Great Lakes region. All drainage north of Lake Huron enters the Hudson Bay system whereas precipitation falling south of the Lake Michigan catchment enters the Mississippi river system flowing to the south.

Great Lakes Michigan and Huron are considered in some hydrologic studies as a single lake (Lake Michigan-Huron; Neff and Nicholas 2005) as the two lakes share a common water level. This is reasonable for studies on the water levels of Lakes Michigan and Huron (Hanrahan et al. 2009; Hanrahan et al. 2010). Lakes Michigan and Huron are - if treated as a single lake - the largest in the world by area. The two lakes cover a combined area of 117 thousand square kilometres with a catchment area representing half the Great Lakes basin. In this study, the two lakes are distinguished geographically and isotopically.

Lake Michigan is slightly smaller than Huron with an open water area of 57,800 km^2. The lake area constitutes 32 percent of Lake Michigan's total catchment area corresponding to a land-to-lake catchment ratio of 2.0. Lakes Superior and Michigan - both headwater lakes as neither has a major connecting channel inflow - comprise the largest percentage of their own catchments. The downstream Great Lakes become progressively smaller relative to their catchment areas (increasing catchment ratios progressing downstream). Lake Winnebago – a large lake (~500 km^2) in the western portion of the catchment – drains into a partially enclosed bay (Green Bay) on Lake Michigan's western shores. Lake Michigan has a net outward flow (roughly 36 km^3/yr; Chapra et al. 2009) into Lake Huron through the Straits of Mackinac at the north end of the lake.

Lake Huron is the second largest by area of the five lakes both in terms of lake area and catchment area. The lake covers 59,600 km^2 and the catchment is 192,900 km^2. Thirty-one percent of the catchment is covered by Lake Huron corresponding to a catchment ratio of 2.2. Georgian Bay - a large semi-enclosed portion of Lake Huron (Figure 1-15) - represents roughly 15,000 km^2 of the lake. Lake Huron drains into Lake St. Clair along the St. Clair River at the southernmost extent of Lake Huron. Lake Huron receives water from Lake Superior and its outflow - the St. Mary's River - at its north end. Lake Huron also receives water inputs from exchange with Lake Michigan to the east. Lake Huron's outlet is located at the southern end of the lake and flows southward into Lake St. Clair by the St. Clair River. Lake St. Clair empties quickly (residence time of roughly two weeks; Quinn 1992) before flowing into Lake Erie via the Detroit River.

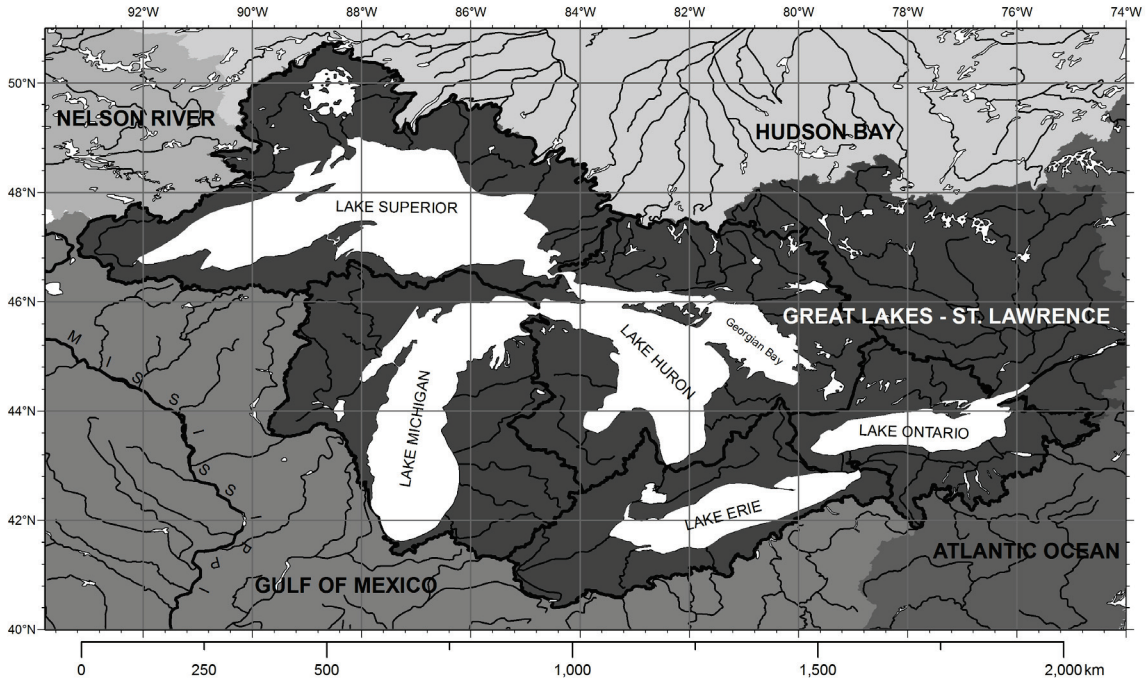

Figure 1-15. Major drainage basins of the North American Laurentian Great Lakes and surrounding region. The Nelson River drains to Hudson Bay; the Great Lakes - St. Lawrence basin drains to the Atlantic Ocean. Catchment areas for each Great Lake are delineated with a thick black line. Catchments for the Nelson, Hudson Bay, Gulf of Mexico, and Atlantic Ocean drainage are represented in greyscale. White areas delineate the Great Lakes shoreline and major lakes in the region. Thin black lines delineate rivers within each of the major catchments.

Lake Erie covers 25,700 km ^{2} and drains a total of 84,500 square kilometres. Its catchment extends the farthest south of all five lakes to a latitude of 40.4ºN. Lake Erie, although the smallest of the Great Lakes by volume, is larger than Lake Ontario by area. Its catchment is bounded to the north by the catchments of Lake Michigan, Huron and Ontario. South of the Lake Erie basin, water enters the Ohio River basin (a major tributary of the Mississippi River system) and drains south toward the Gulf of Mexico. Lake Erie drains north into Lake Ontario through two outlets at the east end of the lake: the Niagara River and the artificial ship canal called the Welland Canal.

The last of the five Great Lakes - Lake Ontario - covers 18,960 km^2 and is the smallest of the Laurentian Great Lakes by area. Lake Ontario's catchment covers 79,560 km^2, leading to a calculated land:lake drainage basin ratio of 3.2, the largest of the five lakes. Water enters the lake from the Niagara River to the south-west and drains into the St. Lawrence River in the east. Water from the St. Lawrence flows east - exiting the Great Lakes basin - and is joined by the Ottawa River before flowing into the Gulf of St. Lawrence and entering the Atlantic Ocean. Table 1–4 summarizes the physiographic data for each of the Great Lakes.

Table 1–4. Physiographic data for the Great Lakes

Lake	Mean elevation (m.a.s.l.)	Lake volume (km^3)	Lake area (km^2)	Total catchment area (km^2)	Catchment ratio (land/lake)	Shoreline length (km)	Depth: average, (maximum) (m)	Maximum length, (maximum width) (km)
Superior	183	12,100	82,100	209,800	1.6	2,780*	147 (405)	563 (257)
Huron	176	3,540	59,600	192,900	2.2	2,970*	59.4 (281)	332 (295)
Michigan	176	4,920	57,800	175,800	2.0	2,250*	85.1 (229)	494 (190)
Erie	173	484	25,700	84,500	2.3	1,290*	18.8 (64)	388 (92)
Ontario	86	1,640	18,960	79,560	3.2	1,020*	86.5 (244)	311 (85)
Lake St. Clair	174	4.2	1,114	13,544	11.2	210*	3.6 (6)	42 (24)
Connecting channels	-	-	446	11,934	25.8	450*	-	-
Totals (only Great Lakes)	-	22,700	244,160	742,560	2.0	10,310*	92.9	-
Totals (with Lake St. Clair and connecting channels)	-	22,700	245,720	768,040	2.1	10,970*	92.3	-

Values reported and calculated from data available in Coordinating Committee on Great Lakes Basin Hydraulic and Hydrologic Data (1977)

* Shoreline length value is scale dependent

1.2.2.2.3 Topography and bathymetry

The Great Lakes basin is a chain lake system and transport of surface water is governed by topography. This section will discuss topography and bathymetry for each of the five Great Lake basins, highlighting similarities and differences within the Great Lakes catchment. Elevation and bathymetric figures are drawn from a geographical information systems analysis of the Great Lakes and catchment. Dataset used includes a 30 arc-second (approximately 1km² grid) digital elevation model: GTOPO30 (Gesch et al. 1999). Bathymetry for the Great Lakes is compiled from a dataset made available by the Great Lakes Information Network (GLIN 2010).

Lake Superior has the highest elevation of the Great Lakes. The long-term lake level is 183 metres above sea level. The catchment elevation is an average of 378 m above sea level (Figure 1-17), reaching its most elevated areas - greater than 550m above sea level - in the western portion of the basin (Vermillion Range). Lake Superior is the deepest of the Great Lakes. Its maximum depth - 406m - occurs in the eastern portion of the lake and is over 200m below sea level. The lake has an average depth of 147m. The lake level drops from 183m to 176m above sea level along the St. Mary's River outflow into Lake Huron.

Lake Huron's catchment has a median value of 300m above sea level, over 100m lower than Lake Superior's median value. The most elevated areas are greater than 500m above sea level and are present in the northern and eastern extents of the catchment (Algoma Highlands and Algonquin Highlands) and south of Georgian Bay. The eastern Lake Huron catchment seldom exceeds 400m above sea level, only doing so in small areas of the Lower Michigan peninsula. The lake has a mean depth of 59.4m and reaches its deepest point (281m below lake level) in the central part of the lake. Georgian Bay reaches depths exceeding 100m between the south-eastern extent of Manitoulin Island - the world's largest island in a freshwater body - and Bruce Peninsula. Saginaw Bay is located in Lake Huron's south-western limits. Depths here rarely exceed 20m. Lake Huron shallows to the south approaching the St. Clair River outlet and to the northwest near its boundary with Lake Michigan at the Straits of Mackinac.

The Lake Michigan catchment is at a lower average altitude than Lake Huron's. The average elevation within the catchment is 284m above sea level. The most elevated areas are in the north-western portion of the catchment (Menominee Range) at the drainage boundaries with Lake Superior and the Mississippi system. The eastern portion of the catchment is generally less elevated. Only small areas in the central and northern lower Michigan Peninsula rise above 400m.a.s.l.. The bathymetry of the lake extends from the lake level at 176m above sea level to a maximum depth of 229m below the lake surface in the north-central region of the lake. From here, the lake bathymetry gradually rises to shallower depths along a southerly transect before dropping off to depths greater than 100m at the lake's southern end in a second deep basin. Green Bay - a partially enclosed embayment on the western flank of the lake - is less than 50m deep and shallows approaching the south-western end. Green Bay is shallow relative to Lake Michigan's main body, but is comparable to Lake St. Clair and western Lake Erie.

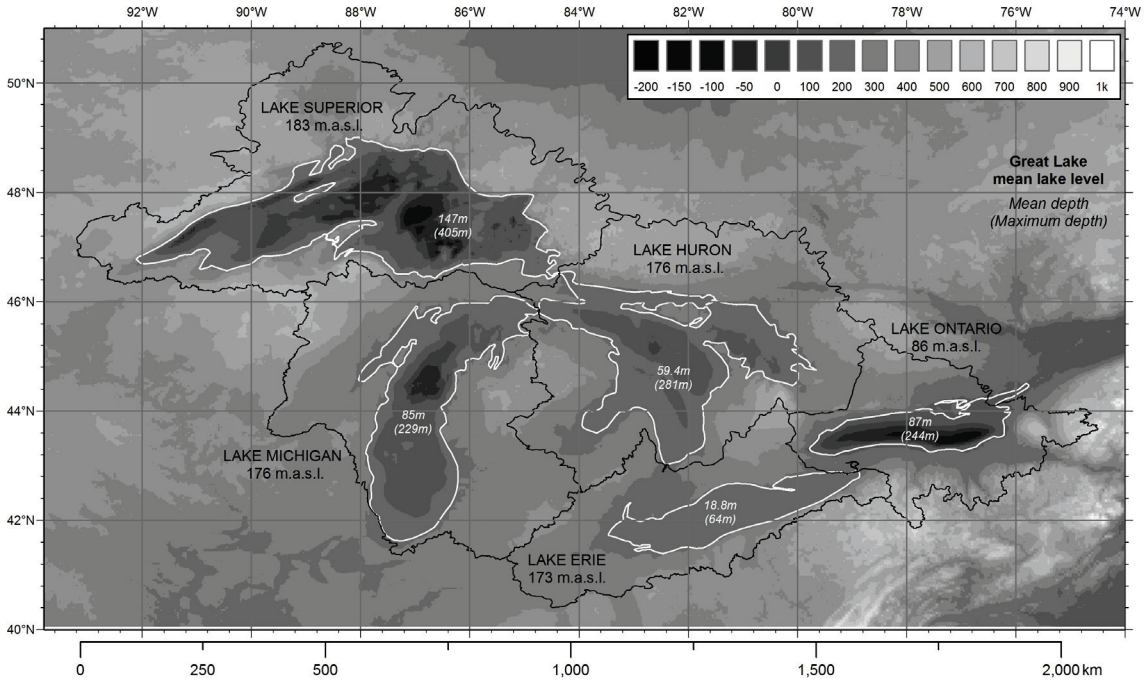

Figure 1-16. Elevation and bathymetry in metres for the Laurentian Great Lakes catchment and surroundings, referenced to sea level (m.a.s.l.). The long-term lake level for each Great Lake is displayed beneath the lake label. Mean (and maximum) depths are displayed within each lake's catchment.

The St. Clair River exits Lake Huron at its southern end at an elevation of 176m above sea level and flows south from Lake Huron. The river travels over 100km before entering Lake Erie's north-western shores. It enters a shallow lake known as Lake St. Clair between Huron and Erie. Lake St. Clair contains 4 cubic kilometres of water; however, this water is spread out over 1,100 km^2, leaving the lake with a mean depth of only 3.6m. Water residence times for Lake St. Clair vary from nine days to a month depending on wind direction (Schwab et al. 1989). Water exits Lake St. Clair and joins the Detroit River which flows south and enters Lake Erie. From the outlet of Lake Huron to the Detroit River's inflow into Lake Erie - known as the Huron-Erie corridor - elevation drops only three metres, 0.9m of which occurs from Lake St. Clair to Lake Erie (Derecki 1984). The gradient along this corridor is so shallow that flow along the river has been documented to reverse when influenced by ice jams in the lower reaches of the river or by seiches produced by strong easterlies blowing across Lake Erie. Twelve reversals were identified prior to 1950 on the Detroit River; one flow reversal occurred in 1986 (April 22; Quinn 1988). Overall, 168km^3 of water enters Lake Erie via the Detroit River each year.

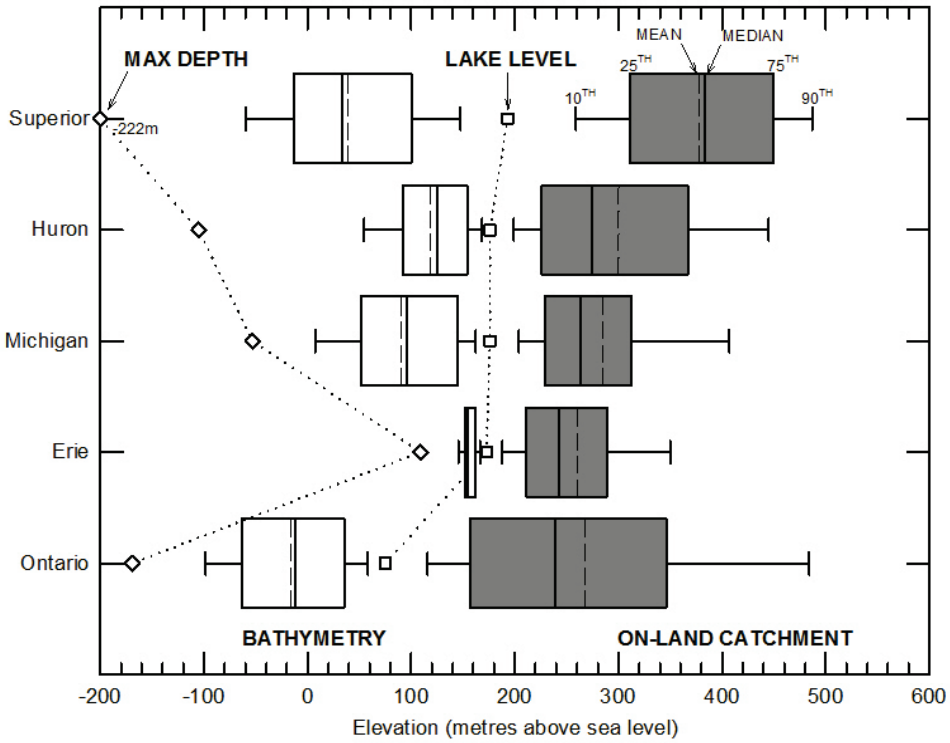

Figure 1-17. Box and whisker plot of elevation in the catchment of the Great Lakes (grey), and bathymetry (white). White squares represent long-term mean lake levels, and white diamonds mark each lake's maximum depth. Box corners indicate the 25th and 75th percentiles; whisker caps mark the 10th and 90th percentiles. The dashed line with each box is the mean elevation; the solid black line is the median value. Data is derived from zonal statistics of a digital elevation model (Gesch et al. 1999).

Lake Erie is the shallowest of all the Great Lakes with a mean depth of only 18.8m. The eastern portion of the lake contains the deepest part, extending to a depth of 64m below surface. Lake Erie's catchment is the least elevated of all the Great Lakes. The average on-land elevation within the basin is 260m. A gridded digital elevation model for the basin demonstrates that 95 percent of the catchment lies below 400m above sea level. The 95th percentile of Erie's on land catchment elevation is over 150m lower than that of Lake Ontario's despite the fact that Lake Erie's catchment resides almost 100m above the surface of Lake Ontario downstream. The most elevated areas are located in the north-eastern and eastern extents of the Lake Erie basin. Similar to the catchment's elevation, the bathymetry of Lake Erie has very little relief relative to the other four Great Lakes. The lake empties at its easternmost extent, flowing northward along the Niagara River and the Welland Canal navigation channel into Lake Ontario's western basin. The Welland Canal flow rate is roughly 6.3 cubic kilometres per year (3.4% of Niagara River discharge).

Lake Ontario is a high-relief lake and catchment basin relative to Great Lakes Erie, Huron and Michigan (Table 1–5). The lake's greatest depth extends 170m below sea level; only Lake Superior extends to greater depths (222m below sea level). Lake Ontario's catchment also has steep relief (Figure

1-17). The on-land catchment extends to elevations greater than 550m above sea level in the southern- and eastern-most areas of the catchment (Allegheny Highlands and Adirondack Mountains). The lake surface is the lowermost in the Laurentian Great Lakes chain, yet the highest regions in its catchment are the highest of any of the Great Lakes (Table 1–5). The most elevated 5% of Lake Ontario's catchment is the highest of all the Great Lake catchments. The mean on-land catchment elevation is 268m above sea level.

Table 1–5. On-land elevation within the Great Lakes basin

Lake	Mean on-land catchment elevation (m.a.s.l.)	95th percentile: on-land catchment elevation (m.a.s.l.)
Superior	384	508
Huron	300	470
Michigan	284	471
Erie	260	402
Ontario	268	566
Great Lakes basin	308	483

1.2.2.3 Climate and limnology

This section discusses climate over the Great Lakes and surrounding areas. Seasonality within the basin is discussed and is linked to the physical limnology of the Great Lakes. Long-term global gridded climate data (New et al. 2002) are presented to describe spatial and intra-annual variability in the basin. A different set of climate gridded datasets developed for the North American continent are used for model inputs in this study.

The Great Lakes basin experiences an array of climates owing to the large area occupied by the drainage basin. Mean annual temperatures for the basin increase in a southerly fashion throughout the basin as a product of latitudinal increases in solar radiation (Figure 1-18). Mean annual temperature ranges from near-zero in the northern extent of Lake Superior's drainage basin to values approaching ten degrees in the southern Lake Michigan and Lake Erie catchments. Seasonality in air temperatures are greatest in the northern portion of the Lake Superior catchment where mean temperatures for July and January are offset by nearly 40 degrees (Figure 1-19). The seasonality in temperatures decreases to the southeast, reaching a minimum of 26 degrees on the south-eastern banks of Lakes Huron and Erie reflecting the moderating role of the lakes in regional climate (Figure 1-19). The heat capacity of the Great Lakes reduces the temperature range of lakeshore climates, increasing the mean minimum temperature during all seasons and decreasing the mean maximum temperature for spring and summer seasons (Scott and Huff 1996). No permafrost exists within the Great Lakes basin despite sub-zero mean annual air temperatures in the northern Lake Superior catchment. The southern extent of isolated permafrost is to the north of the basin near James and Hudson Bay (Figure 1-18).

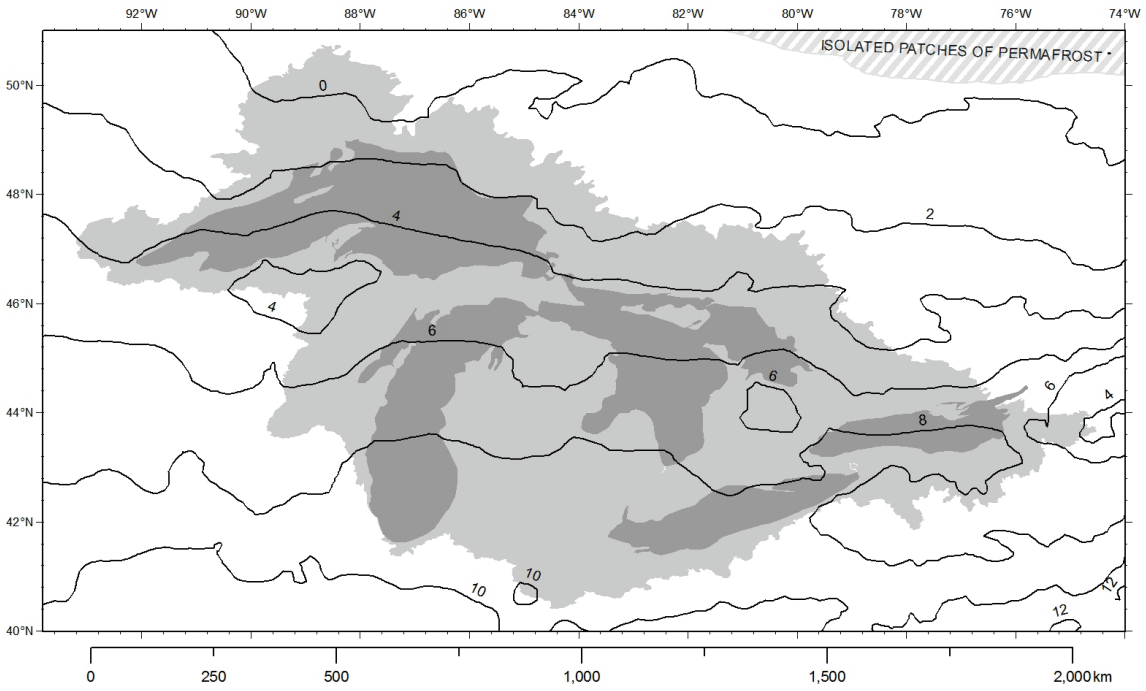

1-18. Mean annual temperature within the Great Lakes basin from New et al. (2002) climate grids. Despite hosting the zero degree isotherm in the northern Lake Superior catchment, no permafrost exists within the Great Lakes basin. Isolated patches of permafrost occur outside of the Great Lakes basin to the north (close to the -1 degree mean annual isotherm).

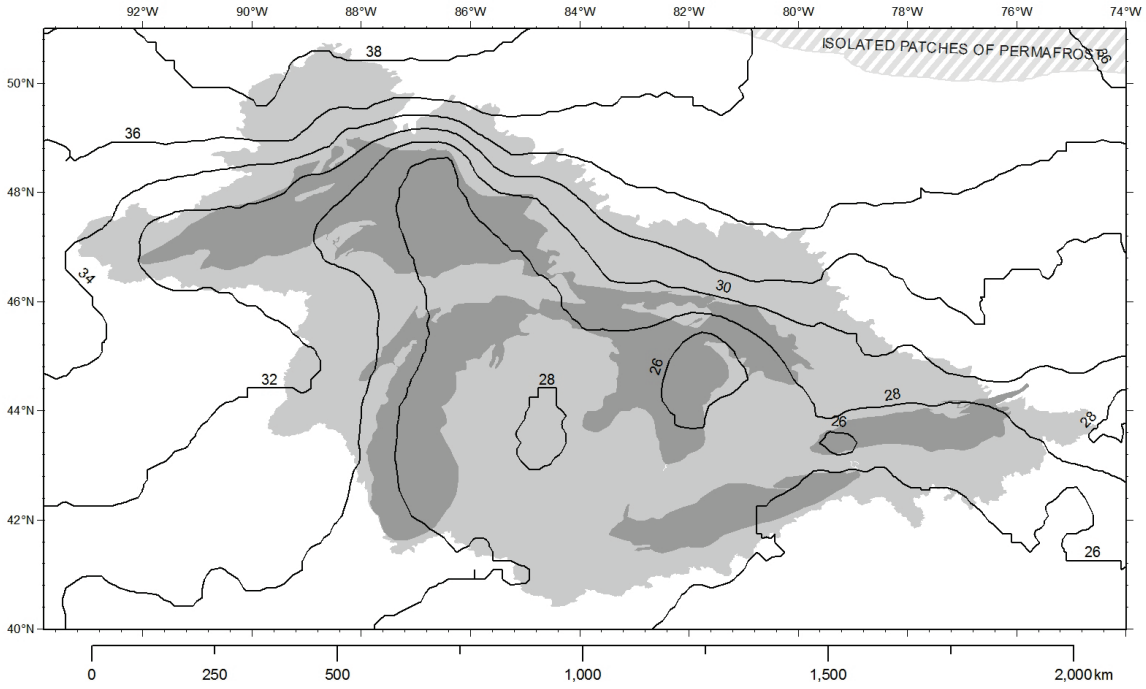

1-19. Difference between mean temperatures for the months of July to January (New et al. 2002). Seasonality in temperatures is greatest in the north (38 degrees), and reaches a minimum on the south-eastern shores of Lakes Huron and Erie.

The dominant winds in the Great Lakes region prevail from the west. The polar jet stream establishes in the southern part of the basin during winter months, allowing cold and dry air masses from the Arctic (cP; continental polar) to penetrate into the Great Lakes basin. The jet stream shifts to the northern portion of the Great Lakes basin in summertime, influencing the entrance of moist and warm air masses from the Gulf of Mexico (mT; maritime tropic) into the Great Lakes catchment from the south (Rasmusen 1968; Magnuson et al. 1997). These air mass trajectories play an important role upon the source of moisture in the Great Lakes basin. Gridded long-term mean wind azimuth and magnitude are presented for the near-surface in the Great Lakes region in Figure 1-22.

Seasonality in precipitation inputs to the Great Lakes basin is influenced by shifts in dominant air masses and by lake-effects. Overall, the Great Lakes and surrounding catchment receive roughly 850mm of precipitation annually (Figure 1-20; data from New et al. 2002). The eastern portions of each lake's catchment receive more precipitation than the upwind, western areas. Air masses prevailing from the west pick up evaporated moisture upon contact with relatively warm waters of the Great Lakes. Downwind over-land climates receive lake effect precipitation ('lake-effect snow') as the land surface cools the overlying air, decreasing saturation vapour pressure and increasing relative humidity (Figure 1-21; Eichenlaub 1970; Niziol et al. 1995). The 'snow belt' lies on the leeward side of the Great Lakes and receives up to four times more snowfall annually than nearby areas without lake-influences. Lake Erie is the only lake of the five that usually freezes over almost entirely (Assel et al. 2003); therefore, lake effect snow persists throughout the majority of snowfall seasons for lakes Superior, Huron, Michigan and Ontario. Lake-effect snow increased during the 20th century, conceivably in response to regional

increases in temperatures and reduced lake ice cover on the surface of the Great Lakes forming a positive feedback with ice-albedo effects (Burnett et al. 2003; Austin and Coleman 2007; Hayhoe et al. 2010). Mean monthly relative humidity within the Great Lakes basin varies between 65% and 80% (Figure 1-21). Monthly humidity minimums occur in April and May (65% to 70%) whereas maximums (~75%) occur in late-summer.

These physical climate data are important components for understanding air-lake interactions. Humidity and temperature fluctuations directly modify an air mass' ability to accept moisture during evaporation of surface waters. Therefore, these data are imperative to the success of water balance studies for the Great Lakes.

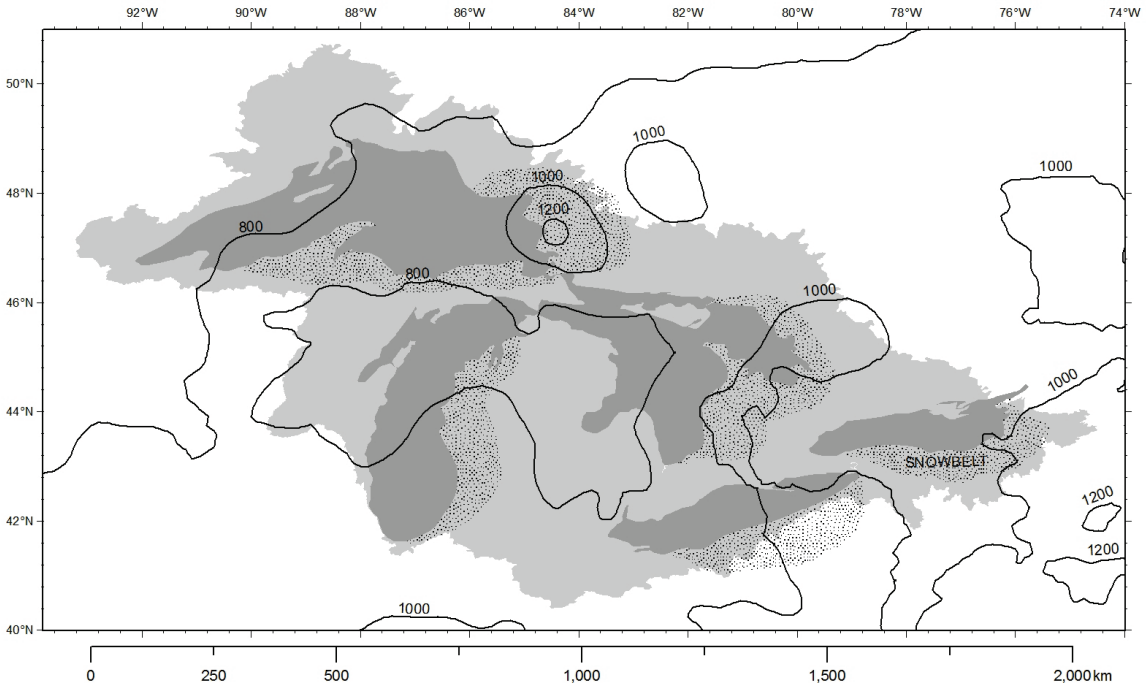

Figure 1-20. Precipitation in the Great Lakes basin. Contours are at 200mm/y intervals following the New et al. (2002) climate grids. Generalized extents of snowbelts (Eichenlaub 1970) are marked with stipple. Precipitation amount generally increases towards the east.

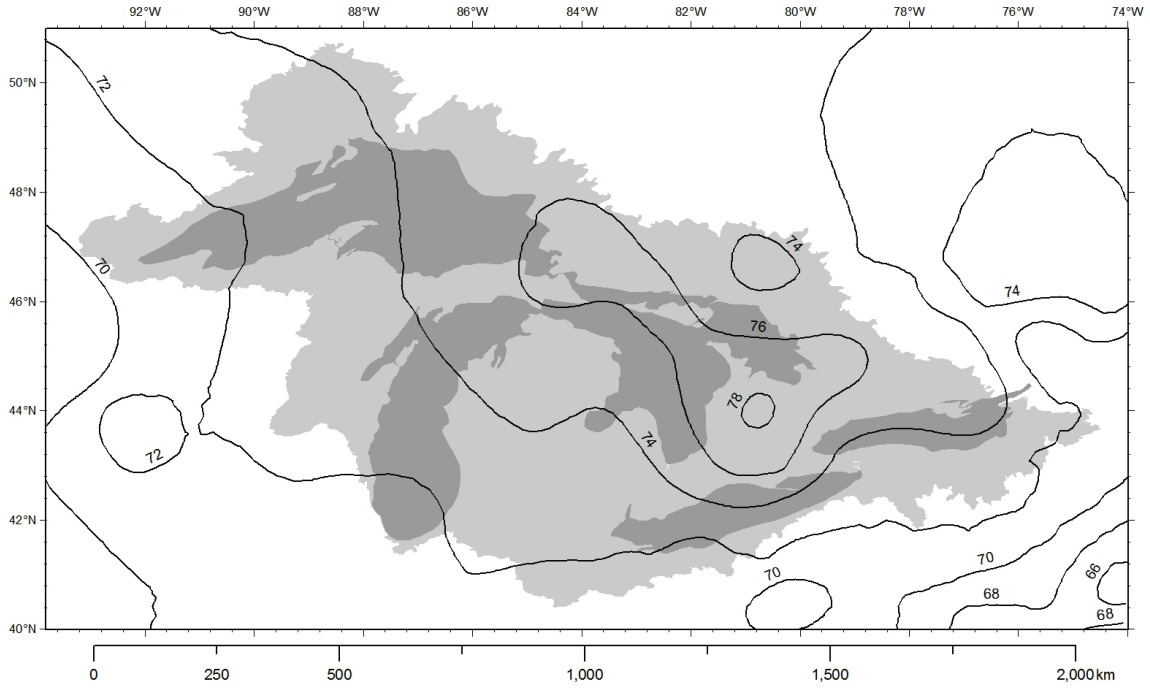

Figure 1-21. Mean annual relative humidity (RH) in the Great Lakes basin. Relative humidity in the Great Lakes basin is greatest on the leeward side of Lake Huron. The mean annual relative humidity is greatest in the eastern portion of the catchments for Great Lakes Superior, Huron and Michigan.

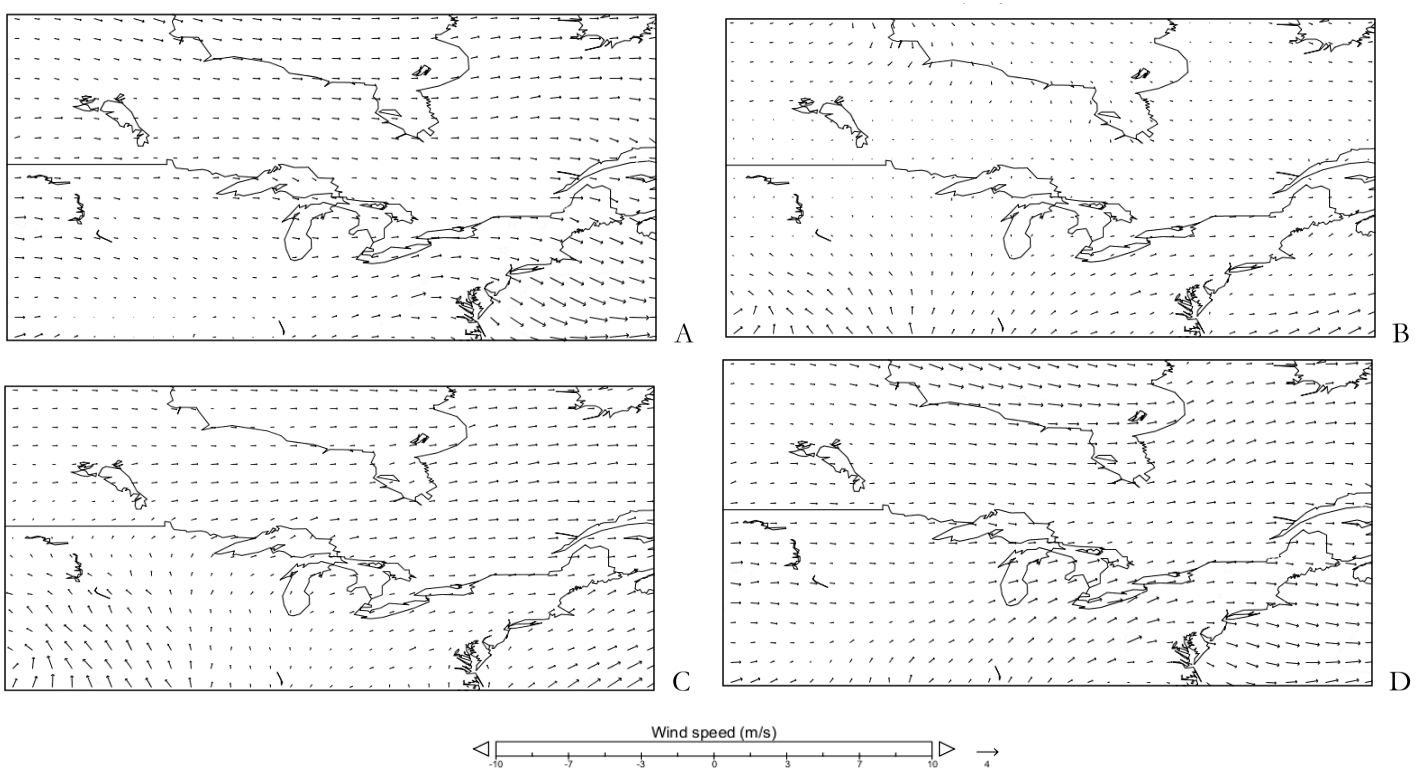

Figure 1-22. Monthly long-term near surface wind vectors for the Great Lakes region (Mesinger et al. 2006). Four months are shown: (A) February, (B) May, (C) August and (D) September. Display software Panoply (National Aeronautics and Space Administration 2011) utilized to produce the above maps. Small arrow in legend denotes a 4 m/s wind speed vector.

1.2.2.4 Previous water balance studies on the Great Lakes

The Great Lakes are a chain lake system. This description pertains to the progression of lake water from the headwater lake - Lake Superior - downstream into Great Lakes Huron, Erie and finally into Ontario. Lake Michigan, as discussed earlier, mixes with Lake Huron but does not receive a direct inflow from an upstream Great Lake. This is similar to Lake Superior. This section quantitatively describes existing estimates for the various fluxes of water into and out of each Great Lake.

Figure 1-23 demonstrates the quantitative fluxes for each Great Lake using values from Neff and Nicholas (2005). When the Great Lakes are examined in this manner, four notable features become apparent.

First, Lake Superior contains more water than all other lakes combined and does not receive a connecting channel inflow; these features explain Lake Superior's extensive residence time of over 100 years that is higher than the downstream Great Lakes' residence times. The volume of Lake Michigan-Huron, considered in this case (Neff and Nicholas 2005) to be one lake, is roughly four times as large in volume as the lower two Great Lakes. The residence time of Lakes Huron and Michigan (10^1 to 10^2) is less than half of Lake Superior's (10^2), but is close to an order of magnitude greater than Lake Erie or Lake Ontario (10^0 to 10^1). The residence time of Lake Michigan is close to 100 years, but if mixing input from Lake Huron is included this estimate drops to roughly 60 years (Quinn 1992).

Secondly, current evaporation estimates suggest this flux to be similar in magnitude to runoff or direct precipitation into each lake. This highlights the importance of evaporation to the water balance of the Great Lakes, particularly for the upper Great Lakes that do not receive a great majority of their water inputs from an upstream lake.

Thirdly, inter-basin diversions are found to be small compared to runoff, precipitation and evaporative fluxes. The Chicago diversion is operational and diverts water to the Mississippi drainage basin at a rate set at 2.9 km^3/yr. Although this flux is small on an annual basis, the prolonged extraction has removed over 150 km^3 from the Great Lakes basin. This extraction has directly lowered the level of Lakes Michigan and Huron by roughly six centimetres and Erie by roughly four centimetres. However, this out-of-basin diversion is complimented by two artificial diversions from the Hudson Bay drainage basin into the Lake Superior basin at Long Lac and Ogaki (Figure 1-14). These two divergences add nearly five cubic kilometres of water to the Great Lakes basin annually.

Finally, the comparatively short residence times lower Great Lakes Erie and Ontario are more akin to rivers when considered in the context of the mean Great Lakes basin residence time (on the order of 150 years). The input of water from upstream Great Lakes is an order of magnitude greater than runoff, precipitation and current estimates of evaporation for Lake Erie and Ontario. Therefore, evaporation for the lower Great Lakes is expected to be small when compared to water inputs to the lake (small evaporation as a proportion of inflow). The fluxes reported by Neff and Nicholas (2005) are shown schematically in Figure 1-23. Viewing the water balance in this manner, the small output of evaporation compared to connecting channel inflows is apparent for Lakes Erie and Ontario.

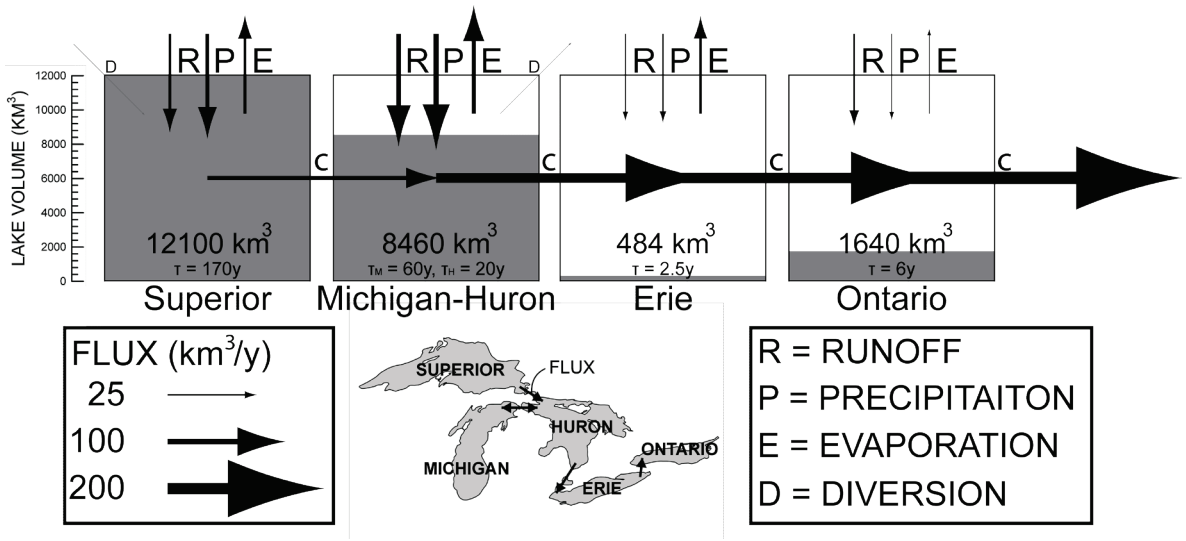

Figure 1-23. Quantitative schematic of the movement of water between the Great Lakes and the atmosphere. Black arrows represent hydrologic fluxes, and the thickness of the lines/arrowheads corresponds to the estimated magnitude of the flux (Neff and Nicholas 2005). The volume of each Great Lake is portrayed by grey shading within each box. The volumes of Lakes Erie and Ontario are small compared to upstream Great Lakes. Runoff, precipitation, inter-basin divergences and connecting channel inflow are represented by R, P, D and C, respectively. Residence times for each lake are displayed (τ) in years (y). Note that the estimates here contain considerable uncertainty thus justifying a alternative (example: stable isotope balance) approach to be taken to constrain uncertainties.

The fluxes portrayed in figure 1-23 are presented again in figures 1-24 and 1-25 for each Great Lake. These figures (1-24, 1-25) differ from Figure 1-23 as they explicitly outline the values for the estimate of each flux and its corresponding estimate of uncertainty. Figure 1-26 reports the surface areas of the Great Lakes and their surrounding catchments in addition to volumetric data.

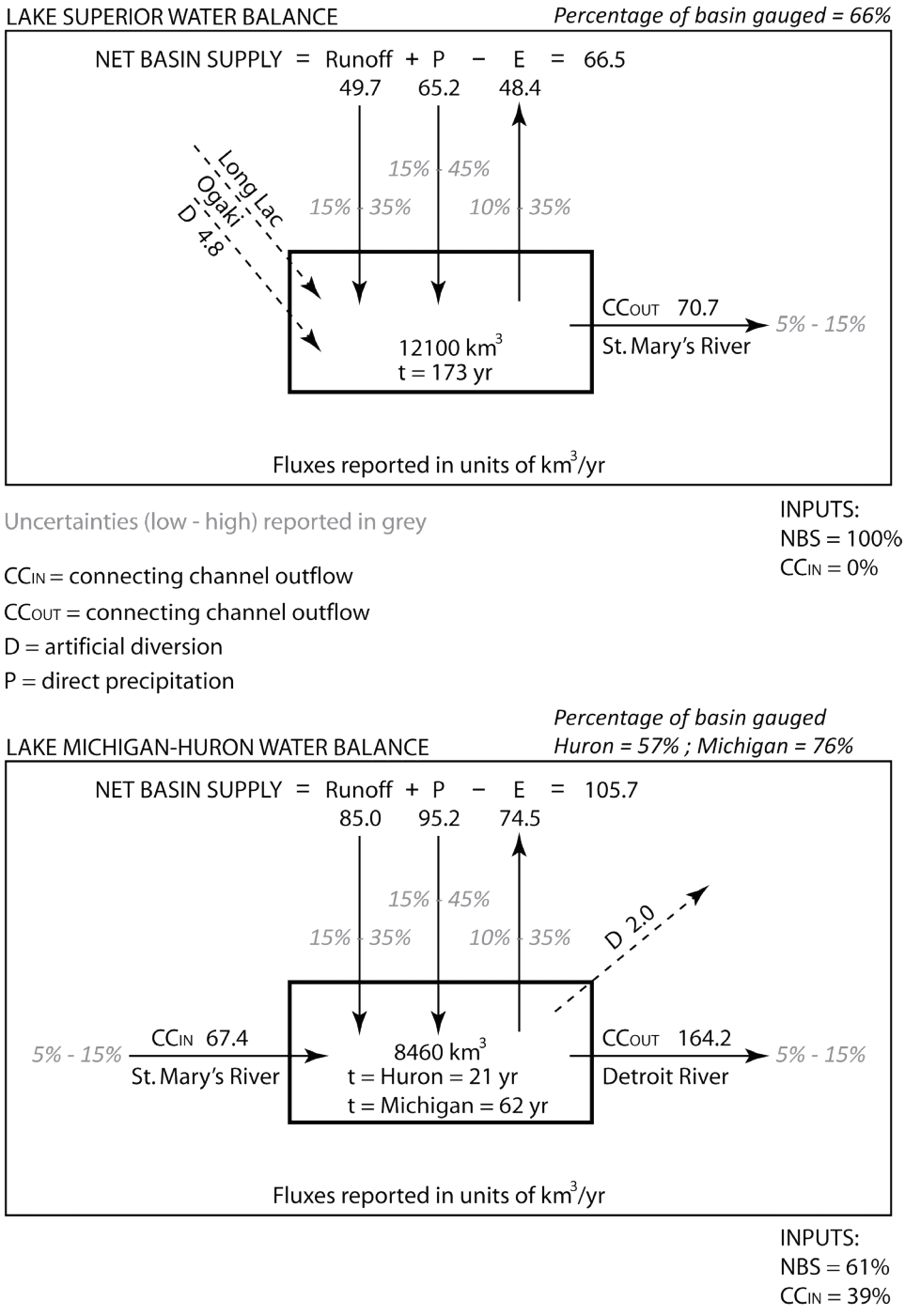

Figure 1-24 - Quantitative schematic for Lake Superior and Lake Michigan-Huron (treated as one lake). Values for percentage of basin gauged, fluxes and uncertainty for each flux presented are those reviewed by Neff and Nicholas (2005). Flushing times (t) for each lake are those reported by Quinn (1992). Great Lake volumes are obtained from the Coordinating Committee on Great Lakes Basin Hydraulic and Hydrologic Data (1977). Net basin supply (NBS) is defined by P + Runoff - E (Neff and Nicholas 2004).

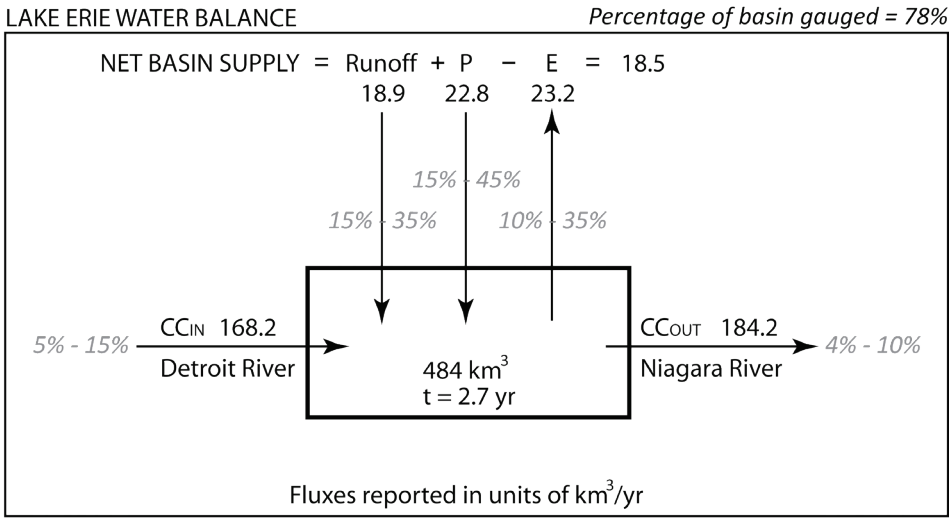

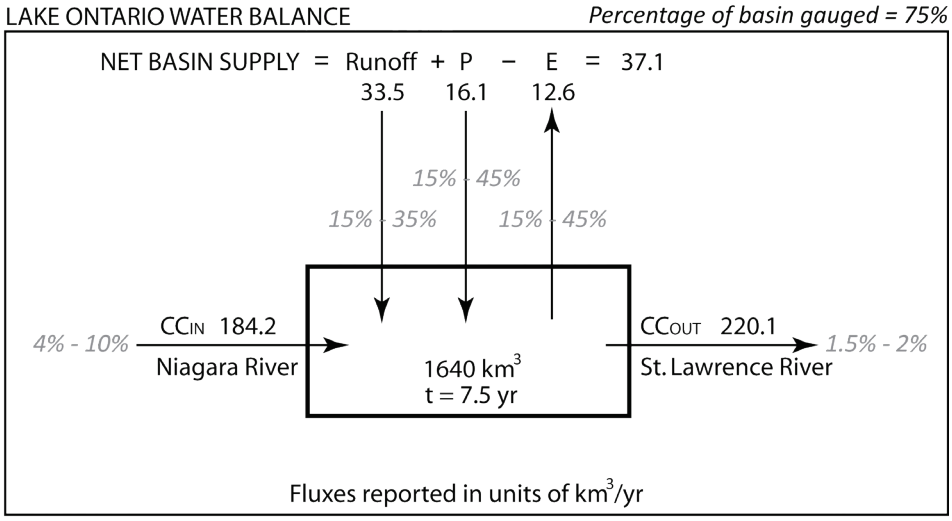

Figure 1-25 - Quantitative schematic for Lake Erie and Lake Ontario. Values for percentage of basin gauged, fluxes and uncertainty for each flux presented are those reviewed by Neff and Nicholas (2005). Flushing times (t) for each lake are those reported by Quinn (1992). Great Lake volumes are obtained from the Coordinating Committee on Great Lakes Basin Hydraulic and Hydrologic Data (1977). Net basin supply (NBS) is defined by P + Runoff - E (Neff and Nicholas 2004).

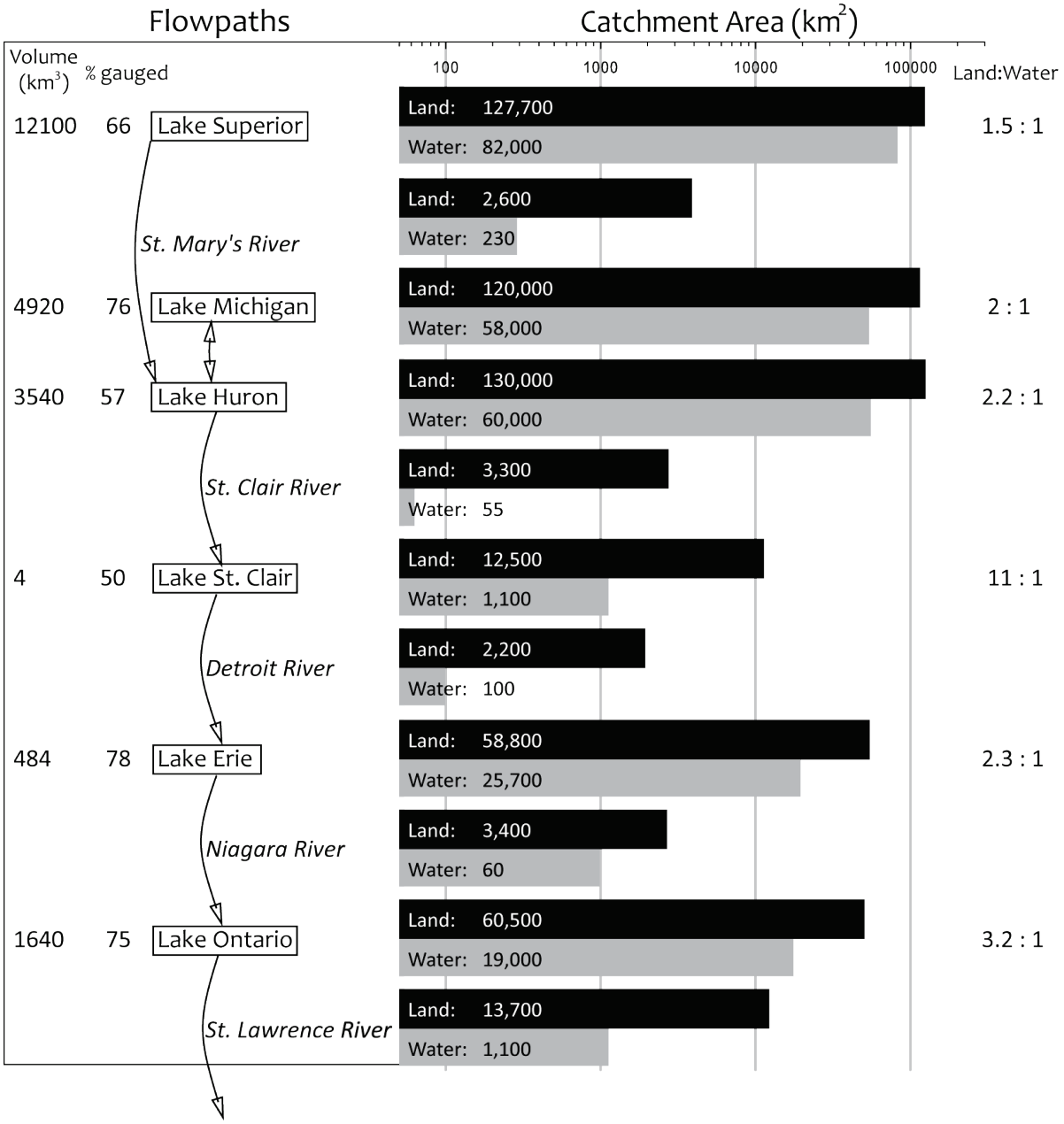

Figure 1-26 - Quantitative schematic of the Great Lakes chain system. Catchment area and Great lake surface areas are compared on a logarithmic scale. Lake St. Clair is also presented as a reservoir in this schematic, despite its small volume and short residence time (roughly two weeks).

Prior to evaluating evaporative losses for the Great Lakes by a stable isotope mass balance, it is important that other methods of estimating evaporation are reviewed. Long-term mean evaporation and direct precipitation values from the Great Lakes Environmental Research Laboratory Model (GLERL) (Croley II 1989; data from personal communication T. Hunter) are summarized in (Figures 1-27a through 1-27e). These figures also present North American Regional Reanalysis (NARR) zonal statistics for air temperature and relative humidity within each Great Lake basin (land and lake area; Mesinger et al. 2006). Physical climate data has already been reviewed. However, evaporation fluxes have not yet been discussed here; the evaporation flux for the Great Lakes will be examined here.

For all Great Lakes, evaporation rates are lowest in summer months and greatest in fall and winter months. This is an interesting seasonal behaviour. Seasonality in evaporation rates diverges from seasonality in air temperatures (evaporation occurs during months with colder air temperature). This seasonality is controlled by the thermal inertia of the water that makes up the Great Lakes. In winter, cold dry continental air masses enter the basin from the northwest. Upon advection over the Great Lakes, the air warms and its ability to accept moisture increases (relative humidity decreases with increasing temperature; following equations of Buck 1981). Furthermore, the average over-lake wind speed of winter months tends to be greater than that of summer months (Mesinger 2006; Figure 1-22). This produces a greater turbulence in the air column and supplies the lake-air boundary layer with under-saturated air (relative humidity < 100%).

During summer months, the northerly shift of the jet stream permits advection of moisture from the Gulf of Mexico. These air masses stagnate over the Great Lakes, and produce less turbulent condition than winter months. Furthermore, the difference between air temperatures and epilimnion surface temperatures is small compared to wintertime. Therefore, model results suggest that summer evaporation rates should be small in comparison to fall and winter rates (Croley II 1989). Eddy covariance approaches suggest that GLERL model (surface flux and heat storage approach) evaporation seasonality is largely correct (C. Spence, personal communication). However, these measurements are only made at certain lakeshore stations, are therefore exposed to localized conditions that may not be representative of processes controlling evaporation over the immense areas covered by each Great Lake. Due to the thermally stratified conditions of the summer months in the Great Lakes, exchange of waters at the near-surface and at-depth is limited. If evaporation enriches an evaporating epilimnion in the heavy stable isotopes of oxygen and hydrogen, then stable isotope ratio measurements have the ability to test the apparent lack of summertime evaporation as suggested in the GLERL energy balance model.

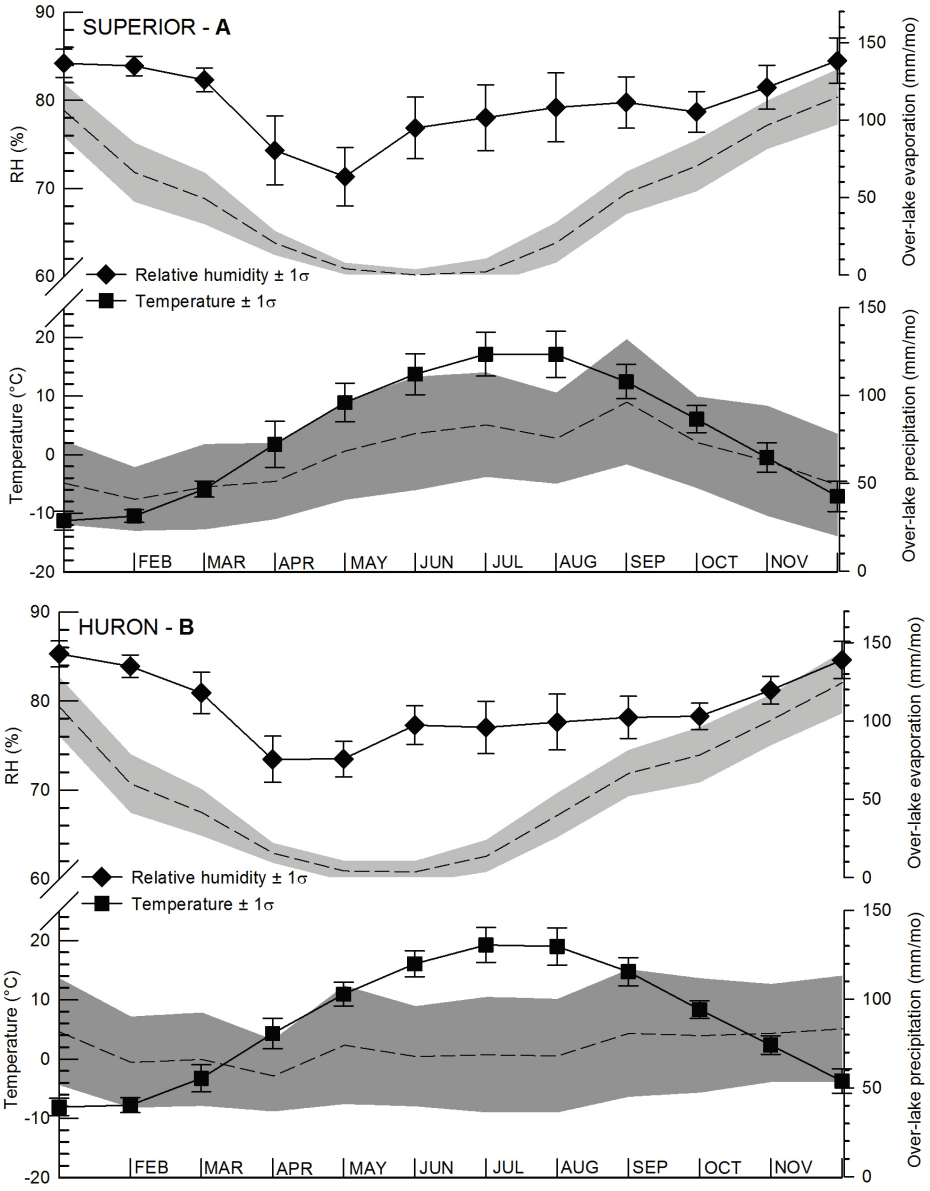

Figure 1-27a and 1-27b. Long-term monthly mean values for over-lake precipitation and evaporation rates from the Great Lakes Environmental Research Laboratory (GLERL) model are presented as a dashed line. Grey shading marks one standard deviation for long-term monthly precipitation and evaporation rates. North American Regional Reanalysis (NARR; Mesinger et al. 2006) monthly mean air temperature and relative humidity (RH) are also plotted. Error bars correspond to one standard deviation of grid values with the basin. Data are shown for Lake Superior (a) and Lake Huron (b).

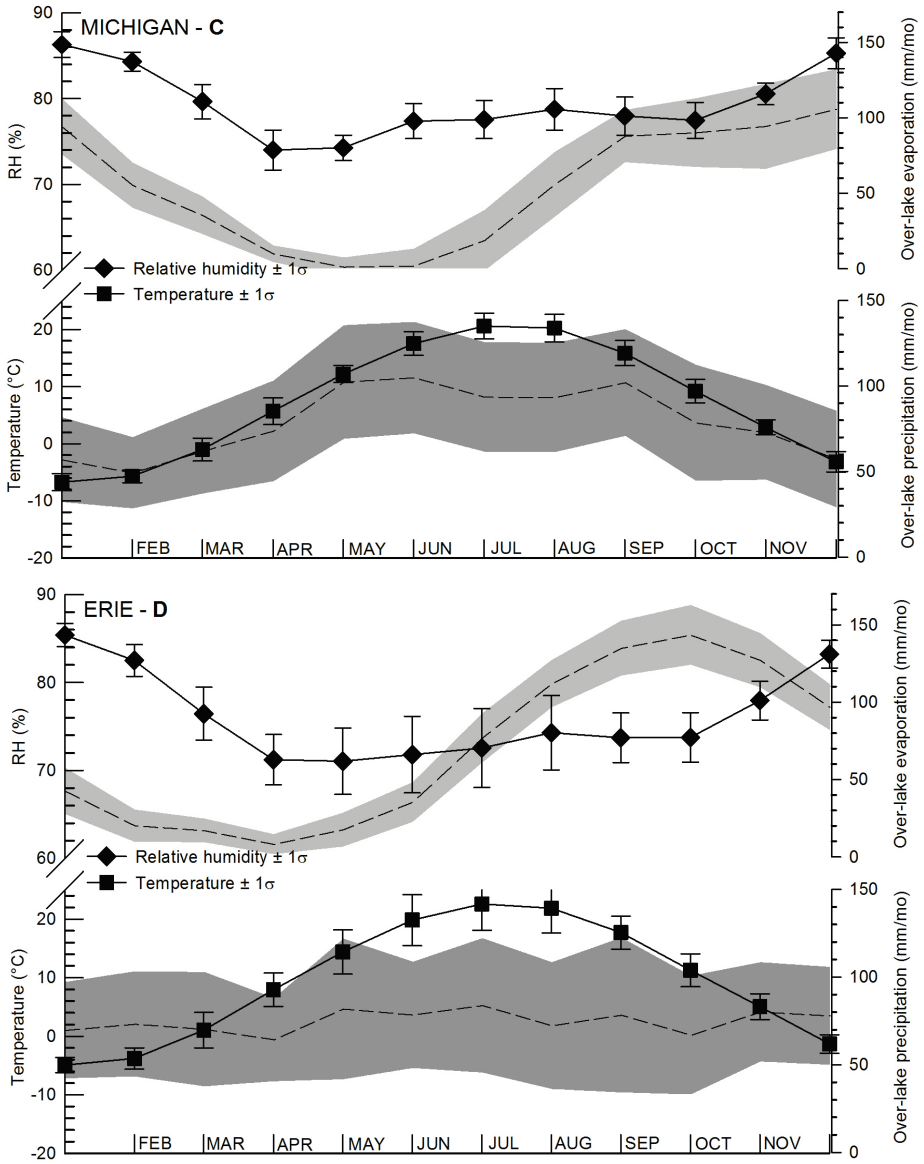

Figure 1-27c and 1-27d. Long-term monthly mean values for over-lake precipitation and evaporation rates from the Great Lakes Environmental Research Laboratory (GLERL) model are presented as a dashed line; grey shading marks one standard deviation for long-term monthly precipitation and evaporation rates. North American Regional Reanalysis (NARR; Mesinger et al. 2006) monthly mean air temperature and relative humidity (RH) are also plotted. Error bars correspond to one standard deviation of grid values with the basin. Data are shown for Lake Michigan (c) and Lake Erie (d).

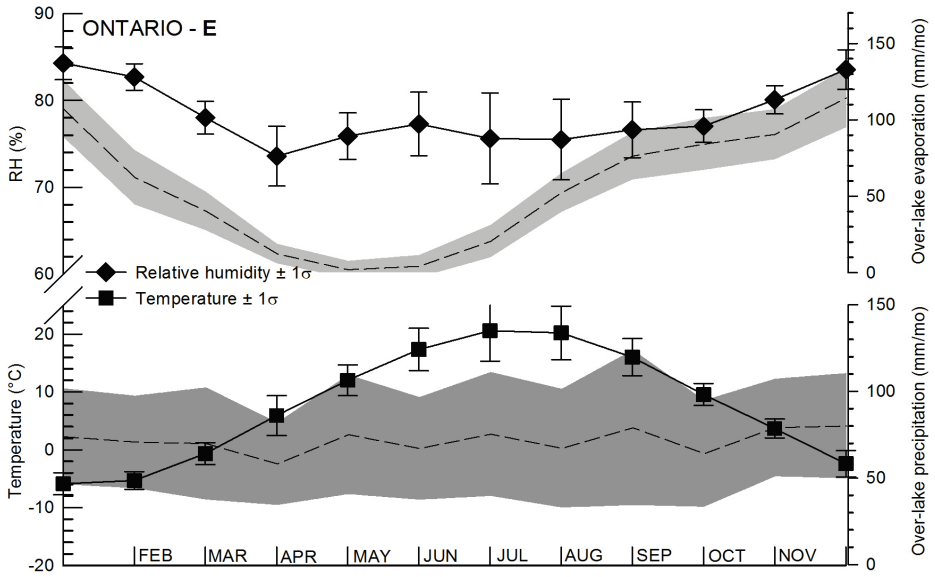

Figure 1-27e. Long-term monthly mean values for over-lake precipitation and evaporation rates from the Great Lakes Environmental Research Laboratory (GLERL) model are presented as a dashed line. Grey shading marks one standard deviation for long-term monthly precipitation and evaporation rates. North American Regional Reanalysis (NARR; Mesinger et al. 2006) monthly mean air temperature and relative humidity (RH) are also plotted. Error bars correspond to one standard deviation of grid values with the basin. Data is shown for Lake Ontario (e).

The GLERL model estimate for the long-term annual evaporation rate of each Great Lake is 603±155 mm/yr, 656±166 mm/yr, 648±205 mm/yr, 830±164 mm/yr and 666±159 mm/yr for Lakes Superior, Huron, Michigan, Erie and Ontario, respectively. Croley II 1989 outputs are in agreement with United States Geological Survey estimates (Neff and Nicholas 2005). A comparison is drawn in Table 1–6.

Table 1–6. Evaporation rates (mm/yr) and fluxes reported by the Great Lakes Environmental Research Laboratory (Croley II 1989) and the United States Geological Survey (Neff and Nicholas 2005).

Lake	Area (km^2)	GLERL		USGS		GLERL		USGS	
		E (km^3/y)	1σ (km^3/y)	E (km^3/y)	+/- (km^3/y)	E (mm/y)	1σ (mm/y)	E (mm/y)	+/- (mm/y)
Superior	82000	49.4	12.7	48.4	16.9	603	155	590	207
Huron	60000	39.4	9.9	74.5	26.1	656	166	624	217
Michigan	58000	37.6	11.9			648	205		
Erie	25700	21.3	4.2	23.2	8.1	830	164	903	316
Ontario	19000	12.6	3.0	12.6	5.7	666	160	663	298

Adding the data in Table 1–6 to long-term input fluxes reported in Neff and Nicholas (2005) produces a value of evaporation as a proportion of inflow for each lake (Table 1–7). These data form a useful comparison tool against stable isotope mass balance outputs. Regarding the uncertainty for the E/I value, it is important to note that the total hydrologic input is well constrained for the lower two Great Lakes. This is a result of the larger proportion contributed by the upstream connecting channel inflow that is gauged and known within 15%. To estimate the uncertainty for the input flux, the uncertainty of the various inputs has been weighted against their proposed fluxes. This produces uncertainties for the total input ranging from ~40% for Lakes Superior, to less than 20% for Lakes Erie and Ontario (Table 1–7, Figure 1-28).

Table 1–7. Evaporation as a proportion of inflow (%) from physical hydrologic approaches

Lake	Total Input		GLERL: Evaporation		USGS: Evaporation		GLERL E/I		USGS E/I	
	km^3/y	+/-	km^3/y	+/-	km^3/y	+/-	%	+/- *	%	+/- *
Superior	115	47	49	13	48	17	43	20-48	42	23-54
Huron	212	68	39	10	75	26	19	8-16	29	10-10
Michigan	123	56	38	12			31	16-44		
Erie	210	42	21	4	23	8	10	3-5	11	5-8
Ontario	234	38	13	3	13	6	5	2-3	5	3-4

* Uncertainty for E/I in %. Low value for uncertainty is presented first, followed by a dash, and then followed by the high uncertainty value.

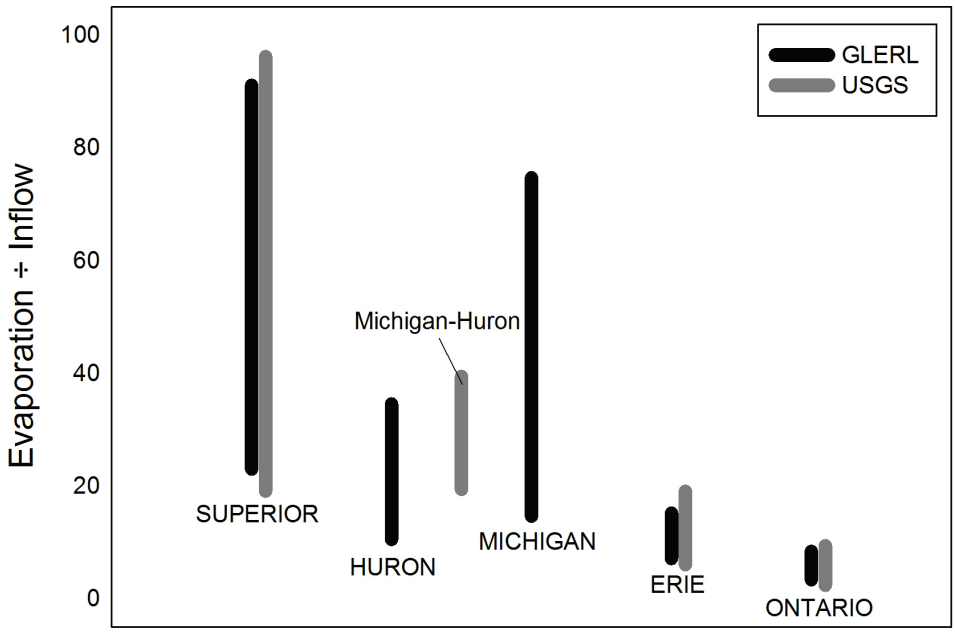

Figure 1-28. Evaporation as a proportion of inflow from the Great Lakes Environmental Research Laboratory model and United States Geological Survey (Neff and Nicholas 2005).

We have now reviewed background literature in isotope hydrology for lake studies, introduced the Great Lakes geography and described previous estimates for evaporation from the Great Lakes using energy and mass balance approaches. Next, the dataset and approach to estimating evaporation using a stable isotope mass balance will be presented.

Chapter 2
Dataset and Methods

2.1 Dataset

Multiple forms of data are required to calculate evaporative losses using a stable isotope approach. This chapter contains four sections. The first (2.1.1) presents data for $\delta^{18}O$ and $\delta^{2}H$ for the Great Lakes, precipitation and other surface waters. The second compiles and reports estimates of lower troposphere relative humidity and temperature over each Great Lake. The third presents lake temperatures and other physical climate data from lake buoys. Finally, estimates of seasonality in lake evaporation as a percentage of mean annual rates are compiled. The sources and values for each referenced dataset are summarized in this section; appendices are referenced for large and new datasets.

2.1.1 Stable isotopes of oxygen and hydrogen in the Great Lakes basin

Several sources of oxygen and hydrogen isotopic data are available for the Great Lakes hydrological system. Isotopic signatures of (1) the Great Lakes, (2) precipitation, and (3) inflows and connecting channels are described in this section.

Two cruises led by the Environmental Protection Agency (EPA) in the spring (late March and early April) and summer (early August) of 2007 collected a total of 514 samples of lake water from the five Great Lakes: 283 samples were collected during the spring cruise and 231 samples were collected in the summer cruise. Lake water samples were acquired from within two metres of the lake surface, at mid-depth(s), and within ten metres of the sediment-water interface at each station. The separation of the two cruises in time and vertical profiling within the water column recovered a set of samples that effectively captures spatial and seasonal variability within Great Lakes waters.

The lake water samples were shipped to the Alberta Research Council's (now a part of Alberta Innovates – Technology Futures) Isotope Hydrology and Geochemistry Laboratory located in Victoria, British Columbia. Stable isotope ratios of oxygen ($^{18}O/^{16}O$) and hydrogen ($^{2}H/^{1}H$) were analyzed for each of the 514 samples. Duplicate runs of samples for quality assurance and quality control (QA/QC) were completed, producing a total of 1224 isotopic analyses of Great Lakes waters (621 for $\delta^{18}O$; 603 for $\delta^{2}H$).

For oxygen isotopic analyses (reported as $\delta^{18}O$ values in ‰ relative to the Vienna Standard Mean Ocean Water (VSMOW) standard, where $\delta^{18}O = 1000 \cdot (R_{sample}/R_{VSMOW} - 1)$ and R is the $^{18}O/^{16}O$ ratio) samples were run on a Delta V Advantage mass spectrometer with a GasBench II peripheral. Water samples were equilibrated in a sealed vial with 0.3% carbon dioxide gas ($CO_{2(g)}$). This permitted the oxygen within the water sample ($H_2O_{(l)}$) to exchange with the oxygen within the $CO_{2(g)}$ at constant temperature. A CTC Analytics autosampler sampled the equilibrated $CO_{2(g)}$ onto the peripheral, where multiple injections of the equilibrated (as $CO_{2(g)}$) were measured against a pure CO_2 monitoring gas. $\delta^{18}O$ results are accurate to within ±0.2‰.

Analyses of the stable isotopes of hydrogen (reported as δ^2H values in ‰ relative to VSMOW, where $\delta^2H = 1000 \cdot (R_{sample}/R_{VSMOW} - 1)$ and R is the $^2H/^1H$ ratio) in each sample were run on a Delta V Advantage mass spectrometer with a HDevice peripheral. A CTC Analytics autosampler was used to inject one microlitre (1 µL) of sample water into the septum port of the HDevice. This duel-inlet peripheral, equipped with chromium metal at 900°C, produced hydrogen gas ($H_{2(g)}$) from the sample water that was then introduced into the mass spectrometer through the duel inlet bellows. The hydrogen isotopic composition was measured relative to a pure hydrogen gas calibrated against international standards. Results are accurate to within ±1‰.

$\delta^{18}O$ and δ^2H results for Great Lakes waters are presented in Appendix A. Sampling stations are displayed in Figure 2-1.

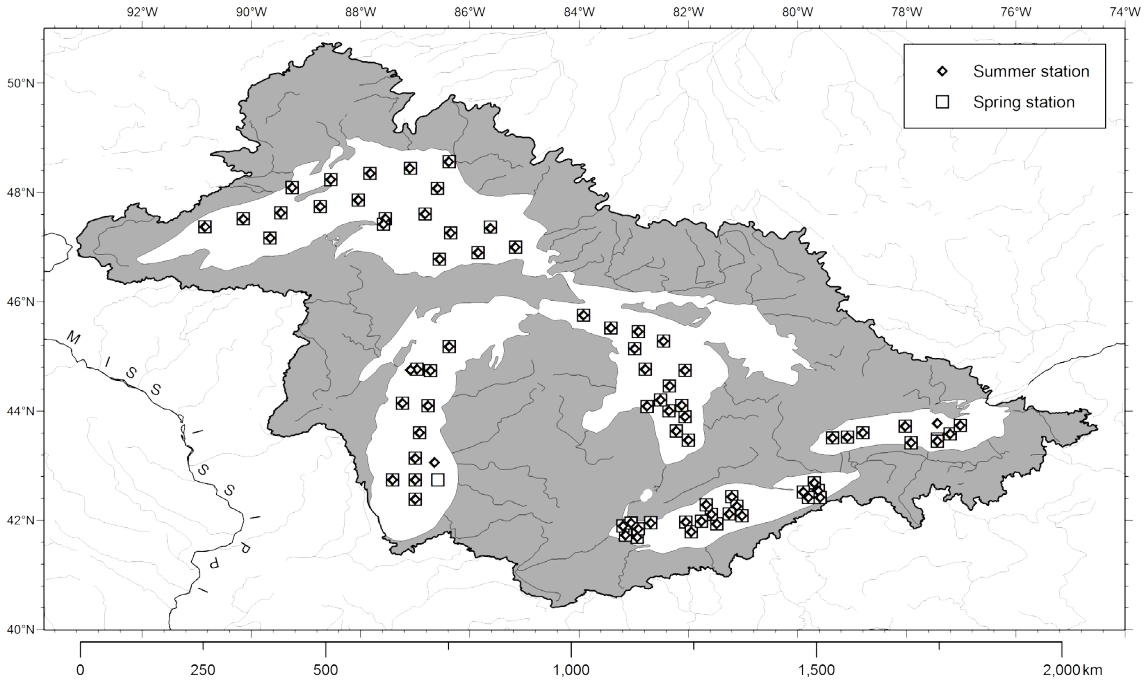

Figure 2-1. Sampling stations for Great Lakes waters. Samples collected during spring months are presented as squares; those collected during summer are presented as diamonds.

Precipitation is collected and analyzed for stable isotopes of oxygen and hydrogen by two regional networks: the Canadian Network for Isotopes in Precipitation (CNIP; http://science.uwaterloo.ca/~twdedwar/cnip/cniphome.html) and the United States Network for Isotopes in Precipitation (USNIP; Welker 2000), and one global network: the International Atomic Energy Agency (IAEA; http://www-naweb.iaea.org/napc/ih/IHS_resources_gnip.html). The regional networks contain isotope data for a combined total of 115 sampling stations (35 CNIP, 80 USNIP). The International Atomic Energy Agency database contains data for over 800 stations worldwide, some of these are jointly operated with the regional networks. In total, 117 precipitation monitoring stations exist over the North American landmass (Figure 2-2).

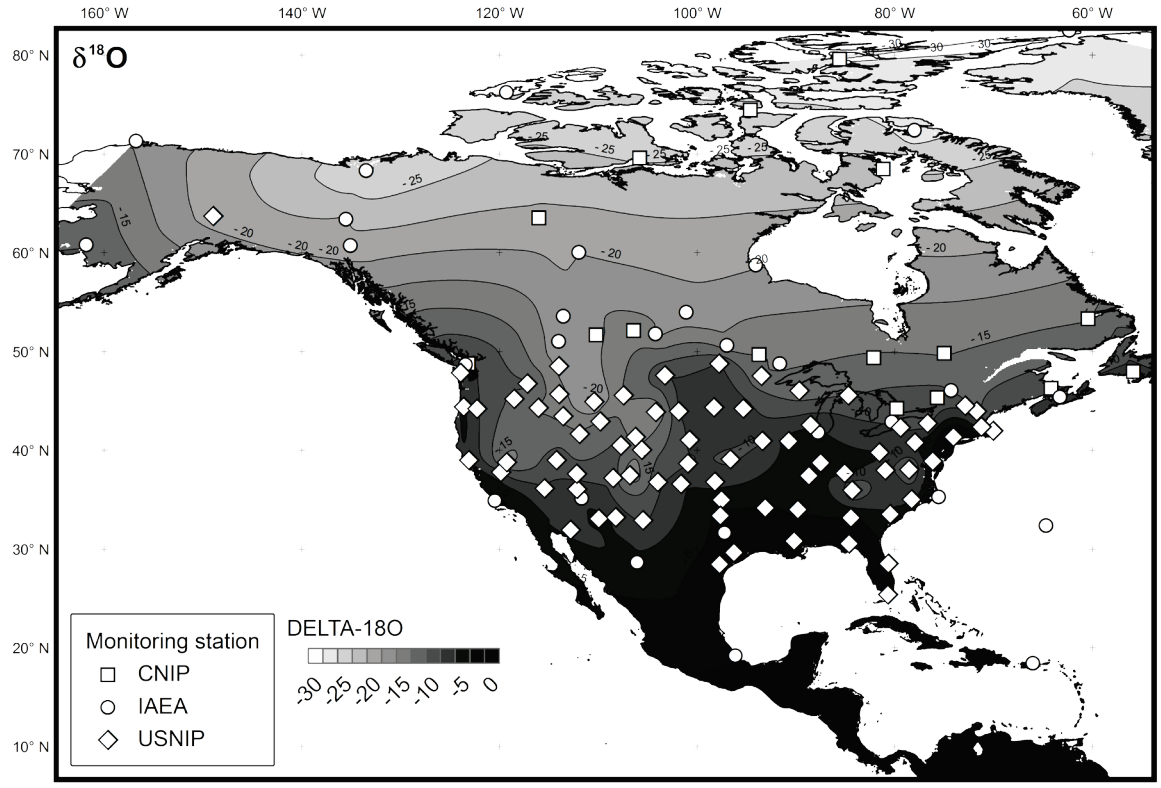

Figure 2-2. North American locations of sampling stations for the Canadian Network for Isotopes in Precipitation (CNIP), United States Network for Isotopes in Precipitation (USNIP), and the International Atomic Energy Agency (IAEA). Average $\delta^{18}O$ values for these stations are presented as a nearest-neighbours interpolation.

Of these stations, 21 are located within or close to the boundary of the Great Lakes drainage basin (13 stations from CNIP, eight from USNIP). The coordinators of each regional network were contacted and provided analytical results and associated precipitation fluxes for each of the stations applicable to the Great Lakes. The combined datasets contain 1943 analyses of $\delta^{18}O$ (1648 from CNIP or IAEA, 286 from USNIP) and 1881 analyses of $\delta^{2}H$ (1600 from CNIP or IAEA, 281 from USNIP). These stations are presented in Table 1–7 and locations are displayed in Figure 2-3.

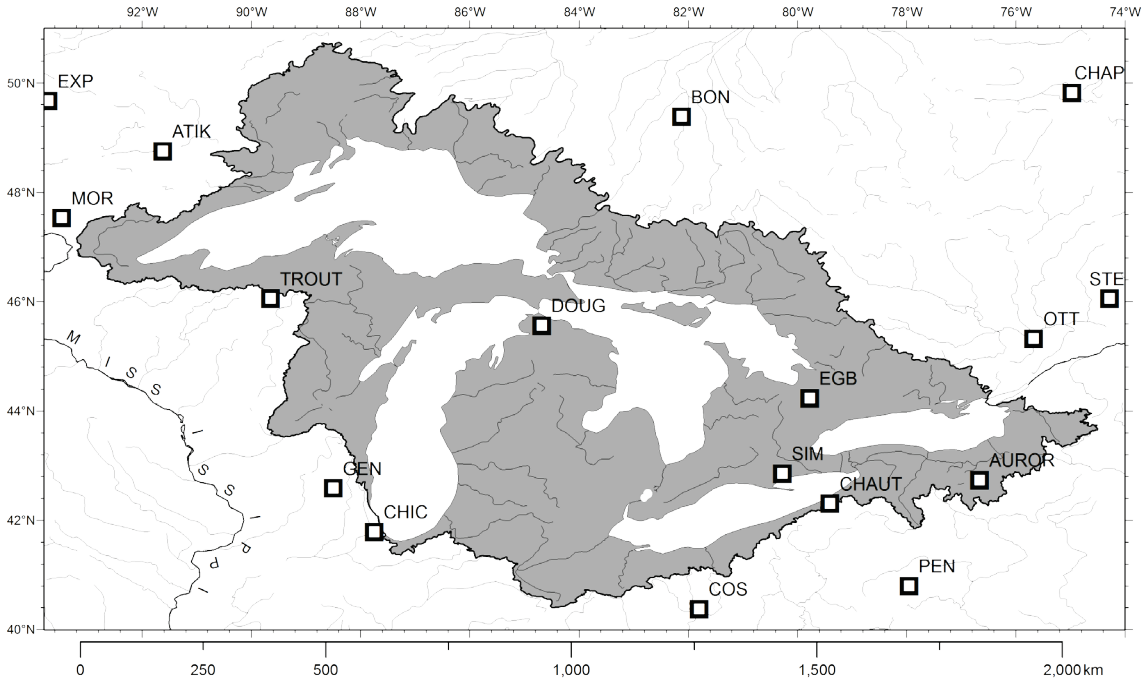

Figure 2-3. Locations of precipitation monitoring stations in the Great Lakes basin and surrounding areas. Stations are abbreviated as follows: Atikokan - ATIK, Aurora Research Farm - AUROR, Bonner Lake - BON, Chapais - CHAP, Chautauqua - CHAUT, Chicago - CHIC, Coshocton - COS, Douglas Lake - DOUG, Egbert - EGB, Experimental Lakes Area - EXP, Lake Geneva - GEN, Morcell Experimental Forest - MOR, Ottawa - OTT , Penn State - PEN, Simcoe - SIM, Ste. Agathe - STE, Trout Lake - TROUT. Not shown here are The Pas, Gimli and Bismarck (west of map extent). Caldwell is located south of the map extent.

Table 2–1. Isotopic monitoring stations for precipitation: spatial and temporal data

Station	Source	Latitude	Longitude	Altitude (m.a.s.l.)	Dates operational	
Atikokan	IAEA	48.75	-91.62	393	1975	1982
Aurora Research Farm	USNIP	42.73	-76.66	249	1989	1994
Bismarck	IAEA	46.77	-100.75	502	1963	1984
Bonner Lake	CNIP	49.38	-82.12	245	1993	2003
Caldwell	USNIP	39.79	-81.53	276	1989	1990
Chapais	CNIP	49.82	-74.97	382	1993	2003
Chautauqua	USNIP	42.30	-79.40	488	1989	1993
Chicago	IAEA	41.78	-87.75	189	1960	1979
Coshocton	IAEA	40.37	-81.80	344	1966	1971
Douglas Lake	USNIP	45.56	-84.68	238	1989	1990
Egbert	CNIP	44.23	-79.77	224	1993	2003
Experimental Lakes Area	CNIP	49.67	-93.72	369	1993	2003
Gimli	IAEA	50.62	-96.98	223	1975	1982
Lake Geneva	USNIP	42.58	-88.50	288	1989	1993
Morcell Experimental Forest	USNIP	47.53	-93.47	431	1989	1994
Ottawa	IAEA	45.32	-75.67	114	1953	2007
Penn State	USNIP	40.79	-77.95	393	1989	1989
Simcoe	IAEA	42.85	-80.27	240	1975	1982
Ste. Agathe	IAEA	46.05	-74.28	395	1975	1982
The Pas	IAEA	53.97	-101.1	272	1975	1982
Trout Lake	USNIP	46.05	-89.65	501	1989	1991

These datasets are used in two ways. First, a local meteoric water line (LMWL) is established for the Great Lakes drainage basin. This is accomplished by producing a linear regression of unweighted results from stations with $\delta^{18}O$ and $\delta^{2}H$. 200 monthly results are randomly selected for Ottawa ($n > 550$ analyses of $\delta^{18}O$) so that this station did not dominate the regression; 200 analyses is close to the next highest number of analyses at a single station (Chicago $n = 192$). Regressions for each individual station are also computed (Table 2–2).

Table 2–2. Meteoric water lines for stations in the Great Lakes basin and vicinity

Station	Source	Precipitation (mm/yr)	MWL slope	MWL intercept	MWL R^2
Atikokan	IAEA	683	7.84	7.49	0.99
Aurora Research Farm	USNIP	1058	7.65	10.47	0.98
Bismarck	IAEA	399			
Bonner Lake	CNIP	882	7.70	5.13	0.99
Caldwell	USNIP	1223			
Chapais	CNIP	1045	7.80	8.53	0.99
Chautauqua	USNIP	864	7.05	4.31	0.96
Chicago	IAEA	908	6.98	0.08	0.96
Coshocton	IAEA	977	7.51	8.81	0.97
Douglas Lake	USNIP	852			
Egbert	CNIP	784	6.86	-2.64	0.95
Experimental Lakes Area	CNIP	687	7.75	5.00	0.99
Gimli	IAEA	557	7.65	2.96	0.99
Lake Geneva	USNIP	1175	7.20	-0.09	0.88
Morcell Experimental	USNIP	934	8.11	11.78	0.99
Ottawa	IAEA	909	7.57	7.06	0.97
Penn State	USNIP	1036			
Simcoe	IAEA	941	7.80	9.40	0.97
Ste. Agathe	IAEA	1200	7.75	9.96	0.98
The Pas	IAEA	445	7.57	-0.42	0.99
Trout Lake	USNIP	1090	8.12	14.88	0.99
Great Lakes basin	(C)(US)NIP, IAEA	-	7.73	6.73	0.98

Second, to establish the annual isotopic composition of precipitation at each site, isotopic results are amount-weighted to monthly precipitation by equation 1:

$$\delta_{P(AW)} = \frac{\Sigma_{i=1}^{n} \delta_i P_i}{\Sigma_{i=1}^{n} P_i} \quad (1)$$

Each month's (i) isotopic analysis (δ) is multiplied by the corresponding monthly precipitation (P). Normalizing to the total precipitation a station received during the sampling period, a flux-weighted isotopic value ($\delta_{P(AW)}$) for each isotopic tracer ($\delta^{18}O$, $\delta^{2}H$) is presented for the ten precipitation monitoring stations in Table 2–3. For interest, the combined datasets of all three networks produce an amount-weighted value of $\delta^{18}O$ = -7.1 ‰ for (n = 5543 analyses of $\delta^{18}O$ and monthly precipitation) from 94 stations over North America.

Table 2–3. Data for isotopic monitoring stations for precipitation

Station	Source	n: $\delta^{18}O$	n: $\delta^{2}H$	$\delta^{18}O$ * (‰$_{SMOW}$)	$\delta^{2}H$ * (‰$_{SMOW}$)	Deuterium excess **
Atikokan	IAEA	76	75	-12.61	-91.5	9.4
Aurora Research Farm	USNIP	27	56	-8.12	-57.3	7.6
Bismarck	IAEA	1	1	-22.20	-174.5	3.1
Bonner Lake	CNIP	121	122	-13.82	-100.7	9.9
Caldwell	USNIP	0	30		-40.4	
Chapais	CNIP	122	123	-13.40	-97.3	10.0
Chautauqua	USNIP	27	32	-8.36	-55.5	11.3
Chicago	IAEA	192	170	-6.18	-44.7	4.8
Coshocton	IAEA	65	64	-7.41	-46.6	12.7
Douglas Lake	USNIP	23	0	-10.27		
Egbert	CNIP	65	65	-10.35	-72.8	10.1
Experimental Lakes Area	CNIP	123	123	-12.33	-90.3	8.4
Gimli	IAEA	76	73	-14.21	-103.7	10.0
Lake Geneva	USNIP	69	43	-7.51	-52.4	7.6
Morcell Experimental Forest	USNIP	109	61	-11.17	-89.1	0.3
Ottawa	IAEA	571	556	-10.97	-75.2	12.6
Penn State	USNIP	0	26		-40.4	
Simcoe	IAEA	81	78	-9.27	-62.2	12.0
Ste. Agathe	IAEA	82	80	-12.55	-87.8	12.6
The Pas	IAEA	73	70	-16.55	-125.8	6.6
Trout Lake	USNIP	31	33	-9.06	-67.3	5.2

* $\delta^{18}O$ and $\delta^{2}H$ are amount weighted to precipitation following equation (1).

** Deuterium excess values are computed as (Dansgaard 1964): deuterium-excess = $\delta^{2}H - 8 \cdot \delta^{18}O$

A complementary spatial dataset has been obtained for isotopes in precipitation. The spatially resolved grid (10-minute) provides a continuous spatial dataset with estimates of monthly precipitation values for $\delta^{18}O$ and $\delta^{2}H$ over the Great Lakes (approach reviewed by Bowen 2008; dataset obtained from Bowen 2009).

Isotope analyses of rivers, streams and Great Lakes connecting channels have been drawn from three data sources. Surveys conducted by the United States Geological Survey (USGS), Environment Canada (EC) and the Grand River Conservation Authority (GRCA) provided $\delta^{18}O$ and $\delta^{2}H$ analyses of surface waters. Cumulatively, the three datasets contain over 500 analyses of oxygen and hydrogen stable isotopic ratios.

Between 1984 and 1987, river water samples were collected by the U.S. Geological Survey (USGS) and analyzed for stable isotopes of oxygen and hydrogen. The sampling program utilized stations from existing networks such as the National Stream Quality Accounting Network (NASQAN; Kendall and Coplen 2001) to obtain samples. In the Great Lakes drainage basin, 22 stations were sampled at one- to eight-month intervals over a 30- to 36-month period. Sampling was not evenly dispersed among the basins: five stations were sampled within the Lake Superior catchment, three within Huron, five within Michigan, three within Erie, and six within Ontario. Each of the 22 stations was sampled on at least ten occasions, amounting to a total of 275 analyses for both $\delta^{18}O$ and $\delta^{2}H$ in the Great Lakes drainage system. Two of the 22 sampled stations are connecting channels between Great Lakes (connecting channel inflow to Lake Huron at the St. Mary's River and into Lake Ontario at the Niagara River) and have been considered separately from net basin supply inputs from rivers.

The Grand River was sampled for isotopes of oxygen and hydrogen on the northern shore of Lake Erie's catchment by the Grand River Conservation Authority. Sampling was completed from 2003 through 2005. Over 70 samples were analyzed for $\delta^{18}O$ and $\delta^{2}H$ over this period.

To determine representative isotopic values for the 20 USGS stations and the Grand River, a flux-weighted approach was taken. Discharge data from the sampling period was obtained for each sampled river from the National Water Information System (NWIS; United States Geological Survey) and Hydroclimatological Data Retrieval Program (HYDAT; Environment Canada) databases. Each sample is assumed to represent the monthly average isotopic value. Each sample is matched to the average monthly discharge to produce a discharge-weighted value for the isotopic composition of each station. This was also completed for all sampling stations in the entire 391 station database (Kendall and Coplen 2000)

$$\delta_{R\,(FW)} = \frac{\Sigma_{i=1}^{n} \delta_i Q_i}{\Sigma_{i=1}^{n} Q_i} \qquad (2)$$

where δ is the result of an isotopic analysis for a sample collected during month i; Q is the average river discharge for month i. The data for these stations is presented in Table 2–4. Drainage area of the combined dataset is 30800 km^2. Between <3 and 41 percent of each Great Lake's drainage area is sampled by Kendall and Coplen (2001): Superior: 2.8 %, Huron: 0.9 %, Michigan: 23 %, Erie: 22 %, Ontario: 42 %. The discharge of these rivers represents between <2 and 30 percent of the runoff flux into each Great Lake: Superior: 2.8 %, Huron: 1.7 %, Michigan: 30 %, Erie: 27 %, Ontario: 30 %. Therefore, the isotopic composition of waters flowing into Lakes Michigan, Erie and Ontario is better characterized than that of Lakes Superior and Huron.

Another source of isotope data in surface waters within the Lake Superior basin was a survey led by Environment Canada in 2008. Sampling of Ontario surface waters was completed in six broad sampling blocks; two of the six lie within the northern sector of Lake Superior's catchment and one other lies within the Long Lac diverted drainage into Lake Superior. 312 lake samples were analyzed for both $\delta^{18}O$ and $\delta^{2}H$ from the six sampling regions (Figure 2-4). Aside from providing inflow stable isotope data for Lake Superior, these data also provide a regional evaporation line for the region north of Lake Superior (slope 5.14, $R^2 = 0.85$). This evaporation slope for small lakes is in agreement with predicted slopes for the region (Gibson et al. 2008).

Sampling locations for rivers (GRCA and USGS) and lakes (EC) are presented in Figure 2-4.

Table 2–4. Rivers with stable-isotope analyses in the Great Lakes basin from Kendall and Coplen (2001) and Grand River Conservation Authority.

Station Name	Basin	Station ID	Latitude	Longitude	Elevation (m.a.s.l)	State/ Province	Drainage area (km^2)
Baptism River Near Beaver Bay	Superior	4014500	47.34	-91.20	187	MN	360
Nemadji River Near South Superior	Superior	4024430	46.63	-92.09	191	WI	1090
Tahquamenon River Near Tahquamenon Paradise	Superior	4045500	46.58	-85.27	212	MI	2050
Washington Creek At Windigo	Superior	4001000	47.92	-89.15	184	MI	30
Pigeon River Near Caseville	Huron	4159010	43.94	-83.24	183	MI	320
Rifle River Near Sterling	Huron	4142000	44.07	-84.02	198	MI	830
Manistee River At Manistee	Michigan	4126520	44.25	-86.32	184	MI	5180
Menominee River Near McAllister	Michigan	4067500	45.32	-87.66	192	WI	10180
Milwaukee River At Milwaukee	Michigan	4087000	43.10	-87.91	185	WI	1800
Popple River Near Fence	Michigan	4063700	45.76	-88.46	429	WI	360
St. Joseph River At Niles	Michigan	4101500	41.83	-86.26	193	MI	9500
Cattaraugus Creek At Gowanda	Erie	4213500	42.46	-78.94	225	NY	1130
Grand River At Painesville	Erie	4212200	41.74	-81.27	177	OH	1820
Sandusky River Near Fremont	Erie	4198000	41.31	-83.16	191	OH	3240
Black River At Watertown	Ontario	4260500	43.99	-75.93	114	NY	4850
Genesee River (Charlotte Docks) At Rochester	Ontario	4232006	43.22	-77.62	105	NY	6360
Niagara River (Lake Ontario) At Fort Niagara	Ontario	4219640	43.26	-79.06	75	NY	686350
Oswego River At Lock 7 At Oswego	Ontario	4249000	43.45	-76.51	75	NY	13210
Sandy Creek Near Adams	Ontario	4250750	43.81	-76.08	160	NY	330
Tonawanda Creek At Batavia	Ontario	4217000	43.00	-78.19	267	NY	440
Grand River (Ontario)	Erie	At York	43.02	-79.89	190	ON	6500

Table 2–4 (continued).

Station Name	Basin	$\delta^{18}O$ * (‰$_{SMOW}$)	$\delta^{2}H$ * (‰$_{SMOW}$)	Deuterium excess **	n	Discharge *** (km^3/yr)
Baptism River Near Beaver Bay	Superior	-10.14	-73.3	7.8	10	0.11
Nemadji River Near South Superior	Superior	-12.03	-84.3	11.9	11	0.39
Tahquamenon River Near Tahquamenon Paradise	Superior	-12.31	-85.2	13.2	10	0.89
Washington Creek At Windigo	Superior	-12.42	-87.2	12.2	11	0.01
Pigeon River Near Caseville	Huron	-10.81	-73.9	12.5	10	0.26
Rifle River Near Sterling	Huron	-11.13	-77.7	11.3	9	0.61
Manistee River At Manistee	Michigan	-10.83	-73.9	12.7	16	2.6
Menominee River Near McAllister	Michigan	-10.80	-76.3	10.1	8	3.2
Milwaukee River At Milwaukee	Michigan	-10.24	-69.8	12.1	9	0.95
Popple River Near Fence	Michigan	-10.77	-75.7	10.5	11	0.08
St. Joseph River At Niles	Michigan	-7.98	-52.9	10.9	16	3.9
Cattaraugus Creek At Gowanda	Erie	-10.62	-70.6	14.4	11	0.9
Grand River At Painesville	Erie	-9.25	-60.2	13.9	7	1.4
Sandusky River Near Fremont	Erie	-8.01	-50.7	13.3	12	0.92
Black River At Watertown	Ontario	-11.12	-75.7	13.3	17	3.0
Genesee River (Charlotte Docks) At Rochester	Ontario	-8.95	-60.8	10.7	4	1.9
Niagara River (Lake Ontario) At Fort Niagara	Ontario	-6.76	-51.2	2.9	4	184
Oswego River At Lock 7 At Oswego	Ontario	-9.46	-65.7	9.9	11	4.8
Sandy Creek Near Adams	Ontario	-11.51	-77.0	15.1	17	0.21
Tonawanda Creek At Batavia	Ontario	-11.04	-74.2	14.2	7	0.18
Grand River (Ontario)	Erie	-10.70	-74.0	11.5	72	1.8

* $\delta^{18}O$ and $\delta^{2}H$ are amount weighted to discharge following equation (2).

** Deuterium excess values are computed as (Dansgaard 1964): deuterium excess = $\delta^{2}H - 8 \cdot \delta^{18}O$

*** Discharge reported is an average of daily discharge measurements for days that isotope samples were acquired

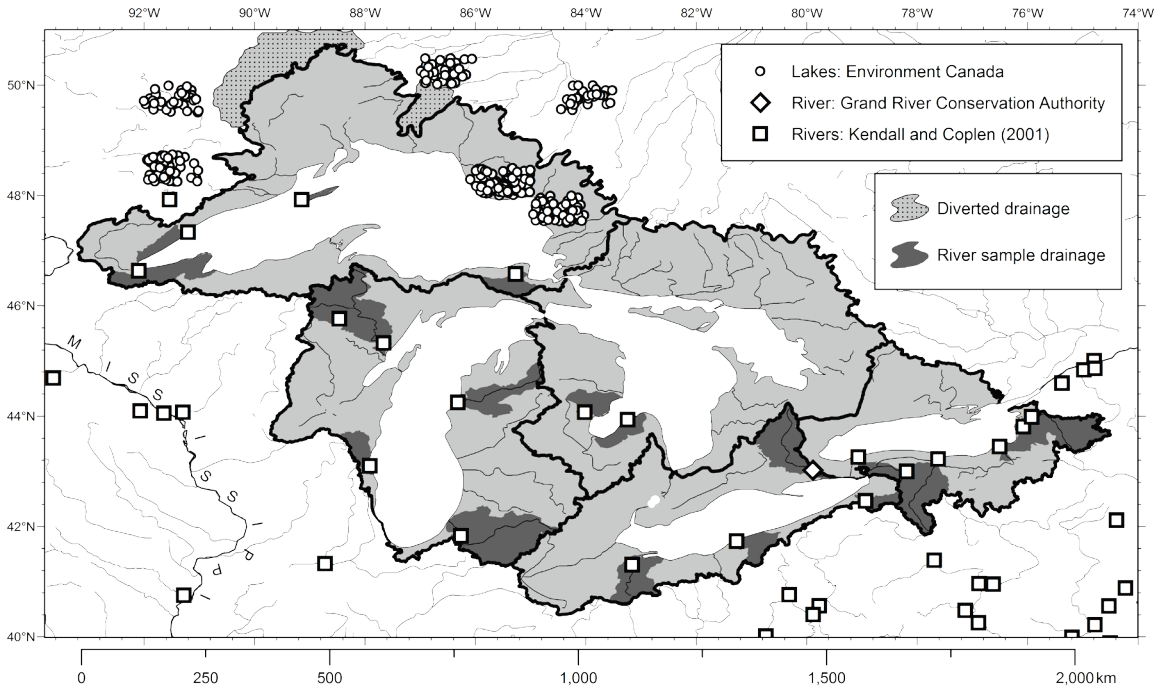

Figure 2-4. Sampling locations for $\delta^{18}O_{H2O}$ and $\delta^{2}H_{H2O}$ in rivers and lakes in the Great Lakes basin (grey) and surrounding region. River data are from Kendall and Coplen (2001) and the Grand River Conservation Authority. Lakes (n = 312) are from an Environment Canada sampling campaign completed in 2008.

The isotopic data collected for this study have now been reviewed. Next, required climatic, hydrologic and spatial data utilized in this study are presented.

2.1.2 Hydrologic, physical climate and spatial data

The EPA-led Great Lakes Environmental Database (GLENDA) provides a large amount of publicly-available data from cruises on the Great Lakes. The physical and chemical data for the spring and summer cruises of 2007 have been united with the isotopic results discussed above to form a single database. Chemical parameters integrated into the database include: pH, alkalinity, conductivity, chloride concentrations, nitrate concentration (as total oxidized nitrate), bulk phosphate concentration, filtrate phosphate concentration, silica concentration (reported as dissolved Si) and dissolved oxygen. Additional analytes available from CTD (conductivity temperature depth) measurements and various analyses include temperature, irradiance, transmittance, fluorescence, beam-attenuation and chlorophyll-a concentration. Major ion geochemistry was not analyzed for samples collected during the 2007 cruise, with the exception of chloride and bicarbonate (expressed in units of alkalinity as $CaCO_3$). However, analytical results of (Ca^{2+}), (Mg^{2+}) and (Na^{+}) are available for 271 samples collected in 2004 and 144 samples from 2005 (EPA, personal communication).

Various sources of climate data exist for the Great Lakes basin. Relative humidity values have been obtained from 10-minute grids described by New et al. (2002) and Mesinger et al. (2006). These sources also provide monthly average temperature values for the lower troposphere. Atmospheric temperature data were also obtained from the National Ocean and Atmospheric Administration (NOAA; Tim Hunter, personal communication). These datasets were produced from land-based temperature monitoring stations. A Voronoi (Thiessen) polygon approach was taken to develop average over lake temperatures.

Monitoring buoys deployed over the Great Lakes provide additional relative humidity (calculated from reported dew point temperatures) and air and lake temperature data (NOAA 2011). This dataset is crucial for estimating over-lake conditions. Locations of monitoring buoys used in this study are shown in Figure 2-5.

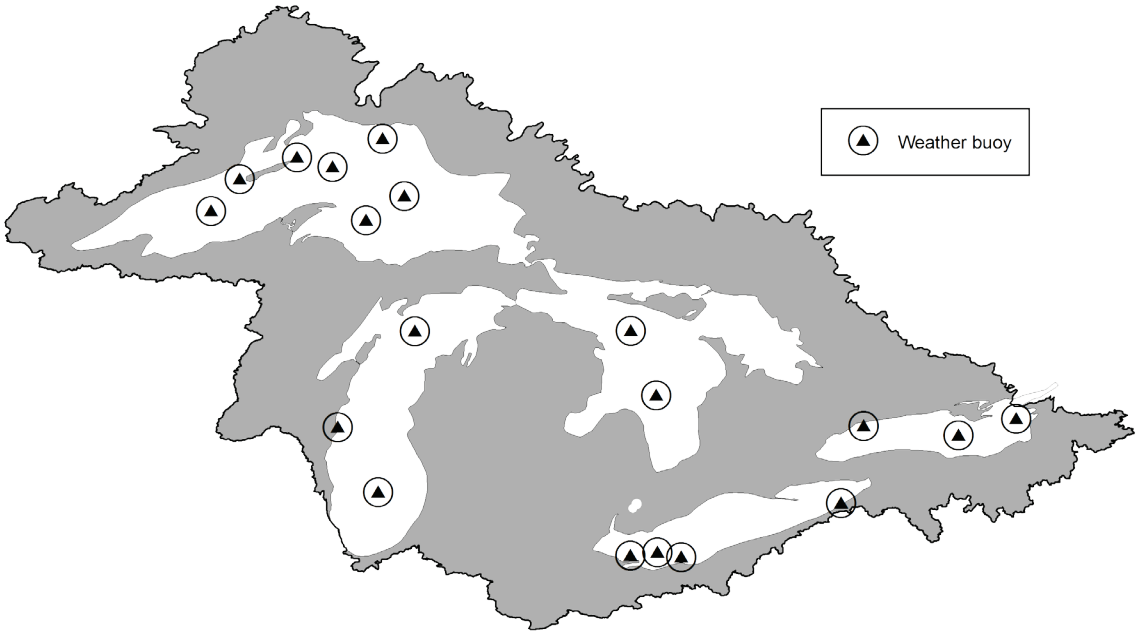

Figure 2-5. Locations of National Data Buoy Center (NDBC) monitoring buoys used in this study. Long-term monthly mean temperature and relative humidity have been extracted for each of the 19 stations in the map.

In addition to the temperature dataset, NOAA provided historical datasets for total daily gauged inflows to each Great Lake and estimates for over lake precipitation by a Voronoi-polygon approach. Connecting channel inflows have also been compiled. These fluxes are crucial for calculating the total hydrologic input to each Great Lake and for isotopic flux weighting of inputs to each Great Lake.

Spatial data acquired in the Great Lakes basin include: catchment delineations for each Great Lake basin, Great Lake coastlines and bathymetry, a digital elevation model, and Great Lakes basin hydrography. Many of these datasets were obtained from the Great Lakes Information Network (GLIN). Hydrographic catchment delineations for the United States were obtained from the United States Geological Survey (USGS 2010).

2.2 Stable isotope approach to calculating over lake evaporation

This section presents a development of the stable isotope mass balance approach to estimating lake evaporation as a proportion of inflow. First, the equations and theoretical formulation of the existing model and the proposed additions for large lake systems are presented. Next, the input values for the calculation are presented.

2.2.1 Equations and proposed modifications for large surface waters

The water balance of any reservoir can be calculated by a mass balance equation:

$$I - O = \Delta S \tag{3}$$

where I is the sum of all hydrologic inputs, O is the sum of all hydrologic outputs and ΔS is the change in storage per unit time. Inputs to a lake are in three general forms: river inputs (runoff), direct groundwater discharge and direct precipitation. Lake hydrologic outputs are lake evaporation, river outflows, or groundwater recharge. ΔS = 0 for lakes in hydrologic steady state (constant volume). Furthermore, if groundwater recharge by the lake is negligible - as is the case for the Great Lakes (Neff and Nicholas 2004) - it is useful to rearrange Equation 3 to the following form:

$$I = Q + E \tag{4}$$

where Q is surface outflow flux from the lake and E is the flux of water lost to evaporation. Next, we add a tracer term to each flux:

$$\delta_I I = \delta_Q Q + \delta_E E \tag{5}$$

where δ is the flux-weighted value for either $\delta^{18}O$ or $\delta^{2}H$ and the subscript corresponds to the flux. The balance now expresses the balance of a lake in terms of its stable isotope mass balance. Since stable isotopes are a conservative tracer - as oxygen and hydrogen are directly incorporated into the water molecule - there is no reactive or biological component to this stable isotope mass balance. For the Great Lakes, the surface outflow represents the isotopic composition of the upstream Great Lake ($\delta_{OUTFLOW} = \delta_L$). Combining Equations (4) and (5) produces an expression for evaporation as a proportion of inflow to a lake.

$$\delta_I I = \delta_L (I - E) + \delta_E E \tag{6}$$

solving for E/I, we have:

$$\frac{E}{I} = \frac{\delta_I - \delta_L}{\delta_E - \delta_L} \tag{7}$$

Evaporation as a proportion of inflow (E/I) is the target value for the stable isotope water balance in most lake studies. However, the E/I value is not the ideal format for the water balance of a North American Great Lake. The value of outflow is very well constrained for most of the Great Lakes (Figures 1-24 and 1-25) with the exception of Lake Michigan and Lake Huron's mixing fluxes. To take advantage of this, I substitute Equation (4) into Equation (7):

$$\frac{E}{Q+E} = \frac{\delta_I - \delta_L}{\delta_E - \delta_L} \quad (8)$$

Rearranging Equation (8), I produce a new expression for the total evaporative flux from a lake in terms of its isotope mass balance and gauged outflow:

$$E = \left(\frac{\delta_I - \delta_L}{\delta_E - \delta_I} \right) \cdot Q \quad (9)$$

The expression presented in Equation (9) capitalizes on the well established liquid surface outflow flux for each Great Lake to produce a quantitative estimate of total evaporation losses by a stable isotope mass balance method. This approach has potential to yield an estimate of the net outgoing evaporate flux that is better constrained than existing uncertainties in evaporation rates (±35 to ±45 percent; Neff and Nicholas 2005). Values of Q are constrained within 10% for the Great Lakes (Figures 1-24 and 1-25; Neff and Nicholas 2005); therefore, if uncertainties associated with the isotopic balance $\left(\frac{\delta_I - \delta_L}{\delta_E - \delta_I} \right)$ can be constrained within about 25% for the Great Lakes, then this may be the superior approach to estimating evaporation.

In order to utilize Equation (7) and Equation (9) to calculate an evaporative estimate for each Great Lake, the various input parameters: δ_I, δ_L and δ_E - must be discussed.

The isotope composition of lake waters is the simplest parameter. Lake water is sampled and analyzed by isotope ratio mass spectrometry. This step is complete for the Great Lakes; data are presented in Appendix A.

The isotope composition of inputs is slightly more complex than that of lake waters. Inputs to a Great Lake are either direct precipitation, intra-basin inflows (runoff) or connecting channel inputs from another Great Lake. Direct groundwater input is neglected here as the maximum discharge flux calculated (Grannemann et al. 2000) is less than the uncertainties for the other fluxes. The flux-weighted values for each of the inputs to a Great Lake are weighted against one another following:

$$\delta_I = \frac{U\delta_U + P\delta_P + R\delta_R}{I} \quad (10)$$

where U is the inflow from an upstream lake, including mixing inputs for Lakes Michigan and Huron. P represents direct over lake precipitation. R represents inflows from intra-basin rivers. Using Equation (10), the flux-weighted isotope composition of the combined inputs to each Great Lake (δ_I) is calculated.

This leaves the $\delta^{18}O$ and $\delta^{2}H$ value for the flux-weighted evaporate from each Great Lake (δ_E). δ_E is calculated following the approach proposed by Craig and Gordon (1965; Equation 14) with significant modifications to account for lake effects on the atmosphere. As a surface water body evaporates both equilibrium and kinetic isotope effects produce an isotopic fractionation between the liquid and vapour phases. First, the equilibrium separation (ε^*) is calculated by equation (11).

$$\varepsilon^* = (\alpha_{l-v}^* - 1) \quad (11)$$

where α* is the liquid-vapour fractionation factor, and is calculated as a third order function of air temperature following equations for $\delta^{18}O$ (Equation 12) and $\delta^{2}H$ (Equation 13) developed by Horita and Wesolowski (1994). All temperatures are weighted against estimates for monthly evaporation percentage.

$$1000 \cdot \ln \alpha_{l-v} * (\delta^{18}O) = -7.685 + 6.7123\left(\frac{10^3}{T}\right) + 1.6664\left(\frac{10^6}{T^2}\right) + 0.35041\left(\frac{10^9}{T^3}\right) \quad (12)$$

$$1000 \cdot \ln \alpha_{l-v} * (\delta^{2}H) = 1158.8\left(\frac{T^3}{10^9}\right) - 1620.1\left(\frac{T^2}{10^6}\right) + 794.84\left(\frac{T}{10^3}\right) - 161.04 + 2.9992\left(\frac{10^3}{T^3}\right) \quad (13)$$

Secondly, a kinetic separation factor (ε_K) represents a second vapour-liquid fractionation for an evaporating water body when the atmosphere is subsaturated (relative humidity: $h < 1$):

$$\varepsilon_K = C_K(1-h) \quad (14)$$

The C_K term for continental systems is derived from wind-tunnel experiments and is input as 0.0142 and 0.0125 for $\delta^{18}O$ and $\delta^{2}H$, respectively. However, the immense surface areas of the Great Lakes and marine-like moderating effects suggest the need to explore C_K values developed for laminar (smooth surface) conditions (0.0186 and 0.0165 for $\delta^{18}O$ and $\delta^{2}H$ following molecular isotopologue diffusivities from Merlivat 1978). Laminar conditions are chosen to best represent the Great Lakes region, as mean monthly wind speeds are generally less than seven metres per second (data from Mesinger et al. 2006; laminar wind speed conditions defined by Araguás-Araguás et al. 2000).

The composition of the atmospheric moisture (δ_A) in equilibrium with the isotope composition of precipitation weighted to seasonality in evaporation ($\delta_{P(E)}$) is calculated following Equation (15).

$$\delta_A = (\delta_{P(E)} - 10^3\varepsilon^*)/\alpha_{l-v}^* \quad (‰) \quad (15)$$

Finally, we add the outputs of equations 11, 14 and 15 for each Great Lake to calculate the isotope composition of the evaporate following the equation of Craig and Gordon (1965), as formulated by Gonfiantini (1986).

$$\delta_E = \left[\frac{(\delta_L/10^3 - \varepsilon^*)/\alpha_{l-v}^* - h(\delta_A/10^3) - \varepsilon_K}{1-h+\varepsilon_K}\right]\cdot 10^3 \quad (‰) \quad (16)$$

Now, a first estimate of evaporation as a proportion of all hydrologic inputs to each Great Lake (E/I) can be formulated following Equation 7. δ_L is the median isotope value of isotope analyses of water samples for each Great Lake, with the exception of Lake Erie (discussed in Chapter 3).

However, the first iteration of the E/I calculation produces awkward results that do not successfully match E/I results for the two isotopic tracers ($\delta^{18}O$ and $\delta^{2}H$; see results section, Table 3–4: E/I_i values). To successfully account for the effects the Great Lakes have upon their own downwind atmosphere, it is important to revisit the evaporation model to account for the incorporation of Great Lake surface waters into the overlying atmosphere through evaporation:

$$Z_{DOWN} = Z_{UP}\cdot(1-x) + Z_{SAT}\cdot(x) \quad (17)$$

The mixing term x represents the amount of the evaporated air parcel (A_{SAT}) incorporated into the overlying atmosphere. Z_{UP} represents an upwind value for the partial pressure of water vapour, air temperature, or δ_A weighted to monthly evaporation. Z_{SAT} represents a saturated air parcel (h = 1) with a temperature representative of a Great Lake surface water temperature during the evaporative season (accounting for latent heat of vaporization) and an isotope composition of δ_E (Equation (16) using initial upwind atmospheric conditions). The calculated "downwind" air-parcel (Z_{DOWN}) is computed following Equation (17) for three parameters: (i) air temperature, (ii) the isotope composition of atmospheric moisture (δ_A) and (iii) specific humidity (converted to relative humidity by calculating the saturation vapour pressure as a function of temperature (i) from Buck (1981)). The calculation for E/I is iterated with varying percentages of saturated air input (x: 0 to 25%) until E/I outputs for ^{18}O and ^{2}H agree..

An evaporate mixing approach was first proposed by Gat et al. (1996; pp. 6448), although the authors' did not include temperature effects on the saturation vapour pressure of the overlying air mass (mixed relative humidity values instead of specific humidity as is proposed by Equation (17). The approach utilizes a model that adds humidity and δ_E in one step. Another δ_A-δ_E mixing model was for small lakes downwind of Great Slave Lake, although lake-effects on humidity and temperature were not included (Brock et al. 2009; Benkert 2010). This approach utilized an estimated value of δ_E advecting via onshore winds from Great Slave lake to constrain E/I values for small lakes leeward of Great Slave Lake. δ_E for Great Slave Lake is calculated by the coupled approach first presented by Yi et al. (2008). Yi et al. use an index lake with a closed water balance (E/I = 1) and a sufficiently long residence time to integrate the isotope signature of input waters (~10 years). Using this index lake with a known E/I value of 1 and a reasonably well constrain input value (δ_I) a value for δ_A is calculated for this ~1000km^2 region. Yi et al. capitalize on the well-constrained δ_A to estimate a unique value for the isotope input to each lake (δ_I) by assuming δ_I must fall on the local meteoric water line and that using a conservation of isotopes:

$$\left(E/I_{^{18}O} = E/I_{^{2}H} \;\; OR \;\; \frac{\delta_I^{\,18O} - \delta_L^{\,18O}}{\delta_E^{\,18O} - \delta_L^{\,18O}} = \frac{\delta_I^{\,2H} - \delta_L^{\,2H}}{\delta_E^{\,2H} - \delta_L^{\,2H}} \right)$$

Kinetic isotope effects govern the δ^2H-$\delta^{18}O$ position of each of the lake below the meteoric water line (Figure 3-1; Figures 3-12a to e). The ratio of to kinetic isotope separation to equilibrium separation between the lake and vapour phases for the Great Lakes (ε_K /ε^*) ranges between 0.39 to 0.40 for $\delta^{18}O$, and 0.037 to 0.045 for δ^2H. Clearly, kinetic effects are much more important to $^{18}O/^{16}O$ ratios than $^{2}H/^{1}H$ under evaporation, as kinetic effects are only ~5 percent of mass-dependent equilibrium separation for deuterium-protium ratios. For $^{18}O/^{16}O$, separation factors for kinetic effects are ~40% of those for equilibrium effects, a much larger proportion than that of deuterium. These ratios explain the lower slopes observed for arid regions. In arid areas, kinetic effects become much more important to the evaporation process. The ratio of kinetic separation factors for the two isotope tracers ($\varepsilon_{K(18O)}$/ $\varepsilon_{K(2H)}$ of 0.88) plays a larger role, as it is inversely and linearly proportional to relative humidity (Equation 14). The equilibrium defined slope ($\varepsilon^*_{18O}/\varepsilon^*_{2H}$) is temperature dependent, and is close to 8.5. It is the competing effect of these two slopes, controlled dominantly by humidity and less so by temperature - that produces observed isotopic ^{18}O- and ^{2}H-enrichment trends in δ^2H-$\delta^{18}O$ space.

2.2.2 E/I calculation inputs for the Great Lakes

To calculate evaporation using the aforementioned equations (Section 2.2.1) we require an accurate determination of input values for several isotopic and physical climate parameters. These are (i) $\delta^{18}O$ and $\delta^{2}H$ values of precipitation weighed to seasonality in evaporation ($\delta_{P(EW)}$, evaporation weighted), (ii) $\delta^{18}O$ and $\delta^{2}H$ values of precipitation weighted to precipitation amount ($\delta_{P(AW)}$, amount weighted), (iii) $\delta^{18}O$ and $\delta^{2}H$ values of intra-basin runoff weighed to river discharge ($\delta_{R(FW)}$, flux weighted), (iv) $\delta^{18}O$ and $\delta^{2}H$ values of waters from each of the Great Lakes, (v) temperatures of each Great Lake and the overlying atmosphere, weighted to the evaporation season and (vi) over lake relative humidity weighted to the evaporation season.

Section 2.2.2.1 presents the method used for $\delta_{P(EW)}$ (i) and $\delta_{P(AW)}$ (ii). Section 2.2.2.2 will present values for $\delta_{R(FW)}$ (iii) for each of the Great Lakes. Sampling sites and analytical techniques for measuring $^{18}O/^{16}O$ and $^{2}H/^{1}H$ in Great Lakes waters (iv) is presented in Section 2.2.1 (Figure 2-1). Finally, Section 2.2.2.4. will present physical climate and lake data (v and vi). After a description of calculation input parameters have been presented the results of the evaporation calculation will be discussed in Chapter 3.

2.2.2.1 Isotope composition of over lake precipitation: δ_P

Characterization of δ_P is a crucial input for a stable isotope mass balance for two reasons. First, δ_P is assumed to be in equilibrium with atmospheric moisture during the vapour condensation process. This has been shown not to be the case for ice crystal formation, but is a suitable assumption for liquid vapour phase changes (Merlivat and Jouzel 1978). The value of δ_P is useful for calculating the isotope composition of atmospheric moisture in order to formulate a value for the outgoing evaporate. However, this approach requires weighting to seasonal evaporation (Gibson 2002a). The isotope composition of precipitation weighted to evaporation is denoted by $\delta_{P(EW)}$ (EW: evaporation weighted). Secondly, $\delta_{P(AW)}$ is the isotope composition of precipitation weighted to precipitation amount (AW: amount weighted). This is a large hydrologic input to the Great Lakes, particularly so for Lakes Superior and Michigan that do not have a connecting channel inflow. The formulation of δ_P weighted to the evaporation season ($\delta_{P(EW)}$) and weighted to over-lake precipitation amount ($\delta_{P(AW)}$) will be presented here.

The isotope composition of direct precipitation can be estimated from a variety of approaches. Fortunately, many isotope precipitation monitoring stations are present in the Great Lakes region (reviewed in section 2.1.1). Four approaches are tested to examine the differences in outputs: a Voronoi-polygon area-precipitation amount weighting approach, a stepwise regression approach with Cressman (1959) corrections, an inverse distance weighted interpolation approach and use of an existing empirical stepwise grid that is corrected to nearby station outputs (Bowen 2009).

The Voronoi (or Thiessen) polygon approach creates a series of polygons from a set of points in space. One polygon is constructed for each data point. All area within the polygon is closer to the measurement site within the polygon than any other point in the dataset (Figure 2-1). If the area within the polygon is assumed to be best represented by precipitation collected at the most proximal CNIP, USNIP or IAEA monitoring station. Finally, the amount weighted isotope composition of direct precipitation is weighted by area and precipitation amount for each of the Great Lakes by Equation (18):

$$\delta_{P(THIESSEN)} = \sum_{i=1}^{i} \delta_{i,\,P(AMOUNT)} \cdot \frac{(A_{i,\,THIESSEN} \cdot P_{i,\,THIESSEN})}{\sum_{i=1}^{n} A_{i,\,THIESSEN} \cdot P_{i,\,THIESSEN}} \quad (18)$$

where $\delta_{P(THIESSEN)}$ is an estimate for the value of $\delta^{18}O$ or $\delta^{2}H$ computed by a Voronoi-area and precipitation amount weighting method. $A_{i,\,THIESSEN}$ represents the percentage of a Great Lake (by area) that is closest to the sampling station i. $P_{i,\,THIESSEN}$ is the mean annual precipitation at sampling station i. $\delta_{i,\,P(AMOUNT)}$ is the amount-weighted value of $\delta^{18}O$ or $\delta^{2}H$ for station i. Results for the Voronoi-polygon area and precipitation amount weighting approach are presented in Table 2–5. The weighting term in Table 2–5 refers to $\frac{(A_{i,\,THIESSEN} \cdot P_{i,\,THIESSEN})}{\sum_{i=1}^{n} A_{i,\,THIESSEN} \cdot P_{i,\,THIESSEN}}$.

Table 2–5. Voronoi-area and precipitation-amount weighting results for each Great Lakes basin.

Station	AREA %	$\delta^{18}O$ * (‰SMOW)	$\delta^{2}H$ * (‰SMOW)	Precip. (mm/yr)	Weighting (%)	Over lake precipitation ($\delta^{18}O$, $\delta^{2}H$, deuterium excess)
LAKE SUPERIOR						
Morcell Experimental Frst.	0.8	-11.17	-89.1	934	0.8	-9.58, -69.8, 6.8
Atikokan	4.4	-12.61	-91.5	683	3.1	
Trout Lake	57.4	-9.06	-67.3	1090	63.7	
Douglas Lake	37.5	-10.27**	-72.2	852	32.5	
LAKE HURON						
Egbert	37.4	-10.35	-72.8	784	35.0	-10.14, -70.9, 10.2
Douglas Lake	48.9	-10.27	-72.2	852	49.7	
Simcoe	13.7	-9.27	-62.2	941	15.4	
LAKE MICHIGAN						
Lake Geneva	27.0	-7.51	-52.4	1175	32.9	-8.15, -57.7, 7.5
Trout Lake	3.3	-9.06	-67.3	1090	3.7	
Douglas Lake	39.5	-10.27	-72.2	852	34.9	
Chicago	30.2	-6.18	-44.7	908	28.4	
LAKE ERIE						
Simcoe	48.0	-9.27	-62.2	941	47.8	-8.42, -55.2, 12.2
Coshocton	38.2	-7.41	-46.6	977	39.5	
Chautauqua	13.8	-8.36	-55.5	864	12.6	
LAKE ONTARIO						
Egbert	28.6	-10.35	-72.8	784	23.4	-8.79, -61.6, 8.7
Simcoe	2.5	-9.27	-62.2	941	2.5	
Ottawa	4.0	-10.97	-75.2	909	3.8	
Chautauqua	5.5	-8.36	-55.5	864	4.9	
Aurora Research Farm	59.4	-8.12	-57.3	1058	65.5	

* $\delta^{18}O$ and $\delta^{2}H$ are amount weighted to precipitation following equation (1).

** Only $\delta^{2}H$ data available; $\delta^{18}O$ is estimated by the local meteoric water line for the Great Lakes basin.

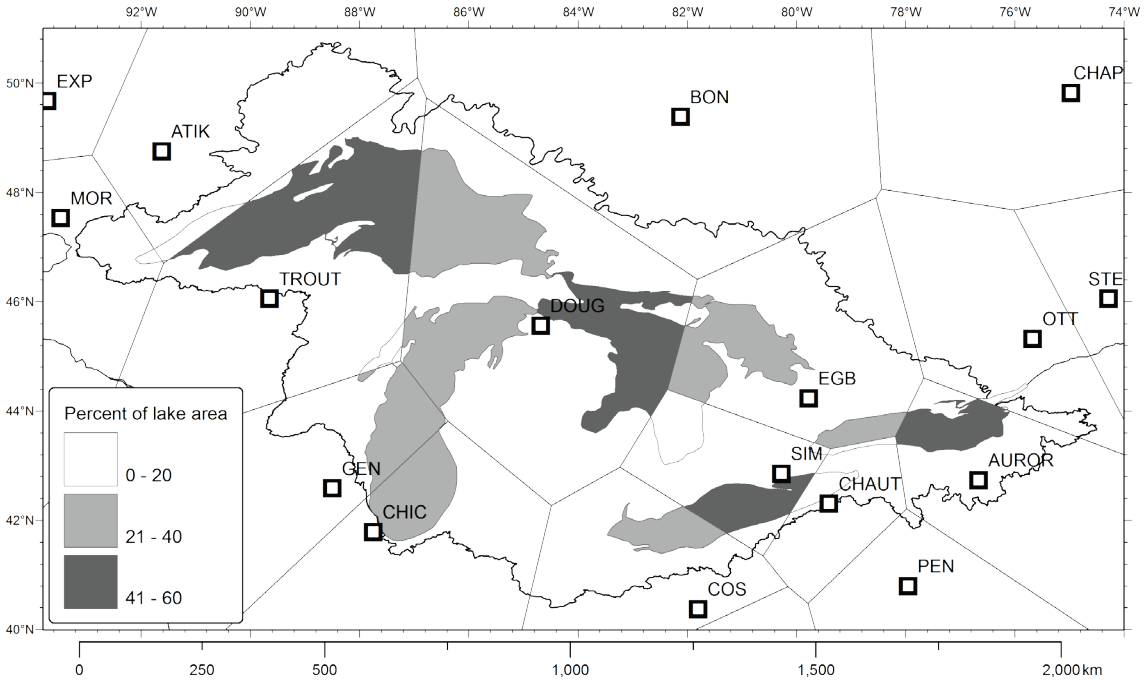

Figure 2-6. Voronoi-polygons in the Great Lakes basin based upon the ten CNIP/USNIP stations with analyses for both $\delta^{18}O$ and $\delta^{2}H$. Shading portrays the percentage of a Great Lake basin most-proximate to a given CNIP/USNIP station.

The Voronoi-polygon approach to estimating δ_P for over lake precipitation has drawbacks. The approach does not consider air mass advection trajectories. This may be a source of considerable error for the Great Lakes region as the dominant wind direction pays a significant role on the source of moisture and consequently the $\delta^{18}O$ and $\delta^{2}H$ values of precipitation. For example, the Voronoi-polygon for Trout Lake covers a significant portion of Lake Superior (57.4 percent; Figure 2-6). However, westerly and north-westerly winds control air mass advection in the region (Figure 1-22); therefore, this station may not represent precipitation over Lake Superior.

Another approach is attempted applying a Cressman-type (1959) correction technique to a stepwise regression model at a monthly time step. To accomplish this, monthly mean $\delta^{18}O$ and $\delta^{2}H$ values are computed for each precipitation monitoring station. Data are presented are Table 2–6.

Table 2–6. Average monthly $\delta^{18}O$ and $\delta^{2}H$ (next page) values for stations within or directly surrounding the Great Lakes basin.

Station	$\delta^{18}O$ (monthly average of all reporting years for a sampling station)											
	Jan	Feb	Mar	Apr	May	Jun	Jul	Aug	Sep	Oct	Nov	Dec
Atikokan (Ontario)	-26.01	-22.90	-18.39	-11.53	-9.72	-9.59	-8.83	-8.72	-10.39	-15.16	-18.01	-22.69
Bonner Lake Ontario	-23.91	-20.91	-16.98	-10.93	-10.20	-9.36	-9.96	-10.38	-11.46	-12.61	-17.82	-21.58
Chapais Quebec	-22.08	-21.37	-18.85	-13.26	-11.52	-10.26	-10.69	-10.39	-11.92	-14.40	-16.36	-19.90
Chicago (Midway Illinois)	-13.99	-11.90	-7.86	-6.68	-4.68	-2.93	-2.77	-3.58	-4.70	-5.38	-9.54	-11.28
Coshocton (Ohio)	-11.75	-11.14	-9.24	-6.01	-5.62	-4.23	-5.64	-4.52	-6.90	-6.86	-9.67	-11.29
Douglas Lake	-20.12	-20.05	-16.88	-6.36	-6.15	-6.49	-11.51	-7.11	-10.86	-9.59	-14.33	-21.11
Egbert Ontario	-15.86	-13.65	-15.92	-9.31	-7.26	-6.78	-6.71	-6.99	-9.06	-11.53	-13.99	-14.11
Experimental Lakes Area	-23.31	-21.72	-19.44	-13.51	-11.02	-10.07	-8.80	-9.19	-10.07	-13.09	-18.62	-18.71
Morcell Experimental Forest	-20.72	-21.38	-15.33	-13.37	-9.38	-8.87	-7.85	-9.02	-10.42	-11.51	-19.34	-19.65
Aurora Research Farm	-13.92					-6.08	-5.43	-7.04	-6.04	-4.97	-11.52	-18.25
Chautauqua	-16.43			-11.03	0.98	-6.17	-6.49	-6.37	-7.23	-9.31	-10.40	-19.89
Ottawa Ontario	-17.03	-16.39	-13.65	-10.28	-8.20	-7.94	-7.72	-7.68	-8.53	-10.88	-12.49	-16.34
Simcoe (Ontario)	-17.25	-16.83	-11.07	-8.16	-7.00	-7.03	-5.64	-6.37	-8.54	-11.50	-10.90	-13.29
Trout Lake		-14.67	-15.85		-7.29	-6.40	-7.87	-7.42	-9.22	-9.50	-12.40	-21.80
Lake Geneva	-12.61	-15.63	-7.47	-10.50	-9.01	-4.48	-4.59	-5.63	-7.35	-6.91	-11.10	-11.09

Table 2–6 (continued).

Station	δ^2H (monthly average of all reporting years for a sampling station)											
	Jan	Feb	Mar	Apr	May	Jun	Jul	Aug	Sep	Oct	Nov	Dec
Atikokan (Ontario)	-194.8	-171.6	-138.7	-77.4	-71.0	-68.0	-62.3	-60.8	-74.3	-110.0	-132.5	-170.2
Bonner Lake Ontario	-179.9	-157.8	-125.2	-78.3	-74.2	-68.3	-73.4	-74.0	-81.2	-90.0	-129.8	-161.7
Chapais Quebec	-163.6	-160.3	-140.5	-97.6	-82.8	-72.0	-76.5	-72.8	-81.9	-102.3	-116.3	-145.4
Chicago (Midway Illinois)	-102.6	-91.6	-55.0	-39.3	-36.2	-24.2	-19.9	-28.6	-37.8	-35.2	-62.1	-79.9
Coshocton (Ohio)	-80.7	-75.3	-60.2	-37.0	-34.0	-22.6	-34.8	-28.2	-39.7	-41.4	-55.9	-76.8
Douglas Lake												
Egbert Ontario	-112.9	-96.8	-115.8	-67.8	-52.5	-45.6	-47.5	-49.1	-62.7	-82.0	-95.8	-103.0
Experimental Lakes Area	-175.7	-164.5	-146.9	-99.7	-82.0	-72.5	-63.0	-67.3	-74.0	-93.2	-137.6	-140.1
Morcell Experimental Forest	-169.7	-161.0	-120.3	-94.5	-54.1	-54.6	-63.5	-70.9	-84.8	-120.6	-153.1	-154.4
Aurora Research Farm				-65.2	-80.7	-33.3	-28.3	-48.0	-56.3	-52.5	-67.4	-97.9
Chautauqua	-126.3			-86.2	-3.6	-43.9	-38.2	-39.6	-43.4	-57.8	-77.3	-135.7
Ottawa Ontario	-121.6	-120.3	-97.6	-71.4	-56.8	-51.6	-54.0	-51.3	-58.8	-71.5	-82.6	-114.1
Simcoe (Ontario)	-124.2	-106.0	-80.3	-59.6	-48.6	-45.6	-37.9	-40.9	-56.8	-77.3	-72.6	-89.7
Trout Lake	-128.9	-104.0	-114.3	-80.3	-17.1	-40.3	-48.7	-59.5	-74.9	-92.4	-92.4	-144.1
Lake Geneva	-105.0	-109.8	-50.4	-73.4	-45.4	-30.0	-30.1	-28.8	-52.0	-58.4	-56.3	-115.0

Next, a second-order polynomial fit is regressed for latitude and $\delta^{18}O$ or $\delta^{2}H$ at a monthly time step for all stations in the Great Lakes region (stepwise method inspired by works of Bowen and Wilkinson (2002)). A $\delta^{18}O$ lapse rate of 0.21 per mille per 100 metres is added (Chamberlain and Poage 2000). Sample regressions are presented in Figure 2-7. Utilizing digital elevation model data and latitude, a monthly grid for the Great Lakes region is prepared following the latitude-altitude relationships presented in Table 2–7.

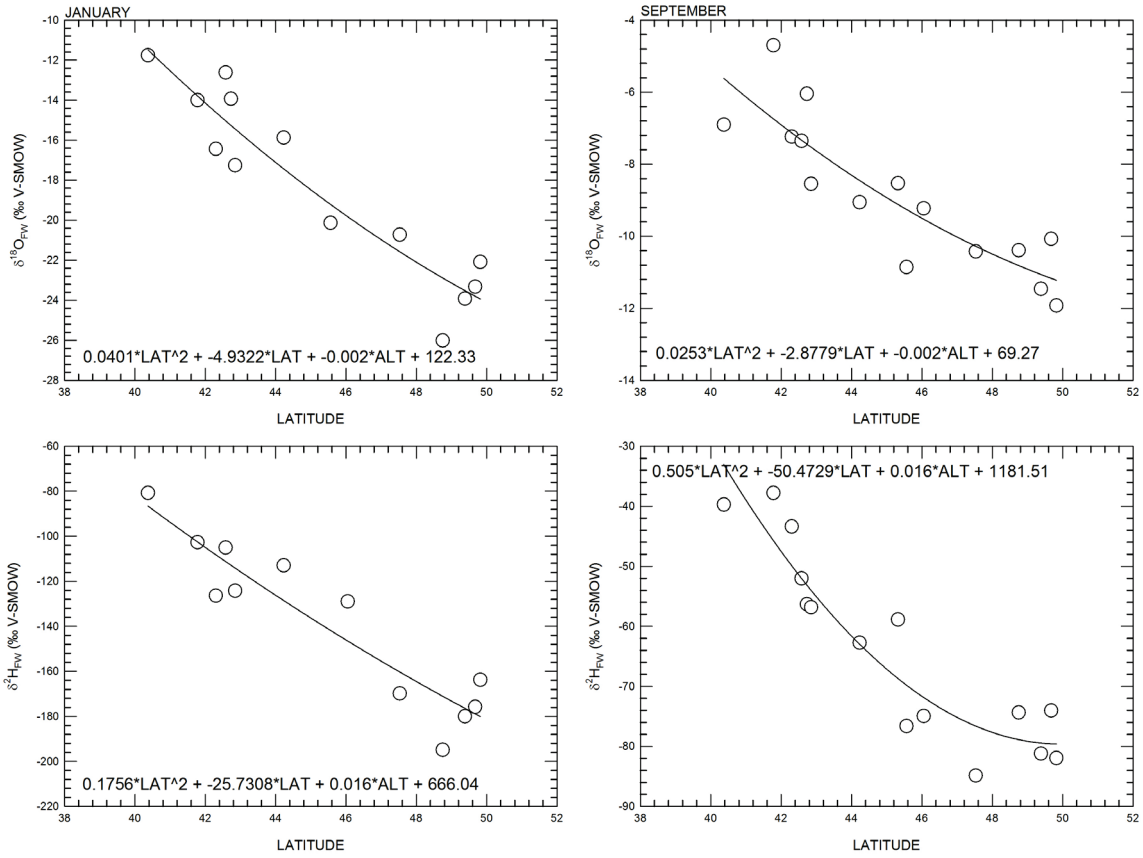

Figure 2-7 - Second-order polynomial fit between $\delta^{18}O$ and latitude (upper plots) or $\delta^{2}H$ and latitude (lower plots) for stations in the Great Lakes region. Two months are shown here: January (left plots) and September (right plots).

Table 2–7. Regressions for stations measuring isotopes in precipitation within the Great Lakes region.

$\delta^{18}O = a_{18O}\cdot LAT^2 + b_{18O}\cdot LAT + c_{18O}\cdot ALT + d_{18O}$ $\delta^{2}H = a_{2H}\cdot LAT^2 + b_{2H}\cdot LAT + c_{2H}\cdot ALT + d_{2H}$								
Month	a_{18O}	b_{18O}	c_{18O}	d_{18O}	a_{2H}	b_{2H}	c_{2H}	d_{2H}
Jan	0.0401	-4.9322	-0.002	122.33	0.1756	-25.7308	-0.016	666.04
Feb	0.0098	-2.0201	-0.002	54.31	-0.0433	-5.5234	-0.016	215.01
Mar	0.0536	-6.0040	-0.002	147.31	0.447	-50.1703	-0.016	1249.43
Apr	-0.0157	0.8666	-0.002	-16.88	0.0811	-11.8099	-0.016	296.39
May	-0.3580	2.8029	-0.002	61.49	-0.7224	62.0280	-0.016	-1375.43
Jun	-0.0013	-0.5280	-0.002	19.37	-0.1416	7.9745	-0.016	-117.16
Jul	0.0326	-3.5624	-0.002	86.88	0.2475	-27.5924	-0.016	688.77
Aug	0.0097	-1.4613	-0.002	38.78	0.1445	-17.9033	-0.016	461.82
Sep	0.0253	-2.8779	-0.002	69.27	0.5050	-50.4729	-0.016	1181.51
Oct	0.0021	-1.0105	-0.002	31.13	0.6449	-65.4261	-0.016	1557.31
Nov	0.0016	-1.1419	-0.002	34.72	0.2112	-28.3025	-0.016	750.64
Dec	0.1235	-12.1999	-0.002	280.56	0.7738	-78.4132	-0.016	1831.18

* Units are decimal degrees for latitude and metres above sea level for altitude (ALT)

Finally, the regressions in Table 2–7 are plotted as gridded data within the Great Lakes region. However, a final step is required to correct for localized differences in $^{18}O/^{16}O$ and $^{2}H/^{1}H$ in precipitation. Cressman (1959) analyses apply a correction on the basis of inverse distance radius of influence and have been applied to successfully map stable isotopes in precipitation in previous works of Birks et al. (2002). The approach requires an initial estimated value that is then corrected to nearby points of a known value (in this case these are monitoring stations for isotopes in precipitation).

$$\delta_{i,j} = \delta(LAT, ALT)_{i,j} + C_{i,j} \tag{19}$$

where $\delta_{i,j}$ is a Cressman-type corrected value for month i and grid cell j. $\delta(LAT,ALT)_{i,j}$ is the result of the empirical formulae presented in Table 2–7 for values of $\delta^{18}O$ or $\delta^{2}H$. $C_{i,j}$ is the Cressman (1959) correction applied to $\delta(LAT,ALT)_{i,j}$ to calculate an appropriate value of $\delta^{18}O_{i,j}$ or $\delta^{2}H_{i,j}$ and is defined as:

$$C_{i,j} = \frac{\sum_{k=1}^{n_k}\left(\left(\delta_k - \delta(LAT, ALT)_{i,j}\right)\cdot\frac{R^2 - D_{k,j}}{R^2 + D_{k,j}}\right)}{n_k} \tag{20}$$

where δ_k is the average value of $\delta^{18}O$ or $\delta^{2}H$ for month i at any grid cell j. R is the radius of influence that a measurement will extend to on the $\delta(LAT,ALT)_{i,j}$ grid, and $D_{k,j}$ is the distance of any given grid cell j to a measurement station k, and the analysis is completed for all measurement stations (n_k). The

Cressman approach and its application to stable isotopes in precipitation were reviewed by Bowen (2010). The procedure is completed for the Great Lakes basin using a radius of influence of 500 km (a 500 km buffer around monitoring stations provides each grid cell within the Great Lakes basin with at least one influencing station). The resulting precipitation grids are presented in Figure 2-9 and 2–11.

Finally, an estimate for $\delta^{18}O$ and $\delta^{2}H$ of over lake precipitation is calculated for each lake. Zonal statistics are applied to the Cressman-type (1959) corrected grid to calculate the isotopic composition of monthly mean over lake precipitation for each Great Lake and are reported in Table 2–8 and shown in Figure 2-8. Zonal is referred to here as the statistics of a raster within a defined area (examples: a Great Lake's catchment area, or the over-lake area of a Great Lake).

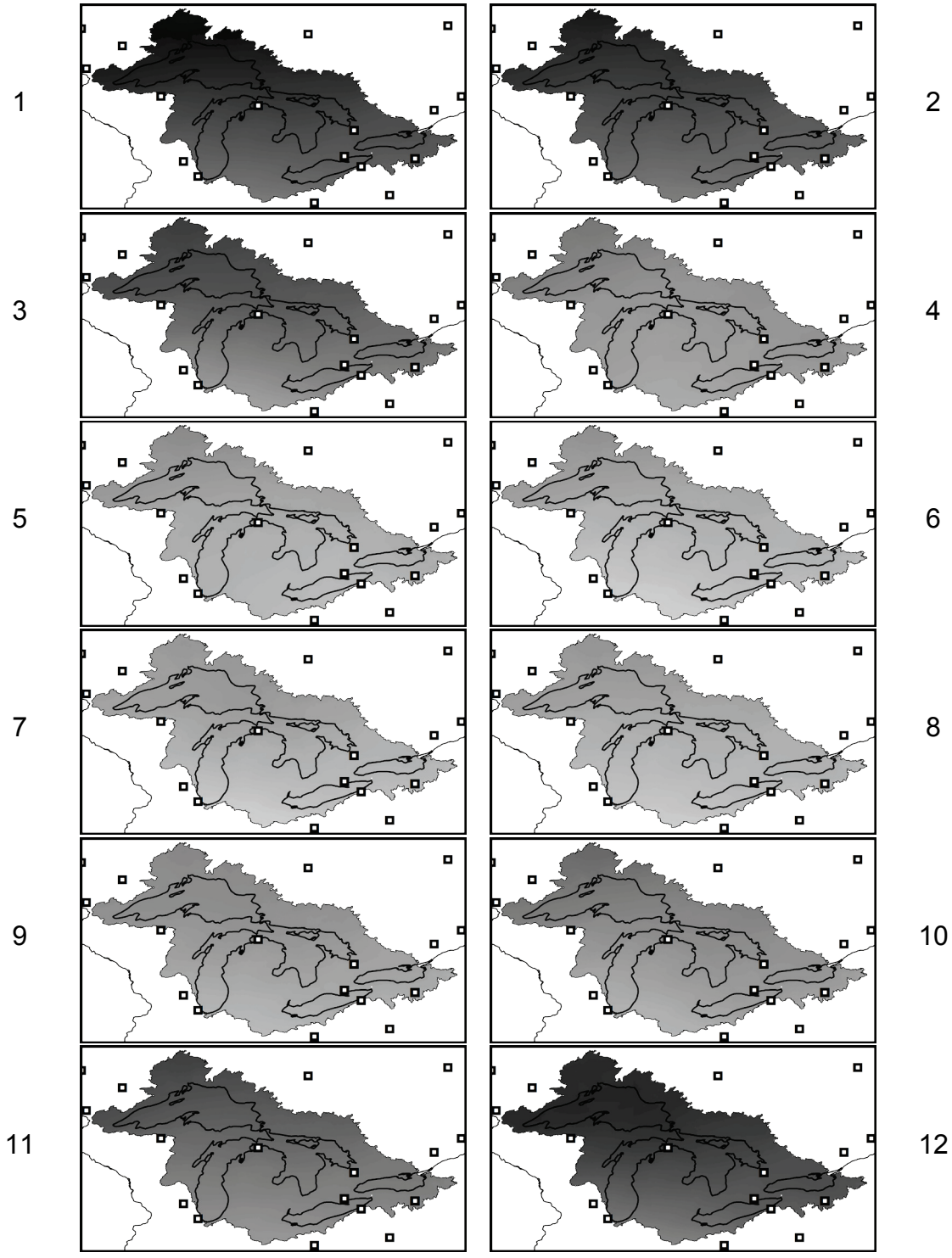

Figure 2-8. Cressman (1959) corrected values for monthly $\delta^{18}O$ in H_2O in precipitation. Monitoring stations are presented as white squares. Greyscale is from $\delta^{18}O$ = 0‰ (black) to $\delta^{18}O$ = -30‰ (white). Months are numbered from one to 12 next to each subplot.

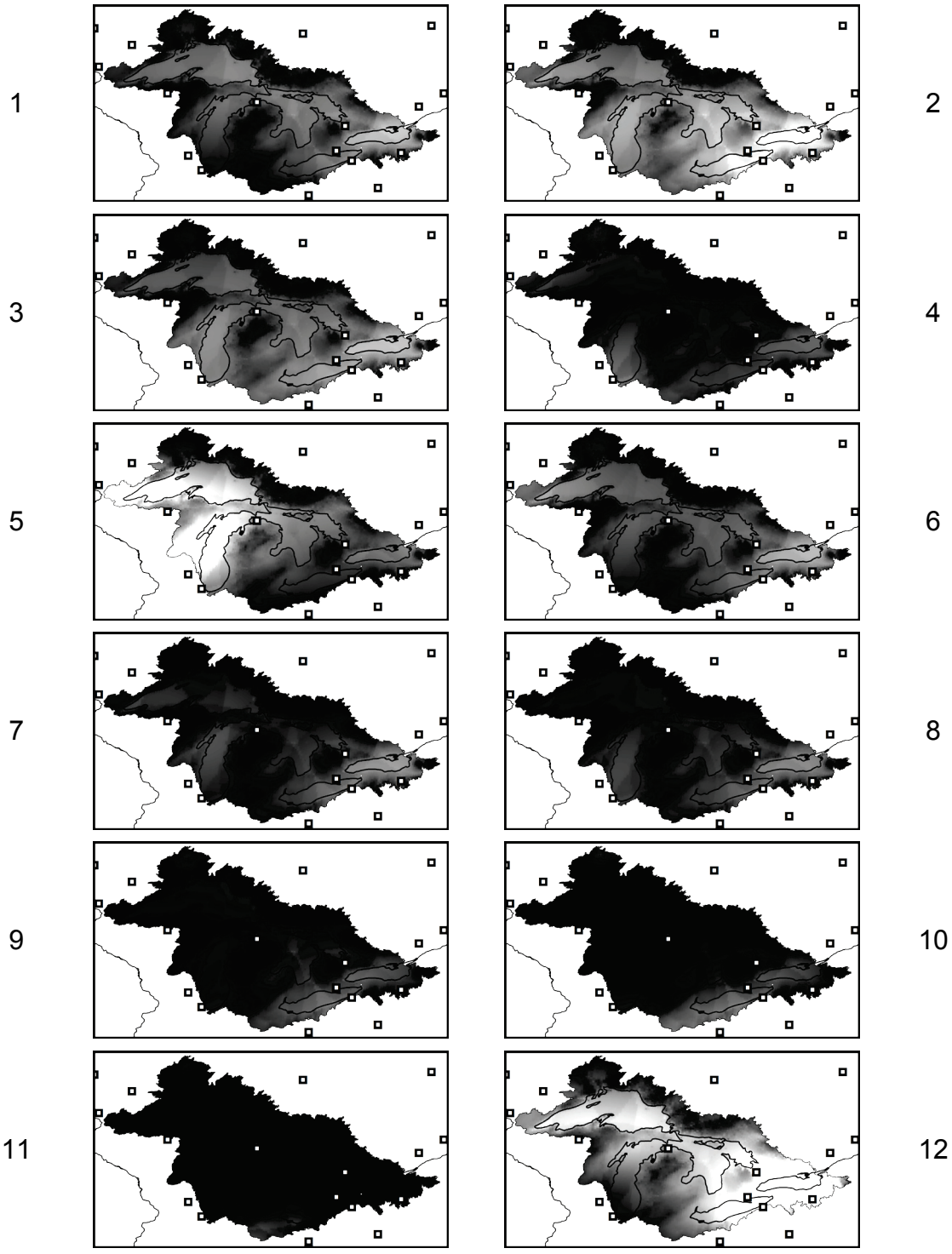

Figure 2-9. Monthly deuterium excess ($\delta^2H - 8 \cdot \delta^{18}O$) computed using the correction method of Cressman (1959) δ^2H and $\delta^{18}O$ grids of in H_2O in precipitation. Monitoring stations are presented as white squares. Greyscale is from 0 (black) to 12 (white). Months are numbered from one to 12 next to each subplot.

Table 2–8. Monthly zonal means for the Great Lakes: Cressman (1959) correction method from CNIP, USNIP and IAEA monitoring stations

Month	Zonal mean values for over lake $\delta^{18}O$ and $\delta^{2}H$				
	Superior	Huron	Michigan	Erie	Ontario
January	-21.25, -163.4	-18.03, -137.2	-16.27, -125.2	-14.65, -110.9	-16.08, -118.7
February	-19.34, -147.9	-16.57, -123.4	-15.42, -115	-13.6, -97.6	-14.72, -105
March	-16.72, -128.3	-14.28, -107.6	-12.14, -89.7	-11.06, -79.9	-12.67, -91.3
April	-10.55, -81.8	-8.97, -69.6	-8.49, -64.1	-8.28, -62	-9.26, -68.1
May	-8.62, -57.9	-7.04, -48.8	-6.98, -43.6	-5.87, -43.2	-6.88, -48.1
June	-8.16, -59.1	-6.7, -47.8	-5.51, -39.5	-5.44, -37.7	-6.43, -42.1
July	-8.63, -66.1	-7.44, -56.1	-6.41, -47.2	-5.51, -38.2	-6.33, -42.4
August	-8.32, -64.6	-6.98, -52.4	-6.09, -44.9	-5.67, -39.8	-6.66, -45.7
September	-10.05, -79.1	-8.88, -68.7	-7.94, -61.9	-7.19, -51.6	-7.85, -57.5
October	-11.72, -97.8	-10.01, -80.6	-8.33, -68.8	-8.32, -60.5	-9.18, -68.8
November	-15.7, -132	-13.13, -108.9	-11.92, -104.8	-10.66, -87.3	-11.86, -98.8
December	-20.45, -153.1	-17.74, -130.8	-16.15, -122.7	-14.54, -102.4	-16.4, -111.4
Amount weighted	-10.81, -78.1	-9.59, -67.2	-8.56, -60.5	-9.14, -63.3	-8.15, -55.4
Evaporation weighted	-15.70, -122.6	-13.74, -105.4	-11.78, -92.2	-8.93, -65.7	-12.16, -88.8

Two more approaches for estimating $\delta^{18}O$ and $\delta^{2}H$ in precipitation over the Great Lakes are taken here for comparison against the Voronoi-polygon and Cressman approaches described earlier. First, values from a global stepwise regression approach (Bowen and Wilkinson 2002) are used to produce zonal monthly mean $\delta^{18}O$ and $\delta^{2}H$ in precipitation. This approach selected low altitude IAEA isotope monitoring stations from around the world and produced a latitude-$\delta^{18}O$ regression. Next, Bowen and Wilkinson reported that high altitude stations plotted with significantly lower $\delta^{18}O$ values than the latitude-$\delta^{18}O$ relationship predicted. A second regression of the residuals from the $\delta^{18}O$-latitude relationship was plotted against altitude. This regression suggested a global $\delta^{18}O$ lapse rate of -2 per mille per kilometre in elevation. The grids used here (Bowen 2009) have been further corrected using the residuals of IAEA monitoring stations. Zonal means are presented in Table 2–9.

Secondly, an inverse distance weighting interpolation is completed at a monthly time step using precipitation monitoring station data from CNIP, USNIP and IAEA networks. Monthly $\delta^{18}O$ values are displayed in Figure 2–11. Amount weighted values and monthly zonal means are presented in Table 2–10.

Outputs for $\delta^{18}O$ monthly zonal means for each Great Lake are compared in Figure 2-10. The three comparisons are drawn between the Bowen (2009) grids, the Cressman correction method and the inverse distance weighting approach and are shown in Figure 2-10. Results for each monthly output are displayed as a series of maps in Table 2–11.

Table 2–9. Monthly zonal means for the Great Lakes: Bowen (2009) gridded data

Month	Zonal mean values for over lake $\delta^{18}O$, $\delta^{2}H$ and deuterium excess from Bowen (2009) gridded data				
	Superior	Huron	Michigan	Erie	Ontario
January	-18.04, -131.6, 12.7	-15.27, -109.2, 12.9	-14.79, -106.7, 11.6	-15.26, -108.3, 13.8	-14.14, -100.5, 12.6
February	-16.52, -118.1, 14	-14.53, -98.9, 17.3	-13.1, -94.6, 10.2	-14.83, -99.7, 18.9	-13.37, -91, 15.9
March	-12.67, -87.4, 13.9	-10.64, -68.6, 16.6	-9.34, -61, 13.7	-10.7, -68.5, 17.1	-9.8, -61.3, 17.1
April	-8.94, -60.9, 10.6	-7.69, -51.7, 9.8	-7.25, -44.4, 13.6	-7.73, -52.5, 9.3	-7.06, -45.9, 10.6
May	-7.01, -50.1, 6	-6.35, -43.6, 7.2	-5.69, -40.3, 5.3	-6.38, -43.2, 7.8	-5.92, -40.2, 7.1
June	-6.58, -45.2, 7.4	-5.71, -37.3, 8.3	-4.55, -32.1, 4.4	-5.95, -38.2, 9.4	-5.1, -33, 7.7
July	-6.12, -42.7, 6.3	-5.46, -35.8, 7.9	-4.65, -30.3, 6.9	-5.55, -35.6, 8.8	-5.18, -33, 8.5
August	-6.48, -44.6, 7.3	-5.6, -36.4, 8.4	-4.74, -33, 4.9	-5.75, -36.2, 9.8	-5.08, -33, 7.7
September	-8.08, -56.1, 8.6	-7.38, -49, 10.1	-6.31, -43.6, 6.9	-7.5, -49.4, 10.6	-6.94, -45.3, 10.3
October	-10.54, -72.1, 12.2	-9.32, -61, 13.6	-8.12, -49.6, 15.4	-9.51, -62.4, 13.7	-8.57, -54.1, 14.4
November	-12.67, -86.8, 14.5	-10.57, -68.9, 15.6	-10.47, -68.9, 14.9	-10.31, -66.9, 15.6	-10.04, -64.2, 16.1
December	-15.9, -113.3, 13.8	-13.42, -92.5, 14.8	-12.75, -88.2, 13.8	-13.42, -92, 15.3	-12.57, -86.1, 14.5
Amount weighted*	-10.87, -76.5, 10.5	-9.44, -63.7, 11.8	-7.71, -52.4, 9.3	-9.31, -53.5, 21.0	-8.71, -42.8, 26.9
Evaporation weighted	-12.82, -90.6, 11.9	-11.22, -76.4, 13.4	-9.98, -68.5, 11.4	-9.09, -44.2, 28.5	-10.22, -60.9, 20.9

* Amount weighted to precipitation flux from the Great Lakes Environmental Research Laboratory outputs (T. Hunter, personal communication)

Table 2–10. Monthly zonal means for the Great Lakes: Inverse distance weighting (IDW) of CNIP, USNIP and IAEA monitoring station monthly data

Month	Zonal mean values for over lake $\delta^{18}O$ and $\delta^{2}H$				
	Superior	Huron	Michigan	Erie	Ontario
January	-18.65, -130.1, 19.1	-15.98, -111.4, 16.4	-13.48, -102.7, 5.1	-14.46, -21.6, 94.0	-13.9, -94.9, 16.3
February	-15.68, -111.1, 14.4	-13.92, -97.9, 13.4	-12.00, -92.5, 3.5	-14.55, -101.3, 15.1	-13.06, -86.0, 18.5
March	-14.63, -107.4, 9.6	-12.58, -90.9, 9.7	-7.89, -55.7, 7.4	-12.70, -97.9, 3.7	-10.56, -73.8, 10.7
April	-6.99, -69.5, -13.5	-6.39, -63.0, -11.9	-6.41, -41.9, 9.4	-9.03, -66.7, 5.6	-7.29, -51.7, 6.7
May	-6.39, -27.6, 23.5	-5.84, -42.4, 4.4	-4.77, -36.9, 1.3	-4.02, -38.1, -5.9	0.74, -9.3, -15.3
June	-6.51, -43.6, 8.5	-6.10, -40.0, 8.9	-2.98, -24.9, -1.1	-6.25, -36.5, 13.5	-5.16, -32.5, 8.8
July	-7.76, -46.0, 16.1	-6.48, -40.3, 11.6	-2.83, -20.9, 1.7	-5.72, -32.5, 13.3	-5.66, -37.3, 8.0
August	-7.06, -50.4, 6.1	-6.34, -41.9, 8.9	-3.64, -29.0, 0.2	-6.54, -43.9, 8.5	-5.39, -35.2, 7.9
September	-9.18, -62.5, 11.0	-8.28, -54.0, 12.2	-4.77, -39.0, -0.9	-6.49, -54.3, -2.4	-7.27, -45.0, 13.1
October	-9.65, -75.3, 1.9	-9.28, -66.5, 7.7	-5.43, -37.3, 6.2	-6.00, -56.7, -8.7	-8.13, -54.7, 10.4
November	-13.09, -92.3, 12.4	-11.73, -77.2, 16.6	-9.59, -61.7, 15	-11.56, -71.0, 21.5	-10.43, -66.7, 16.8
December	-18.78, -124.2, 26.0	-14.34, -102.7, 12	-11.32, -82.8, 7.7	-14.98, -101.6, 18.3	-13.33, -91.7, 15.0
Amount weighted*	-11.37, -79.0, 12.0	-9.94, -69.8, 9.7	-6.32, -46.6, 4.0	-9.27, -59.8, 14.4	-8.35, -57.0, 9.8
Evaporation weighted	-13.60, -95.3, 13.5	-11.91, -83.2, 12.1	-8.54, -62.5, 5.8	-8.80, -58.7, 11.6	-10.42, -69.7, 13.6

* Amount weighted to precipitation flux from the Great Lakes Environmental Research Laboratory outputs (T. Hunter, personal communication)

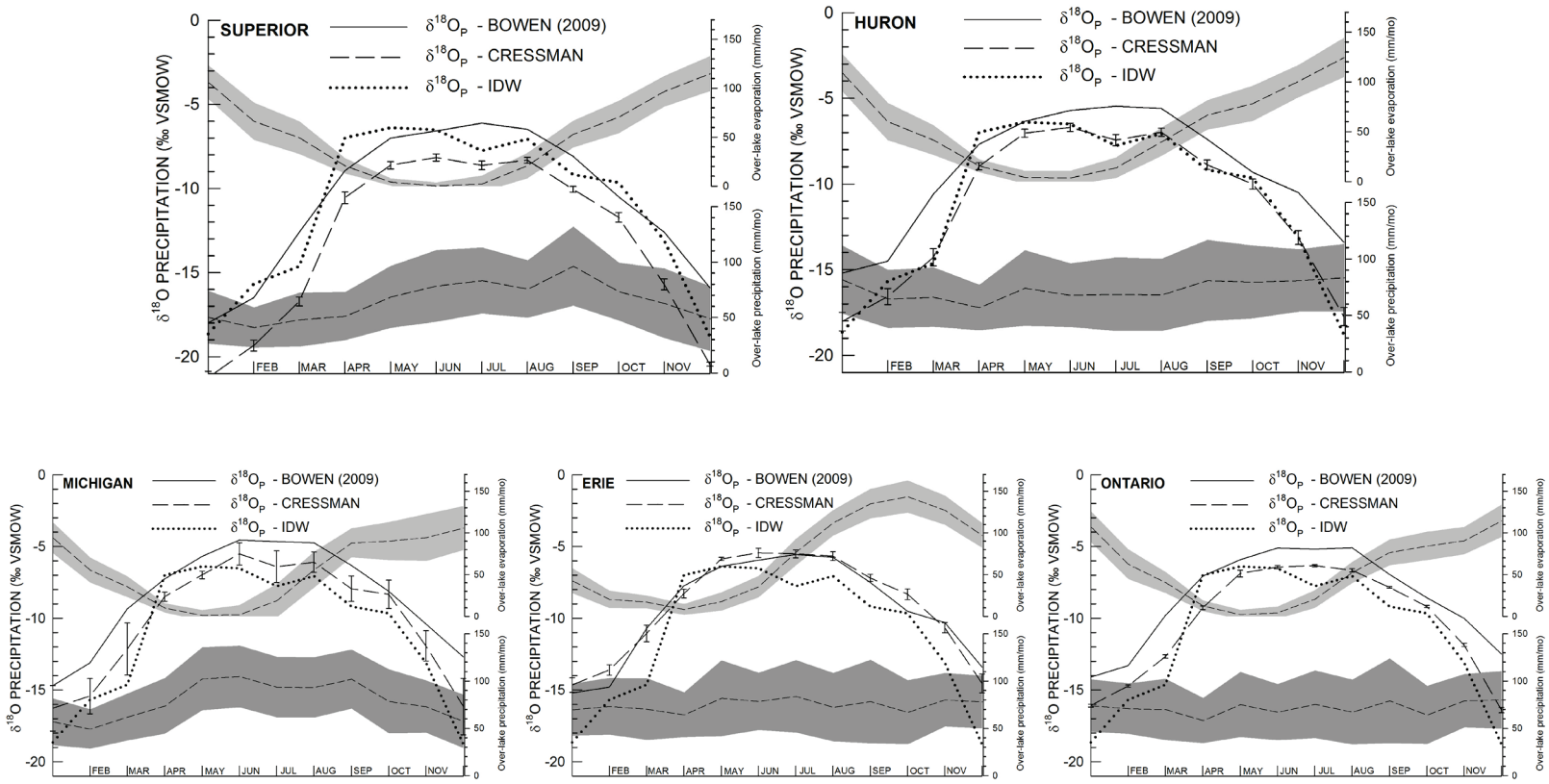

Figure 2-10. Monthly $\delta^{18}O$ estimates for over lake precipitation for each of the five lakes (separate figure for each lake). Bowen (2009) gridded data is plotted as a black solid line; results from the regression and Cressman corrected values from CNIP, USNIP and IAEA datasets are presented as a dashed line; results from an inverse distance weighting method of monthly means of CNIP, USNIP and IAEA stations are presented as a dotted line. Great Lakes Environmental Research Laboratory (GLERL) monthly over lake precipitation (short dashed line, one standard deviation in dark grey) and evaporation rates (short dashed line, one standard deviation in light grey) are shown.

Table 2–11. $\delta^{18}O$ in precipitation. Scale shown for $\delta^{18}O$ is -30 per mille (white) to 0 per mille (black).

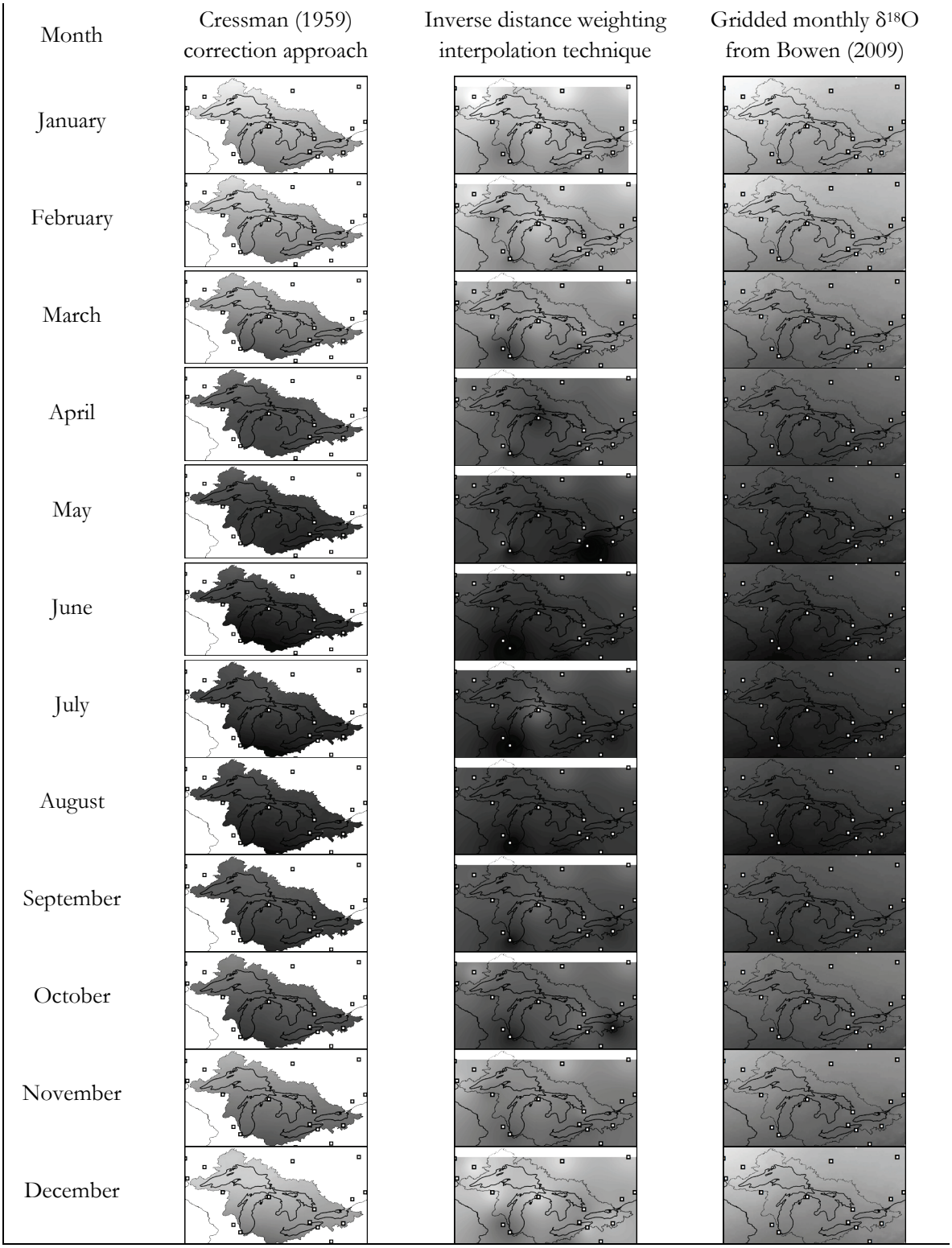

Four approaches to estimating $\delta^{18}O$ and $\delta^{2}H$ of over lake precipitation are outlined in this section: (i) Voronoi-polygon and precipitation amount weighting using CNIP/USNIP and IAEA monitoring stations, (ii) Cressman corrections applied monthly to a latitude-regression model based on CNIP, USNIP and IAEA monthly mean values with an additional lapse rate (altitude effect), (iii) a global step-wise regression model for $\delta^{18}O$ in precipitation based on latitude and altitude corrected to interpolated residuals (grids available from Bowen 2009; approach described in Bowen and Wilkinson 2002; Bowen and Revenaugh 2003), and (iv) an inverse distance weighting interpolation of monthly mean $\delta^{18}O$ and $\delta^{2}H$ from CNIP, USNIP and IAEA stable isotope precipitation sampling stations. The amount weighted $\delta^{18}O$ and $\delta^{2}H$ values for each of the five Great Lakes are presented for the four approaches in Tables: (i) 2–5, (ii) 2–8, (iii) 2–9 and (iv) 2–10. Results of amount weighted $\delta^{18}O$ ($\delta_{P(AW)}$) and evaporation weighted $\delta^{18}O$ ($\delta_{P(EW)}$) are shown in Figure 2-11. Precipitation isotope composition values input into the calculation of E/I are an average of the Bowen (2009), 500km-radius Cressman-corrected IAEA and C(US)NIP data, and monthly inverse distance weighting of IAEA and C(US)NIP data.

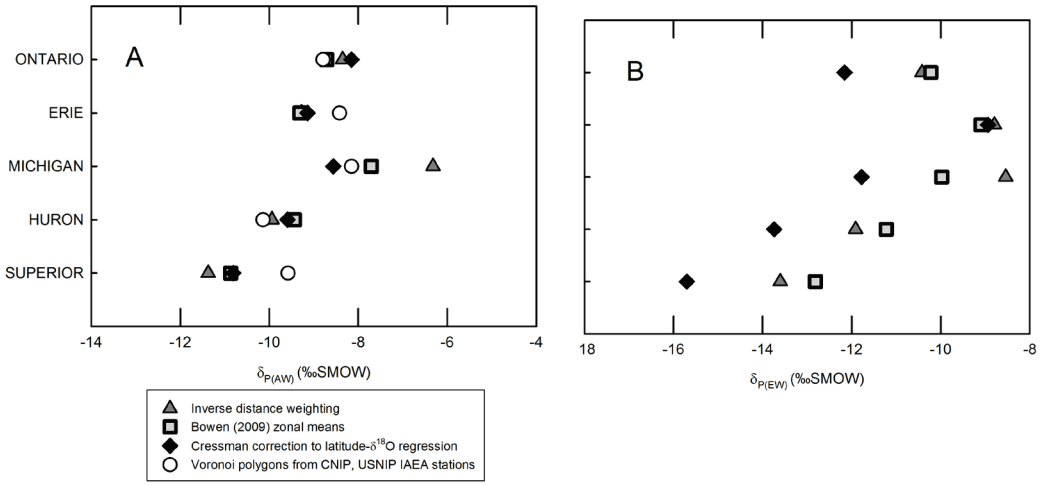

Figure 2-11. Amount weighted (a) and evaporation weighted (b) precipitation $\delta^{18}O$ estimates from four different approaches: (i) inverse distance weighting of monitoring station means (dark grey triangles), (ii) zonal means from an existing grid (Bowen 2009; grey squares), (iii) a monthly latitude-$\delta^{18}O$ regression model corrected using the Cressman (1959) approach (black diamonds) and (iv) Voronoi-polygon area and precipitation amount weighting using existing monitoring stations (white circles).

2.2.2.2 Flux-weighted isotope composition of intra-basin runoff ($\delta_{R(FW)}$) to each Great Lake

A calculation of the intra-basin water input to each Great Lake - river inputs - is calculated here. This is an important hydrological component of each Great Lake. A value of $\delta_{R(FW)}$ is used afterwards within Chapter 2 to calculate the isotope composition of water inputs to each Great Lake. The isotope composition of water inputs to each Great Lake is a direct input to the calculation of evaporation by a stable isotope mass balance.

Data for rivers in the Great Lakes basin from Kendall and Coplen (2001) are presented in section 2.1.1. As mentioned in that section, between three and 30 % of each Great Lake's total runoff flux is explained by this dataset (Superior: 2.8 %, Huron: 1.7 %, Michigan: 30 %, Erie: 27 %, Ontario: 30 %.). For Lakes Michigan, Erie and Ontario the isotope composition of runoff is reasonably well constrained by this survey (all ~30 %). For Lakes Superior and Huron this is likely not the case (<3 %). Furthermore, since this survey is a United States initiative, the majority of samples are collected in the southern (often leeward) portions of each Great Lake basin; this potentially biases the sampling network.

As a solution, the zonal means of amount-weighted annual $\delta_{P(AW)}$ for each catchment sampled within the Great Lakes basin have been calculated. These are compared to outputs from the Kendall and Coplen (2001) datasets to evaluate the representativeness of $\delta_{P(AW)}$ grids for streamflow. Areas used to compute zonal statistics are presented in Figure 2-12. Results for each sampled drainage area in Figure 2-12 are presented in Table 2–12.

A comparison of stable isotope compositions of gridded amount-weighted precipitation ($\delta_{P(AW)}$) and flux-weighted river discharge ($\delta_{R(FW)}$) is completed next. This discrepancy analysis will be useful for E/I calculation sensitivity analyses.

Table 2–12. Zonal mean values for precipitation within drainage areas presented in Figure 2-12
(Inverse distance weighting: IDW, Bowen (2009) grids or Cressman corrected latitude-regression approach)

STATION		RIVER	IDW	BOWEN (2009)	CRESSMAN
Baptism River Near Beaver Bay	USGS	-10.14, -73.3	-13.72, -101.8	-10.90, -78.4	-10.82, -80.2
Black River At Watertown	USGS	-11.12, -75.7	-10.84, -72.4	-10.65, -71.3	-8.78, -60.7
Cattaraugus Creek At Gowanda	USGS	-10.62, -70.6	-10.15, -70.1	-9.68, -64.5	-8.38, -57.1
Genesee River (Charlotte Docks) At Rochester	USGS	-8.95, -60.8	-10.13, -68.0	-9.77, -65.0	-8.43, -57.6
Grand River At Painesville	USGS	-9.25, -60.2	-9.59, -63.7	-8.67, -57.2	-8.03, -54.0
Manistee River At Manistee	USGS	-10.83, -73.9	-11.36, -72.6	-9.42, -65.1	-8.82, -62.0
Menominee River Near McAllister	USGS	-10.80, -76.3	-11.34, -80.3	-10.01, -70.6	-9.48, -67.7
Milwaukee River At Milwaukee	USGS	-10.24, -69.8	-9.05, -63.6	-8.63, -59.8	-7.95, -56.2
Nemadji River Near South Superior	USGS	-12.03, -84.3	-13.19, -97.8	-10.57, -75.7	-10.56, -77.7
Oswego River At Lock 7 At Oswego	USGS	-9.46, -65.7	-10.14, -64.5	-9.67, -64.3	-9.01, -62.3
Pigeon River Near Caseville	USGS	-10.81, -73.9	-10.79, -71.3	-9.04, -61.3	-8.82, -61.2
Rifle River Near Sterling	USGS	-11.13, -77.7	-11.40, -73.3	-9.29, -63.5	-8.99, -62.9
Sandusky River Near Fremont	USGS	-8.01, -50.7	-8.96, -59.1	-8.11, -53.4	-7.11, -47.7
Sandy Creek Near Adams	USGS	-11.51, -77	-10.55, -68.9	-10.19, -68.1	-9.04, -62.6
St. Joseph River At Niles	USGS	-7.98, -52.9	-9.22, -62.6	-8.14, -54.7	-7.26, -49.8
Tahquamenon River Near Tahquamenon Paradise	USGS	-12.31, -85.2	-12.18, -81.4	-10.22, -71.7	-10.15, -72.3
Washington Creek At Windigo	USGS	-12.42, -87.2	-12.58, -91.2	-11.02, -79.1	-10.99, -79.8
Grand River (Ontario)	GRCA	-10.70, -74.0	-10.47, -71.6	-9.67, -65.0	-8.74, -60.1

LAKE BLOCK		Average	Lowest $\delta^{18}O$	IDW	BOWEN (2009)
BLOCK L	EC	-9.74, -76.0	-13.29, -92.6	-14.65, -108.3	-12.57, -91.5
BLOCK M	EC	-7.71, -63.9	-10.59, -76.6	-15.00, -109.8	-11.92, -86.2
BLOCK N	EC	-10.17, -81.8	-13.39, -98.4	-15.08, -110.4	-12.27, -88.5
BLOCK O	EC	-10.84, -84.4	-12.18, -87.5	-13.40, -97.3	-11.92, -85.0
BLOCK P	EC	-9.76, -73.3	-12.35, -89.1	-12.27, -87.7	-11.47, -81.6
BLOCK Q	EC	-9.69, -75.2	-12.45, -90.0	-12.32, -87.7	-11.14, -78.6

Table 2–13. $\delta^{18}O$ of sampled rivers and lakes compared to zonal mean $\delta^{18}O_{P(AW)}$ within drainage areas presented in Figure 2-12.

STATION		$\delta^{18}O_{R(FW)}$	$\delta^{18}O_{R(FW)}$ – IDW	$\delta^{18}O_{R(FW)}$ – BOWEN (2009)	$\delta^{18}O_{R(FW)}$ – CRESSMAN
Baptism River Near Beaver Bay	USGS	-10.14	3.58	0.76	0.68
Black River At Watertown	USGS	-11.12	-0.28	-0.47	-2.34
Cattaraugus Creek At Gowanda	USGS	-10.62	-0.47	-0.94	-2.24
Genesee River (Charlotte Docks) At Rochester	USGS	-8.95	1.18	0.82	-0.52
Grand River At Painesville	USGS	-9.25	0.34	-0.58	-1.22
Manistee River At Manistee	USGS	-10.83	0.53	-1.41	-2.01
Menominee River Near McAllister	USGS	-10.80	0.54	-0.79	-1.32
Milwaukee River At Milwaukee	USGS	-10.24	-1.19	-1.61	-2.29
Nemadji River Near South Superior	USGS	-12.03	1.16	-1.46	-1.47
Oswego River At Lock 7 At Oswego	USGS	-9.46	0.68	0.21	-0.45
Pigeon River Near Caseville	USGS	-10.81	-0.02	-1.77	-1.99
Rifle River Near Sterling	USGS	-11.13	0.27	-1.84	-2.14
Sandusky River Near Fremont	USGS	-8.01	0.95	0.10	-0.90
Sandy Creek Near Adams	USGS	-11.51	-0.96	-1.32	-2.47
St. Joseph River At Niles	USGS	-7.98	1.24	0.16	-0.72
Tahquamenon River Near Tahquamenon Paradise	USGS	-12.31	-0.13	-2.09	-2.16
Washington Creek At Windigo	USGS	-12.42	0.16	-1.40	-1.43
Grand River (Ontario)	GRCA	-10.70	-0.23	-1.03	-1.96
AVERAGE ± STANARD DEVIATION:			**0.41±1.05 ‰**	**-0.81±0.90 ‰**	**-1.50±0.85 ‰**
BLOCK L (lowest $\delta^{18}O$ value in block compared)	EC	-13.30	1.36	-0.72	
BLOCK M (lowest $\delta^{18}O$ value in block compared)	EC	-10.60	4.41	1.33	
BLOCK N (lowest $\delta^{18}O$ value in block compared)	EC	-13.40	1.69	-1.12	
BLOCK O (lowest $\delta^{18}O$ value in block compared)	EC	-12.20	1.22	-0.26	
BLOCK P (lowest $\delta^{18}O$ value in block compared)	EC	-12.30	-0.08	-0.88	
BLOCK Q (lowest $\delta^{18}O$ value in block compared)	EC	-12.40	-0.13	-1.31	

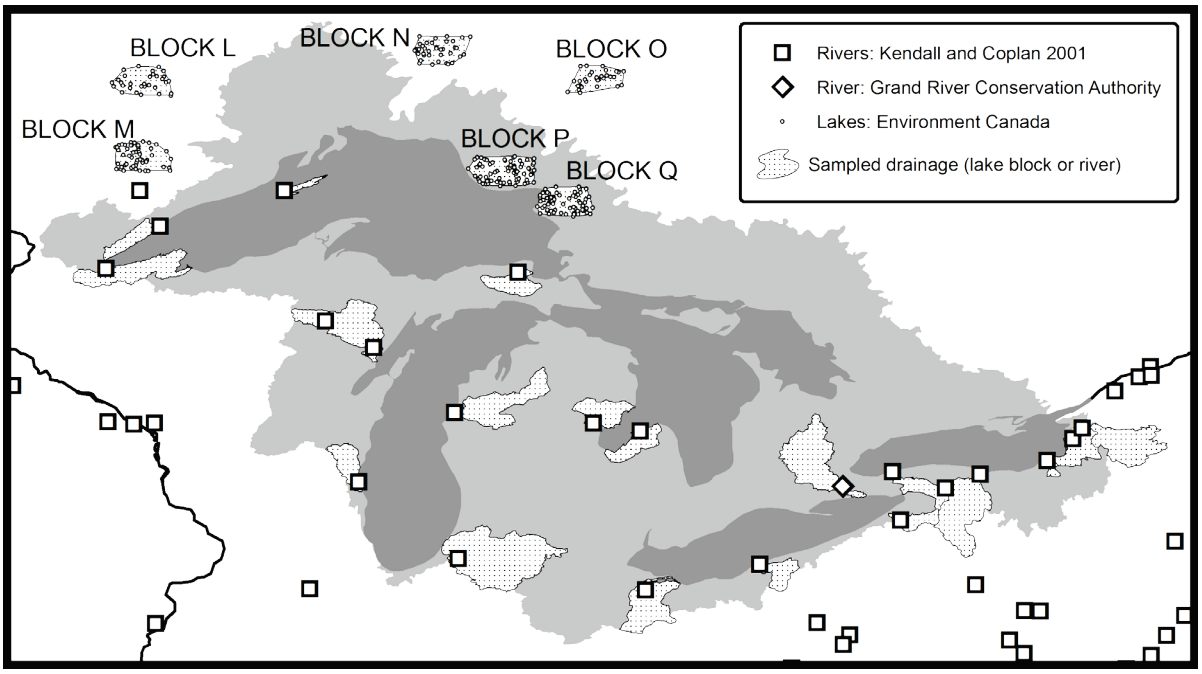

Figure 2-12. Sampling stations and associated drainage areas used to compute zonal means for grids of $\delta^{18}O$ and $\delta^{2}H$ in precipitation ($\delta_{P(AW)}$).

In general, gridded precipitation $\delta^{18}O_{P(AW)}$ is shown to be representative of flux-weighted $\delta^{18}O_{R(FW)}$ of the catchment it is deposited within to ±1 per mille (Table 2–13). The Cressman corrected latitude-regression technique predicts higher $\delta^{18}O$ values within a river's sample catchment than calculated flux-weighted $\delta^{18}O_{R(FW)}$ values in most cases (average of 1.5 ‰ higher**,** 1σ = 0.9 ‰). This is likely a product of the lapse rate that was artificially added to a latitude-$\delta^{18}O$ regression that already encompasses altitude effects (the northern Lake Superior basin is also at the highest elevations, Figure 1-17). Zonal means from Bowen (2009) also predict higher $\delta^{18}O_{R(FW)}$ values by 0.8 ‰ on average (1σ = 0.9**‰**). Zonal $\delta^{18}O_{P(AW)}$ means from the inverse distance weighting approach predicts results that are lower than $\delta^{18}O_{R(FW)}$ by 0.4 per mille on average (1σ = 1.1**‰**). Variations ($\pm1\sigma$) in the computation $\delta^{2}H_{R(FW)}$ – $\delta^{2}H_{P(AW)}$ for the three gridded approaches are: 2.5±8.7 ‰, -5.6±6.0 ‰ and -8.7±6.0 ‰ for the IDW, Bowen (2009) and Cressman grids respectively.

A convex hull (area plot surrounding outermost points in a group) was created for each of the six sampling blocks of an Environment Canada lake survey (Figure 2-12). Small lakes undergo surface evaporation during the open water season (summertime). This produces a heavy oxygen- and hydrogen-isotope enrichment that skews the use of isotope compositions of lake waters as indicators of the isotope composition of runoff. Zonal mean $\delta_{P(AW)}$ from gridded values are 2 to 3 ‰ lower than the average $\delta^{18}O$ values for each of the six lake blocks (10 to 20 ‰ lower in $\delta^{2}H$), likely produced by surface evaporation and heavy isotope enrichment as is suggested by low d-excess values. However, this discrepancy is much smaller if the lake within each sampling block with the lowest $\delta^{18}O$ value is selected instead of computing an average (Table 2–12).

Overall, a river catchment's zonal mean of gridded amount-weighted precipitation captures the flux weighted river discharge within 1‰ in $\delta^{18}O$ and 6‰ in $\delta^{2}H$. To produce a basin-wide estimate of flux-weighted isotope composition of river runoff, gridded $\delta_{P(AW)}$ catchment means $\delta^{18}O$ and $\delta^{2}H$ values in precipitation for the terrestrial catchment of each Great Lake is computed (not including Great Lake area). The average discrepancy for each grid cell to the resulting zonal mean estimates for $\delta^{18}O_{R(FW)}$ and $\delta^{2}H_{R(FW)}$ ($\delta^{18}O$ presented in Table 2–13; $\delta^{2}H$ stated in previous paragraph) are added. Results of these estimates for the flux-weighted isotope composition of runoff into each Great Lake are presented in Table 2–14.

Table 2–14. $\delta_{R(FW)}$ values for each of the Great Lakes derived from three grids

Lake	$\delta^{18}O$ (‰ SMOW)			$\delta^{2}H$ (‰ SMOW)			Deuterium-excess		
	IDW	CRES	BOW	IDW	CRES	BOW	IDW	CRES	BOW
Superior	-12.3	-12.4	-12.2	-89.8	-87.6	-78.1	9.0	11.9	19.9
Huron	-11.0	-11.1	-11.0	-75.1	-75.3	-63.0	12.7	13.6	24.9
Michigan	-10.1	-10.1	-10.0	-69.1	-69.4	-55.5	11.8	11.3	24.6
Ontario	-10.1	-10.5	-10.8	-67.7	-72.1	-61.4	12.8	11.5	24.7
Erie	-9.3	-9.3	-9.5	-62.8	-63.1	-51.7	11.9	11.5	24.0

The agreement in $\delta^{18}O$ between the three approaches presented in Table 2–14 is within 0.5‰ in all cases except for one (Lake Ontario: Bowen (2009) and inverse distance weighting). Agreement in $\delta^{2}H$ is also very promising. The Bowen (2009) grid produces very large deuterium excess values for the Great Lakes region and therefore the values of $\delta^{2}H$ do not match with the other approaches as close as the inverse distance weighting and Cressman correction approaches match (within 5 per mille in all cases, and <1 per mille for three of the five lakes). An average of the outputs in Table 2–14 from the three grids is assumed to represent the amount weighted isotope composition of intra-basin runoff to each Great Lake.

2.2.2.3 The isotope composition of hydrologic inputs to each Great Lake: δ_I

All hydrologic inputs to each Great Lake (connecting channel inflows, direct precipitation and runoff) must be weighted according to their respective fluxes in order to develop a representative value for the input to each Great Lake (δ_I, Equation (10)). The development of appropriate $\delta^{18}O$ and $\delta^{2}H$ values for the net input to each Great Lake from amount-weighted precipitation ($\delta_{P(AW)}$) and connecting channel inflow (δ_U) and intra-basin river inflows (δ_R) has been presented previously. Here, we will present the magnitude of runoff, direct precipitation and connecting channel inflow to each Great Lake. The three fluxes and their respective $\delta^{18}O$ and $\delta^{2}H$ values are used to produce an estimate of the values of both $\delta^{18}O$ and $\delta^{2}H$ for the net hydrologic input to each Great Lake.

Amount weighted values for $\delta^{18}O$ and $\delta^{2}H$ in direct precipitation falling on each Great Lake were presented previously ($\delta_{P(AW)}$, Section 2.2.2.1). In summary, four approaches were taken to estimating a representative value of $\delta_{P(AW)}$ for each Great Lake. The results are shown in Figure 2-11a. The long-term direct precipitation falling on each Great Lake is calculated as an average of the GLERL (T. Hunter,

personal communication) and the USGS (Neff and Nicholas 2005) reported fluxes (Figure 1-24 and 1-25). The direct precipitation flux for the period of one residence time prior to the sampling date are chosen for Lakes Huron, Erie and Ontario.

The isotope composition of connecting channel inflows (δ_U) is the only remaining flux to be presented, as $\delta^{18}O$ and δ^2H values for direct precipitation (Section 2.2.2.1) and runoff (Section 2.2.2.2) have been formulated. Connecting channel inflows are assumed to be well represented by the isotope composition of an upstream Great Lake ($\delta_U = \delta_{L(UPSTREAM)}$). Since the $\delta^{18}O$ and δ^2H values of lake waters are not stratified (as shown in Chapter 3) this is a reasonable assumption.

δ_U is straightforward for lakes with one connecting channel inflow, assuming negligible evaporation occurs between upstream lakes and discharge into a lower chain lake compared to evaporation over the upstream Great Lake. A representative value for the upstream Great Lake is chosen for δ_U for Lakes Erie and Ontario. However, for Lakes Michigan and Huron the setting is more complicated.

Lake Michigan and Lake Huron exchange water between both bodies at the Straits of Mackinac. The estimated fluxes for these exchanges are similar to that of the St. Mary's river, which flows from Lake Superior to Lake Huron. Lake Huron is estimated to add 36 km^3/yr to Lake Michigan by diffusion (calculated by Chapra et al. 2009). It is currently uncertain whether these waters fully mix and enter the Lake Michigan reservoir before flowing back into Lake Huron (Chapra et al. 2009), although isotopic tracers may be a useful technique to test this. Existing estimates of flow from Lake Michigan to Lake Huron generally fall between 45 and 50 km^3/yr (Powers and Ayers 1960; Saylor and Sloss 1976). Lake Huron's connecting channel input is two fold as it receives 45 to 50 km^3/yr from Lake Michigan and ~67±7 km^3/yr from Lake Superior (Neff and Nicholas 2005). These two inputs are weighted against each another using $\delta^{18}O$ and δ^2H values for Lake Michigan and Lake Superior to produce a value of δ_U for Lake Huron. The isotope composition for upstream lake inflow to each of the Great Lakes (δ_U) is presented in Table 2–15.

Table 2–15. Isotope composition of connecting channel inflows to each Great Lake: δ_U

Lake	Upstream Lake(s)	Connecting channel inflow (km^3/yr)	$\delta^{18}O_U$ (‰ SMOW)	δ^2H_U (‰ SMOW)
Superior	-	-	-	-
Huron	Superior, Michigan	67, 45	-7.50	-57.0
Michigan	Huron	36	-7.07	-53.8
Erie	Huron	168	-7.07	-53.8
Ontario	Erie	184	-6.76	-51.2

Next, the flux weighted isotope composition of waters that enter each Great Lake (δ_I) is calculated. Equation (1) - which weights runoff, direct precipitation and upstream hydrologic inputs against one another - is applied to accomplish this. The calculation and outputs are presented for each Great Lake in Table 2–16.

Table 2–16. Flux weighted $\delta^{18}O$ and $\delta^{2}H$ to each Great Lake.

Lake	U	$\delta^{18}O_U$	$\delta^{2}H_U$	P	$\delta^{18}O_{P(AW)}$*	$\delta^{2}H_{P(AW)}$*	R	$\delta^{18}O_{R(FW)}$	$\delta^{2}H_{U(FW)}$	$\delta^{18}O_I$	$\delta^{2}H_I$
Superior	-			63.6	-11.02	-77.8	44.2	-12.30	-85.2	-11.5	-80.8
Huron	112	-7.50	-57.0	52.3	-9.65	-66.9	48.4	-11.03	-71.1	-8.8	-62.7
Michigan	36	-7.07	-53.8	54.8	-7.53	-53.2	35.8	-10.07	-64.7	-8.1	-56.6
Erie	168	-7.07	-53.8	23.0	-9.24	-58.8	19.1	-10.47	-67.1	-7.6	-55.6
Ontario	184	-6.76	-51.2	16.3	-8.40	-51.7	34.0	-9.37	-59.2	-7.3	-52.4

* $\delta^{18}O_{P(AW)}$ value is an average of Bowen (2009), IDW, and Cressman-corrected (1959) IAEA, C(US)NIP

2.2.2.4 Physical climate parameters: relative humidity, air temperature, lake temperature

Physical climate data for over-lake conditions is available from gridded North American Regional Reanalysis dataset (NARR; Mesinger et al. 2006). The outputs from these grids are verified against monitoring buoy data (NOAA 2011). An example of outputs for Lake Superior is presented in Figure 2-13. Monthly NARR air temperatures match those recorded at monitoring buoys within a few degrees Celsius. However, the NARR outputs produce lower winter temperatures than monitoring buoys, and higher summer temperatures. Relative humidity zonal means for Lake Superior from NARR grids are lower than over lake monitoring buoys by five to ten percent, likely a product of over-lake humidity build-up as the lake evaporates (whereas the NARR grid output presented in Figure 2-13 is a zonal mean that includes near shore data).

Temperature and relative humidity data are inputs for the calculations of a liquid-vapour stable isotope equilibrium fractionation factor (α^*), a kinetic separation factor (ε_K), ultimately leading to the calculation of the isotope composition of the net lake evaporate (δ_E) and from the an estimate of the lake evaporation flux.

In order for an appropriate value for air temperature and over lake humidity to be entered into the formulation of δ_E, these parameters must be weighted to seasons where evaporation is occurring. To do so, the monthly mean values for air temperature, lake temperature and relative humidity are calculated and weighted against monthly lake evaporation from the Great Lakes Environmental Research Laboratory's lumped parameter heat storage and surface flux evaporation model outputs. Monthly mean air and lake temperatures and relative humidity for each Great Lake are shown in Table 2–17. Evaporation weighted climate parameters ready for input into evaporation calculations are presented in Table 2–18.

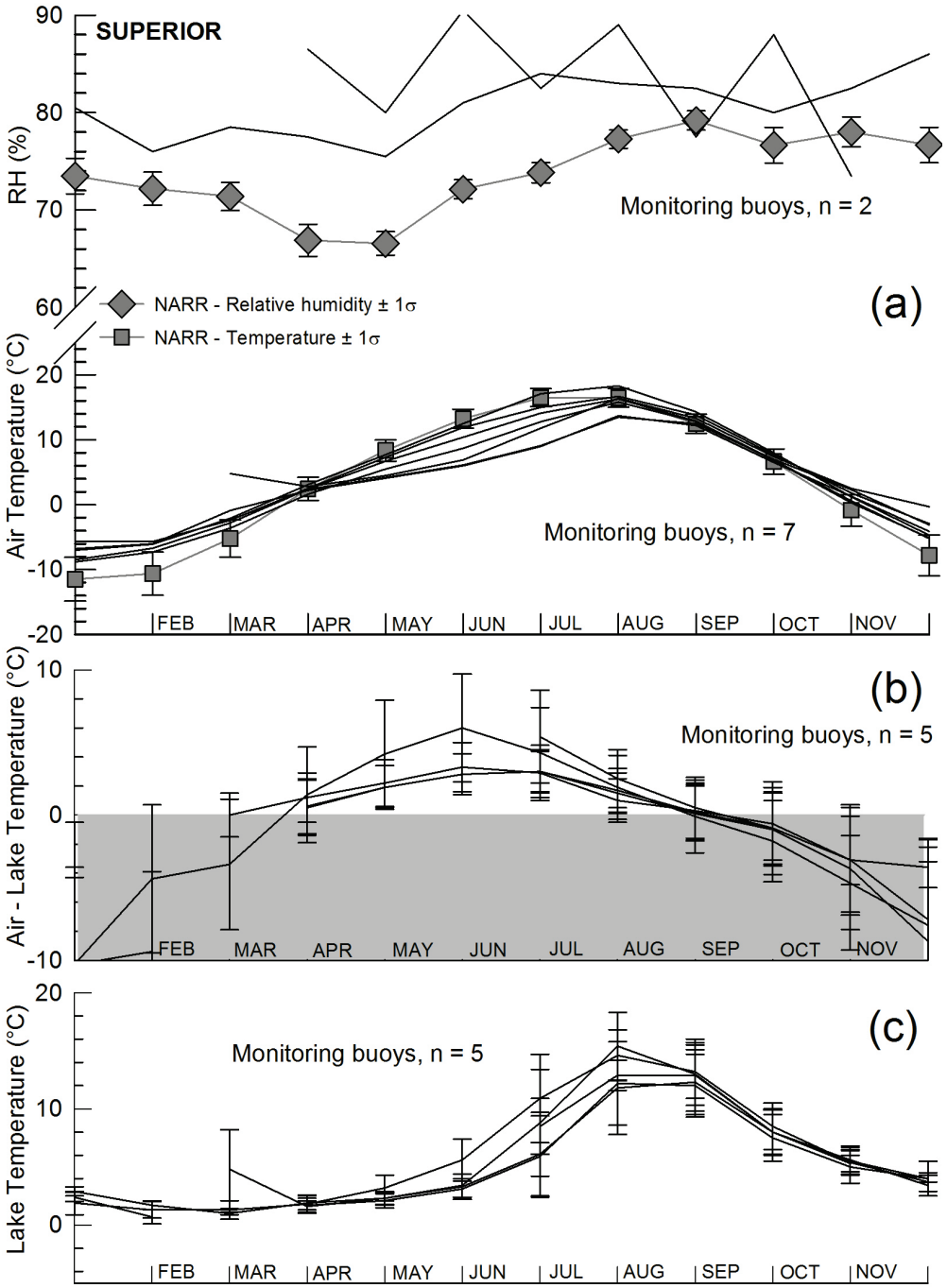

Figure 2-13. A comparison of zonal means and standard deviations of gridded North American Regional Reanalysis (Mesinger et al. 2006; grey diamonds/squares; data for 2m above surface) and long-term means for National Oceanic and Atmospheric Administration over lake monitoring buoys (black lines and error bars). The following parameters are compared: (a) relative humidity and air temperature data, (b) air minus lake temperature and (c) lake temperature. Error bars show ±1σ from long-term mean value.

Table 2–17. Monthly physical climate inputs for each Great Lake. Evaporation is expressed as a monthly percentage of total annual evaporation.

Lake	Month	RH (%)	Air T (°C)	Lake T (°C)	Evaporation (%)		Lake	Month	RH (%)	Air T (°C)	Lake T (°C)	Evaporation (%)
Superior	1	73.5	-6.6	2.4	17.6		Huron	1	79.2	2.1	1.9	16.6
Superior	2	72.2	-6.4	1.2	11.0		Huron	2	77.3	1.3	1.5	9.1
Superior	3	71.4	-1.2	2.4	8.2		Huron	3	75.5	1.5	1.5	6.3
Superior	4	66.9	2.4	1.8	3.4		Huron	4	70.2	2.8	2.8	2.4
Superior	5	66.6	5.7	2.5	0.6		Huron	5	68.4	4.5	4.5	0.6
Superior	6	72.1	8.9	3.9	0.0		Huron	6	72.0	9.0	9.0	0.5
Superior	7	73.8	12.7	8.0	0.4		Huron	7	72.3	15.5	16.5	2.1
Superior	8	77.3	15.8	13.4	3.4		Huron	8	76.3	18.3	19.0	6.1
Superior	9	79.2	13.1	12.7	8.8		Huron	9	78.7	16.3	16.0	10.1
Superior	10	76.6	7.2	8.0	11.7		Huron	10	77.4	11.0	10.8	11.9
Superior	11	78.0	1.4	5.4	16.0		Huron	11	80.1	6.0	5.9	15.3
Superior	12	76.7	-3.6	3.8	19.0		Huron	12	81.4	2.5	2.0	19.0
Michigan	1	75.5	-4.3	2.5	14.5		Erie	1	76.2	-1.0	3.0	5.1
Michigan	2	74.1	-4.3	1.9	8.5		Erie	2	75.5	-2.5	1.9	2.4
Michigan	3	72.1	1.2	3.0	5.4		Erie	3	72.9	1.5	4.4	2.0
Michigan	4	67.3	4.0	3.6	1.5		Erie	4	67.8	7.3	6.4	1.0
Michigan	5	66.2	8.0	7.0	0.1		Erie	5	67.7	15.5	11.9	2.1
Michigan	6	69.5	13.0	10.7	0.3		Erie	6	70.1	19.9	17.4	4.2
Michigan	7	71.6	18.7	17.3	2.9		Erie	7	70.9	22.6	22.0	9.2
Michigan	8	75.2	20.0	19.5	8.6		Erie	8	74.2	21.3	23.0	13.5
Michigan	9	76.5	16.7	17.5	13.5		Erie	9	75.4	17.4	22.0	16.2
Michigan	10	74.4	10.8	12.2	13.9		Erie	10	73.4	11.3	15.5	17.3
Michigan	11	76.7	5.2	7.7	14.5		Erie	11	75.8	5.8	11.9	15.3
Michigan	12	78.3	-0.7	5.3	16.3		Erie	12	77.9	0.4	4.1	11.6

Table 2–17. (continued)

Lake	Month	RH (%)	Air T (°C)	Lake T (°C)	Evaporation (%)
Ontario	1	76.7	-2.0	4.2	16.1
Ontario	2	75.9	-2.0	1.8	9.3
Ontario	3	73.6	0.0	2.6	6.0
Ontario	4	68.3	5.3	3.0	1.8
Ontario	5	68.5	9.0	6.3	0.3
Ontario	6	71.1	16.0	14.0	0.6
Ontario	7	71.0	19.3	18.0	3.1
Ontario	8	74.3	21.7	21.5	7.9
Ontario	9	76.7	18.0	19.3	11.5
Ontario	10	75.9	11.0	10.5	12.6
Ontario	11	77.8	6.0	9.0	13.6
Ontario	12	79.3	1.0	7.0	17.2

Table 2–18. Evaporation weighted climate parameters for each Great Lake.

Lake	Relative humidity (%)	Air temperature (°C)	Lake Temperature (°C)
Superior	75.2	0.3	4.9
Huron	78.5	6.5	6.4
Michigan	75.5	5.8	9.0
Erie	74.4	11.8	15.0
Ontario	76.4	6.5	9.4

A review of required data for this study of Great Lakes waters is complete. The E/I calculation input parameter δ_I is presented for each lake in Table 2–16. Physical climate inputs are shown in Table 2–18. All required data for a calculation of δ_E are presented in this review, and a calculation can now be completed following the procedure outlined in Section 2.2.1. Results are presented next (Chapter 3).

Chapter 3
Results and Discussion

This section presents $\delta^{18}O$ and $\delta^{2}H$ in waters sampled in the Great Lakes basin (Section 3.1). These are compared to other analytes measured during the cruises of the Great Lakes. Semi-quantitative interpretations of water parcel mixing, stratification and seasonality in evaporation are discussed. Next, results for evaporation modelling by a stable isotope mass balance model are presented for each Great Lake simultaneously matching outputs from two conservative geochemical tracers (^{18}O and ^{2}H; Section 3.2.1). Uncertainty and calculation sensitivity analysis is completed to assess error associated with the calculation for each of the Great Lakes (Section 3.2.1).

3.1 $^{18}O/^{16}O$ and $^{2}H/^{1}H$ ratios in Great Lakes waters and the regional water cycle

A new dataset of $^{18}O/^{16}O$ and $^{2}H/^{1}H$ in the North American Great Lakes is presented here. The Environmental Protection Agency collected 514 samples of water from the North American Great Lakes during two sampling campaigns in spring and summer of 2007. Samples were collected at surface, mid depth(s) and within ten metres of the sediment-water interface at 75 over lake stations. $\delta^{18}O$ and $\delta^{2}H$ values for each of the Great Lakes are presented in Figure 3-1.

First, results are compared to previous isotope investigations of Great Lakes waters. The waters of the Great Lakes are fairly homogenous over time, reflecting the long basin residence time (roughly a century).. Deuterium concentration data is plotted for the Great Lakes in Figure 3-2. Two of the early publications (Friedman et al. 1964; Brown 1970) may be subject to analytical uncertainty or sampling bias (single result reported for each Lake. The observed isotopic-homogeneity provides an opportunity to assess the long-term hydrologic operation for each Great Lake. This is an advantage of the isotopic approach over conventional means, since the latter are subject to interannual variations in precipitation, ice-cover and physical climate that effect processes such as evaporation and water inputs. Further, these approaches are limited to periods where sufficient data has been collected to estimate evaporation, whereas the isotope approach integrates the long-term signature of the lakes within the residence time of each. This time-frame surpasses the physical climate data record for Lake Superior, providing a glimpse into the Lake's long-term behaviour.

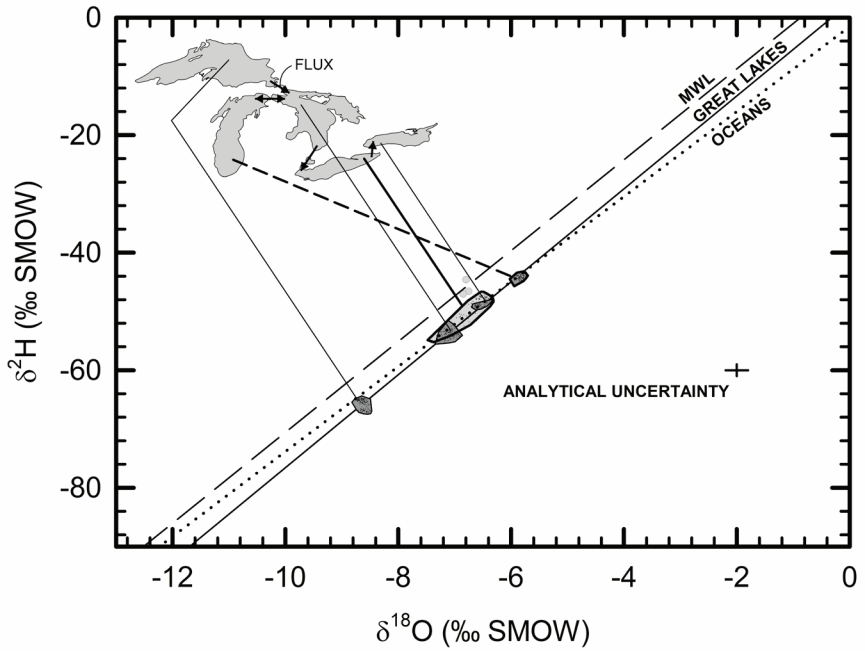

Figure 3-1. (previous page) $\delta^{18}O$ and $\delta^{2}H$ values in the North American Great Lakes. A convex hull (area bounding outermost points) surrounding results for each Great Lake; lines connect each convex hull to the appropriate Great Lake on the map in the upper left. Unweighted regressions are shown for meteoric waters (labelled MWL; IAEA, CNIP, and USNIP; dashed line; $\delta^{2}H = 7.73 \cdot \delta^{18}O + 7.26$, n = 1699, R^2 = 0.982), Great Lake waters (solid line; $\delta^{2}H = 7.90 \cdot \delta^{18}O + 2.49$, n = 514, R^2 = 0.979), and world oceans (Schmidt 1999; Bigg and Rohling 2000; Schmidt et al. 1999; $\delta^{2}H = 7.23 \cdot \delta^{18}O - 1.54$, n = 1362, R^2 = 0.980). Three points for Lake Erie are plotted separately as grey circles.

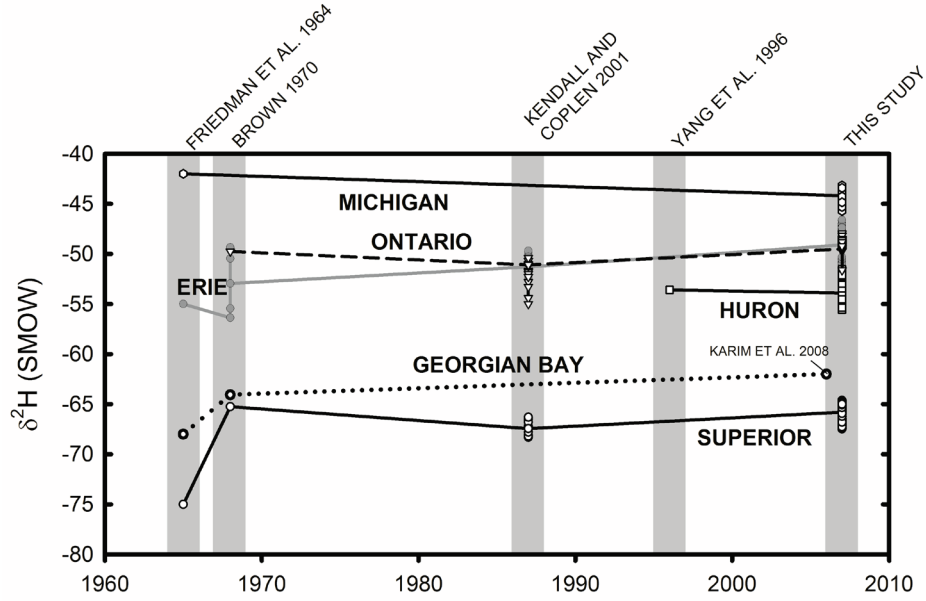

Figure 3-2. $\delta^{2}H$ results for Great Lakes waters over time. $\delta^{18}O$ values are not reported for early works.

Table 3–1. $\delta^{18}O$ and $\delta^{2}H$ results for samples of the North America Great Lakes

Lake	Samples analyzed			Average $\delta^{18}O$	Average $\delta^{2}H$	1σ $\delta^{18}O$	1σ $\delta^{2}H$
	Spring	Summer	Total				
Superior	80	60	140	-8.62	-65.8	0.07	0.88
Huron	60	45	105	-7.07	-53.9	0.09	0.69
Michigan	44	36	80	-5.83	-44.2	0.06	0.47
Erie	63	63	126	-6.65	-49.2	0.28	2.36
Ontario	36	27	63	-6.57	-49.1	0.08	0.46

Next, we examine variations in $\delta^{18}O$-$\delta^{2}H$ space. Figure 3-1 shows results of δ18O and δ2H analyses for Great Lakes waters. The Great Lakes plot along a trajectory that is subparallel and offset from meteoric waters, similar to present day oceans (Schmidt 1999; Bigg and Rohling 2000; data available from Schmidt et al. 1999: slope 7.23) and also to several of the world's major rivers (Mississippi: $\delta^{18}O$-$\delta^{2}H$ slope of 7.6, Kendall and Coplan 2001; Amazon: $\delta^{18}O$-$\delta^{2}H$ slope of 7.7, Longinelli and Edmonds 1983; Mackenzie: $\delta^{18}O$-$\delta^{2}H$ slope of 7.0, Yenisey: $\delta^{18}O$-$\delta^{2}H$ slope of 7.0, personal communication, Y. Yi; Yi et al. submitted).

The offset from the meteoric water line is a product of kinetic isotope effects resulting in an ^{18}O and ^{2}H enrichment during evaporation for the Great Lakes (Craig 1961). $\delta^{18}O$ and $\delta^{2}H$ values progressively increase from headwaters (Lake Superior) to the lowermost lake (Ontario) with the exception of Lake Michigan (Figure 3-1). The range in $\delta^{18}O$ and $\delta^{2}H$ values is very small for Lakes Superior, Huron, Michigan and Ontario. Results for Lake Erie show the largest range in $\delta^{18}O$ and $\delta^{2}H$ of all the Great Lakes; values for Lake Erie plot between Lake Huron (upstream) and Lake Ontario (downstream). Average and standard deviation for $\delta^{18}O$ and $\delta^{2}H$ values of the Great Lakes water is presented in Table 3–1. Lake Michigan waters have the highest concentrations of ^{18}O and ^{2}H of all the Great Lakes. The average $\delta^{18}O$ value is 1.2 per mille higher than the average value for Lake Huron. This is significant, as the two lakes share a similar lake level and are considered as one body in some hydrological studies (Neff and Nicholas 2005). Stable isotopic ratios in water show that the water in Lake Michigan is distinct from Lake Huron waters, supporting separate treatment of Lake Michigan and Lake Huron in water balance studies. The distinct isotopic-separation of these water bodies may provide insights into the magnitude of exchange between these lakes.

The $\delta^{2}H/\delta^{18}O$ slope of 7.90 found for a regression of all Great lakes samples analyzed deserves further consideration (Figure 3-1). Predicted $\delta^{2}H/\delta^{18}O$ slopes for lake systems at this location are close to a value of five (Gibson et al. 2008). This is shown to be true for $\delta^{18}O$ and $\delta^{2}H$ analysis of 312 small lakes in the Lake Superior region in Figure 3-3 ($\delta^{2}H/\delta^{18}O$ slope of 5.14, $R^2 = 0.85$). However, evaporation from small lakes is limited to a shorter ice free season than the Great Lakes due to a much lower thermal inertia. Therefore these lakes are exposed to a different climate during evaporation. Differences in hydrological operation between large and small lake systems is an important consideration for isotopic investigations. Differences between large and small lake systems include lake effects on the atmosphere, the degree of stratification and mixing, and the effects of thermal inertia (reductions or seasonal delays in

ice cover for larger lakes). A large amount of evaporation from the Great Lakes is expected to occur during the winter months while the Great Lakes remain ice-free. However, winter evaporation is inhibited by a shielding ice cover for smaller systems. Despite these expected differences, the δ^2H-$\delta^{18}O$ slopes of regional lake systems are a useful comparative tool for larger systems, and fall along a slope similar to that of Lake Superior (5.3; Figure 3-3).

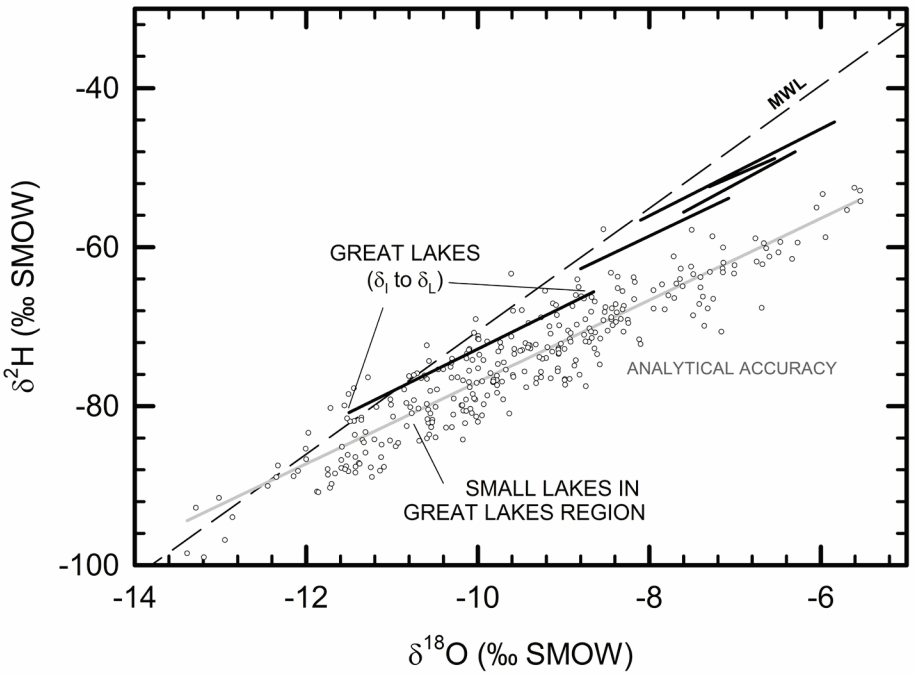

Figure 3-3. $\delta^{18}O$ and δ^2H values for 312 lakes ranging in size from <1 to 100 square kilometres (white circles). A regression of all 312 lake values is shown as a thick grey line ($\delta^2H = 5.14 \cdot \delta^{18}O - 25.5$; $R^2 = 0.852$). δ_I and δ_L for all five Great Lakes are connected by thick black lines.

However, a regression of $\delta^{18}O$ and δ^2H of waters from all the Great Lakes (n = 514) plot along a significantly higher slope (7.90) than smaller lakes in the Great Lakes region (5.14) as shown in Figure 3-3. This is interpreted as a result of continuous inputs of meteoric waters via streams and direct precipitation into each Great Lake, in addition to evaporation losses. If no additional water was added to the chain lake system as it proceeded downstream (Superior to Huron to Erie to Ontario) then Great Lakes waters would be expected to plot along a slope close to a value of five. The same effect controls the slope of oceanic waters and rivers, made evident by similar $\delta^{18}O$-δ^2H regressions for the oceans in comparison to the Great Lakes (Figure 3-1). This interpretation is qualitatively presented in Figure 3-4.

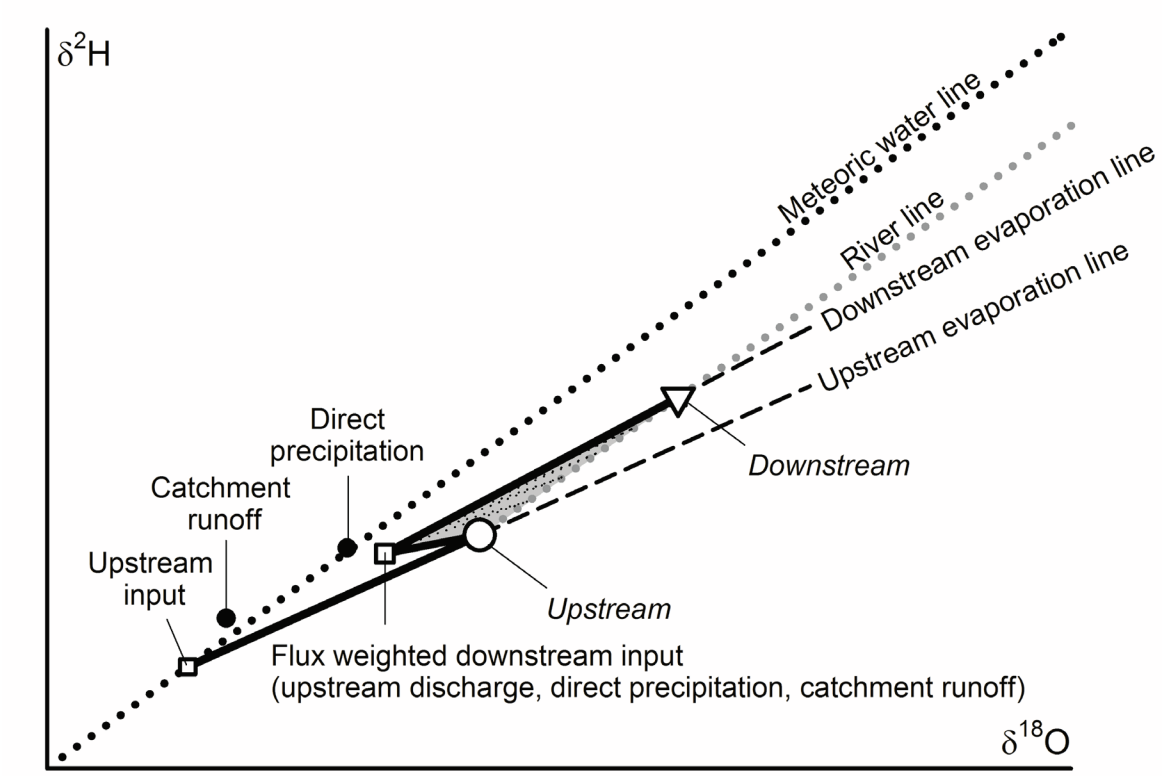

Figure 3-4. $\delta^{18}O$-$\delta^{2}H$ schematic of a chain lake system - such as the Great Lakes - or most river systems. An upstream lake (or river sampling station) is shown as a white circle. A downstream lake (or river sampling station) is represented by a white triangle. Between the two stations two dominant processes affect the signature of the river or chain lake system: (1) evaporation (thick black arrow; refers to evaporation both over lake/river and within the catchment intermediate to the sampling stations) and (2) water inputs from catchment runoff (and groundwater discharge if significant to the water budget), and direct precipitation that falls on the river- or lake-surface between the sampling stations (labelled black circles). Flux-weighting the isotope compositions of direct precipitation (δ_P), catchment runoff (δ_R) and the upstream lake outflow (or upstream river gauging station) produces a weighted input isotope composition for the downstream sampling station. The relative proportions of hydrologic input to evaporation losses control the isotope composition of the downstream lake or river sampling station. This schematic shows different evaporation slopes (dashed grey lines) for the upstream and downstream stations to reflect the geographical separation between river stations or chain-lakes, that produces varying climatic conditions for each river reach or lake and in turn determines the evaporation slope. A grey dotted line shows how these processes could produce a river- or chain-lake- regression that falls subparallel but offset (below) that of meteoric waters (shown here as a black dotted line). The relative positions of isotope compositions and evaporation trajectories portrayed in this schematic is not applicable to all rivers; however, the governing concepts shown are applicable to all chain-lake and river systems.

The schematic presented in Figure 3-4 shows how a chain-lake or river system with multiple sampling stations may plot subparallel to meteoric waters in $\delta^{18}O$-$\delta^{2}H$ space. The trajectory that a river or chain-lake system plots along is dependent upon atmospheric conditions (humidity, temperature. isotope composition of water vapour), the degree of evaporation of catchment waters prior to input into the main channel, the isotope composition of precipitation along a particular reach, and the relative proportions of evaporation losses to catchment water and direct precipitation inputs. The isotope composition of inputs is shown as a flux-weighted mixture of the isotope compositions of upstream discharge, direct precipitation, and catchment runoff (including groundwater discharge, if significant to the water budget). These three input components form a triangle, with the flux-weighted input value plotting within the triangles boundaries. The position of the flux-weighted input is - by definition - weighted to the isotope composition of the flux with the greatest input and will plot nearest to the input with the greatest flux.

For the Great Lakes, evaporation losses are expected to be roughly 25 to 50 percent of the magnitude of runoff and direct precipitation, although the uncertainties associated with each of these are large (up to 45%). Water entering each Great Lake via precipitation and runoff is assured to be larger than water exiting the system, since connecting channel inflows entering each Great Lake are less than connecting channel outflows. The different is runoff + precipitation - evaporation, and is referred to as net basin supply in earlier studies (Neff and Nicholas 2004). Since more water enters by streams and precipitation than are exported by evaporation losses, it is reconcilable that the slope of all Great Lakes waters plots subparallel to meteoric waters and not along a slope of five as is expected for a system only undergoing evaporation at this location.

Next, the distribution of stable isotopes within Great Lakes waters will be examined. Figures 3-5a to 3-5e show an at-depth transect along the long axis of each Great Lake (east-west for Lakes Superior, Erie and Ontario; north-south for Lakes Michigan and Huron). Colour contours display a third variable: $\delta^{18}O$, temperature or chloride concentrations. Spring and summer results are shown on the same page so that seasonal variations can be distinguished. Consistent spatial patterns of $\delta^{18}O$, temperature and chloride for all of the Great Lakes emerge from Figures 3-5a - 3-5e.

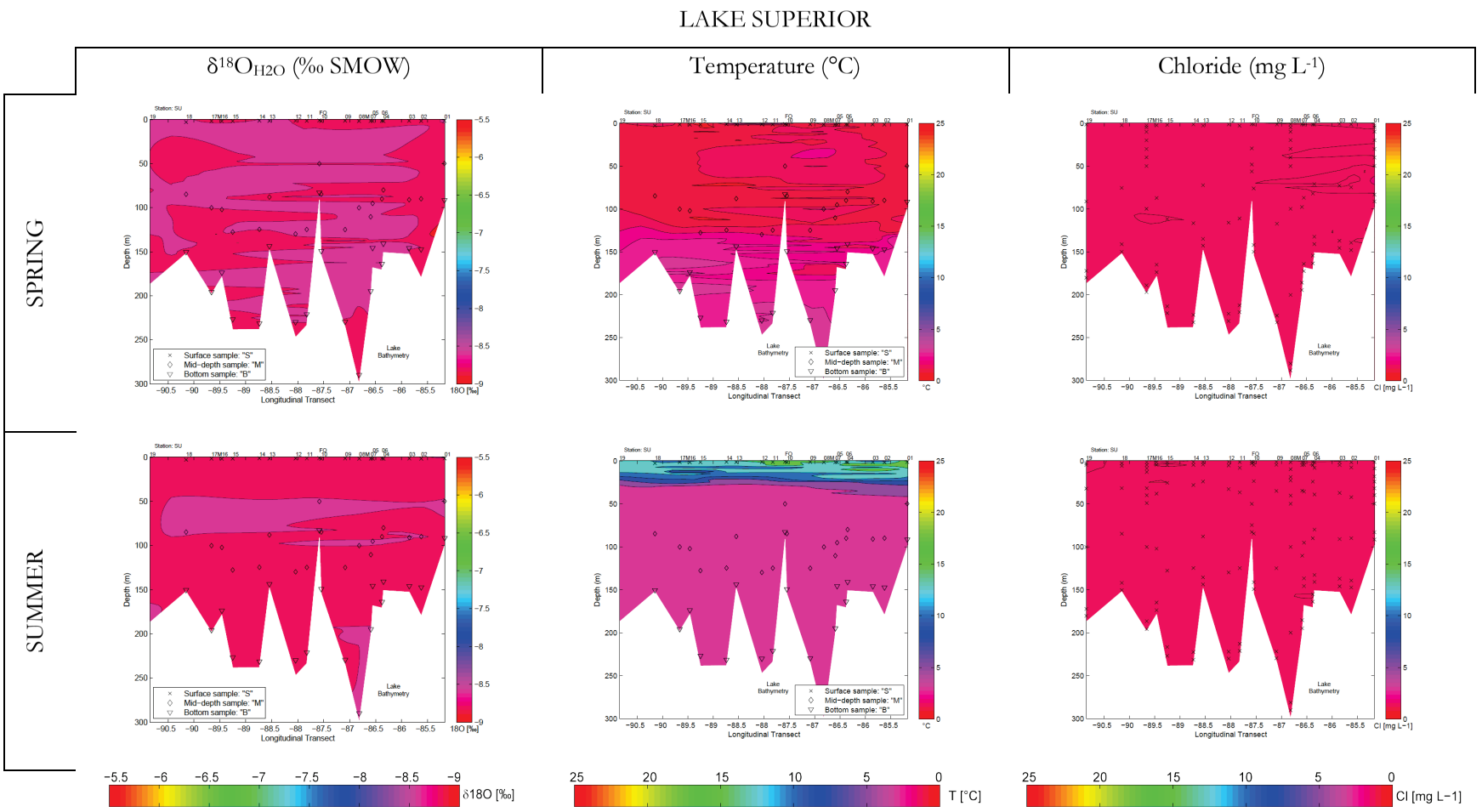

Figure 3-5a. At-depth longitudinal profile for Lake Superior waters (2007): (from left to right) $\delta^{18}O$, temperature and chloride concentration. Spring results are shown in the upper three plots, summer results are shown in the bottom three plots. Isotope sampling locations are marked by a cross (surface), diamond (mid depth) or a triangle (near bottom) in temperature and $\delta^{18}O$ plots. Chloride measurement sites are shown as crosses.

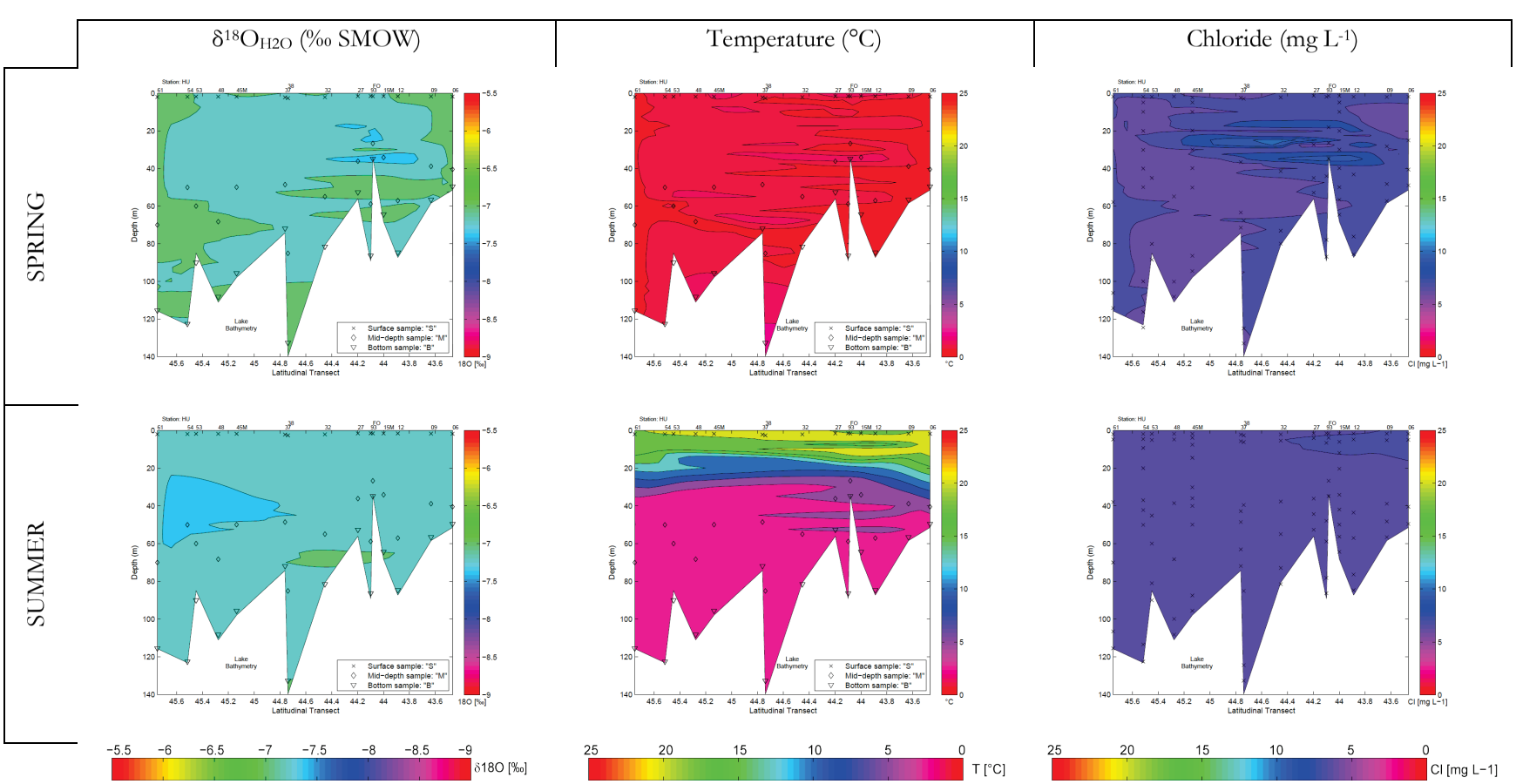

Figure 3-5b. At-depth latitudinal profile for Lake Huron waters (2007): (from left to right) $\delta^{18}O$, temperature and chloride concentration. Spring results are shown in the upper three plots, summer results are shown in the bottom three plots. Isotope sampling locations are marked by a cross (surface), diamond (mid depth) or a triangle (near bottom) in temperature and $\delta^{18}O$ plots. Chloride measurement sites are shown as crosses.

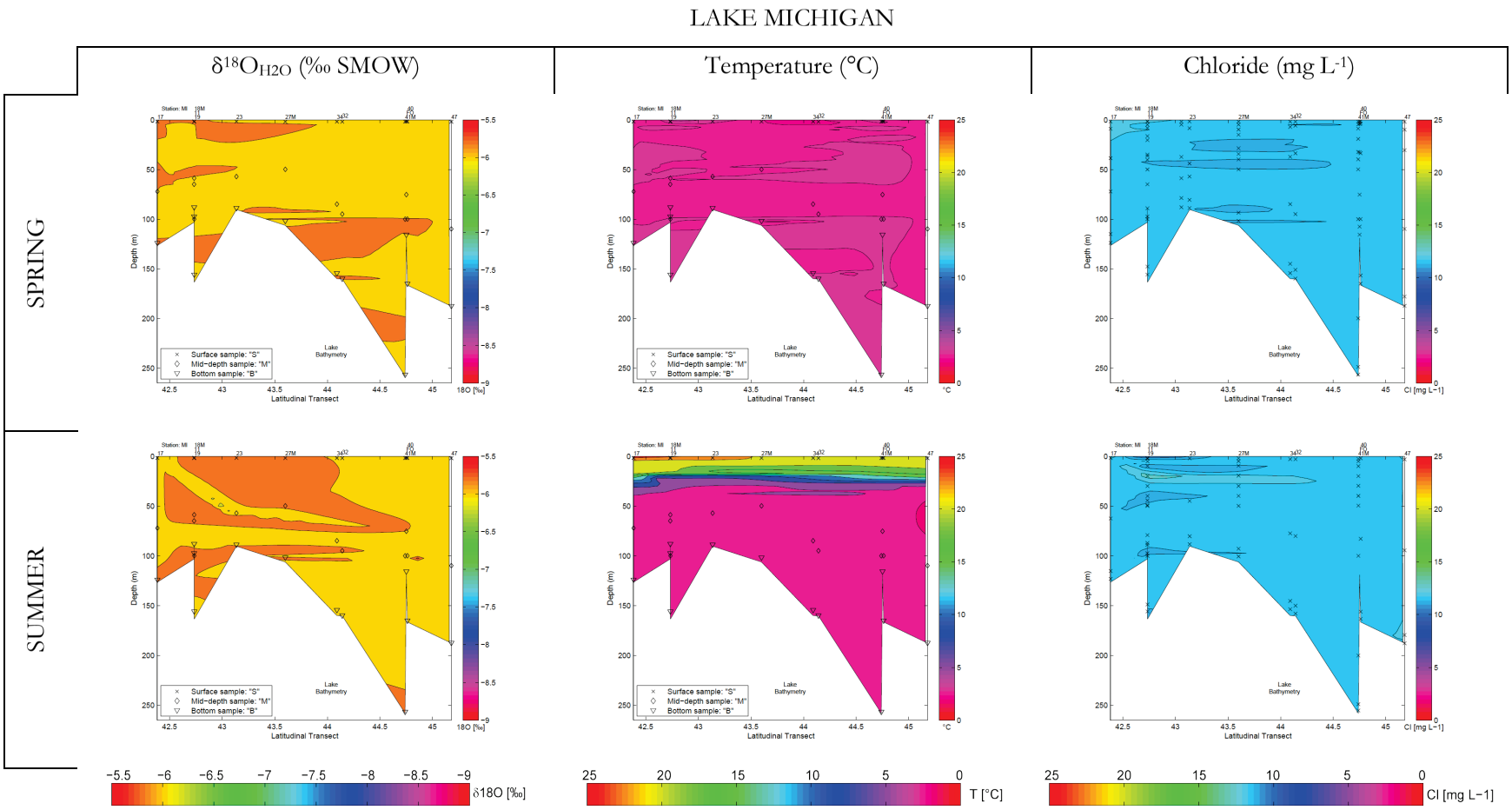

Figure 3-5c. At-depth latitudinal profile for Lake Michigan waters (2007): (from left to right) $\delta^{18}O$, temperature and chloride concentration. Spring results are shown in the upper three plots, summer results are shown in the bottom three plots. Isotope sampling locations are marked by a cross (surface), diamond (mid depth) or a triangle (near bottom) in temperature and $\delta^{18}O$ plots. Chloride measurement sites are shown as crosses.

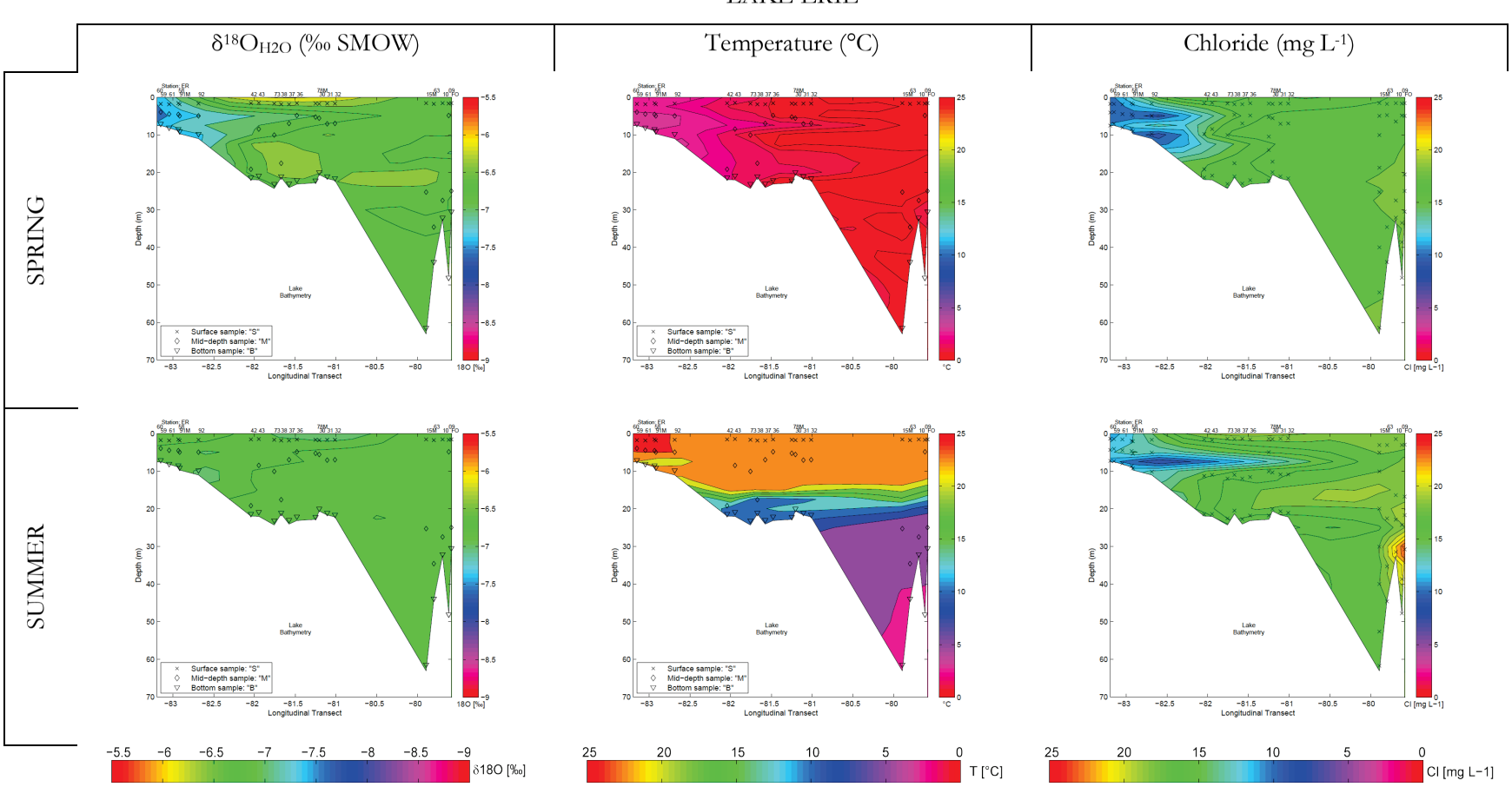

Figure 3-5d. At-depth longitudinal profile for Lake Erie waters (2007): (from left to right) $\delta^{18}O$, temperature and chloride concentration. Spring results are shown in the upper three plots, summer results are shown in the bottom three plots. Isotope sampling locations are marked by a cross (surface), diamond (mid depth) or a triangle (near bottom) in temperature and $\delta^{18}O$ plots. Chloride measurement sites are shown as crosses.

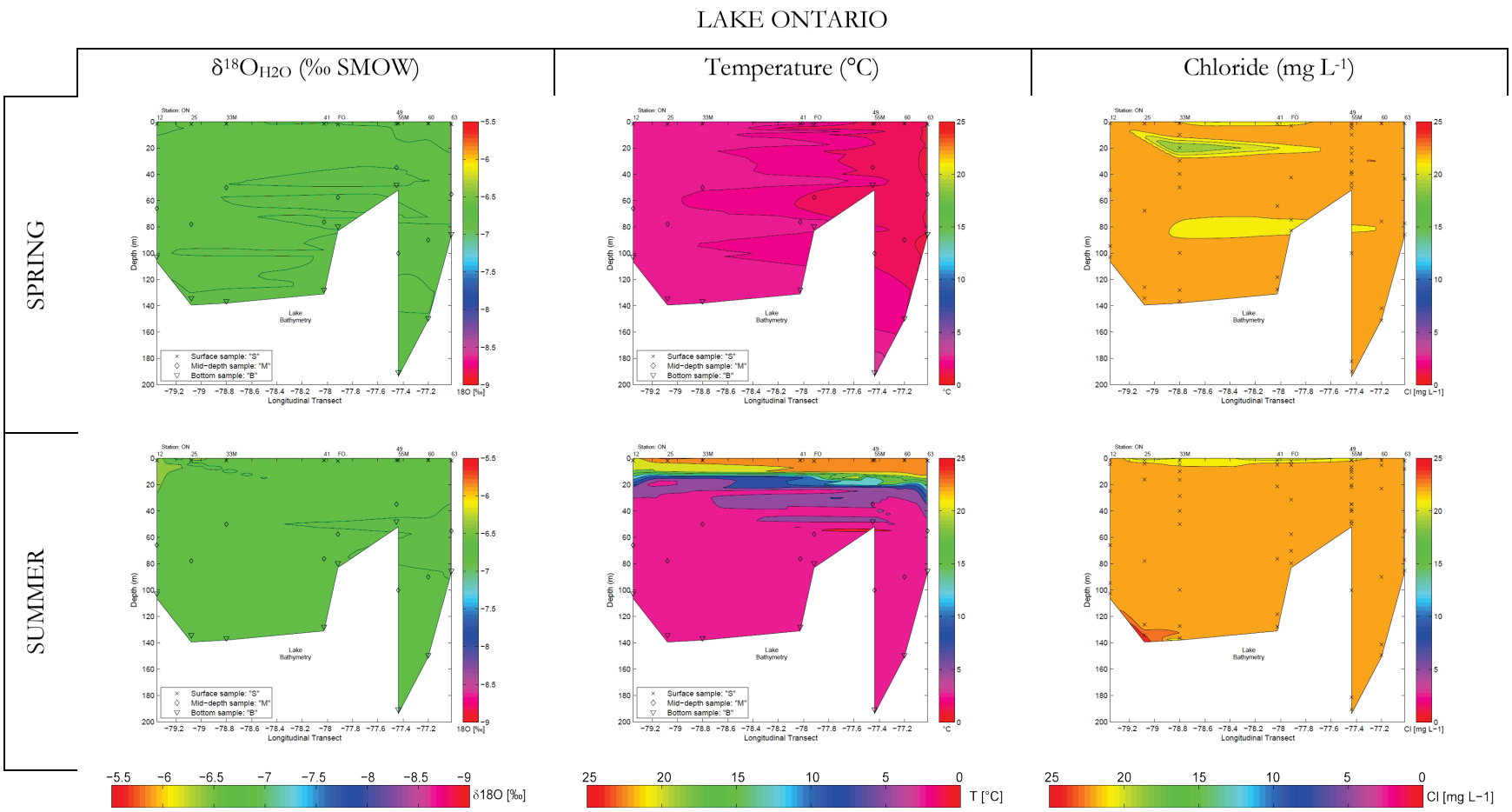

Figure 3-5e. At-depth longitudinal profile for Lake Ontario waters (2007): (from left to right) $\delta^{18}O$, temperature and chloride concentration. Spring results are shown in the upper three plots, summer results are shown in the bottom three plots. Isotope sampling locations are marked by a cross (surface), diamond (mid depth) or a triangle (near bottom) in temperature and $\delta^{18}O$ plots. Chloride measurement sites are shown as crosses.

Overall, stable oxygen and hydrogen isotopes in each Great Lake are fairly homogenous both spatially and seasonally, with the exception of Lake Erie. Perhaps the most revealing result of at-depth transects is shown by $\delta^{18}O$ values and temperatures during the summer cruise. A thermally-induced density stratification develops in the summer months for all Great Lakes (Figures 3-5a - e). This stratification limits exchange between surface and deep waters to diffusion, largely removing water mass mixing. Isotopic stratification is expected if lake evaporation is significant since summer epilimnion waters only weakly exchange with underlying waters by diffusion and turbulent mixing and evaporated waters will be depleted in the heavy isotopes of oxygen and hydrogen, thus enriching the remaining epilimnion waters. Despite sampling in the late-summer (August) - and thus sampling waters that have had potential to interact with the atmosphere for several months - a surface ^{18}O-enrichment is not apparent for any of the Great Lakes. The lack of $^{18}O/^{16}O$ stratification in waters of the Great Lakes during the summer months is explained by a very small evaporate flux during the summer. This result is supported by energy balance evaporation estimates that suggest little evaporation occurs during the warm, humid summer months (Croley II 1989).

At-depth $\delta^{18}O$ transects also provide information on Lake Michigan and Lake Huron exchange. Lake Michigan-Huron are treated as a single lake in some works (Neff and Nicholas 2004). Isotopic results for waters in Lake Michigan and Huron show that these two water bodies are isotopically-distinct, in addition to their geographical separation. Furthermore, a large flux of water is proposed to migrate through the Straits of Mackinac that connect the two water bodies. The flux into Lake Michigan is proposed to be $36 km^3/yr$. However, Schwab et al. (2005) point out that it is unclear whether the water entering Lake Michigan actually integrates with into Lake Michigan, or if it simply mixes in the Straits of Mackinac and is advected back into Lake Huron. ^{18}O is a conservative tracer of water masses, and unlike chloride does not have an important anthropogenic component in the Great Lakes basin. From at-depth profiles, the isotope composition of Lake Michigan appears to be fairly homogenous, and an overwhelming isotopic signature of Lake Huron waters (more ^{18}O-depleted than Lake Michigan's) is not evident. This result suggests that Lake Michigan-Huron water exchange may not fully integrate into the downstream lake, with important implications for residence and flushing times for the Lakes, particularly Lake Michigan that does not have a direct connecting channel inflow.

As mentioned in the above paragraph, chloride is a hydrophilic anion and is sometimes a useful tracer of water parcel advection and mixing in absence of - or with consideration of - artificial sources. Like $\delta^{18}O$ and $\delta^{2}H$ values, chloride levels are found to have a reasonably consistent spatial and seasonal distribution within each Great Lake. The Great Lakes use of chloride as a water balance tracer is lessened due to additions from road salts (NaCl, CaCl solutions) and possibly from water softeners in the Great Lakes basin (Chapra et al. 2009). Chloride concentrations are highest in the lower Great Lakes where the average population density is higher (Michigan, Erie, Ontario). A cross plot of $\delta^{18}O$ values against chloride (Figure 3-6a), sodium (Figure 3-6b), calcium(Figure 3-6c), and magnesium (Figure 3-6d) concentrations in Great Lakes water samples is shown in Figure 3-6. $\delta^{18}O$-Mg^{2+} concentrations show a linear trend for all Great Lakes samples ($R^2 = 0.954$). Mg^{2+} is not added in the same large quantities as sodium, chloride and calcium are for road de-icing applications (in the forms of halite - NaCl - and CaCl solution). Regressions for $\delta^{18}O$ against (Ca^{2+}), (Na^{+}) or (Cl^{-}) show lower correlation values ($R^2 = 0.90$, 0.68 and 0.58), reflecting an additional source of these solutes such as road de-icing materials, water

softeners or natural groundwater discharge from Paleozoic formations that crop out in the lower Great Lakes.

Temperature is the most seasonally and temporally variant of the three parameters shown in Figure 3-5a - 3-5e ($\delta^{18}O$, chloride concentration and temperature). All five of the Great Lakes develop a thermally-induced density stratification in summer (density is a function of temperature; density transects for each Great Lake in spring and summer are available in the appendices). The depth of this epilimnion layer reaches 15 to 25 metres. Temperature also shows an east-west variation in Lake Erie waters. Waters to the west are warmer by roughly three degrees than those in the eastern part of the basin in the spring. This could reflect latent cooling during evaporation as the waters proceed downstream (east).

The combination of temperature and $\delta^{18}O$ measurements at-depth is shown here to successfully assess a lack of both summertime evaporation and metalimnion-epilimnion mixing in the Great Lakes. This sampling technique could be applied to other large surface waters and may be the least expensive method available to assess seasonality in evaporation rates for certain lakes. This is especially significant when considering logistical difficulties associated with establishing numerous physical climate monitoring stations over large areas of open water, and that near-shore sites are subject to annual freeze-thaw cycles.

Depth-$\delta^{18}O$ plots highlight the vertical homogeneity of the Great Lakes. The homogenous isotope composition of the lakes' water is produced by seasonal overturn (spring and fall seasons), coupled with very low evaporation during stratified seasons (summer). Data for ten other lakes and semi-enclosed or endorheic seas are shown in Figure 3-7 to highlight at-depth changes in $\delta^{18}O$ for lakes that are perennially stratified. Perennially stratified lakes shown are Lake Tanganyika and Lake Kivu. The Great Lakes plot in a similar fashion to other large lakes that undergo seasonal mixing such as Lake Garda, Italy (data from Longinelli et al. 2008). Lake Erie's surface $\delta^{18}O$ values are slightly more ^{18}O-depleted than deeper waters. This is the result of mixing in the epilimnion with catchment runoff and inputs from Lake Huron by the Detroit River. Two of Lake Ontario's most ^{18}O-enriched samples are located at the surface. These may reflect localized water mass stagnation during the evaporation season, which would impart an ^{18}O-enrichment via isotope effects during evaporation.

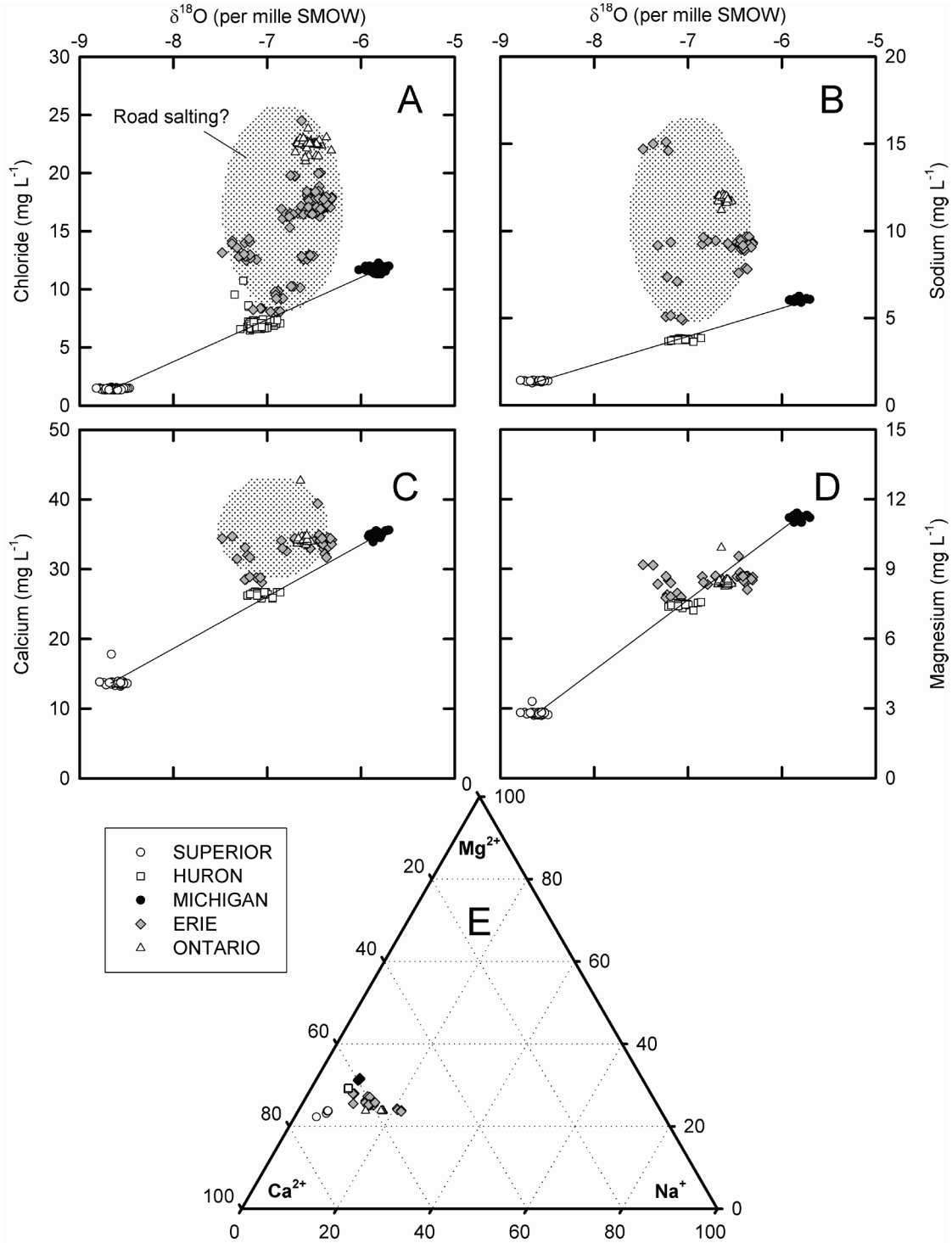

Figure 3-6. $\delta^{18}O$- (a) Chloride, (b) Sodium, (c) Calcium, and (d) Magnesium cross plots for the Great Lakes. Stipple marks a deviation from a linear trend in the upper Great Lakes (solid line), perhaps induced by the prolonged addition of road de-icing materials (halite, CaCl solutions). (e) A ternary plot of major cation concentrations (milliequivilents per litre) is shown in (e).

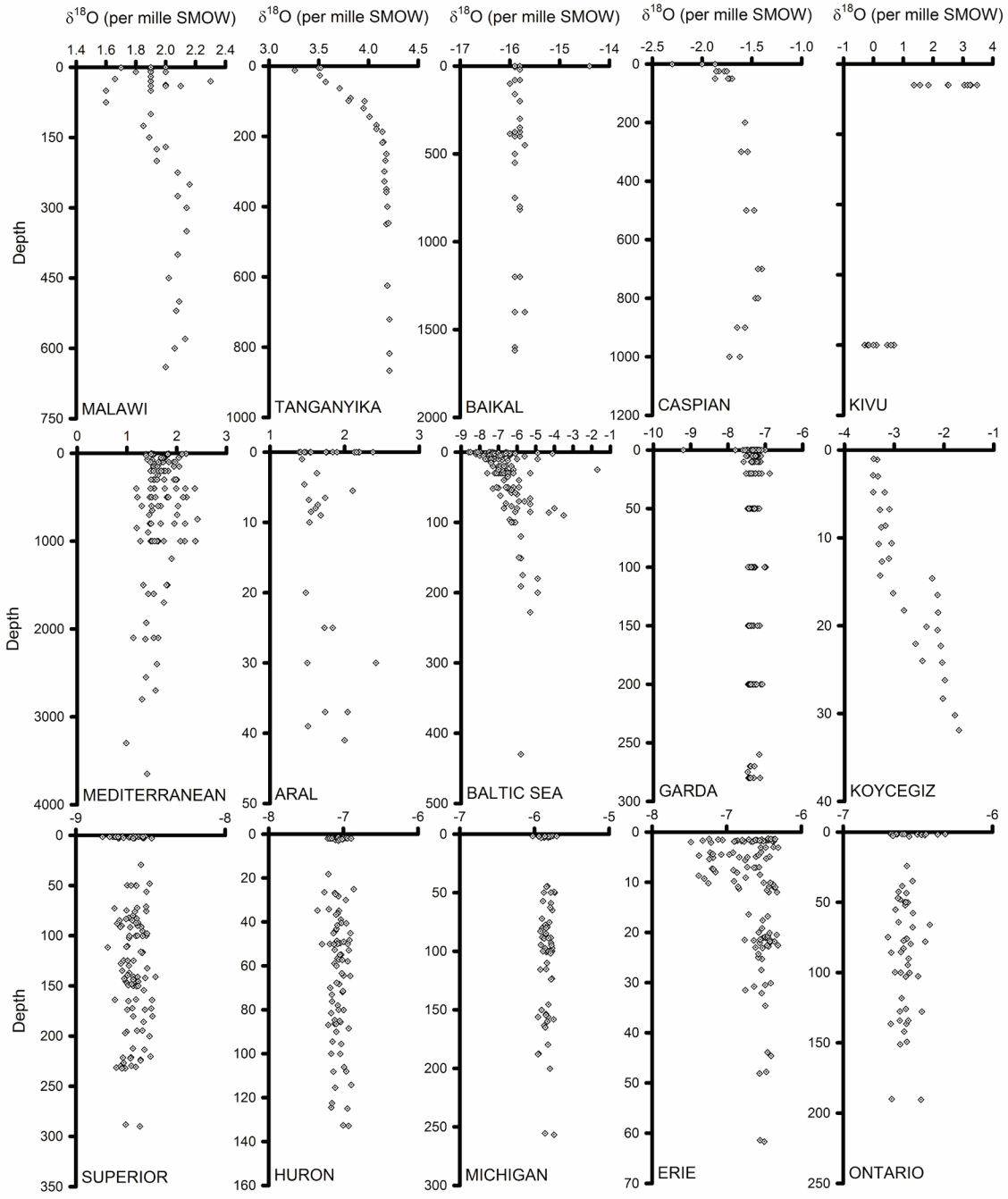

Figure 3-7. Depth-$\delta^{18}O$ plots for large lakes and semi-enclosed or enclosed seas. The lowermost row of plots shown data from the Great Lakes (this work). The isotope-composition of the Great Lakes are relatively homogenous at depth, with the exception of Lake Erie that shows variability in $\delta^{18}O$ values at depths <10 metres. Also, the highest $\delta^{18}O$ values in Lake Ontario are at the lake's surface. For other water bodies, surface waters are either more concentrated in ^{18}O than deep waters (Lake Kivu, Mediterranean Sea); or, ^{18}O is more concentrated at depth than at the surface (Tanganyika, Caspian Sea, Baltic Sea, Lake Koycegiz).

$\delta^{18}O$, temperature and chloride concentrations in Lake Erie show the greatest seasonal and spatial variability of all the Great Lakes. Spring results show east to west differences in all parameters. Waters in the western portion of Lake Erie (ER-59, -60, -61) are characterized by: $\delta^{18}O \approx -7.2$ ‰, $T \approx 3.4$ °C and $(Cl^-) \approx 11$ mg L^{-1}. In the easternmost Lake Erie waters (ER-09, -10, -FO) $\delta^{18}O$ values are higher ($\delta^{18}O \approx -6.6$ ‰) temperatures are lower ($T \approx 0.5$ °C) and chloride concentrations are higher ($(Cl^-) \approx 18$ mg L^{-1}). The observed temperature decrease from west-to-east in Lake Erie may be a result of latent effects imparted during lake evaporation, or input of runoff and precipitation with temperatures lower than Lake Erie's. At the southernmost Lake Huron station (HU06) these parameters are : $\delta^{18}O = -6.9$ ‰, $T = 0.8$ °C and $(Cl^-) = 7.1$ mg L^{-1}. Therefore, the waters found in western Lake Erie in springtime are similar to those of southern Lake Huron, but have higher chloride concentrations, higher temperatures and slightly lower $\delta^{18}O$ values. This may be explained by an addition of runoff between Lake Huron and Lake Erie along the St. Clair and Detroit Rivers (runoff with elevated chloride concentrations - potentially from road salt - and lower $\delta^{18}O$ values compared to Lake Huron's). A tabular synoptic profile from Lake Huron to eastern Lake Ontario is presented in Table 3–2.

Table 3–2 - $\delta^{18}O$, temperature and chloride concentration from Lake Huron to Lake Ontario

	Southern Lake Huron (HU06)	Western Lake Erie (ER 59, 60, 61)	Eastern Lake Erie (ER 09, 10, FO)	Western Lake Ontario (12, 25, 33M)	Eastern Lake Ontario (60, 63)
	Spring / Summer average values shown				
$\delta^{18}O$ (‰ SMOW)	-6.92 / -7.08	-7.15 / -6.79	-6.57 / -6.48	-6.61 / -6.49	-6.61 / -6.55
Temperature (°C)	0.8 / 15.0	3.4 / 25.5	0.5 / 17.6	2.7 / 10.8	1.7 / 13.1
Chloride (mg L^{-1})	7.1 / 7.0	10.8 / 10.2	18.0 / 17.8	21.9 / 22.3	20.3 / 22.8

The isotope composition of Lake Erie varies seasonally. Additionally, the offset of lake waters in δ^2H-$\delta^{18}O$ space varies seasonally. The most ^{18}O-enriched and ^2H-enriched waters in Lake Erie are those of the spring season (Figure 3-8). This is interpreted to be the heavy isotope enrichment signal of elevated evaporation rates in the fall and winter seasons. Quadratic fits for both spring and summer results show a negative coefficient for the squared term, demonstrating a greater offset from the meteoric water line for high $\delta^{18}O$ and δ^2H values (Figure 3-8). Spring season also shows the most ^{18}O- and ^2H-depleted samples. These results plot within the boundaries of Lake Huron results (dark grey area plot in Figure 3-8) and are located in the western portion of Lake Erie; these may be Lake Huron waters that have not been exposed to isotope effects associated with evaporation from Lake Erie.

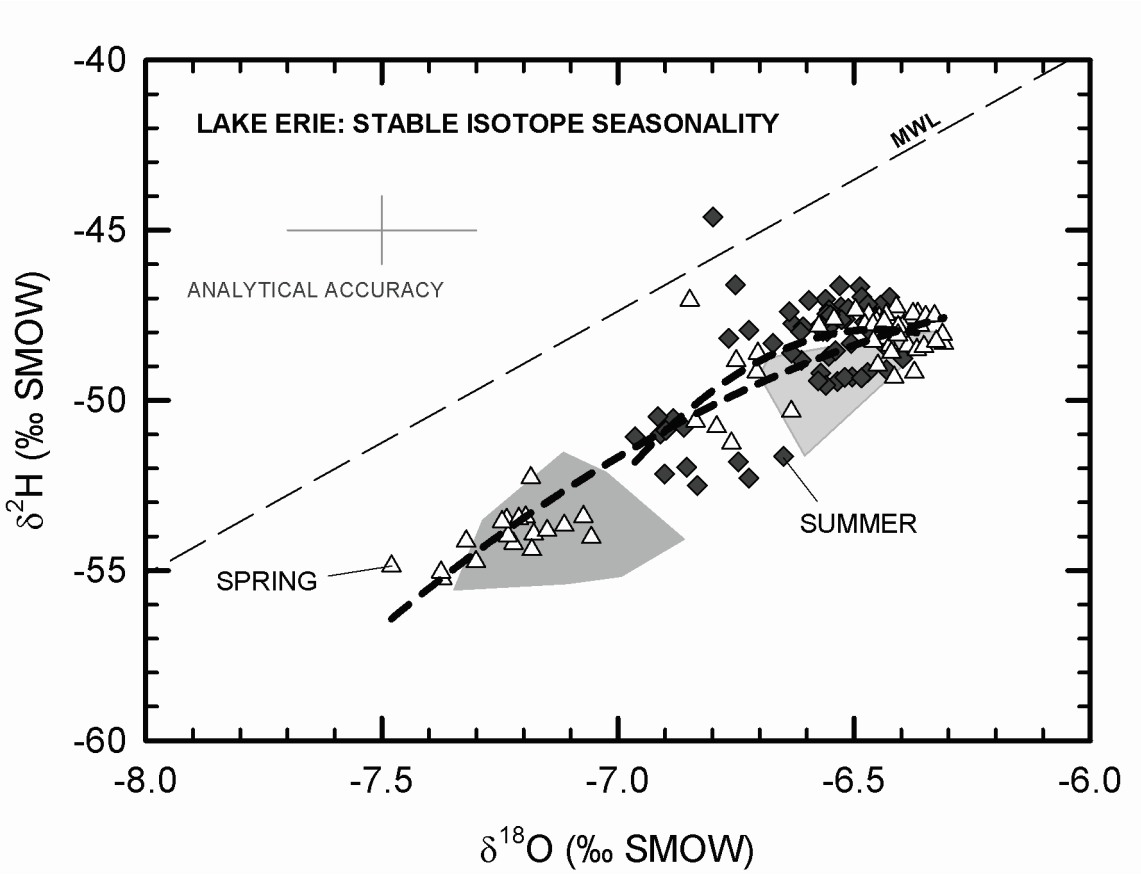

Figure 3-8. Stable isotope composition and seasonality of Lake Erie waters. Spring samples are presented as white triangles, summer as dark grey diamonds. The isotope composition of Lake Huron (upstream of Lake Erie) is presented as a dark grey area plot; that of Lake Ontario (downstream) is shown in light grey. Second order fits are shown for Lake Erie waters for spring (dark grey dashed line) and summer (black dashed line) results.

As mentioned previously, stable isotopes in Lakes Michigan and Huron may contain information on the magnitude of exchange between these lakes. Stations near the Straits of Mackinac (north in Figure 3-5b, and Figure 3-5c) in Lakes Michigan and Huron do not show an influence of the other lake in any geochemical, temperature or nutrient data collected. Quinn (1977) suggested that an immense amount of water exchanges between the two lakes (35 km^3 each year from Huron into Michigan), and used this exchange to justify decreasing Lake Michigan's estimated residence time from ~100 years to 62 years (Quinn 1992; 36 km^3/yr is roughly half the discharge of the St. Mary's River draining lake Superior - 70 km^3/y). However, the assumption embedded in Quinn's calculation is that exchanging between Lake Michigan and Lake Huron completely mixes with the waters in the downstream lake. Given that the average fluxes between Lake Michigan and Lake Huron are comparable (Michigan to Huron flux is higher), it is reasonable to suggest that waters simply mix in the Straits of Mackinac but do not integrate into the downstream Great Lake's waters. The north-south homogeneity in isotopic data in Lakes Michigan and Huron (Figures 3-5b and 3-5c) do not support complete integration of waters flowing in the Straits of Mackinac.

Additional isotopic examination of Quinn's (1992) assumption of integration for flows in the Straits of Mackinac is derived from a sample analyzed for $^{18}O/^{16}O$ and $^{2}H/^{1}H$ by Karim et al. (2008). This survey collected a sample of surface waters in the Straits of Mackinac. The isotopic data for this point plots intermediate to Lakes Huron and Michigan: $\delta^{18}O$ = -6.4 (GLB-66 from Karim et al. 2008; Lake Michigan average $\delta^{18}O$ is -5.83 and Lake Huron's average $\delta^{18}O$ value is -7.07 per mille). This value reflects a 1:1 mixture of Lake Huron and Lake Michigan water with lesser amounts of meteoric water as reflected by the trajectory of the sample towards the meteoric water line (Figure 3-9). This sample is a mixture of the two Great Lakes' waters. However, a sample of Lake Huron water collected less than 100 kilometres to the east shows no indication of mixing with Lake Michigan waters, and instead shows a signature of average Lake Huron water (Karim et al. 2008). Quinn (1977) proposes that the exchange in the Straits is highest in mid-summer months. If this is the case, an isotopic or geochemical signature of Lake Michigan waters in Lake Huron (and Lake Huron in Lake Michigan) samples is expected in the analysis of summer samples. This is not reflected in the isotopic data shown here, suggesting waters flowing in the Straits of Mackinac are not entirely incorporated into the "downstream" Lake.

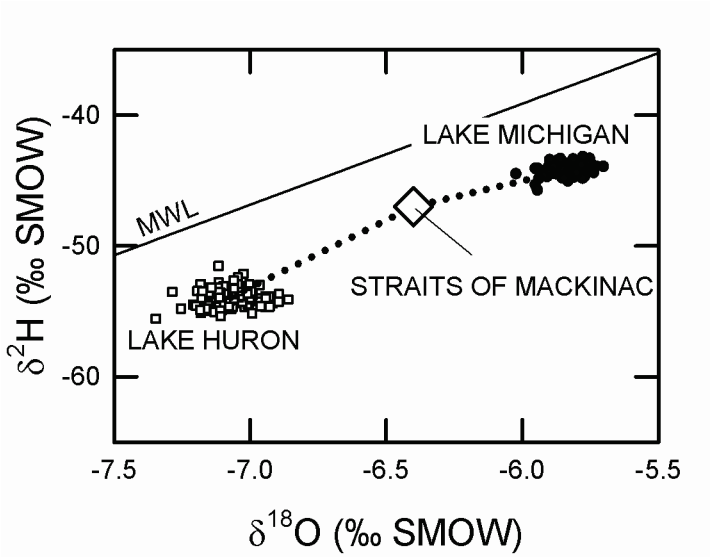

Figure 3-9. $\delta^{18}O$-$\delta^{2}H$ plot showing the mixed sample collected from the Straits of Mackinac (large white diamond; data from Karim et al. 2008; sampled ID GLB-66). Lake Huron and Lake Michigan data (this study) are shown as white squares and dark grey circles, respectively.

If the assumption of Quinn (1992) that flow in the Straits of Mackinac fully mixes with the incoming Great Lake is removed, the residence and flushing times of both Lake Huron and Michigan increases. Using the net outward flow from Lake Michigan into Lake Huron the residence time for Lake Michigan is recalculated here. Two scenarios are used to produce a range of residence time values: (1) that flow from Lake Huron to Lake Michigan does not fully integrate into Lake Michigan waters (2) that mixed waters fully integrate into the opposing lake. There also appears to be some confusion between residence time and flushing times in Quinn (1977), as Equation 6 in this publication uses only liquid outflows to calculate the "residence time." This is instead referred to as a flushing time, since the calculation examines only liquid fluxes and ignores vapour exchange via evaporation. Furthermore, no uncertainty analysis is

shown in earlier residence and flushing time estimates; therefore, the errors associated with these estimates are also unknown.

The residence time of each Great Lake is recalculated using both GLERL estimates, and using an isotopic approach. For Lake Michigan, an evaporation estimate of 38±12 km^3/yr (GLERL long-term average ±1σ) and a net outflow of zero of 51±30 km^3/yr from Lake Michigan to Huron are applied. The residence time (liquid and vapour fluxes) for Lake Michigan is between 29 and 106 years. The flushing time (liquid fluxes only) time of Lake Michigan is between 42 and 239 years. The large uncertainties associated with these estimates originate from large uncertainties associated with the mixing, outflow and evaporate fluxes for Lake Michigan. The isotope and geochemical transect data suggest that the Huron to Michigan water flux may be less than that 36km^3/yr originally proposed (Quinn 1992),

It is possible to compute the residence time of a lake using an isotopic approach as first proposed by Gibson and Edwards (2002). A lake's residence time can by computed by the relation: $\tau = V \cdot x_{E/I} \cdot (1/E)$ where τ, V, $x_{E/I}$ and E represent residence time, volume, E/I ratio and an estimate for the evaporative flux. Alternatively, τ may be calculated by $\tau = V \cdot [Q \cdot (x_{E/Q} + 1)]^{-1}$ where $x_{E/Q}$ is calculated by an isotope mass balance. The liquid outflow from the lake (Q) is known well for the Great Lakes (±5 to ±15 percent) as it is measured daily therefore the second equation for residence time using $x_{E/Q}$ carries the lower certainty for lakes with a single gauged outflow. However, the amount of fully integrating exchange of water is poorly known between Lakes Michigan and Huron. For these lakes - and others where the liquid outflows are not well known - the form $\tau = V \cdot x_{E/I} \cdot (1/E)$ produces less uncertainty. Results for physical balance and isotopically-derived residence times are shown in Table 3–3.

Table 3–3. Hydraulic residence (τ) and flushing times (liquid flux only) for the Great Lakes.

Lake	Volume (km^3)	Q (km^3/yr)	E (km^3/yr)	Exchange (km^3/yr)	τ (IMB)*** (yrs)	τ (EB)** (yrs)	Flushing time (yrs)	Quinn (1992)
Superior	12,100	71±11	49±13		69 (30-132)	84 - 126	149 - 201	173
Huron	3,540	164±25	39±10		16 (8-29)	12 - 21	15 - 25	21
Michigan	4,920	51±30	38±12	0 - 36	27 (13-45)*	29 - 106	42 - 239	62
Erie	484	184±18	21±4		2.3 (1.5-3.5)	2.1 - 2.6	2.4 - 2.9	2.7
Ontario	1,640	220±4	13±3		7.9 (3-17)	6.8 - 7.3	7.3 - 7.6	7.5

* isotope mass balance calculation used large flux from Lake Huron from results of Quinn (1992)
** computed using GLERL values for E and Q
*** E/I or E/Q values obtained by a isotope mass balance

The isotope-derived water residence time estimates are consistently lower than energy balance estimates. As Horita (2008) describes, the isotopic approach

This result may be explained by recycling of evaporated moisture as over lake precipitation. This "recycled" moisture is embedded within conventional hydrologic estimates, and is included in the total evaporation flux estimates as calculated by these methods. The isotopic approach provides a different perspective to large lake evaporation. Equation (3) sets up a water balance, where inputs are equal to

outputs at a hydrologic steady state. This equation is used to set up the relationship for E/I by a stable isotope mass balance. However, since a portion of water leaving a Great Lake's surface is recycled as over lake precipitation, this water is included in conventional estimates for both evaporation and direct precipitation. This isotope approach only considers waters that are evaporated and advected from the lake surface, as is defined by outputs in Equation 3.

3.2 Stable isotope mass balance: E/I for the North American Laurentian Great Lakes

Here, calculation outputs of a stable isotope mass balance approach to estimating evaporation as a proportion of inflow are shown. Equations used here are presented earlier in Section 2.2.1. Calculation of isotopic, physical climate and hydrologic inputs to the calculation are presented in Section 2.2.2.

Calculation inputs are either stable isotope or physical climate data. Calculation inputs are: (1) a flux-weighted isotope composition of all hydrologic inputs to a lake (δ_I), (2) the measured isotopic composition of lake water (δ_L), the isotope composition of precipitation weighted to (3) precipitation amount and (4) weighted to seasonality in evaporation, (5) the temperature of the lower troposphere, (6) the temperature of waters at the surface of the lake, and (7) the relative humidity of the lower troposphere (all of 5, 6 and 7 weighted to seasonality in evaporation). Here, results of the calculation using the computed input parameters for each Great Lake (Section 2.2.2) and evaporation equations (Section 2.2.1) are presented. Tabular results are shown in Table 3–4. Table 3–5 provides an explanation for all parameters listed in Table 3–4.

Table 3–4. Evaporation calculation for each Great Lake under smooth and rough kinetic fractionation scenarios.

	LAKE	Superior	Superior	Huron	Huron	Michigan	Michigan	Erie	Erie	Ontario	Ontario
(i) Input data	e_K scenario	Smooth	Rough	Smooth	Rough	Smooth	Rough	Smooth	Rough	Smooth	Rough
	δ_I ^{18}O	-11.5	-11.5	-8.8	-8.8	-8.1	-8.1	-7.6	-7.6	-7.3	-7.3
	δ_I ^{2}H	-80.8	-80.8	-62.7	-62.7	-56.6	-56.6	-55.6	-55.6	-52.4	-52.4
	δ_L ^{18}O	-8.6	-8.6	-7.1	-7.1	-5.8	-5.8	-6.3	-6.3	-6.5	-6.5
	δ_L ^{2}H	-65.6	-65.6	-53.9	-53.9	-44.2	-44.2	-48.0	-48.0	-48.9	-48.9
	$\delta_{P\ EVAP}$ ^{18}O	-14.0	-14.0	-12.3	-12.3	-10.1	-10.1	-8.9	-8.9	-10.9	-10.9
	$\delta_{P\ EVAP}$ ^{2}H	-102.6	-102.6	-88.3	-88.3	-74.4	-74.4	-56.2	-56.2	-73.1	-73.1
	T_{LAKE}	4.9	4.9	6.4	6.4	9.0	9.0	15.0	15.0	9.4	9.4
	T_{AIR}	0.3	0.3	6.5	6.5	5.8	5.8	11.8	11.8	6.5	6.5
	RH	75.2	75.2	78.5	78.5	75.5	75.5	74.4	74.4	76.4	76.4
	MIX	17.4	15.8	15.3	13.9	18.0	16.5	17.7	14.6	13.4	10.4
	$C_{K\ 18O}$	18.6	14.2	18.6	14.2	18.6	14.2	18.6	14.2	18.6	14.2
	$C_{K\ 2H}$	16.5	12.5	16.5	12.5	16.5	12.5	16.5	12.5		12.5
(ii) Iteration one	$T_{AIR\text{-}KELVIN}$	273.5	273.5	279.7	279.7	279.0	279.0	285.0	285.0	279.7	279.7
	α^* ^{18}O	1.01178	1.01178	1.01109	1.01109	1.01117	1.01117	1.01055	1.01055	1.01109	1.01109
	α^* ^{2}H	1.11131	1.11131	1.10188	1.10188	1.10290	1.10290	1.09455	1.09455	1.10188	1.10188
	ε^* ^{18}O	0.01178	0.01178	0.01109	0.01109	0.01117	0.01117	0.01055	0.01055	0.01109	0.01109
	ε^* ^{2}H	0.11131	0.11131	0.10188	0.10188	0.10290	0.10290	0.09455	0.09455	0.10188	0.10188
	ε_K ^{18}O	0.00462	0.00352	0.00400	0.00305	0.00456	0.00348	0.00477	0.00364	0.00439	0.00335
	ε_K ^{2}H	0.00410	0.00310	0.00356	0.00269	0.00405	0.00306	0.00423	0.00320	0.00390	0.00295
	$\delta_{P\ EVAP} - \varepsilon^*$ ^{18}O	-25.5	-25.5	-23.1	-23.1	-21.0	-21.0	-19.2	-19.2	-21.8	-21.8
	$\delta_{P\ EVAP} - \varepsilon^*$ ^{2}H	-192.5	-192.5	-172.6	-172.6	-160.8	-160.8	-137.7	-137.7	-158.8	-158.8
	T	0.3	0.3	6.5	6.5	5.8	5.8	11.8	11.8	6.5	6.5
	e_S	6.2	6.2	9.6	9.6	9.2	9.2	13.8	13.8	9.6	9.6
	q_S	4.7	4.7	7.6	7.6	6.9	6.9	10.3	10.3	7.4	7.4

Table 3–4 (continued).

	E/I_i ^{18}O	21.0	30.5	16.5	28.0	13.9	18.8	6.2	7.8	5.0	7.0
	E/I_i ^{2}H	191.7	359.6	-81.0	-60.0	60.6	74.1	10.1	10.6	11.1	12.6
(iii) Downwind air parcel	δ_E ^{18}O	-22.3	-18.0	-17.5	-13.2	-22.1	-17.9	-27.3	-23.1	-21.7	-17.4
	δ_E ^{2}H	-73.5	-69.8	-43.0	-39.1	-64.6	-60.9	-123.0	-119.5	-80.7	-77.0
	T_{DW}	2.6	2.6	6.5	6.5	7.4	7.4	13.4	13.4	8.0	8.0
	e_S	7.3	7.3	9.6	9.6	10.3	10.3	15.3	15.3	10.6	10.6
	q_S	7.3	7.3	9.6	9.6	10.3	10.3	15.3	15.3	10.6	10.6
(iv) Mixed air parcel	$\delta_{A\ MIX}$ ^{18}O	-24.9	-24.3	-22.2	-21.7	-21.2	-20.5	-20.7	-19.8	-21.7	-21.3
	$\delta_{A\ MIX}$ ^{2}H	-171.8	-173.1	-152.7	-154.1	-143.5	-144.3	-135.1	-135.1	-148.4	-150.3
	T_{MIX}	0.7	0.7	6.5	6.5	6.1	6.1	12.1	12.0	6.7	6.7
	$q_{S\ MIX}$	5.1	5.1	7.9	7.8	7.5	7.5	11.2	11.0	7.8	7.7
	$e_{S\ MIX}$	6.4	6.4	9.6	9.6	9.4	9.4	14.0	14.0	9.8	9.7
	RH_{MIX}	80.3	79.8	81.8	81.5	80.4	80.0	79.4	78.5	79.9	79.1
(v) Iteration two	α^* ^{18}O	1.01174	1.01174	1.01109	1.01109	1.01114	1.01114	1.01052	1.01053	1.01107	1.01108
	α^* ^{2}H	1.11067	1.11073	1.10189	1.10189	1.10248	1.10251	1.09417	1.09424	1.10160	1.10166
	ε^* ^{18}O	0.01174	0.01174	0.01109	0.01109	0.01114	0.01114	0.01052	0.01053	0.01107	0.01108
	ε^* ^{2}H	0.11067	0.11073	0.10189	0.10189	0.10248	0.10251	0.09417	0.09424	0.10160	0.10166
	ε_K ^{18}O	0.00367	0.00286	0.00339	0.00263	0.00365	0.00284	0.00384	0.00305	0.00375	0.00297
	ε_K ^{2}H	0.00326	0.00252	0.00301	0.00232	0.00325	0.00250	0.00341	0.00268	0.00333	0.00261
	δ_E ^{18}O	-18.9	-17.6	-17.1	-15.4	-17.0	-16.0	-19.4	-19.0	-18.5	-16.7
	δ_E ^{2}H	-120.0	-113.2	-105.0	-96.4	-105.2	-99.7	-124.5	-122.4	-104.6	-96.1
	δ^* ^{18}O	-6.0	-6.3	-4.8	-5.1	-3.0	-3.2	-2.8	-2.7	-3.4	-3.8
	δ^* ^{2}H	-50.0	-51.7	-40.8	-42.8	-27.1	-28.3	-25.3	-24.8	-32.7	-34.5
	E/I_{ii} ^{18}O	27.9	31.9	17.3	20.8	20.3	22.3	9.9	10.2	6.3	7.5
	E/I_{ii} ^{2}H	27.9	31.9	17.3	20.8	20.3	22.3	9.9	10.2	6.3	7.5
	GLERL E/I	43	43	19	19	31	31	10	10	5	5

Table 3–5. Explanation of parameters listed in Table 3–4.

	LAKE	Lake title	Weighting
(i) Input data	e_K scenario	Rough or smooth kinetic fractionation factors, based on wind speeds of Araguás-Araguás et al. (2000)	-
	δ_I	Isotope composition of water inputs	Amount
	δ_L	Isotope composition of lake surface waters	-
	$\delta_{P\ EVAP}$	Isotope composition of precipitation	Evap.
	T_{LAKE}	Lake surface temperature	Evap.
	T_{AIR}	Temperature of overlying air	Evap.
	RH	Relative humidity of overlying air	Evap.
	MIX	Amount of mixing of air temperature, δ_E, and specific humidity required to match E/I for ^{18}O and ^{2}H tracers	-
	C_K	Kinetic isotope effect coefficient for calculating ε_K	-
(ii) Iteration one	$T_{AIR-KELVIN}$	Temperature of overlying air (Kelvin)	Evap.
	α^*	Equilibrium water-vapour fractionation factor	Evap.
	ε^*	Equilibrium water-vapour separation factor	Evap.
	ε_K	Kinetic water-vapour separation factor	Evap.
	$\delta_{P\ EVAP}$ - ε^*	Isotope composition of ambient atmospheric moisture	Evap.
	T	Temperature of the overlying air	Evap.
	e_S	Saturation vapour pressure of an evaporating air parcel (calculated using equations of Buck 1981)	-
	q_S	Saturation vapour pressure of an evaporating air parcel	-
	E/I_i	Initial E/I output using above parameters	-
(iii) D.wind	δ_E	Isotope composition of evaporated moisture advected beyond the lake area	-
	T_{DW}	Temperature of an evaporating air parcel; assumed to be an average of the lake surface and air temperatures	-
	e_S	Saturation vapour pressure of the overlying air (calculated using equations of Buck 1981)	-
	q_S	Specific vapour pressure of the overlying air	-
(iv) Mixed air parcel	$\delta_{A\ MIX}$	Mixed isotope composition of ambient atmospheric moisture	-
	T_{MIX}	Mixed temperature of the overlying air	-
	$q_{S\ MIX}$	Mixed saturation vapour pressure of the overlying air (calculated using equations of Buck 1981)	-
	$e_{S\ MIX}$	Mixed specific vapour pressure of the overlying air	-
	RH_{MIX}	Mixed relative humidity ($q_{s\ MIX}/e_{s\ MIX}$)	-
(v) Iteration two	α^*	Mixed equilibrium water-vapour fractionation factor	-
	ε^*	Mixed equilibrium water-vapour separation factor	-
	ε_K	Mixed kinetic water-vapour separation factor	-
	δ_E	Mixed isotope composition of evaporated moisture advected beyond the lake area	-
	δ^*	Mixed isotope composition of desiccating lake	-
	E/I_{ij}	Evaporated moisture exported from the lake area as a proportion of inflow	-
	GLERL E/I	Great Lakes Environmental Research Laboratory E/I output	-

Evaporation as a proportion of inflow, as a first iteration, produces unrealistic and poor results (some negative values). This is a product of poor accounting for lake effects on the overlying atmosphere into the model, but also suggests that climate parameter inputs do not accurately describe the atmosphere that the Great Lakes evaporate into. A second model iteration is completed that accounts for lake effects and matches E/I value outputs for both ^{18}O and ^{2}H tracers following the procedure outlined in the methods section (mixing of evaporate into the atmospheric moisture). A schematic showing the procedure taken is shown in Figure 3-11.

To constrain both isotopes and mass, the δ_A, air temperature and humidity parameters are modified in accordance with an air mass advecting over a large water body and incorporating a certain amount of evaporated moisture. Between 10 and 17 percent mixing of a saturated air mass with isotope composition δ_E - as defined by initial climate input estimates - is required to constrain E/I outputs for both oxygen and hydrogen isotopes. These values are similar to previous estimates of evaporated moisture in precipitation on the leeward shores of the Great Lakes. These estimates are 4.6 to 15.7 percent (Gat et al. 1994) and 9 to 21 percent for Lake Michigan (Machavaram and Krishnamurthy (1995).

The isotope composition of atmospheric moisture is influenced by the Great Lakes (Gat et al. 1994). This is a well known phenomenon, and is the result of an evaporate signature that plots with a deuterium excess value (Dansgaard 1964) greater than that of waters entering from outside the basin (allochthonous sources). Upon condensation and deposition of vapour - which are governed mostly by equilibrium isotope effects - the isotope composition of precipitation retains the - often elevated - deuterium excess signature imparted by evaporated moisture. For large lakes and semi-enclosed seas that have a liquid discharge (not terminal) this is the case for precipitation on the leeward part of the catchment (see Lake Biwa, Japan - influence of Sea of Japan evaporate (Taniguchi et al. 2000) - is the only large lake to plot above the global meteoric water line in Figure 1-2. As a lake loses a larger and larger proportion of its water by evaporation the lake $\delta^{18}O$ and $\delta^{2}H$ values increase along a slope usually between 4 and 6. As a lake proceeds along this trajectory under a high-evaporation scenario, the deuterium excess of evaporated moisture approaches that of meteoric waters. Therefore, the effect on the isotope composition of atmospheric moisture is expected to be less significant for a terminal, non-chain lake that loses water only by evaporation. In any case, the Great Lakes all have a liquid outflow and the isotope composition of outgoing evaporated moisture from the lakes must be of lower $\delta^{18}O$ and $\delta^{2}H$ values and higher deuterium excess values than that of input waters. This description is portrayed schematically in Figure 3-10a. Note δ_A is recalculated using values of δ_E by rearranging Equation 16 to the form:

$$\delta_A = [-1]\cdot\left[\frac{\left[(1-h+\varepsilon_K)\cdot(\delta_E/1000)-(\delta_L/10^3-\varepsilon^*)/\alpha_{l-v}{}^*+\varepsilon_K\right]}{h}\right]\cdot 10^3 \quad (‰)$$

This is shown in previous works of Gat et al. (1994) and Machavaram and Krishnamurthy (1995); however, these studies examine only summer precipitation in order to avoid complications from kinetic isotope effects during ice crystal formation for winter. The authors' estimates of ~5 to 20 percent of Great Lakes moisture in leeward precipitation seem rather high when compared to energy balance models that produce near-zero values for the summer evaporation flux. This apparent difference between energy and isotopic approaches may reflect moisture exchange between the atmosphere and the lake surface without a net evaporation loss from the lake. However, if this exchange is large enough, then its signal would be expected to be observed in epilimnion waters of the Great Lakes; this is not seen in at-depth

transects shown in this work. Re-examination of precipitation datasets - that have been enhanced since the work of Gat et al., and Machavaram and Krishnamurthy - may provide spatially resolved estimates for the sources of atmospheric vapour on the region. Furthermore, the amount of Great Lakes moisture in winter season lake-effect snowfall could be quantified if the kinetic effects during snow formation can be decoupled from the expectedly higher deuterium excess values of Great Lakes evaporate. Winter precipitation would be expected to show a larger amount of recycled Great Lakes moisture as the majority of evaporation occurs during winter months.

No direct measurement of evaporate over the Great Lakes or of the free atmosphere is measured in this study. However, Gat (2008) reports a value from the work of Vrooman (1948) for vapour over Lake Ontario for ^{18}O abundance of 0.97. Lake Ontario's abundance is reported as 1.00. The meaning of "abundance" is unknown; however, since Lake Ontario's isotope composition is known ($\delta^{18}O$ = -6.57‰ SMOW) the "abundance" can be converted into per mille notation. Doing so, the $\delta^{18}O$ value of the atmosphere over Lake Ontario is -36‰ SMOW. Modelled values are close to -21‰. This work is dated, and analytical techniques in isotope ratio mass spectrometry have advanced significantly since 1948. However, this difference in modelled and measured atmospheric vapour isotope compositions calls for in-situ measurement or over-lake vapour collection to test modelled outputs.

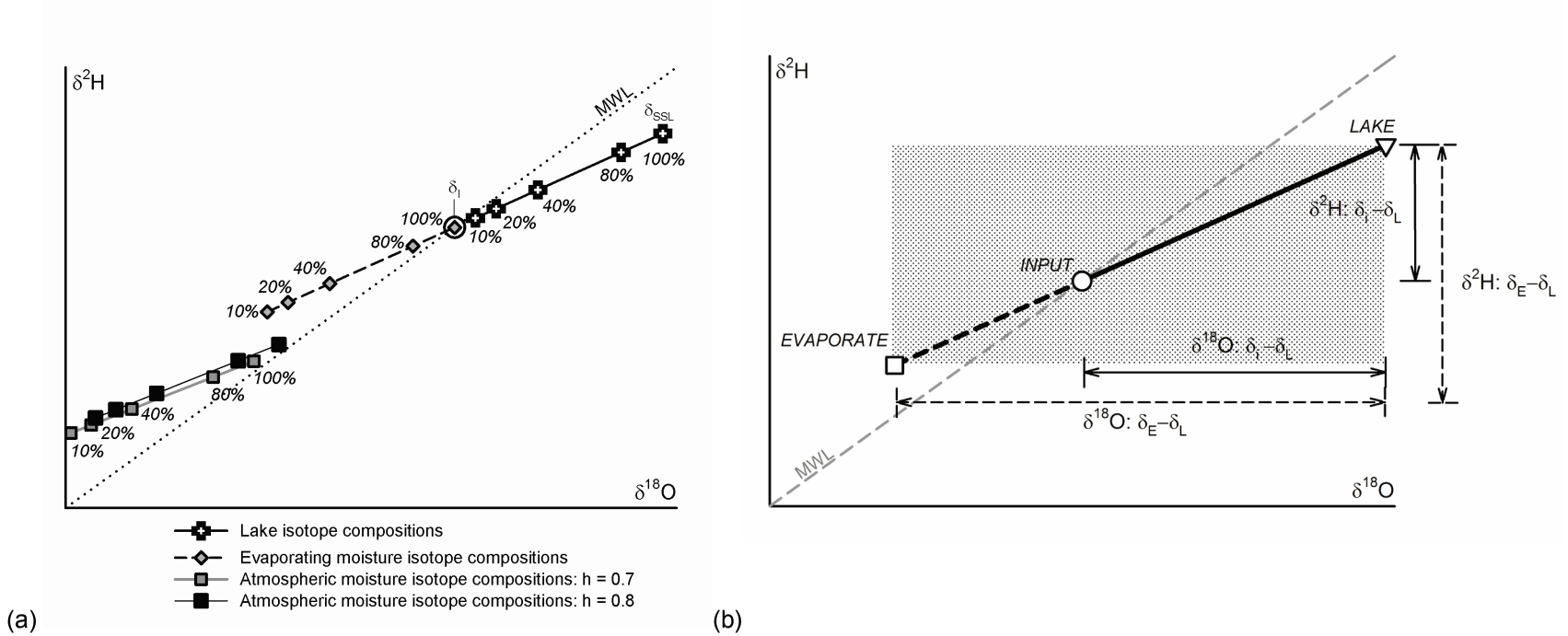

Figure 3-10. (a) Schematic of different E/I scenarios (shown as % values in plot) for the isotope composition of a lake (δ_L; black crosses) and its outgoing evaporated moisture (δ_E; gray diamonds). It is shown here that the isotopic composition of evaporate for lakes with a low E/I value has the greatest separation in deuterium excess values from that of meteoric waters. This isotope composition of inputs is shown as a white circle (with δ_E at E/I = 100% embedded within the circle). δ_A is recalculated from values of δ_E using air temperature (0.3 degrees C), relative humidity (70% to 80%) and lake temperature (4.9) from Lake Superior. For terminal lakes with a known input and lake isotope composition and negligible groundwater discharge, δ_E is also known, since it must equal the isotope composition of input waters exactly to retain an isotopic steady state ($\delta_E = \delta_I$). This makes calculation of δ_A possible for this special scenario, as long as the residence time of the water body is sufficiently long to smooth seasonal variability (Yi et al. 2008). δ_{SSL} refers to the lake isotope composition in this special scenario where E/I = 100% ($\delta_E = \delta_I$). A regression of meteoric waters is plotted for reference (Craig 1961a). (b) Schematic of the calculation of E/I. The isotope compositions (δ^2H and $\delta^{18}O$) of evaporate (square), hydrologic inputs (circle) and the lake (triangle) are shown. the line connecting these isotope compositions is known as an evaporation line, and is shown as a black dashed line between the evaporate and input isotope compositions and as a solid line between the input and the lake isotope compositions.

In order to visualize the mixing technique employed here for the Great Lakes, a $\delta^{18}O$-$\delta^{2}H$ plot is shown for mixing scenarios of zero to 25 percent of Great Lakes evaporate integration into the atmosphere ($0 < x < 0.25$ from Equation 17; Figure 3-12a through 3-12e). It is also useful to envision this procedure in an E/I (^{18}O)-E/I (^{2}H) cross plot. This mixing scenario is presented for each Great Lake in Figures 3-13a through 3-13e. Mixing scenarios of evaporated moisture into the overlying atmosphere are presented as grey shading from black (0%) to white (25%). The trajectory of three variables as mixing increases are shown: δ_A, δ_E and δ^*.

The isotope composition of the atmosphere is calculated to be offset from measured precipitation (weighted to the evaporation season) by equilibrium isotope effects alone. The isotope composition of precipitation weighted to evaporation is shown in Figures 3-12a through 3-12e as $\delta_{P\ (EVAP\ WEIGHTED)}$. This value is used to calculate an initial estimate for δ_A. As shown in Figure 3-10, this initial estimate is unlikely to represent the natural setting, as the value plots near that of meteoric waters instead of at an elevated deuterium excess value (defined by Dansgaard 1964; $d > 10$) as expected for a non-terminal lake system large enough to influence the overlying atmosphere such as the Great Lakes.

As the lakes evaporate, the evaporated moisture mixes with that of the overlying atmosphere. This is shown in the model results, where δ_A values trend towards that of δ_E as greater amounts of evaporate is integrated. The two other mixing parameters are temperature and humidity. As mixing proceeds, the value of δ_E is influenced because the Craig and Gordon (1965) model calculates δ_E as a function of δ_A, air temperature and humidity (see Equation 16). δ_E values follow a trend roughly towards the isotope composition of the lake in equilibrium with the atmosphere (defined as δ_A^* in Craig and Gordon 1965 - pp. 99; redefined here as δ_L^* in Figures 3-12a through 3-12e). This is significant, since this is the expected isotope composition of evaporate under marine conditions (Craig and Gordon 1965). The trajectory toward this value shows a semi-ocean like behaviours of the Great Lakes.

Higher humidity values shift the initial δ_E value towards that of standard mean ocean water for the climate scenario of the Great Lakes. Consequently, the value of δ_E at the intersection with the extrapolation of the local evaporation line as the δ_E-δ_A mixing model proceeds is nearer to that of the isotope composition of the input to the lake. Therefore, a greater amount of evaporation is required to balance the isotope composition of the lake (higher E/I values for higher humidity inputs). Two humidity scenarios are shown in Figures 3-12a through 3-12e because humidity is the most sensitive input parameter for E/I, particularly for values in the Great Lakes basin that approach $h = 80\%$ (Horita et al. 2008).

As the trajectory of δ_E descends below the meteoric water line, it does not equal δ_L^* at a mixing scenario of 100%. This is the result of the initial δ_E estimates that lie well above values intersecting the extrapolation of the local meteoric water line. However, examining the equation of δ_E (Equation 16) more closely, this formula becomes undefined at $h = 100\%$. The denominator ($1-h+\varepsilon_K$) is equal to zero at $h = 100\%$ (since kinetic isotope effects are removed under for a saturated air mass).

For the E/I (^{18}O)-E/I (^{2}H) cross plots, rough kinetic isotope effect conditions produce higher E/I values than laminar conditions. From wind speed data (Mesinger et al. 2006) and kinetic isotope effect scenarios (<7 m/s; Araguás-Araguás et al. 2000) evaporation from the Great Lakes is proposed to be best represented by smooth (laminar) kinetic isotope effect conditions. The difference between smooth and rough E/I outputs is greatest for high humidity input scenarios (Figures 3-13a through 3-13e). The

isotope composition of the evaporate (δ_E) follows a trajectory that intersects an extrapolation of a regression δ_I-δ_L. At this point, the E/I outputs for both ^2H and ^{18}O are synchronized to a common value.

For evaporate mixing scenarios for the Great Lakes, δ_A values follow a trajectory towards that of δ_E as the percent of evaporate mixture is increased. This is consistent with elevated deuterium excess in precipitation on the leeward side of the Great Lakes (Gat et al. 1994; Machavaram and Krishnamurthy 1995). Since vapour condensation is governed primarily by equilibrium isotope effects, the deuterium excess parameter should not vary significantly between atmospheric vapour and its condensed phase, since $\varepsilon^*_{18O}/\varepsilon^*_{2H}$ varies between 8.42 at 25°C and 9.41 at 1°C (Horita and Wesolowski 1994). This does not apply to deposition as kinetic effects are associated with vapour-solid phase transitions (Merlivat and Jouzel, 1979; Jouzel and Merlivat 1984). δ_A values shown have a large separation from precipitation for both $\delta^{18}O$ and δ^2H. This is caused by two converging factors: (1) weighting of precipitation to the evaporation (winter) season leads to low $\delta_{P(EW)}$ values, and (2) weighting of temperature to the evaporation season produces higher equilibrium separation (ε^*) values.

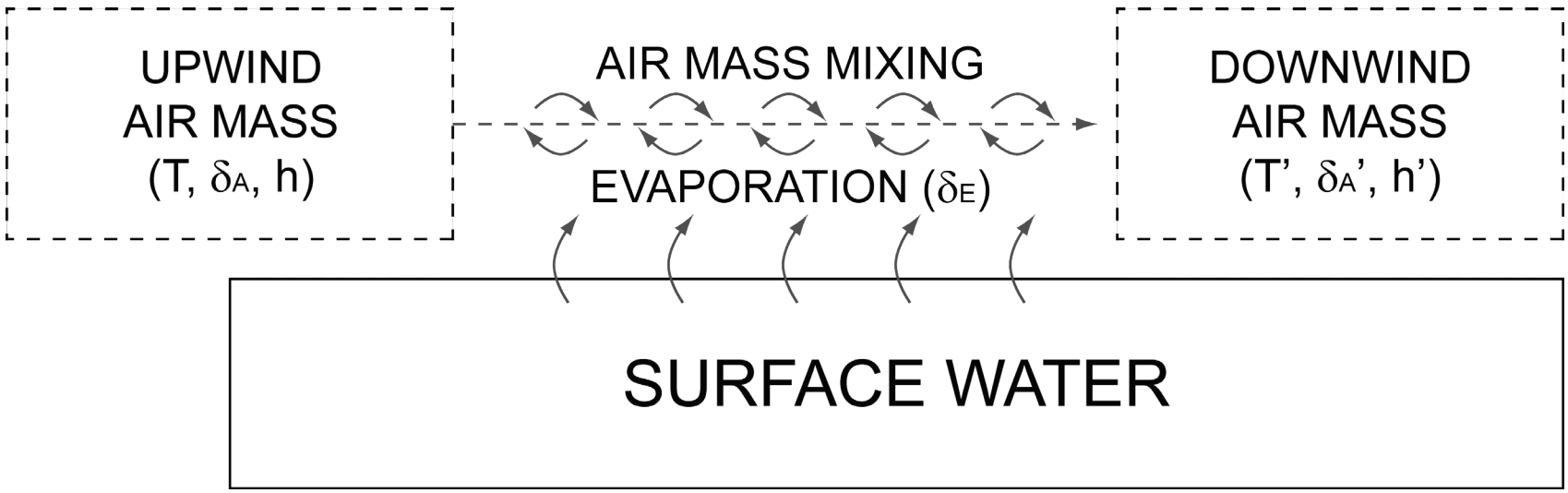

Figure 3-11 - Schematic of the mixing model applied to reiterate the calculation of evaporation as a proportion of inflow for the Great Lakes. An upwind air mass with climate parameters T (air temperature weighted to the evaporation season), δ_A (isotope composition of the free atmosphere - calculated to be in isotopic equilibrium with precipitation weighted to the evaporation season) and h (relative humidity weighted to the evaporation season). These parameters are influenced by large areas of open water, and produce a downwind air mass with a moderated temperature (to a value closer to that of the lake: T'), modified atmospheric vapour isotope composition (δ_A' - approaches a value of the isotope composition of lake evaporate: δ_E) and an elevated humidity (from lake evaporation: h'). The model is reiterated applying the climate scenario shown schematically in the downwind air mass.

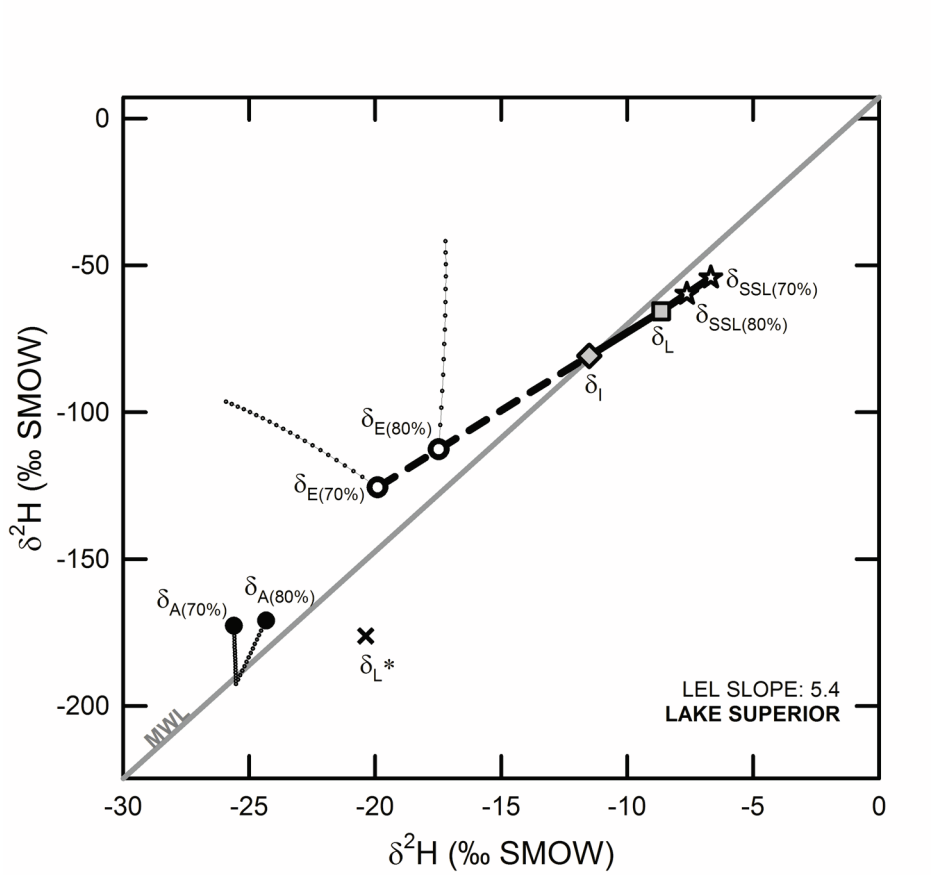

Figure 3-12a. Isotope mass balance scenario for Lake Superior. Two relative humidity input value scenarios are shown: 70% and 80%. Parameters shown in the diagram are the isotope compositions of atmospheric moisture (δ_A; black circles), evaporated vapour (δ_E; white circles), and the isotope composition of a closed lake (δ_{SSL}; white stars, where E/I = 100% for $\delta_E=\delta_I$). The isotope composition of the Great Lake (δ_L, grey square) and the isotope composition of hydrologic inputs to the Great Lake (δ_I; grey square) are shown. Also, the modelled isotope composition of vapour in equilibrium with the Great Lake is shown (δ_L*, black cross; after Craig and Gordon 1965).

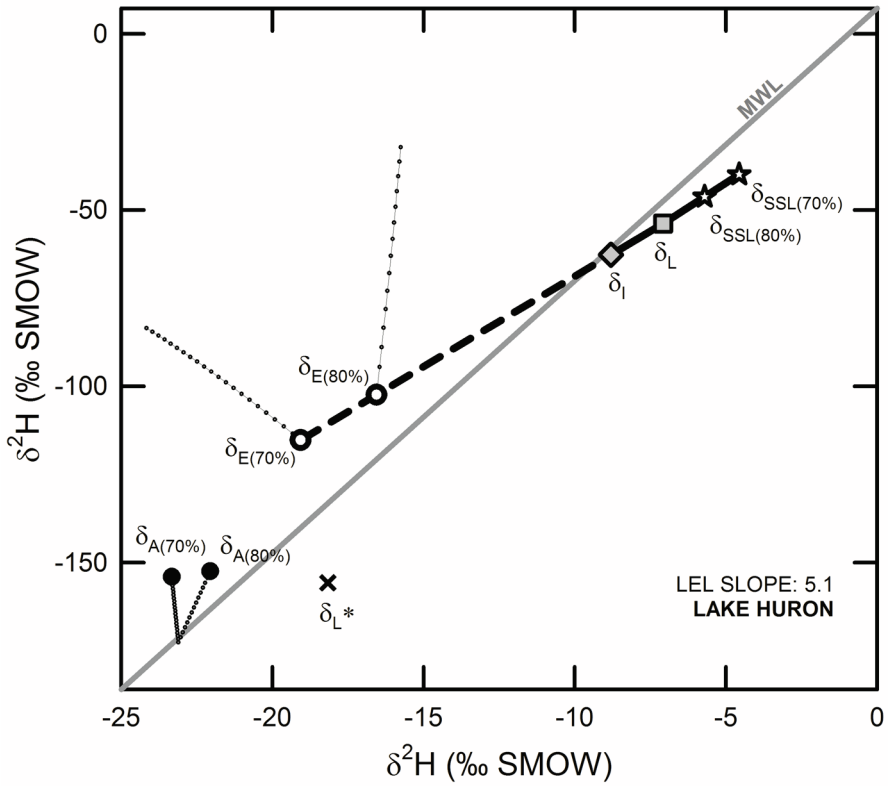

Figure 3-12b. Isotope mass balance scenario for Lake Huron. Two relative humidity input value scenarios are shown: 70% and 80%. Parameters shown in the diagram are the isotope compositions of atmospheric moisture (δ_A; black circles), evaporated vapour (δ_E; white circles), and the isotope composition of a closed lake (δ_{SSL}; white stars, where E/I = 100% for $\delta_E=\delta_I$). The isotope composition of the Great Lake (δ_L, grey square) and the isotope composition of hydrologic inputs to the Great Lake (δ_I; grey square) are shown. Also, the modelled isotope composition of vapour in equilibrium with the Great Lake is shown (δ_L*, black cross; after Craig and Gordon 1965).

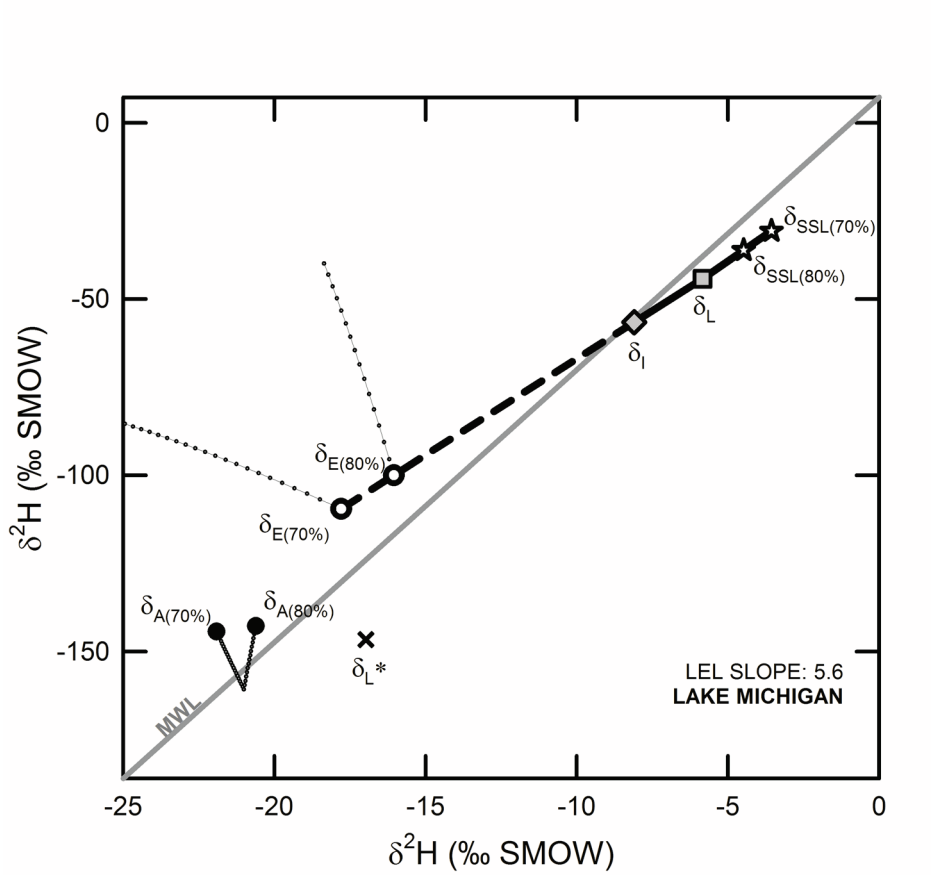

Figure 3-12c. Isotope mass balance scenario for Lake Michigan. Two relative humidity input value scenarios are shown: 70% and 80%. Parameters shown in the diagram are the isotope compositions of atmospheric moisture (δ_A; black circles), evaporated vapour (δ_E; white circles), and the isotope composition of a closed lake (δ_{SSL}; white stars, where E/I = 100% for $\delta_E=\delta_I$). The isotope composition of the Great Lake (δ_L, grey square) and the isotope composition of hydrologic inputs to the Great Lake (δ_I; grey square) are shown. Also, the modelled isotope composition of vapour in equilibrium with the Great Lake is shown (δ_L*, black cross; after Craig and Gordon 1965).

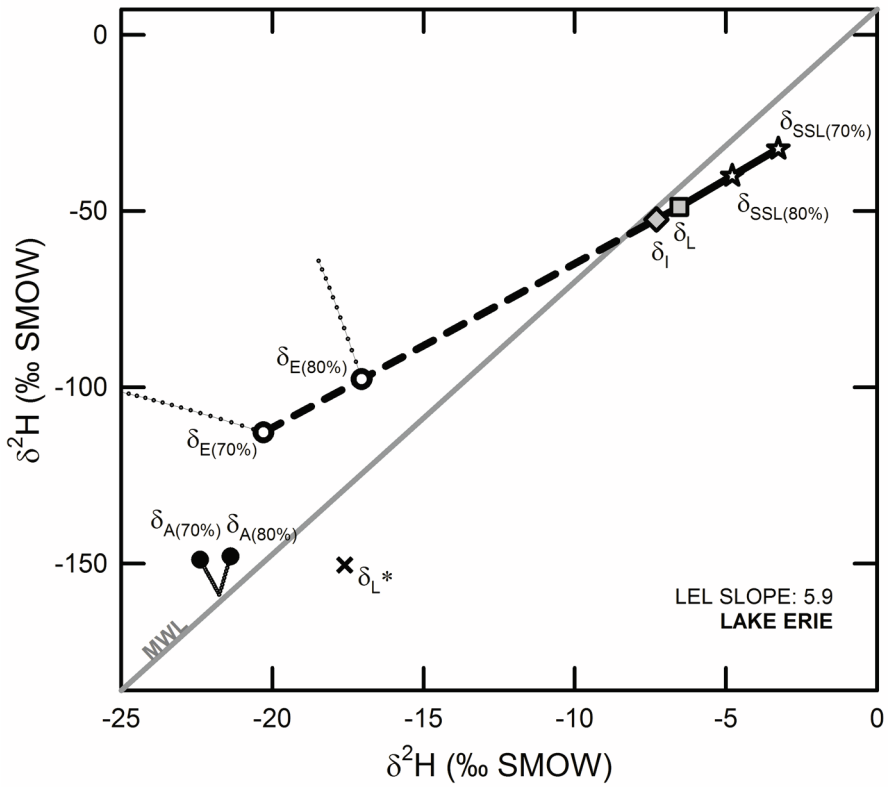

Figure 3-12d. Isotope mass balance scenario for Lake Erie. Two relative humidity input value scenarios are shown: 70% and 80%. Parameters shown in the diagram are the isotope compositions of atmospheric moisture (δ_A; black circles), evaporated vapour (δ_E; white circles), and the isotope composition of a closed lake (δ_{SSL}; white stars, where E/I = 100% for $\delta_E=\delta_I$). The isotope composition of the Great Lake (δ_L, grey square) and the isotope composition of hydrologic inputs to the Great Lake (δ_I; grey square) are shown. Also, the modelled isotope composition of vapour in equilibrium with the Great Lake is shown (δ_L*, black cross; after Craig and Gordon 1965).

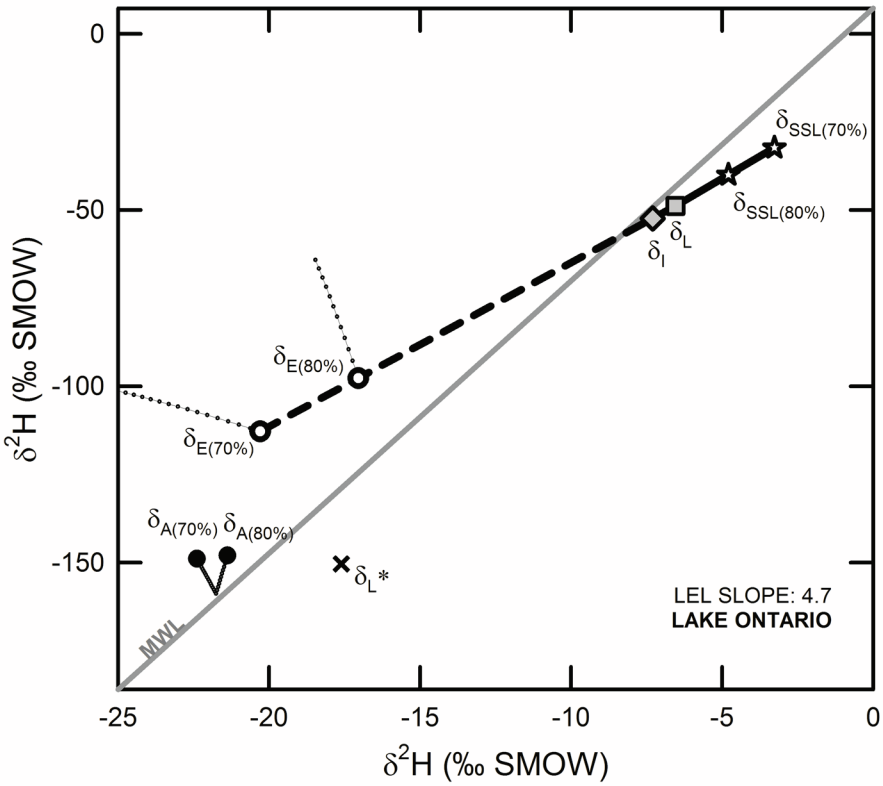

Figure 3-12e. Isotope mass balance scenario for Lake Ontario. Two relative humidity input value scenarios are shown: 70% and 80%. Parameters shown in the diagram are the isotope compositions of atmospheric moisture (δ_A; black circles), evaporated vapour (δ_E; white circles), and the isotope composition of a closed lake (δ_{SSL}; white stars, where E/I = 100% for $\delta_E=\delta_I$). The isotope composition of the Great Lake (δ_L, grey square) and the isotope composition of hydrologic inputs to the Great Lake (δ_I; grey square) are shown. Also, the modelled isotope composition of vapour in equilibrium with the Great Lake is shown (δ_L*, black cross; after Craig and Gordon 1965).

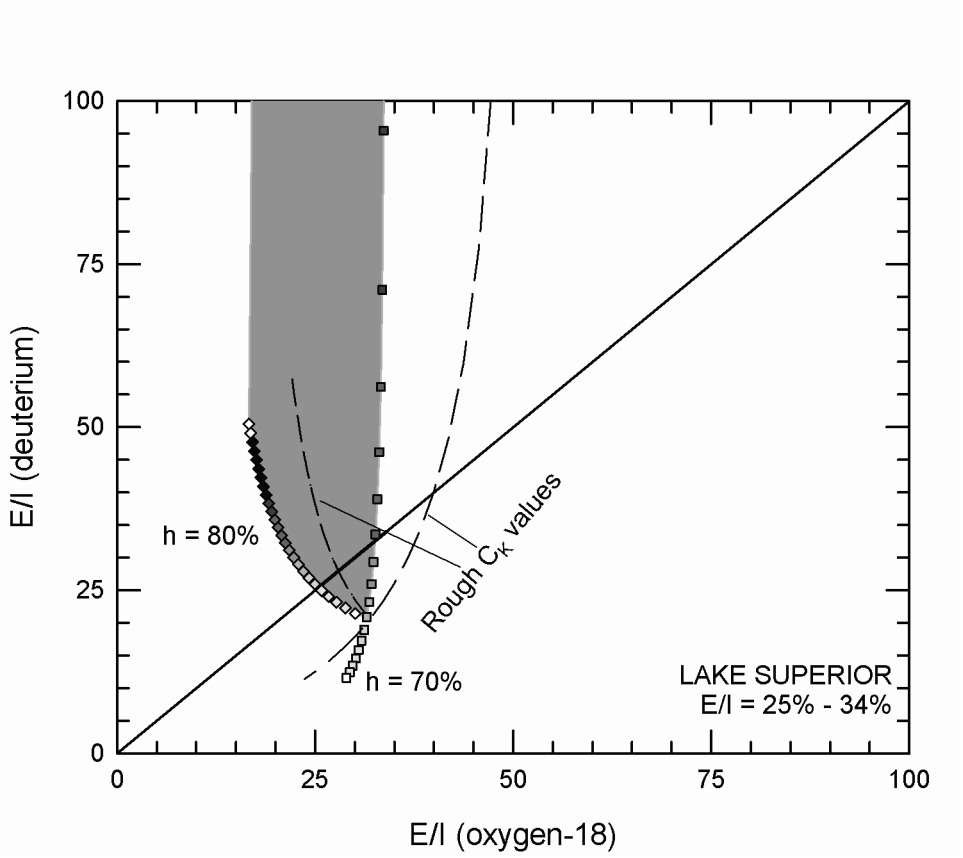

Figure 3-13a. Evaporation as a proportion of inflow (E/I) for Lake Superior computed by an isotope mass balance for two geochemical tracers (deuterium, oxygen-18) following the lake-effect mixing model presented in this thesis. Two relative humidity (h) scenarios are shown: low (squares) and high (diamonds). The greyscale shade of the symbol represents the degree of mixing (x term in Equation 17). Black represents x = 0%, white represents x = 25%. Grey shading bounds E/I values between the two humidity scenarios under laminar (smooth) kinetic isotope effect conditions. Also, a "rough conditions" kinetic isotope effect scenario is presented as dashed lines for both humidity scenarios as well. A one-to-one line is shown as a thick black line. E/I values that fall on the one-to-one line for the two humidity scenarios are shown numerically in the bottom right corner.

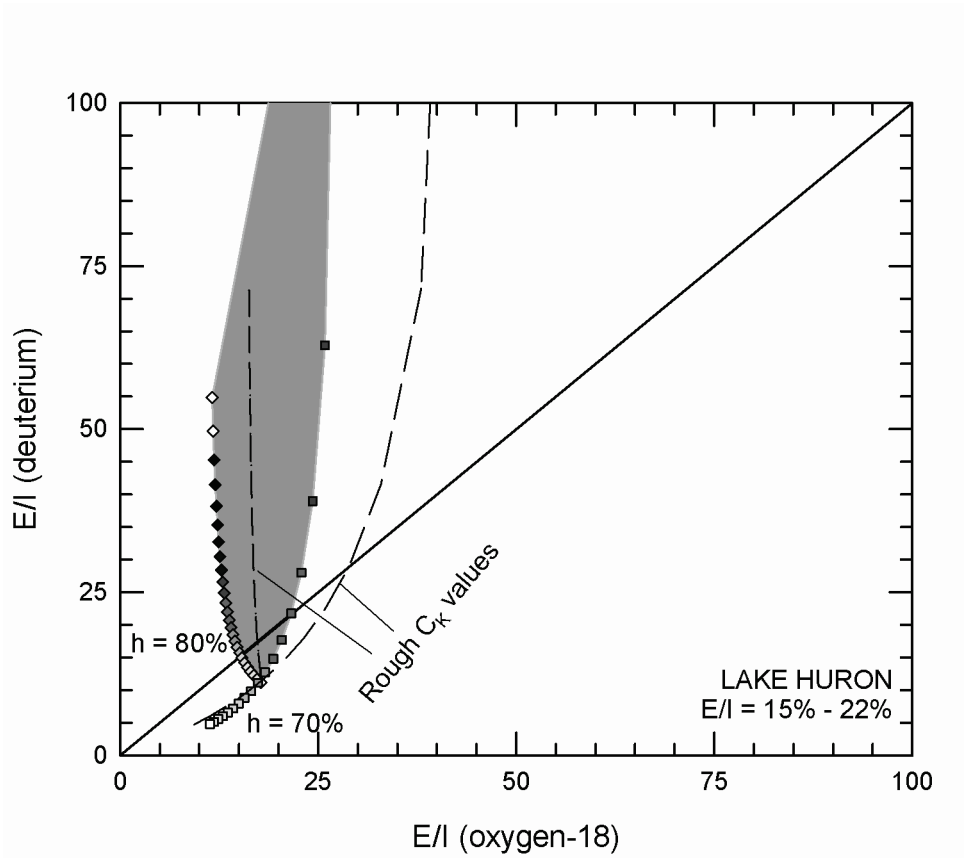

Figure 3-13b. Evaporation as a proportion of inflow (E/I) for Lake Huron computed by an isotope mass balance for two geochemical tracers (deuterium, oxygen-18) following the lake-effect mixing model presented in this thesis. Two relative humidity (h) scenarios are shown: low (squares) and high (diamonds). The greyscale shade of the symbol represents the degree of mixing (x term in Equation 17). Black represents x = 0%, white represents x = 25%. Grey shading bounds E/I values between the two humidity scenarios under laminar (smooth) kinetic isotope effect conditions. Also, a "rough conditions" kinetic isotope effect scenario is presented as dashed lines for both humidity scenarios as well. A one-to-one line is shown as a thick black line. E/I values that fall on the one-to-one line for the two humidity scenarios are shown numerically in the bottom right corner.

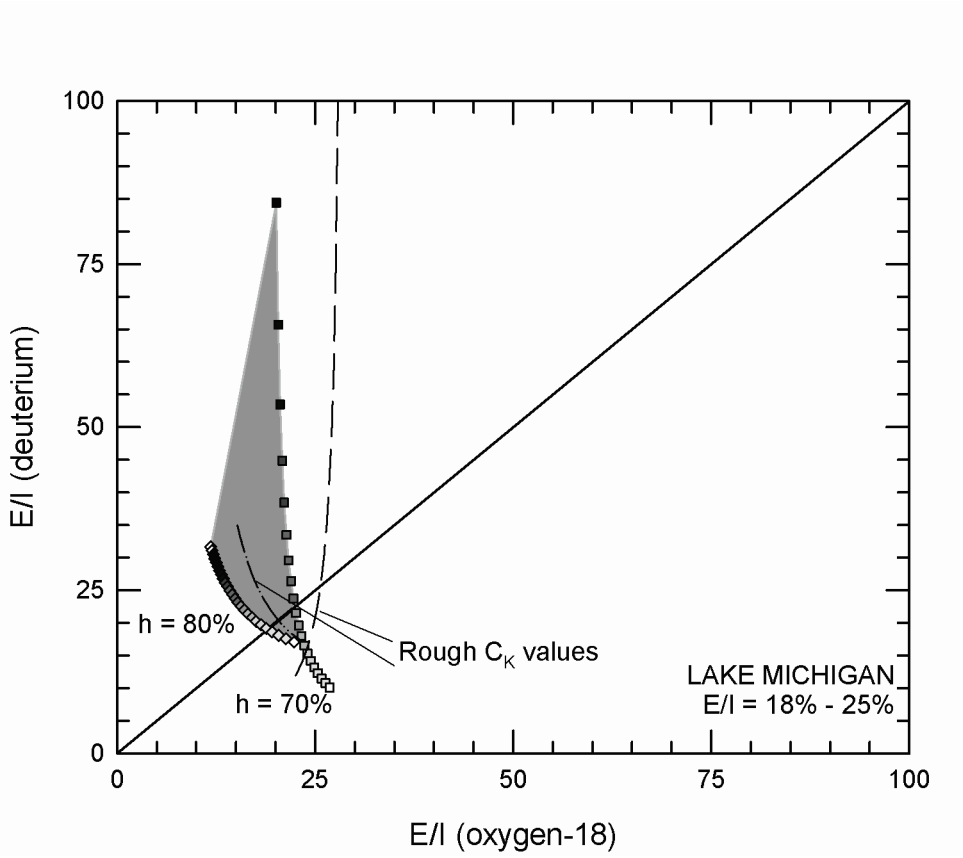

Figure 3-13c. Evaporation as a proportion of inflow (E/I) for Lake Michigan computed by an isotope mass balance for two geochemical tracers (deuterium, oxygen-18) following the lake-effect mixing model presented in this thesis. Two relative humidity (h) scenarios are shown: low (squares) and high (diamonds). The greyscale shade of the symbol represents the degree of mixing (x term in Equation 17). Black represents x = 0%, white represents x = 25%. Grey shading bounds E/I values between the two humidity scenarios under laminar (smooth) kinetic isotope effect conditions. Also, a "rough conditions" kinetic isotope effect scenario is presented as dashed lines for both humidity scenarios as well. A one-to-one line is shown as a thick black line. E/I values that fall on the one-to-one line for the two humidity scenarios are shown numerically in the bottom right corner.

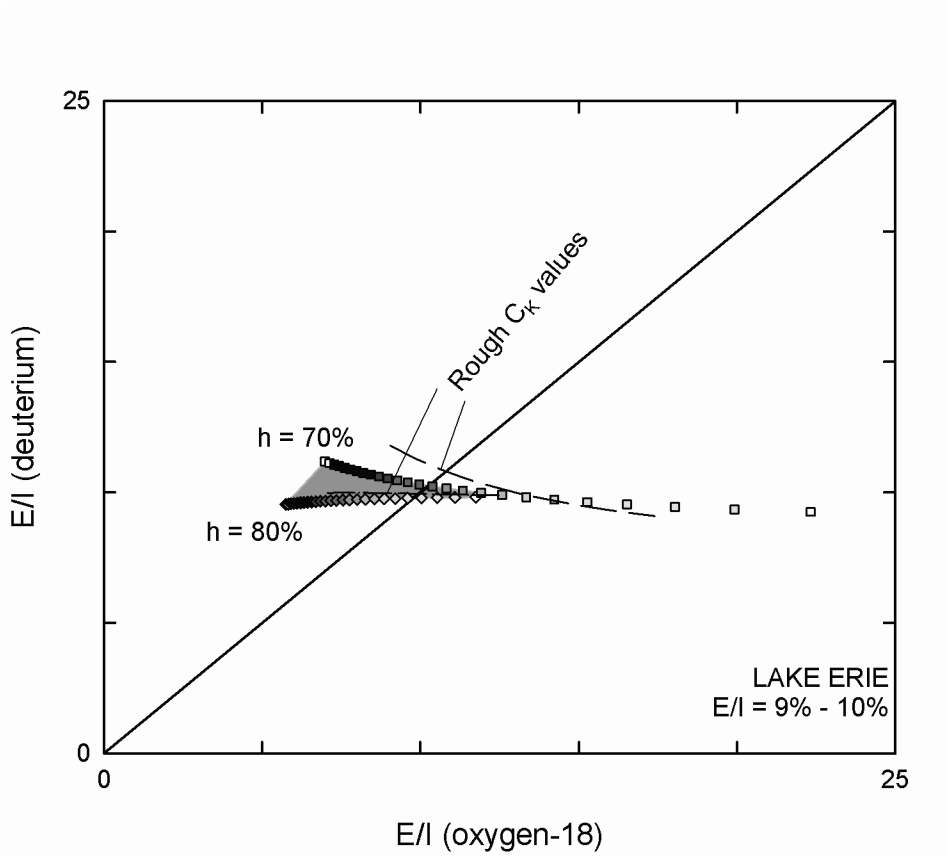

Figure 3-13d. Evaporation as a proportion of inflow (E/I) for Lake Erie computed by an isotope mass balance for two geochemical tracers (deuterium, oxygen-18) following the lake-effect mixing model presented in this thesis. Two relative humidity (h) scenarios are shown: low (squares) and high (diamonds). The greyscale shade of the symbol represents the degree of mixing (x term in Equation 17). Black represents x = 0%, white represents x = 25%. Grey shading bounds E/I values between the two humidity scenarios under laminar (smooth) kinetic isotope effect conditions. Also, a "rough conditions" kinetic isotope effect scenario is presented as dashed lines for both humidity scenarios as well. A one-to-one line is shown as a thick black line. E/I values that fall on the one-to-one line for the two humidity scenarios are shown numerically in the bottom right corner.

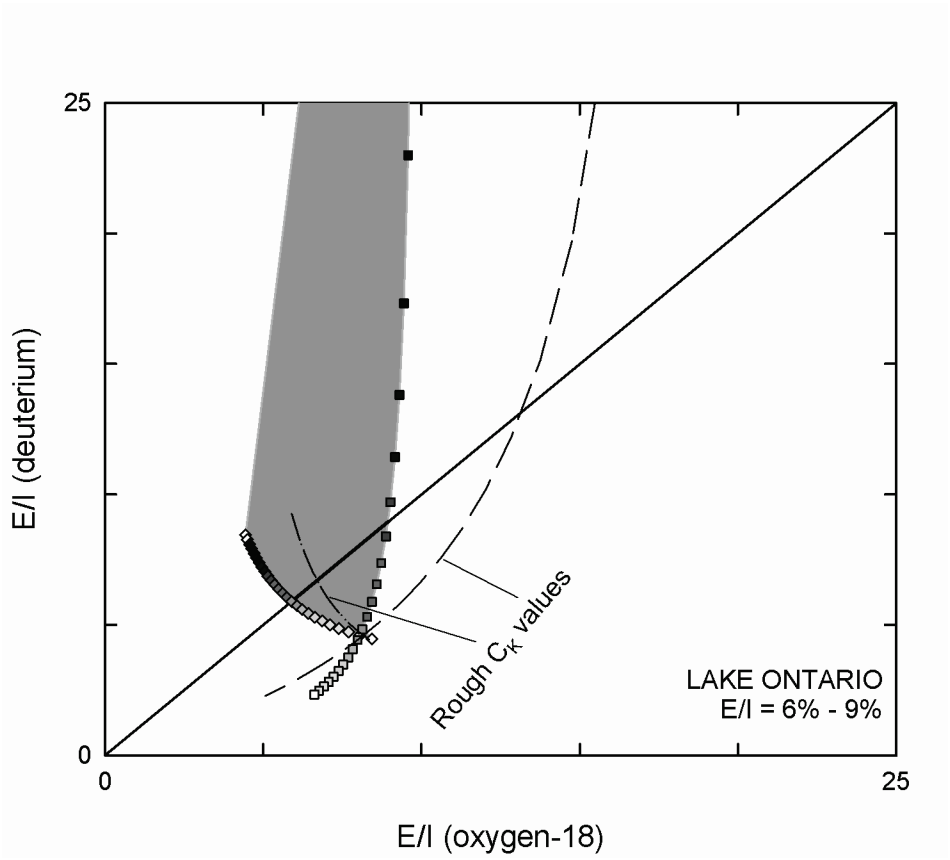

Figure 3-13e. Evaporation as a proportion of inflow (E/I) for Lake Ontario computed by an isotope mass balance for two geochemical tracers (deuterium, oxygen-18) following the lake-effect mixing model presented in this thesis. Two relative humidity (h) scenarios are shown: low (squares) and high (diamonds). The greyscale shade of the symbol represents the degree of mixing (x term in Equation 17). Black represents x = 0%, white represents x = 25%. Grey shading bounds E/I values between the two humidity scenarios under laminar (smooth) kinetic isotope effect conditions. Also, a "rough conditions" kinetic isotope effect scenario is presented as dashed lines for both humidity scenarios as well. A one-to-one line is shown as a thick black line. E/I values that fall on the one-to-one line for the two humidity scenarios are shown numerically in the bottom right corner.

Output values for E/I are similar to GLERL laboratory outputs (Figure 3-14, Table 3–4). A comparison of the two methods shows a nearly identical E/I values for Lakes Huron and Erie. Isotope mass balance results for Lake Michigan and Lake Superior are two-thirds of the Great Lakes Environmental Research Laboratory (GLERL) model outputs. Lake Ontario is the only Great Lake that has an isotope mass balance with a greater E/I estimate than that of the GLERL model. However, before comparisons of the GLERL outputs and stable isotope mass balance approach may be drawn, a model sensitivity analysis for each Great Lake is completed. This approach will produce an range of uncertainty for the E/I value derived from a stable isotope mass balance for each Great Lake.

A rigorous uncertainty analysis is not completed for the vast majority of stable isotope mass balance evaporation studies. This is likely due to large uncertainties for input parameters that quickly proliferate into unrealistic estimates for E/I. However, if a rigorous uncertainty analysis is completed for physical and energy water balances, errors are often large as well. Here, reasonable uncertainties for all input parameters into the stable isotope mass balance are tested and the calculation is rerun with an aim of assessing calculation uncertainty. Input parameters for the stable isotope mass balance approach and associated uncertainties are shown in Table 3–6.

Table 3–6. Uncertainties associated with input parameters to the stable isotope mass balance

Calculation input	Uncertainty (±)	Effect on E/I as value increases
δ_I ^{18}O [‰]	1.0, 0.5, 0.7, 0.3, 0.3 *	Decreases E/I output value
δ_I ^{2}H [‰]	8.0, 4.2, 6, 2.2, 2.3 *	Decreases E/I output value
δ_L ^{18}O [‰]	±1σ of lake results	Increases E/I output value
δ_L ^{2}H [‰]	±1σ of lake results	Increases E/I output value
$\delta_{P\ EVAP}$ ^{18}O [‰]	1.0	Decreases E/I output value
$\delta_{P\ EVAP}$ ^{2}H [‰]	8	Decreases E/I output value
T_{LAKE} [°C]	0.5	Increases E/I output value
T_{AIR} [°C]	1	Decreases E/I output value
RH [%]	5	Increases E/I output value

* δ_I uncertainties vary between lakes. These values assume a known (zero uncertainty) connecting channel inflow isotope composition, and an uncertainty of ±1 per mille for $\delta^{18}O$ (±8 per mille for $\delta^{2}H$) for runoff and direct precipitation inputs. Values are listed in order as Superior, Huron, Michigan, Erie, Ontario (delimitated by commas).

Maximizing uncertainties uses low values for δ_I, $\delta_{P\ EVAP}$ and air temperatures and a high value for relative humidity and lake temperature. Minimizing E/I uses the opposite uncertainty end member for each of these inputs. The model converges on a single value for E/I for both ^{18}O and ^{2}H in all cases, including the case where uncertainties are selected to maximize or minimize E/I values (all-increase or all-decrease E/I scenarios for each parameter shown in Table 3–6). This produces an absolute maximum

and minimum scenario for E/I for each Great Lake by an isotopic approach. These values can be compared to energy and mass transfer estimates shown earlier in Figure 1-28. Maximized and minimized E/I values are presented in Table 3–7.

Table 3–7. Maximum and minimal E/I values applying uncertainties for input parameters (Table 3–6)

LAKE	E/I (calculated inputs scenario)	E/I (minimum-maximum)	E/I (minimum)	GLERL estimate
SUPERIOR	27.9	12-54	12.3	23-91
HURON	17.3	8-32	8.6	10-35
MICHIGAN	20.3	9-35	9.7	14-74
ERIE	9.9	6-15	6.3	7-15
ONTARIO	6.3	2-14	2.0	3-8

Now a comparison of the stable isotope mass balance evaporation estimates can be made to conventional hydrologic approaches. A comparison of uncertainties and outputs is shown in Figure 3-14. The isotope mass balance model constrains the value of evaporation as a proportion of inflow better than estimates from conventional hydrologic means for Lakes Superior and Michigan. Lake Huron uncertainties for the GLERL and isotope mass balance (IMB) models are similar. Evaporation estimates for the lower two Great Lakes - Erie and Ontario - are reported to be slightly better constrained by conventional hydrologic approaches (Neff and Nicholas 2005). Lake Erie evaporation loss estimates calculated by an isotope mass balance are very similar to conventional hydrologic estimates (Figure 3-14). Lake Ontario E/I values are similar for all methods as well. An isotope mass balance approach suggests that evaporation as a proportion of inflow from Lake Ontario may be slightly higher than conventional hydrologic approaches estimate.

Values of evaporation as a proportion of inflow (E/I) are lower for the isotope mass balance approach than E/I values obtained from energy and mass balance techniques (Croley II 1989; Neff and Nicholas 2004) for Lake Superior, Huron, and Michigan. Returning to Equation (4), we note that water inputs are presumed to equal connecting channel outflow in addition to evaporation losses ($I = Q + E$, assuming steady state). However, a more accurate description of evaporation losses is that evaporated water is advected from beyond the extent of the lake surface. Water that evaporates from a Great Lake and subsequently reprecipitates onto its surface is not included in isotope mass balance model estimates. This recycling is invoked to ensure that the isotopic residence time is always less than that of a lake's waters (Horita (2008) proposes $\tau_i = (1–h)\cdot\tau_L$ where τ_i and τ_L represent the residence time of isotopes and that of the lake).

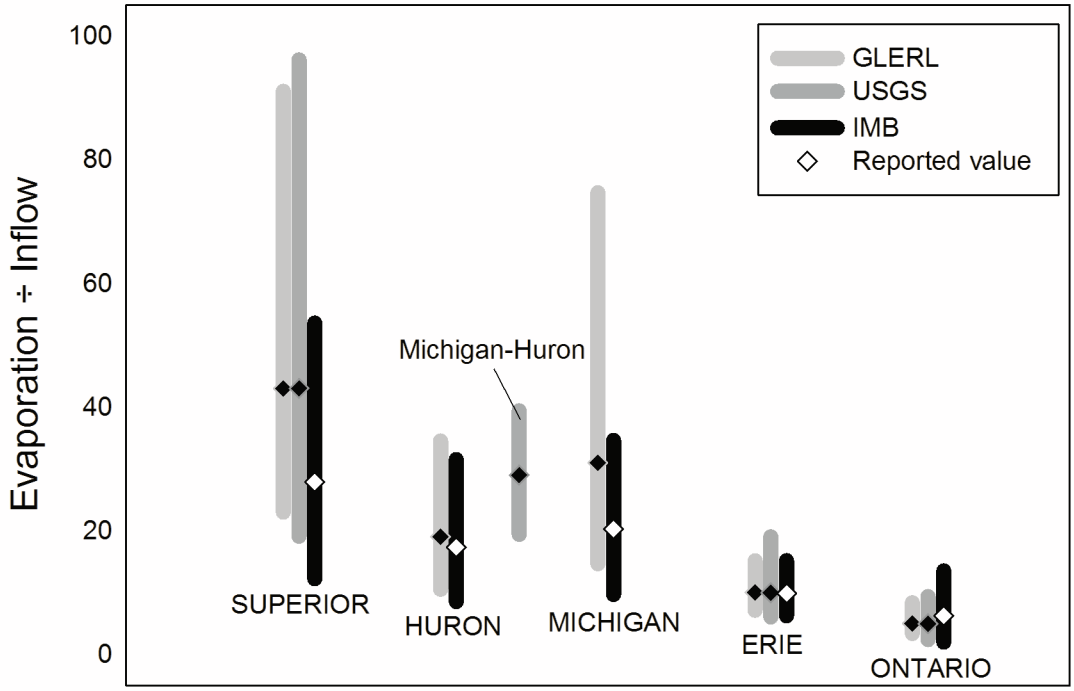

Figure 3-14. Maximum and minimum uncertainty scenarios for the Great Lakes Environmental Research Laboratory (GLERL; light grey) and United States Geological Survey (USGS; dark grey) water balances. The isotope mass balance E/I outputs (IMB; black) is shown to have a similar or better constrained uncertainty in comparison to conventional hydrological approaches. Reported estimates for E/I are shown as diamonds for each of the three models.

Recycled water is embedded in energy balance estimates. The result of this is that recycled water may be counted as evaporate for these approaches. Therefore, it is reasonable that the isotope mass balance E/I ratios are lower than conventional hydrologic estimates. This shows an added advantage of an isotope approach, particularly from an atmospheric water budget perspective, as ^{18}O and ^{2}H tracers demonstrate an ability to estimate the net water evaporated into the atmosphere and advected from the lake surface.

Changes to the climate and hydrology of Lake Superior is another - so far unaccounted for - source of certainty in the isotope mass balance and conventional hydrologic estimates. Lake Superior's residence time is greater than 100 years. If the equation of lake-isotope residence time from Horita (2008) is considered the residence time of oxygen and hydrogen isotopes in Lake Superior waters is still >70 years (for h ~75%). This reflects a time-lag in the Lake's isotopic signature, and suggests that - like Lake Baikal (Seal and Shanks 1998) - Lake Superior may not be in isotopic equilibrium with current climate conditions. Therefore, fluctuations or long-term changes to climate and hydrology of a lake will

experience a time lag before changes to the isotopic signature of waters are observed. From historical isotope data, it seems that the $^{2}H/^{1}H$ ratio of Lake Superior's waters has remained fairly consistent from 1963 to 2007. The long residence provides an advantage for isotope investigations as it permits an interpretation of Lake Superior's hydrologic cycle over the past ~100 years.

A stable isotope study adds new insights into the hydrologic operation of lakes. The ability to "look into the past" when sampling lakes with long residence times is one advantage of an isotopic study over conventional approaches limited to instrumental records. Another advantage is the removal of moisture recycling from evaporation over inflow (E/I estimates). Taking this a step further, the contribution of lake evaporate in lake-effect precipitation can be determined if sufficient collection stations are set up (Gat et al. 1994). Also, the concentrations of ^{18}O and ^{2}H in water are a conservative tracer of a water parcel, and can be applied to estimate exchange between lakes as has been investigated here for Lake Michigan. The separation of Lake Michigan and Huron shows that these waters are distinct, and require separate hydrologic evaluation despite sharing a common lake level.

Overall implications for this study support use of stable isotopes to compliment conventional hydrologic investigations of lakes. Stable isotopes add information where conventional techniques are limited, such as the existence of physical climate monitoring in the past. The advantages of adding stable isotopes fall into two main categories for the Great Lakes: (1) cost and simplicity, and (2) new perspectives and hydrologic information. (1) A stable isotope study is cost-efficient compared to logistically challenges and costs associated with over-lake monitoring. Furthermore, continuous sampling is not a necessity for large, well-mixed lakes with multi-year residence times. Climate data required for evaporation modeling using stable isotopes is often already in place, as temperature and humidity are standard measurements. (2) Stable isotopes add new information for large lake hydrology such as: (a) new estimates for the long-term mean value of evaporation as a proportion of inflow within the residence time of a lake, often extending beyond the period of instrumental records for large lakes, (b) monthly sampling shows an ability to determine seasonality in over lake evaporation, (c) permits a direct measurement and calculation of the contribution of lake evaporate into the regional atmosphere, (d) can trace and distinguish water masses as they exchange between lakes. Finally, (e) combined with paleo-ecology, isotope records from lake cores can determine past changes to a lake hydrology (100s-10,000s of years); however, a thorough understanding of modern controls on isotope variations is required to interpret past fluctuations, advocating for a contemporary isotope hydrology investigation compliment all paleo-limnology studies using stable isotopes.

Further work for the Great Lakes could help to address Lake Michigan-Huron water exchanges, the contribution of Great Lakes evaporate and importance of Great Lake ice cover to lake-effect snowfalls, and long-term changes to Lake Superior's hydrology, and direct measurement of moisture during evaporation seasons. (1) Several at-depth continuous sampling stations along the Straits of Mackinac can directly quantification of the amount of mixing between Lake Michigan and Lake Huron, therefore constraining the large uncertainties in residence time calculations for Lake Michigan. (2) More precipitation collection stations - both upwind and downwind of a Great Lake - could be used to calculate the percentage of Great Lake evaporate in lake-effect precipitation. Coupled with daily ice-cover data for the Great Lakes, an assessment potential changes in magnitude and frequency of lake-effect snowfalls could be projected for a warmer climate. (3) Lake Superior is an immense water body, with a

residence time so long (~100 years) that its isotope signature integrates changes on a century time scale. Since Lake Superior is well mixed, and its outflow represents the isotope composition of the Lake, changes to Lake Superior could be evaluated by collection of monthly samples of the St. Mary's river in a multi-decadal effort to track changes to the system's hydrology. (4) Evaporation as a proportion of inflow to each Great Lake is constrained to uncertainties that approach conventional estimates. However, the isotope mass balance E/I outputs could be greatly improved by analyzing vapour eddy covariance towers during the evaporation season. This would significantly constrain uncertainties in δ_E values inn the computation of E/I, which is the largest uncertainty in this computation as all other parameters can be directly measured. Option (4) could be coordinated with ongoing efforts to measure evaporation by eddy covariance methods by either sampling moisture or by measuring in-situ using a laser-based instrument.

Summary

Waters from each of the five Great Lakes were collected during two sampling campaigns in spring and summer of 2007 aboard the Environmental Protection Agency's (EPA) Research Vessel, the Lake Guardian. A total of 514 samples distributed throughout the Great Lakes were collected for isotopic analysis from 75 offshore sampling stations at surface, mid depth(s) and within 10m of the sediment-water interface. Analysis of $^{18}O/^{16}O$ and $^{2}H/^{1}H$ ratios for all 514 samples was completed by the Alberta Research Council's Isotope Hydrology and Geochemistry Laboratory located in Victoria B.C. in 2009.

A modified calculation approach to estimating evaporation as a proportion of inflow is developed here. The approach capitalizes on previous works that quantify isotope effects during the liquid-vapour phase transition of H_2O in natural and laboratory settings; however, an additional modification is proposed to account for lake effects on the overlying atmosphere during the evaporation process. We apply this new model to the dataset of $\delta^{18}O$ and $\delta^{2}H$ values of water in the Great Lakes coupled with data for surface waters and precipitation from other networks (Canadian and United States Network(s) for Isotopes in Precipitation). This approach has improved the understanding of the Great Lakes hydrologic system by assessing seasonality in evaporation rates, providing a new estimate of evaporation as a proportion of inflow for each lake, and identifying moisture recycling as an important process in the basin.

Stable isotopes of oxygen and hydrogen are found to constrain uncertainties in E/I values comparably to conventional hydrologic methods, without the need for extensive over-lake climate monitoring stations. For Lakes Michigan and Huron, the isotope mass balance approach provides a new perspective into water exchange and evaporation from these lakes, and demonstrates that the waters in each Lake are distinct despite sharing a similar lake level. E/I ratios are highest for the headwater Great Lakes (Superior and Michigan, (30% and 20%) and lowest for Lakes Erie and Ontario (10% and 6%), controlled by large inputs from connecting channels into lower chain-lakes, and by variations in evaporation rates between the Great Lakes. E/I values for Lakes Superior and Michigan calculated by the isotope mass balance approach are lower than values computed by the Great Lakes Environmental Laboratory (GLERL), perhaps demonstrating the isotopic approach's ability to calculate evaporated moisture that is advected from the basin and not subsequently recycled as over lake precipitation. At-depth and intra-annual sampling and isotope ratio measurement of lake waters confirm a lack of significant summer evaporation over the Great Lakes.

References

Araguás-Araguás, L., K. Froehlich, and K. Rozanski (2000). Deuterium and oxygen-18 isotope composition of precipitation and atmospheric moisture, Hydrological Processes 14: 1341–1355.

Assel, R., K. Cronk, and D. Norton (2003). Recent trends in Laurentian Great Lakes ice cover, Climatic Change 57: 185–204, doi:10.1023/A:1022140604052.

Austin, J.A., and Colman, S.M. (2007). Lake Superior summer water temperatures are increasing more rapidly than regional air temperatures: A positive ice-albedo feedback. Geophysical Research Letters 34: L06604, doi:10.1029/2006GL029021.

Bauch, D., P. Schlosser and R.G. Fairbanks (1995). Freshwater balance and the sources of deep and bottom waters in the Arctic Ocean inferred from the distribution of H,180. Progress in Oceanography 35: 53–80.

Benkert B. (2010). Isotope hydrology and paleohydrology of the Slave River Delta, NWT, Ph.D. thesis, University of Waterloo, Ontario, Canada.

Bigg, G.R., and Rohling, E.J. (2000). An oxygen isotope data set for marine water. Journal of Geophysical Research 105: 8527–8535.

Birge, R.T., and Menzel, D.H. (1931). The relative abundance of the oxygen isotopes and the basis of the atomic weight system, Physical Review 37: 1669–1671.

Birks, S.J., J.J. Gibson, L. Gourcy, P.K. Aggarwal, and T.W.D. Edwards (2002). Maps and animations offer new opportunities for studying the global water cycle, Eos Transactions American Geophysical Union 83(37). AGU Electronic Supplement: accessed May 21, 2011 at http://www.agu.org/pubs/eos-news/supplements/1995-2003/020082e.shtml.

Blackett, P.M.S. (1927). The Ejection of Protons from Nitrogen Nuclei, Photographed by the Wilson Method. Proceedings of the Royal Society of London: 349–360.

Baertchi, I.H., and Macklin, W.C. (1976). Absolute 18O content of standard mean ocean water, Earth Planetary Science Letters 31: 341–344.

Bolfan-Casanova, N., S. Mackwell, H. Keppler, C. McCammon and D.C. Rubie (2002). Pressure dependence of H solubility in magnesiowüstite up to 25 GPa: implications for the storage of water in the Earth's lower mantle. Geophysical Research Letters 29 (10): 1029–32.

Bond, G., W. Broecker, S. Johnsen, J. McManus, L. Labeyrie, J. Jouzel and G. Bonani (1993). Correlations between climate and records from North Atlantic sediments and Greenland ice. Nature 365: 143–147.

Bootsma, H.A., and Hecky R.E. (1993). Conservation of the African Great Lakes: A limnological perspective. Conservation Biology 7: 644–656.

Bottinga, Y., and Craig, H. (1969). Oxygen isotope fractionation between COP and water and the isotopic composition of marine atmosphere. Earth and Planetary Science Letters 5: 285–295.

Bowen, G.J. (2008). Spatial analysis of the intra-annual variation of precipitation isotope ratios and its climatological corollaries. Journal of Geophysical Research 113: doi:10.1029/2007JD009295.

Bowen, G.J. (2009). Waterisotopes.org. Accessed February 23, 2010 at http://wateriso.eas.purdue.edu/waterisotopes/.

Bowen, G.J., and Wilkinson, B. (2002). Spatial distribution of $\delta^{18}O$ in meteoric precipitation. Geology 30: 315–318.

Bowen, G.J., and Revenaugh J. (2003). Interpolating the isotopic composition of modern meteoric precipitation. Water Resources Research 39: doi:10.1029/2003WR002086.

Brock, B.E., Y. Yi, K.P. Clogg-Wright, T.W.D. Edwards, B.B. Wolfe (2009). Multi-year landscape-scale assessment of lakewater balances in the Slave River Delta, NWT, using water isotope tracers. Journal of Hydrology 379: 81–91. DOI:10.1016/j.jhydrol.2009.09.046.

Brown, R.M. (1970). Environmental isotope variations in the precipitation, surface waters and in tree rings in Canada. In: Interpretation of environmental isotope data in hydrology, International Atomic Energy Agency, Vienna, held 24-28 June 1968: 4–6.

Bryson, B. (2003). A Short History of Nearly Everything. Doubleday, London. 515 pp.

Buck, A.L. (1981). New equations for computing vapour pressure and enhancement factor. Journal of Applied Meteorology 20: 1527–1532.

Burnett, A.W., M.E. Kirby, H.T. Mullins W.P. Patterson (2003). Increasing Great Lake-effect snowfall during the twentieth century: A regional response to global warming?. Journal of Climate 16, 3535–3542.

Center for International Earth Science Information Network (CIESIN), Columbia University; and Centro Internacional de Agricultura Tropical (CIAT) (2005). Gridded Population of the World Version 3 (GPWv3): Population Density Grids. Palisades, NY: Socioeconomic Data and Applications Center (SEDAC), Columbia University. Accessed November 22, 2010 at http://sedac.ciesin.columbia.edu/gpw.

Cerling, T.E., J.R. Bowman and J.R. O'Neil (1988). An isotopic study of a fluvial-lacustrine sequence: the Plio-Pleistocene Koobi Fora sequence, East Africa. Palaeogeography, Palaeoclimatology, Palaeoecology 63: 335–356.

Chamberlain, C.P., and M.A. Poage (2000). Reconstructing the paleotopography of mountain belts from the isotopic composition of authigenic minerals. Geology 28: 115–118.

Chapra, S.C., A. Dove and D.C. Rockwell (2009). Great Lakes chloride trends: Long-term mass balance and loading analysis. Journal of Great Lakes Research 35: 272–284.

Clementz, M.T., and Sewall, J.O. (2011). Latitudinal Gradients in Greenhouse Seawater $\delta^{18}O$: Evidence from Eocene Sirenian Tooth Enamel. Science 332 (6028): 455.

Coordinating Committee on Great Lakes Basic Hydraulic and Hydrologic Data (1977). Coordinated Great Lakes Physical Data, U.S. Army District Engineer, Detroit, pp. 33.

Craig, H. (1961a). Isotopic variations in meteoric waters. Science 133: 1702–1703.

Craig, H. (1961b). Standards for reporting concentrations of deuterium and oxygen-18 in natural waters. Science 133: 1833–34.

Craig, H. (1966). Isotopic composition and origin of the Red Sea and Salton Sea geothermal brines, Science 54: 1544-1547.

Craig, H. (1975). Lake Tanganyika geochemical and hydrographic study: 1973 expedition. Scripps Institute of Oceanography, Reference 75-5, La Jolla, California, 83 pp.

Craig, H., and Gordon, L.I. (1965) Deuterium and oxygen-18 variations in the ocean and the marine atmosphere. In E Tongiorgi, ed, Proceedings of a Conference on Stable Isotopes in Oceanographic Studies and Paleotemperatures. Spoleto, Italy: 9–130.

Cressman, G.P. (1959), An operational objective analysis system. Monthly Weather Reviews 87: 367–374, doi:10.1175/1520-0493(1959)087<0367:AOOAS>2.0.CO;2.

Croley II, T.E. (1989). Verifiable evaporation modeling on the Laurentian Great Lakes. Water Resources Research 25: 781–792.

Dansgaard, W. (1964). Stable isotopes in precipitation. Tellus 16: 436–468.

Dansgaard, W., Johnsen S.J., Clausen H.B., Dahl-Jensen D., Gundestrup N.S., Hammer G.U., Hvidberg C.S., Steffenaen J.P., Sveinbjornsdottir A.E., Jouzel J., Bond G. (1993). Evidence for general instability of past climate from a 250-kyr ice-core record. Nature 364: 218-220.

de Wit J.C., C.M. van der Straaten, W.G. Mook (1980). Determination of the absolute hydrogen isotopic ratio of V-SMOW and SLAP. Geostandards Newsletter 4: 33-36.

Derecki, J.A. (1984). Detroit River, physical and hydraulic characteristics. National Oceanographic and Atmospheric Administration, Great Lakes Environmental Research Laboratory, GLERL Contribution No. 417. Ann Arbor, MI.

Dinçer, T. (1968). The use of oxygen-18 and deuterium concentrations in the water balance of lakes. Water Resources Research 4: 1289–1305.

Downing, J. A., Y.T. Prairie, J.J. Cole, C.M. Duarte, L.J. Tranvik, R.G. Striegl, W.H. McDowell, P. Kortelainen, N.F. Caraco, J.M. Melack, J.J. Middelburg (2006). The global abundance and size distribution of lakes, ponds, and impoundments. Limnology and Oceanography 51: 2388–2397.

Earth Impact Database (2011). Earth impact database. Accessed June 2, 2011 at www.unb.ca/passc/ImpactDatabase

Edwards, T.W.D., B.B. Wolfe and G.M. MacDonald (1996). Influence of changing atmospheric circulation on precipitation $\delta^{18}O$ temperature relations in Canada during the Holocene. Quaternary Research 46: 211–218.

Edwards T. W. D., and Fritz P. (1986). Assessing meteoric water composition and relative humidity from ^{18}O and ^{2}H in wood cellulose: Paleoclimatic implications for southern Ontario, Canada. Applied Geochemistry 1: 715–723.

Eichenlaub, V.L. (1970). Lake-effect snowfall to the lee of the Great Lakes: Its role in Michigan. Bulliten of American Meteorlogical Society 51: 403–412.

Emiliani, C. (1955). Pleistocene temperatures. Journal of Geology 63: 538–578.

Environmental Protection Agency (2011). Great Lakes: Basic Information. Accessed June 11, 2011 at http://www.epa.gov/glnpo/basicinfo.html.

Farrand, W.R. (1988). Glacial Lakes around Michigan. Geological Survey Division, Michigan Department of Environmental Quality, Bulletin 4.

Fontes, J-Ch., R. Gonfiantini, and M.A. Roche (1970). Deuterium et oxygene-18 dans les eaux du lac Tchad. In: Isotope Hydrology 1970. International Atomic Energy Agency, Vienna: 387–404.

Fontes, J-Ch., B. Boulange, J.P. Carmouze and T. Florkowski (1979). Preliminary oxygen-18 and deuterium study of the dynamics of Lake Titicaca. In: Isotopes in Lake Studies. International Atomic Energy Agency, Vienna: 145–150.

Friedman, I. (1953). Deuterium content of natural water and other substances. Geochimica Cosmochimica Acta 4: 89–103.

Friedman, I., A.C. Redfield, B. Schoen (1964). The variation of the deuterium content of natural waters in the hydrologic cycle. Review of Geophysics 2: 177–224.

Froehlich, K. (2000). Evaluating the water balance of inland seas using isotopic tracers: the Caspian Sea experience. Hydrological Processes 14: 1371–1383.

Gat, J.R. (1970). Environmental isotope balance of Lake Tiberias. In: Isotope Hydrology 1970. International Atomic Energy Agency, Vienna: 109–127.

Gat, J.R. (1979). Isotope hydrology of very saline surface waters. I: Isotopes in Lake Studies. International Atomic Energy Agency. Vienna: 153–162.

Gat, J.R. (1984). The stable isotope composition of Dead Sea waters. Earth and Planetary Science Letters 71: 361–376.

Gat J.R. (1995). Stable isotopes of fresh and saline lakes. In: A. Lerman, D. Imboden and J. Gat, Editors, Physics and Chemistry of Lakes, Springer-Verlag, New York (1995): 139–165.

Gat J.R. (1996). Oxygen and hydrogen isotopes in the hydrologic cycle. Annual Reviews of Earth and Planetary Science 24: 225–262

Gat J.R. (2008). The isotopic composition of evaporating waters - review of the historical evolution leading up to the Craig-Gordon model. Isotopes in Environmental and Health Studies 44(1): 5–9.

Gat, J.R., and Bowser C. (1991). The heavy isotope enrichment of water in coupled evaporative systems. In: Stable Isotope Geochemistry: a Tribute to Samuel Epstein (eds H.P. Taylor, J.R. O'Neil & I.R. Kaplan), pp. 159–168. The Geochemical Society, St Louis, MO, USA.

Gat, J.R., C.J. Bowser and C. Kendall (1994). The contribution of evaporation from the Great Lakes of North America to the continental atmospheric moisture: detection by means of the stable isotope signature of the evaporated waters. Geophysical Research Letters 21: 557–560.

Gat, J.R., A. Shemesh, E. Tziperman, A. Hecht, D. Geogopoulos, O. Basturk (1996). The stable isotope composition of waters of the Eastern Mediterranean Sea. Journal of Geophysical Research 101(C3): 6441–6451.

Gat, J.R., and Airey, P.L. (2006). Stable water isotopes in the atmosphere/biosphere/lithosphere interface: scaling-up from the local to continental scale, under humid and dry conditions. Global Planetary Change 51: 25–33.

Gesch, D.B., K.L. Verdin and S.K. Greenlee (1999). New land surface digital elevation model covers the earth: Eos Transactions, American Geophysical Union 80 (6): 69–70.

Giauque, W.F., and Johnson, H.L. (1929a). An isotope of oxygen of mass 17 in the earth's atmosphere. Nature 123: 831.

Giauque, W.F., and Johnson, H.L. (1929b). An isotope of oxygen, mass 18. Nature 123: 318.

Gibson, J.J. (1996). Non-steady isotopic methods for estimating lake evaporation: development and validation in Arctic Canada, Ph.D. thesis, University of Waterloo, Ontario, Canada.

Gibson, J.J. (2002a). A new conceptual model for predicting isotope enrichment of lakes in seasonal climates. PAGES News 10: 10–11.

Gibson, J.J. (2002b). Short-term evaporation and water budget comparisons in shallow arctic lakes using non-steady isotope mass balance. Journal of Hydrology 264: 247–266

Gibson, J.J., and Edwards, T.W.D. (2002). Regional water balance trends and evaporative-transpiration partitioning from a stable isotope survey of lakes in northern Canada. Global Biogeochemical Cycles 16: doi:10.1029/2001GB001839.

Gibson, J.J., T.W.D. Edwards and T.D. Prowse (1996). Development and validation of an isotopic method for estimating lake evaporation. Hydrological Processes 10: 1369–1382.

Gibson, J.J., R. Reid and C. Spence (1998). A six-year isotopic record of lake evaporation in the Canadian Subarctic. Hydrological Processes 12: 1779–1792.

Gibson, J.J., E.E. Prepas and P. McEachern (2002). Quantitative comparison of lake throughflow, residency, and catchment runoff using stable isotopes: Modelling and results from a survey of boreal lakes. Journal of Hydrology 262: 128–144.

Gibson, J.J., S.J. Birks and T.W.D. Edwards (2008). Global prediction of δ_A and δ^2H-$\delta^{18}O$ evaporation slopes for lakes and soil water accounting for seasonality. Global Biogeochemical Cycles 22, GB2031, doi:10.1029/2007GB002997

GLIN: Great Lakes Information Network (2010). Maps and GIS of the Great Lakes Region, accessed July 5, 2009 at http://gis.glin.net/

Gonfiantini, R., G.M. Zuppi, D.H. Eccles and W. Ferro. (1979). Isotope investigation of Lake Malawi. In: Isotopes in lake studies. International Atomic Energy Agency, Vienna, Austria.

Gonfiantini, R. (1986). Environmental isotopes in lake studies. In: Fritz, P., Fontes, J.Ch. (Eds.), Handbook of Environmental Isotope Geochemistry, vol. 3. Elsevier, New York: 113–168.

Grannemann, N.G., and Weaver, T.L. (1998). An annotated bibliography of selected references on the estimated rates of direct groundwater discharge to the Great Lakes. USGS Water-Resources Investigations Report 98–4220

Grannemann N.G., R.J. Hunt, J.R. Nicholas, T.E. Reilly and T.C. Winter (2000). The importance of ground water in the Great Lakes Region. United States Geological Survey Water Resources Investigations Report 00-4008.

Green II, H.W., C. Wang-Ping and M.R. Brudzinski (2010). Seismic evidence of negligible water carried below 400-km depth in subducting lithosphere. Nature 467: 828–831.

Grieve, R.A.F., D. Stoffler and A. Deutsch (1991). The Sudbury structure: Controversial or misunderstood: Journal of Geophysical Research 96 (E5): 22753–22754.

Hanrahan, J.L., S.V. Kravtsov and P.J. Roebber (2009). Quasi-periodic decadal cycles in the levels of Lakes Michigan and Huron. Journal of Great Lakes Research 35: doi:10.1016/j.jglr.2008.11.004.

Hayhoe, K., J. VanDorn, T. Croley II, N. Schlegal, D. Wuebbles (2010). Regional climate change projections for Chicago and the US Great Lakes. Journal of Great Lakes Research 36 (Supplement 2): 7–21.

Herdendorf, C.E. (1982). Large lakes of the World. Journal of Great Lakes Research 8: 106-113.

Hirschmann, M. M. (2006). Water, melting, and the deep earth H2O cycle, Annual Reviews of Earth and Planetary Science 34: 629–653, doi:10.1146/annurev. earth.34.031405.125211.

Horita, J. (2008) Isotopic evolution of saline lakes in low-latitude and polar regions. Aquatic Geochemistry 15: 43–69 doi: 10.1007/s10498-008-9050-3

Horita, J. and D. Wesolowski (1994), Liquid-vapour fractionation of oxygen and hydrogen isotopes of water from the freezing to the critical temperature, Geochimica et Cosmochimica Acta 58: 3425–3437.

Horita, J., K. Rozanski and S. Cohen (2008). Isotope effects in the evaporation of water: a status report of the Craig-Gordon model. Isotopes in Environmental and Health Studies 44: 23–49.

International Atomic Energy Agency (2011). Water Resources Programme - Environmental Isotopes in the Hydrological Cycle : Principles and Applications. Accessed September 12, 2011 at http://www-naweb.iaea.org/napc/ih/IHS_resources_publication_hydroCycle_en.html

Jasechko, S., J.J. Gibson, A. Pietroniro and T.W.D. Edwards (2011). Stable isotope mass balance of the Laurentian Great Lakes to constrain evaporative losses. In: International Symposium on Isotopes in Hydrology, Marine Ecosystems, and Climate Change Studies, Principality of Monaco, April 2011: IAEA-CN-085-030.

Jouzel, J., and L. Merlivat (1984). Deuterium and Oxygen 18 in Precipitation: Modelling of the isotopic effects during snow formation, Journal of Geophysical Research 89: 11749–11757.

Karim, A., J. Veizer and J. Barth (2008). Net ecosystem production in the great lakes basin and its implications for the North American missing carbon sink: A hydrologic and stable isotope approach. Global and Planetary Change 61: 15–27, doi: 10.1016/j.gloplacha.2007.08.004.

Kendall, C. and Coplen, T.B. (2001). Distribution of oxygen-18 and deuterium in river waters across the United States. Hydrological Processes 15: 1363–1393, doi: 10.1002/hyp.217.

Lawrence, J.F., and Wysession, M.E. (2006). Seismic evidence for subduction-transported water in the lower mantle. In: Jacobsen, S.D., van der Lee, S. (Eds.). Earth's Deep Water Cycle. American Geophysical Union, Geophysical Monographs Series 168: 251–261.

Lehner, B., and Doll, P. (2004). Development and validation of a global database of lakes, reservoirs and wetlands. Journal of Hydrology 296: 1–22.

Levia, D.F. Jr., and Frost, E.E. (2003). A review and evaluation of stemflow literature in the hydrologic and biogeochemical cycles of forested and agricultural ecosystems. Journal of Hydrology 274: 1–29.

Longinelli, A., B. Stenni, L. Genoni, O. Flora, C. De Francesco, and G. Pellegrini (2008). A stable isotope study of the Garda lake, Northern Italy: its hydrological balance. Journal of Hydrology 360: 103–116.

Longinelli, A. and Edmond, J.M. (1983). Isotope geochemistry of the Amazon Basin: a reconnaissance. Journal of Geophysical Research: 3703–3717.

Macauley, D. (2006). 'The place of the elements and the elements of place: Aristotelian contributions to environmental thought'. Ethics, Place and Environment 9: 187–206.

Machavaram, M.V., and Krishnamurthy R.V. (1995). Earth surface evaporative process: a case study from the Great Lakes region of the United States based on deuterium excess in precipitation. Geochimica et Cosmochimica Acta 59: 4279–4283.

Magnuson, J.J., Webster, K.E., Assel, R.A., Bowser, C.J., Dillin, P.J., Eaton, J.G., Evans, H.E., Fee, E.J., Hall, R.I., Mortsch, L.R., Schindler, D.W., and Quinn, F.H. (1997). Potential Effects of Climate Changes on Aquatic Systems: Laurentian Great Lakes and Precambrian Shield Region. Journal of Hydrological Processes 11: 825–871.

Majoube, M. (1971). fractionment en oxygene- 18 et en deutirium entrel'ean et sa vapour. J. Chim. Phys. 68: 1423–1436.

McCoy, H.N., and Ross, W.H. (1907). The Specific Radioactivity of Thorium and the Variation of the Activity with Chemical Treatment and with Time. Journal of the American Chemical Society 29: 1709–1718.

Merlivat L. (1978). Molecular diffusivities of $H_2{}^{16}O$, $HD^{16}O$, and $H_2{}^{18}O$ in gases. Journal of Chemical Physics 69: 2864–2871, doi:10.1063/1.436884

Merlivat, L., and J. Jouzel (1979). Global climatic interpretation of the deuteriumoxygen18 relationship for precipitation, Journal of Geophysical Research 84: 5029–5033.

Mesinger, F., G. DiMego, E. Kalnay, P. Shafran, W. Ebisuzaki, D. Jovic, J. Woollen, K. Mitchell, E. Rogers, M. Ek, Y. Fan, R. Grumbine, W. Higgins, H. Li, Y. Lin, G. Manikin, D. Parrish and W. Shi (2005). North American Regional Reanalysis. Bulletin of the American Meteorological Society 87: 343–360.

Murakami, M., K. Hirose, H. Yurimoto, S. Nakashima and N. Takafuji (2002). Water in Earth's Lower Mantle. Science 295: 1885–1887.

National Aeronautics and Space Administration (NASA) (2011). NASA GISS: Panoply 3 netCDF, HDF and GRIB Data Viewer. Accessed June 25, 2011 at http://www.giss.nasa.gov/tools/panoply/

Neff, B.P. and Nicholas, J.R. (2005). Uncertainty in Great Lakes Water Balance, US. Geological Survey Scientific Investigations Report 2004-5100, 42 pp.

New, M., D. Lister, M. Hulme, I. Makin (2002). A high-resolution data set of surface climate over global land areas. Climate Research 21: 1–25.

Niziol, T.A., W.R. Snyder and J.S. Waldstreicher (1995). Winter weather forecasting throughout the eastern United States. Part IV: Lake effect snow. Weather Forcasting 10: 61–77.

NOAA (2011). National Data Buoy Center. Accessed June 24, 2011 at http://www.ndbc.noaa.gov/

OneGeology (2011). OneGeology - Making Geological Map Data for the Earth Accessible. Accessed January 21, 2011 at http://www.onegeology.org/

Priestly, J. (1775). Experiments and Observations of Different Kinds of Air. London: J. Johnson.

Quinn, F.H. (1977). Annual and seasonal flow variations through the Straits of Mackinac. Water Resources Research 13(a): 137–144.

Quinn, F.H. (1988). Detroit River flow reversals, Journal of Great Lakes Research: 14 (4): 383–387.

Quinn, F.H. (1992). Hydraulic residence times for the Laurentian Great Lakes. Journal of Great Lakes Research 18: 22–8.

Rasmusen, E.M. (1968). Atmospheric water vapour transport and the water balance of North America, Part II Large-scale water balance investigations, Monthly Weather Reviews 96: 720–734.

Rayleigh, J.W.S. (1896). Theoretical considerations respecting the separation of gases by diffusion and similar processes. Philosophical Magazine 42: 493–498.

Ricketts, R.D., and Johnson, T.C. (1996). Climate change in the Turkana basin as deduced from a 4000 year long 8180 record. Earth and Planetary Science Letters 142: 7–17.

Rozanski, K., Araguás-Araguás, L., and Gonfiantini, R. (1993). Isotopic patterns in modern global precipitation. In: Climate Change in Continental Isotopic Records, Geophysical Monograph 78, American Geophysical Union: 1–36.

Saylor, J.H., and Sloss, P.W. (1976). Water volume transport and oscillatory current flow through the Straits of Mackinac. Journal of Physical Oceanography: 229–237.

Schmidt, G.A. (1999). Forward modeling of carbonate proxy data from planktonic foraminifera using oxygen isotope tracers in a global ocean model. Paleoceanography 14, 482–497.

Schmidt, G.A., G.R. Bigg and E.J. Rohling (1999). Global Seawater Oxygen-18 Database - v1.21. Accessed November 1, 2010 at http://data.giss.nasa.gov/o18data/

Schulte P., L. Alegret, I. Arenillas, J.A. Arz, P.J. Barton, P.R. Bown, T. Bralower, G. Christeson, P. Claeys, C. Cockell, G. Collins, A. Deutsch, T. Goldin, K. Goto, J.M. Grajales-Nishimura, R. Grieve, S. Gulick, K.R. Johnson, W. Kiessling, C. Koeberl, D.A. Kring, K.G. MacLeod, T. Matsui, J. Melosh, A. Montanari, J. Morgan, C. Neal, R.D. Norris, E. Pierazzo, G. Ravizza, M. Rebolledo-Vieyra, W-U. Reimold, E. Robin, T. Salge, R.P. Speijer, A.R. Sweet, J. Urrutia-Fucugauchi, V. Vajda, M. Whalen and T. Willumsen P. S. (2010). The Chicxulub Impact and the Mass Extinction at the Cretaceous-Paleogene Boundary. Science 327: 1214–1218.

Schwab, D.J., A.H. Clites, C.R. Murthy, J.E. Sandall, L.A. Meadows, G.A. Meadows (1989). The effect of wind on transport and circulation in Lake St. Clair. Journal of Geophysical Research 94 (4): 4947–4958.

Schwab, D.J., T.E. Croley II, W.M. Schertzer, (2005). Physical limnological and hydrological characteristics of Lake Michigan. In: Edsall, T., Munawar, M. (Eds.), State of Lake Michigan: ecology, health, and management. Ecovision World Monograph Series, Goodword Books, New Delhi, India.

Scotese, C.R., McKerrow, W.S. (1990). Revised world maps and introduction. In: McKerrow, W. S. & Scotese, C. R. (eds) Palaeozoic Palaeogeography. and Biogeography. Geological Society, London, Memoirs 12: 1–21.

Scott, R. W., and Huff, F. A. (1996). Impacts of the Great Lakes on Regional Climate Conditions. Journal of Great Lakes Research 22: 845–863.

Seal, R.R., and Shanks, W.C. (1998). Oxygen and hydrogen isotope systematics of Lake Baikal, Siberia: implications for paleoclimate studies. Limnology and. Oceanography 43: 1251–1261.

Sharp, Z.D. (2007). Principles of Stable isotope Geochemistry. Prentice Hall, New York. 360 pp.

Soddy, F. (1913). The Radio-elements and the Periodic Law Chemical News 107: 97–99.

Soddy, F. (1966). The Origins of the Conceptions of Isotopes, Nobel Lecture, December 12, 1922. In Nobel Lectures Including Presentation Speeches and Laureates' Biographies: Chemistry 1901–1921. New York: Elsevier, pp. 367–401.

Sofer, Z., and Gat, J.R. (1975). The isotopic composition of evaporating brines: Effect of the isotopic activity ratio in saline solutions. Earth and Planetary Science Letters 26: 179–186.

Solley W.B., R.R. Pierce and H.A. Perlman (1998). Estimated use of water in the United States in 1995: U.S. Geological Survey Circular 1200, 71 pp.

Tanigushi M., T. Nakayama, N. Tase and J. Shimada (2001). Stable isotope studies of precipitation and river water in the Lake Biwa basin, Japan. Hydrological Processes 14: 539–556.

Urey H.C., F.G. Brickwedde, and G.M. Murphy (1932). A Hydrogen Isotope of Mass 2. Physical Review 39: 164–165.

USGS (2011). Active mines and mineral plants in the US. Accessed June 16, 2011 at http://tin.er.usgs.gov/mineplant/

USGS (2010). USGS Water Resources: About USGS Water Resources. Accessed June 2, 2010 at http://water.usgs.gov/GIS/huc.html

Vogt, H.J. (1976). Isotopentrennung bei der Verdampfung von Wasser. Staatsexamensarbeit, Universitat Heidelberg, 78 pp.

Vrooman R.H. (1948). Survey of the occurrence of oxygen 18 in natural sources. M.Sc. Thesis, McMaster University, Hamilton, Ontario, Canada.

Welker, J.M. (2000). Isotopic ($\delta^{18}O$) characteristics of weekly precipitation collected across the USA: an initial analysis with application to water source studies. Hydrological Processes 14: 1449–1464

Wolfe, B.B, T.L. Karst-Riddoch, S.R. Vardy, M.D. Falcone, R.I. Hall and T.W.D. Edwards (2005). Impacts of climate and river flooding on the hydroecology of a floodplain basin, Peace-Athabasca Delta, Canada since A.D. 1700. Quaternary Research 64: 147–162.

World Business Chicago (2011). Great Lakes St. Lawrence Economic Region Profile. Accessed April 13, 2011 at http://www.worldbusinesschicago.com/news/great-lakes-st-lawrence-economic-region-profile

Yang, C., K. Telmer and J. Veizer (1996). Chemical dynamics of the "St. Lawrence" riverine system: δD_{H2O}, $\delta^{13}C_{DIC}$, $\delta^{34}S_{sulphate}$, and dissolved $^{87}Sr/^{86}Sr$. Geochimica et Cosmochimica Acta 60(5): 851–866.

Yi, Y., B.E. Brock, M.D. Falcone, B.B. Wolfe, T.W.D. Edwards (2008). A coupled isotope tracer method to characterize input water to lakes. Journal of Hydrology 350: 1–13.

Yi, Y., J.J. Gibson, L.W. Cooper, J-F. Hélie, S.J. Birks, J.W. McClelland, R.M. Holmes, B.J. Peterson. (submitted). Isotopic signals (^{18}O, ^{2}H, ^{3}H) of six major rivers draining the Pan-Arctic watershed. Global Biogeochemical Cycles.

Zachos, J., M. Pagani, L. Sloan, E. Thomas and K. Billups (2001). Trends, rhythms, and aberrations in global climate 65 Ma to present. Science 292: 686–693.

Zimmermann, U. (1979). Determination by stable isotopes of underground inflow and outflow and evaporation of young artificial groundwater lakes. In: Isotopes in Lake Studies. International Atomic Energy Agency, Vienna: 87–94.

Zuber, A. (1983). On the environmental isotope method for determining the water balance of some lakes. Journal of Hydrology 61: 409–427.

Appendix A:

Tabular data – $\delta^{18}O$ and $\delta^{2}H$ in North American Great Lakes waters

Lake	Cruise ID	Date	Station	Latitude	Longitude	Depth (m)	$\delta^{18}O$ (‰SMOW)	$\delta^{2}H$ (‰SMOW)	T (°C)	EC (µS/cm)	pH
Erie	ER0711	09/04/07	ER09	42.54	-79.62	3.1	-6.54	-47.6	0.3	146.9	8.5
Erie	ER0711	09/04/07	ER09	42.54	-79.62	24.3	-6.57	-47.8	0.3	147.1	8.5
Erie	ER0711	09/04/07	ER09	42.54	-79.62	47.8	-6.47	-47.5	0.3	147.1	8.4
Erie	ER0711	10/04/07	ER10	42.68	-79.69	1.5	-6.70	-48.6	0.5	158.0	8.6
Erie	ER0711	10/04/07	ER10	42.68	-79.69	16.4	-6.71	-49.2	0.6	159.2	8.5
Erie	ER0711	10/04/07	ER10	42.68	-79.69	31.5	-6.75	-48.8	0.6	159.4	8.5
Erie	ER0711	09/04/07	ER15M	42.52	-79.89	3.1	-6.48	-47.8	0.3	149.1	8.4
Erie	ER0711	09/04/07	ER15M	42.52	-79.89	30.1	-6.41	-47.4	0.6	150.3	8.5
Erie	ER0711	09/04/07	ER15M	42.52	-79.89	61.7	-6.50	-47.3	0.9	152.2	8.5
Erie	ER0711	09/04/07	ER30	42.43	-81.21	1.5	-6.37	-47.4	1.9	157.3	8.7
Erie	ER0711	09/04/07	ER30	42.43	-81.21	10.4	-6.38	-47.6	1.9	157.2	8.7
Erie	ER0711	09/04/07	ER30	42.43	-81.21	20.1	-6.43	-47.7	1.9	157.2	8.7
Erie	ER0711	09/04/07	ER31	42.25	-81.11	1.4	-6.41	-47.3	0.9	148.8	8.7
Erie	ER0711	09/04/07	ER31	42.25	-81.11	10.9	-6.85	-47.1	0.8	148.5	8.7
Erie	ER0711	09/04/07	ER31	42.25	-81.11	20.7	-6.45	-47.6	0.8	148.5	8.7
Erie	ER0711	09/04/07	ER32	42.08	-81.01	1.3	-6.44	-47.9	0.3	150.0	8.6
Erie	ER0711	09/04/07	ER32	42.08	-81.01	10.9	-6.43	-47.5	0.5	151.1	8.6
Erie	ER0711	09/04/07	ER32	42.08	-81.01	21.1	-6.45	-47.7	0.5	151.4	8.6
Erie	ER0711	09/04/07	ER36	41.94	-81.48	1.6	-6.40	-47.8	1.0	149.3	8.7
Erie	ER0711	09/04/07	ER36	41.94	-81.48	11.6	-6.46	-47.8	1.0	149.6	8.7
Erie	ER0711	09/04/07	ER36	41.94	-81.48	21.8	-6.36	-47.8	1.3	151.3	8.7
Erie	ER0711	09/04/07	ER37	42.11	-81.58	1.4	-6.45	-48.0	0.6	146.2	8.7
Erie	ER0711	09/04/07	ER37	42.11	-81.58	12.0	-6.44	-47.7	0.6	146.5	8.6
Erie	ER0711	09/04/07	ER37	42.11	-81.58	22.8	-6.44	-48.2	0.7	147.2	8.6
Erie	ER0711	09/04/07	ER38	42.28	-81.67	1.5	-6.38	-47.5	1.7	155.9	8.7
Erie	ER0711	09/04/07	ER38	42.28	-81.67	11.0	-6.35	-47.5	1.7	155.8	8.7

Lake	Cruise ID	Date	Station	Latitude	Longitude	Depth (m)	$\delta^{18}O$ (‰SMOW)	$\delta^{2}H$ (‰SMOW)	T (°C)	EC (µS/cm)	pH
Erie	ER0711	09/04/07	ER38	42.28	-81.67	20.5	-6.33	-47.5	1.7	156.0	8.7
Erie	ER0711	08/04/07	ER42	41.97	-82.04	1.6	-6.79	-50.8	2.0	157.9	8.8
Erie	ER0711	08/04/07	ER42	41.97	-82.04	11.3	-6.84	-50.6	2.0	158.1	8.8
Erie	ER0711	08/04/07	ER42	41.97	-82.04	21.5	-6.76	-51.3	2.0	158.3	8.7
Erie	ER0711	08/04/07	ER43	41.79	-81.95	1.8	-6.39	-48.4	1.5	153.1	8.7
Erie	ER0711	08/04/07	ER43	41.79	-81.95	11.0	-6.37	-48.5	1.5	153.5	8.7
Erie	ER0711	08/04/07	ER43	41.79	-81.95	21.4	-6.42	-48.4	1.5	153.7	8.7
Erie	ER0711	08/04/07	ER58	41.68	-82.93	2.0	-7.48	-54.9	3.4	147.1	8.3
Erie	ER0711	08/04/07	ER58	41.68	-82.93	4.7	-7.37	-55.2	3.4	147.2	8.3
Erie	ER0711	08/04/07	ER58	41.68	-82.93	8.7	-7.37	-55.1	3.4	147.2	8.2
Erie	ER0711	08/04/07	ER59	41.73	-83.15	1.5	-7.11	-53.7	3.6	146.4	8.3
Erie	ER0711	08/04/07	ER59	41.73	-83.15	4.1	-7.22	-54.2	3.6	146.3	8.3
Erie	ER0711	08/04/07	ER59	41.73	-83.15	7.4	-7.18	-53.9	3.6	146.1	8.3
Erie	ER0711	08/04/07	ER60	41.89	-83.20	1.4	-7.24	-53.5	3.3	154.2	8.7
Erie	ER0711	08/04/07	ER60	41.89	-83.20	4.4	-7.18	-52.3	3.3	154.1	8.6
Erie	ER0711	08/04/07	ER60	41.89	-83.20	7.3	-7.20	-53.4	3.3	154.0	8.6
Erie	ER0711	08/04/07	ER61	41.95	-83.05	1.6	-7.06	-54.0	3.2	127.7	8.1
Erie	ER0711	08/04/07	ER61	41.95	-83.05	4.5	-7.07	-53.4	3.2	127.7	8.1
Erie	ER0711	08/04/07	ER61	41.95	-83.05	8.0	-7.15	-53.8	3.2	128.0	8.0
Erie	ER0711	09/04/07	ER63	42.42	-79.80	3.1	-6.31	-48.3	0.1	146.8	8.4
Erie	ER0711	09/04/07	ER63	42.42	-79.80	22.6	-6.31	-48.1	0.1	146.9	8.4
Erie	ER0711	09/04/07	ER63	42.42	-79.80	44.6	-6.41	-47.8	0.1	147.1	8.4
Erie	ER0711	09/04/07	ER73	41.98	-81.76	1.4	-6.35	-48.4	1.5	153.2	8.7
Erie	ER0711	09/04/07	ER73	41.98	-81.76	12.0	-6.33	-48.3	1.5	154.2	8.7
Erie	ER0711	09/04/07	ER73	41.98	-81.76	22.6	-6.46	-48.3	1.6	155.3	8.7
Erie	ER0711	09/04/07	ER78M	42.12	-81.25	1.4	-6.41	-48.1	0.3	144.6	8.6

Lake	Cruise ID	Date	Station	Latitude	Longitude	Depth (m)	$\delta^{18}O$ (‰SMOW)	$\delta^{2}H$ (‰SMOW)	T (°C)	EC (µS/cm)	pH
Erie	ER0711	09/04/07	ER78M	42.12	-81.25	10.1	-6.42	-49.3	0.3	144.9	8.6
Erie	ER0711	09/04/07	ER78M	42.12	-81.25	21.8	-6.42	-48.6	0.5	147.0	8.6
Erie	ER0711	08/04/07	ER91M	41.84	-82.92	2.1	-7.21	-53.5	2.6	142.8	8.5
Erie	ER0711	08/04/07	ER91M	41.84	-82.92	5.4	-7.23	-54.0	2.6	142.8	8.5
Erie	ER0711	08/04/07	ER91M	41.84	-82.92	9.3	-7.30	-54.7	2.6	142.8	8.4
Erie	ER0711	08/04/07	ER92	41.95	-82.69	1.7	-7.32	-54.1	3.0	149.5	8.5
Erie	ER0711	08/04/07	ER92	41.95	-82.69	5.1	-7.18	-54.4	3.0	149.5	8.5
Erie	ER0711	08/04/07	ER92	41.95	-82.69	10.2	-7.25	-53.6	3.0	149.7	8.5
Erie	ER0711	09/04/07	ERFO	42.42	-79.58	3.0	-6.37	-49.2	0.3	146.5	8.5
Erie	ER0711	09/04/07	ERFO	42.42	-79.58	16.8	-6.45	-49.0	0.3	146.7	8.5
Erie	ER0711	09/04/07	ERFO	42.42	-79.58	30.8	-6.63	-50.3	1.6	163.7	8.5
Huron	HU0711	14/04/07	HU06	43.47	-82.00	2.0	-6.90	-54.3	0.8	111.7	8.3
Huron	HU0711	14/04/07	HU06	43.47	-82.00	25.1	-6.86	-54.1	0.8	111.9	8.3
Huron	HU0711	14/04/07	HU06	43.47	-82.00	40.6	-6.96	-54.0	0.8	112.0	8.3
Huron	HU0711	14/04/07	HU06	43.47	-82.00	49.0	-7.00	-53.8	0.8	112.0	8.3
Huron	HU0711	14/04/07	HU09	43.63	-82.22	2.1	-7.04	-54.3	0.9	111.8	8.4
Huron	HU0711	14/04/07	HU09	43.63	-82.22	28.3	-7.07	-54.3	1.0	112.2	8.3
Huron	HU0711	14/04/07	HU09	43.63	-82.22	48.3	-6.92	-54.4	1.0	112.2	8.3
Huron	HU0711	14/04/07	HU09	43.63	-82.22	57.3	-7.01	-54.2	1.0	112.3	8.3
Huron	HU0711	14/04/07	HU12	43.89	-82.06	2.0	-7.05	-54.0	0.7	112.2	8.4
Huron	HU0711	14/04/07	HU12	43.89	-82.06	43.2	-7.09	-54.1	0.6	112.4	8.4
Huron	HU0711	14/04/07	HU12	43.89	-82.06	76.2	-7.15	-53.9	0.7	113.0	8.4
Huron	HU0711	14/04/07	HU12	43.89	-82.06	85.6	-7.04	-54.0	0.7	113.1	8.4
Huron	HU0711	14/04/07	HU15M	44.00	-82.35	1.5	-7.06	-54.1	0.8	111.4	8.4
Huron	HU0711	14/04/07	HU15M	44.00	-82.35	30.0	-6.97	-54.2	0.8	111.5	8.3
Huron	HU0711	14/04/07	HU15M	44.00	-82.35	50.0	-6.94	-53.9	0.8	111.6	8.3

Lake	Cruise ID	Date	Station	Latitude	Longitude	Depth (m)	$\delta^{18}O$ (‰SMOW)	$\delta^{2}H$ (‰SMOW)	T (°C)	EC (µS/cm)	pH
Huron	HU0711	14/04/07	HU15M	44.00	-82.35	64.6	-6.91	-54.1	0.8	111.9	8.3
Huron	HU0711	14/04/07	HU27	44.20	-82.50	1.4	-7.07	-54.8	0.8	111.7	8.3
Huron	HU0711	14/04/07	HU27	44.20	-82.50	27.4	-7.10	-54.9	1.0	112.2	8.3
Huron	HU0711	14/04/07	HU27	44.20	-82.50	45.1	-6.90	-54.1	1.1	112.4	8.3
Huron	HU0711	14/04/07	HU27	44.20	-82.50	52.9	-6.93	-54.2	1.1	112.5	8.3
Huron	HU0711	04/04/07	HU32	44.45	-82.34	2.3	-7.01	-54.2	0.7	111.0	8.2
Huron	HU0711	04/04/07	HU32	44.45	-82.34	41.5	-7.08	-54.0	0.7	111.2	8.3
Huron	HU0711	04/04/07	HU32	44.45	-82.34	73.1	-7.15	-53.9	0.7	111.3	8.3
Huron	HU0711	04/04/07	HU32	44.45	-82.34	80.0	-7.06	-53.4	0.7	111.3	8.3
Huron	HU0711	03/04/07	HU37	44.76	-82.78	2.5	-7.05	-53.8	1.0	111.5	8.3
Huron	HU0711	03/04/07	HU37	44.76	-82.78	36.7	-7.10	-54.6	1.0	111.6	8.3
Huron	HU0711	03/04/07	HU37	44.76	-82.78	63.4	-7.02	-54.7	1.0	111.7	8.3
Huron	HU0711	03/04/07	HU37	44.76	-82.78	71.5	-7.01	-54.4	1.0	111.8	8.2
Huron	HU0711	03/04/07	HU38	44.74	-82.06	3.0	-7.06	-54.7	1.9	115.3	8.3
Huron	HU0711	03/04/07	HU38	44.74	-82.06	67.7	-7.09	-54.0	1.9	115.5	8.3
Huron	HU0711	03/04/07	HU38	44.74	-82.06	125.0	-6.94	-54.7	2.0	116.3	8.2
Huron	HU0711	03/04/07	HU38	44.74	-82.06	132.9	-6.93	-53.9	2.1	116.5	8.2
Huron	HU0711	03/04/07	HU45M	45.14	-82.98	2.4	-7.01	-54.4	1.5	113.6	8.3
Huron	HU0711	03/04/07	HU45M	45.14	-82.98	50.2	-7.13	-54.7	1.5	113.7	8.3
Huron	HU0711	03/04/07	HU45M	45.14	-82.98	86.4	-7.10	-54.3	1.5	113.8	8.3
Huron	HU0711	03/04/07	HU45M	45.14	-82.98	94.5	-7.15	-54.3	1.5	113.8	8.3
Huron	HU0711	03/04/07	HU48	45.28	-82.45	1.8	-6.99	-55.2	1.4	113.7	8.1
Huron	HU0711	03/04/07	HU48	45.28	-82.45	54.9	-7.03	-54.3	1.6	114.6	8.3
Huron	HU0711	03/04/07	HU48	45.28	-82.45	100.1	-7.04	-53.9	1.7	114.8	8.3
Huron	HU0711	03/04/07	HU48	45.28	-82.45	108.1	-6.96	-54.6	1.7	114.9	8.3
Huron	HU0711	03/04/07	HU53	45.45	-82.92	2.0	-7.15	-54.6	1.3	112.8	8.1

Lake	Cruise ID	Date	Station	Latitude	Longitude	Depth (m)	$\delta^{18}O$ (‰SMOW)	$\delta^{2}H$ (‰SMOW)	T (°C)	EC (µS/cm)	pH
Huron	HU0711	03/04/07	HU53	45.45	-82.92	45.1	-7.13	-55.0	1.3	113.1	8.3
Huron	HU0711	03/04/07	HU53	45.45	-82.92	80.1	-7.00	-54.1	1.3	113.2	8.3
Huron	HU0711	03/04/07	HU53	45.45	-82.92	88.5	-6.93	-54.6	1.3	113.2	8.3
Huron	HU0711	03/04/07	HU54M	45.52	-83.42	2.0	-7.21	-54.5	1.4	112.4	8.3
Huron	HU0711	03/04/07	HU54M	45.52	-83.42	50.0	-7.18	-55.1	1.4	112.6	8.3
Huron	HU0711	03/04/07	HU54M	45.52	-83.42	100.0	-7.16	-54.9	1.4	112.8	8.3
Huron	HU0711	03/04/07	HU54M	45.52	-83.42	124.5	-7.16	-54.8	1.4	112.9	8.3
Huron	HU0711	03/04/07	HU61	45.75	-83.92	1.9	-6.94	-53.9	0.9	113.8	8.1
Huron	HU0711	03/04/07	HU61	45.75	-83.92	57.9	-6.94	-54.0	0.8	113.8	8.3
Huron	HU0711	03/04/07	HU61	45.75	-83.92	106.1	-6.99	-53.8	0.8	115.3	8.2
Huron	HU0711	03/04/07	HU61	45.75	-83.92	114.2	-6.89	-53.7	0.8	115.6	8.2
Huron	HU0711	14/04/07	HU93	44.10	-82.12	2.0	-7.11	-54.9	0.4	111.0	8.4
Huron	HU0711	14/04/07	HU93	44.10	-82.12	44.1	-7.11	-55.4	0.4	111.2	8.4
Huron	HU0711	14/04/07	HU93	44.10	-82.12	78.0	-7.07	-54.2	0.5	111.5	8.4
Huron	HU0711	14/04/07	HU93	44.10	-82.12	86.9	-7.20	-54.5	0.5	111.6	8.4
Huron	HU0711	14/04/07	HUFO	44.08	-82.75	1.5	-7.20	-54.5	1.5	122.0	8.4
Huron	HU0711	14/04/07	HUFO	44.08	-82.75	18.2	-7.20	-54.6	1.5	122.3	8.4
Huron	HU0711	14/04/07	HUFO	44.08	-82.75	26.5	-7.25	-54.8	1.5	125.8	8.4
Huron	HU0711	14/04/07	HUFO	44.08	-82.75	34.8	-7.35	-55.6	1.8	136.8	8.4
Michigan	MI0711	31/03/07	MI11	42.38	-87.00	1.8	-5.70	-43.9	3.0	167.1	8.4
Michigan	MI0711	31/03/07	MI11	42.38	-87.00	62.6	-5.79	-43.8	3.0	167.9	8.4
Michigan	MI0711	31/03/07	MI11	42.38	-87.00	115.4	-5.84	-43.6	3.1	168.9	8.4
Michigan	MI0711	31/03/07	MI11	42.38	-87.00	123.3	-5.77	-43.9	3.1	168.9	8.4
Michigan	MI0711	31/03/07	MI17	42.73	-87.42	2.0	-5.78	-44.0	2.7	166.0	8.3
Michigan	MI0711	31/03/07	MI17	42.73	-87.42	49.3	-5.74	-43.9	2.7	166.1	8.4
Michigan	MI0711	31/03/07	MI17	42.73	-87.42	89.1	-5.87	-43.9	2.8	166.6	8.4

Lake	Cruise ID	Date	Station	Latitude	Longitude	Depth (m)	$\delta^{18}O$ (‰SMOW)	$\delta^{2}H$ (‰SMOW)	T (°C)	EC (µS/cm)	pH
Michigan	MI0711	31/03/07	MI17	42.73	-87.42	97.5	-5.86	-44.2	2.8	166.9	8.4
Michigan	MI0711	01/04/07	MI18M	42.73	-87.00	2.4	-5.79	-43.6	3.3	169.2	
Michigan	MI0711	01/04/07	MI18M	42.73	-87.00	50.0	-5.73	-43.9	3.3	169.4	
Michigan	MI0711	01/04/07	MI18M	42.73	-87.00	100.1	-5.82	-43.8	3.3	169.6	
Michigan	MI0711	01/04/07	MI18M	42.73	-87.00	156.0	-5.82	-43.8	3.3	169.8	
Michigan	MI0711	31/03/07	MI19	42.73	-86.58	2.3	-5.79	-44.4	2.6	164.8	8.4
Michigan	MI0711	31/03/07	MI19	42.73	-86.58	44.5	-5.83	-44.5	2.6	165.1	8.4
Michigan	MI0711	31/03/07	MI19	42.73	-86.58	79.3	-5.83	-43.9	2.6	165.3	8.4
Michigan	MI0711	31/03/07	MI19	42.73	-86.58	87.2	-5.87	-44.0	2.6	165.3	8.4
Michigan	MI0711	01/04/07	MI23	43.13	-87.00	2.2	-5.83	-44.1	2.9	166.6	8.3
Michigan	MI0711	01/04/07	MI23	43.13	-87.00	44.9	-5.84	-44.0	2.9	166.8	8.4
Michigan	MI0711	01/04/07	MI23	43.13	-87.00	80.4	-5.90	-44.0	2.9	167.0	8.3
Michigan	MI0711	01/04/07	MI23	43.13	-87.00	88.4	-5.78	-44.6	2.9	167.0	8.3
Michigan	MI0711	01/04/07	MI27M	43.60	-86.92	2.1	-5.85	-44.4	2.6	164.4	8.3
Michigan	MI0711	01/04/07	MI27M	43.60	-86.92	49.9	-5.87	-44.4	2.6	164.8	8.4
Michigan	MI0711	01/04/07	MI27M	43.60	-86.92	93.0	-5.78	-44.3	2.6	165.1	8.4
Michigan	MI0711	01/04/07	MI27M	43.60	-86.92	100.7	-5.84	-44.3	2.6	165.1	8.4
Michigan	MI0711	01/04/07	MI32	44.14	-87.23	3.0	-5.87	-44.3	2.5	163.8	8.4
Michigan	MI0711	01/04/07	MI32	44.14	-87.23	80.2	-5.84	-44.5	2.6	164.9	8.4
Michigan	MI0711	01/04/07	MI32	44.14	-87.23	150.2	-5.90	-43.9	3.0	167.5	8.3
Michigan	MI0711	01/04/07	MI32	44.14	-87.23	158.2	-5.74	-44.1	3.0	167.6	8.3
Michigan	MI0711	01/04/07	MI34	44.09	-86.77	3.0	-5.81	-44.7			8.0
Michigan	MI0711	01/04/07	MI34	44.09	-86.77	77.5	-5.85	-44.8	2.6	164.9	8.4
Michigan	MI0711	01/04/07	MI34	44.09	-86.77	145.5	-5.81	-44.2	2.8	166.6	8.4
Michigan	MI0711	01/04/07	MI34	44.09	-86.77	153.7	-5.84	-44.2	2.8	166.6	8.4
Michigan	MI0711	02/04/07	MI40	44.76	-86.97	2.1	-5.78	-44.4	2.6	164.7	8.4

Lake	Cruise ID	Date	Station	Latitude	Longitude	Depth (m)	$\delta^{18}O$ (‰SMOW)	$\delta^{2}H$ (‰SMOW)	T (°C)	EC (µS/cm)	pH
Michigan	MI0711	02/04/07	MI40	44.76	-86.97	83.0	-5.92	-44.4	2.7	165.7	8.4
Michigan	MI0711	02/04/07	MI40	44.76	-86.97	156.2	-5.95	-45.3	3.0	167.7	8.4
Michigan	MI0711	02/04/07	MI40	44.76	-86.97	163.5	-5.87	-44.5	3.1	167.8	8.4
Michigan	MI0711	02/04/07	MI41M	44.74	-86.72	2.7	-5.90	-44.0	3.3	168.2	8.4
Michigan	MI0711	02/04/07	MI41M	44.74	-86.72	100.1	-5.79	-44.2	3.3	168.5	8.4
Michigan	MI0711	02/04/07	MI41M	44.74	-86.72	200.3	-5.79	-44.2	3.2	168.7	8.4
Michigan	MI0711	02/04/07	MI41M	44.74	-86.72	255.5	-5.86	-44.2	3.2	168.9	8.4
Michigan	MI0711	02/04/07	MI47	45.18	-86.38	3.2	-5.91	-44.7	2.5	164.6	8.5
Michigan	MI0711	02/04/07	MI47	45.18	-86.38	94.5	-5.91	-44.4	2.5	165.1	8.4
Michigan	MI0711	02/04/07	MI47	45.18	-86.38	179.7	-5.82	-43.7	2.8	167.0	8.4
Michigan	MI0711	02/04/07	MI47	45.18	-86.38	187.9	-5.95	-44.1	2.8	167.1	8.4
Ontario	ON0711	10/04/07	ON12	43.50	-79.35	1.5	-6.61	-49.2	2.7	174.7	8.4
Ontario	ON0711	10/04/07	ON12	43.50	-79.35	52.1	-6.58	-48.9	2.7	175.0	8.4
Ontario	ON0711	10/04/07	ON12	43.50	-79.35	94.6	-6.57	-48.8	2.7	175.2	8.4
Ontario	ON0711	10/04/07	ON12	43.50	-79.35	102.9	-6.58	-49.4	2.7	175.3	8.4
Ontario	ON0711	10/04/07	ON25	43.52	-79.08	1.6	-6.67	-48.7	2.7	174.4	8.3
Ontario	ON0711	10/04/07	ON25	43.52	-79.08	67.8	-6.53	-49.1	2.7	174.4	8.4
Ontario	ON0711	10/04/07	ON25	43.52	-79.08	125.9	-6.58	-49.2	2.7	174.7	8.4
Ontario	ON0711	10/04/07	ON25	43.52	-79.08	134.2	-6.62	-48.6	2.7	174.7	8.4
Ontario	ON0711	11/04/07	ON33M	43.60	-78.80	1.4	-6.68	-49.2	2.7	174.5	8.4
Ontario	ON0711	11/04/07	ON33M	43.60	-78.80	50.0	-6.59	-49.2	2.7	174.9	8.4
Ontario	ON0711	11/04/07	ON33M	43.60	-78.80	99.8	-6.65	-49.0	2.7	175.1	8.4
Ontario	ON0711	11/04/07	ON33M	43.60	-78.80	136.5	-6.68	-48.7	2.7	175.2	8.4
Ontario	ON0711	11/04/07	ON41	43.72	-78.03	1.6	-6.64	-48.9	1.7	169.5	8.4
Ontario	ON0711	11/04/07	ON41	43.72	-78.03	64.2	-6.63	-49.1	2.0	171.0	8.4
Ontario	ON0711	11/04/07	ON41	43.72	-78.03	118.2	-6.61	-49.4	2.8	175.6	8.3

Lake	Cruise ID	Date	Station	Latitude	Longitude	Depth (m)	$\delta^{18}O$ (‰SMOW)	$\delta^{2}H$ (‰SMOW)	T (°C)	EC (µS/cm)	pH
Ontario	ON0711	11/04/07	ON41	43.72	-78.03	127.6	-6.62	-49.3	2.8	175.7	8.3
Ontario	ON0711	11/04/07	ON49	43.48	-77.44	1.5	-6.68	-49.0	1.7	169.6	8.4
Ontario	ON0711	11/04/07	ON49	43.48	-77.44	24.2	-6.57	-49.0	1.9	170.3	8.4
Ontario	ON0711	11/04/07	ON49	43.48	-77.44	38.4	-6.60	-51.6	1.9	170.5	8.4
Ontario	ON0711	11/04/07	ON49	43.48	-77.44	47.0	-6.63	-49.7	2.3	172.5	8.3
Ontario	ON0711	11/04/07	ON55M	43.44	-77.44	2.7	-6.67	-49.5	1.8	169.9	8.5
Ontario	ON0711	11/04/07	ON55M	43.44	-77.44	50.0	-6.58	-49.1	1.8	169.9	8.4
Ontario	ON0711	11/04/07	ON55M	43.44	-77.44	100.0	-6.62	-49.3	1.8	170.2	8.4
Ontario	ON0711	11/04/07	ON55M	43.44	-77.44	190.0	-6.67	-49.4	3.2	177.7	8.4
Ontario	ON0711	11/04/07	ON60	43.58	-77.20	1.5	-6.59	-49.4	1.7	169.2	8.5
Ontario	ON0711	11/04/07	ON60	43.58	-77.20	75.9	-6.57	-49.2	1.7	169.6	8.4
Ontario	ON0711	11/04/07	ON60	43.58	-77.20	142.0	-6.59	-48.8	2.2	172.2	8.4
Ontario	ON0711	11/04/07	ON60	43.58	-77.20	151.1	-6.62	-49.1	2.2	172.3	8.4
Ontario	ON0711	11/04/07	ON63	43.73	-77.02	1.6	-6.64	-49.2	1.6	168.7	8.5
Ontario	ON0711	11/04/07	ON63	43.73	-77.02	43.4	-6.58	-49.2	1.5	168.5	8.4
Ontario	ON0711	11/04/07	ON63	43.73	-77.02	77.3	-6.60	-49.1	1.5	168.6	8.4
Ontario	ON0711	11/04/07	ON63	43.73	-77.02	85.8	-6.68	-49.4	1.5	168.6	8.4
Ontario	ON0711	12/04/07	ONFO	43.42	-77.92	3.2	-6.56	-49.1	2.6	173.8	8.4
Ontario	ON0711	12/04/07	ONFO	43.42	-77.92	42.5	-6.63	-49.0	2.6	173.9	8.4
Ontario	ON0711	12/04/07	ONFO	43.42	-77.92	74.8	-6.70	-49.3	2.6	174.1	8.4
Ontario	ON0711	12/04/07	ONFO	43.42	-77.92	82.8	-6.60	-49.3	2.6	174.1	8.4
Superior	SU0711	15/04/07	SU01M	46.99	-85.16	2.8	-8.61	-66.8	1.2	52.6	8.0
Superior	SU0711	15/04/07	SU01M	46.99	-85.16	49.8	-8.66	-66.7	1.2	52.9	8.0
Superior	SU0711	15/04/07	SU01M	46.99	-85.16	83.4	-8.66	-66.9	1.3	53.0	7.9
Superior	SU0711	15/04/07	SU01M	46.99	-85.16	91.3	-8.70	-66.8	1.3	53.1	7.9
Superior	SU0711	16/04/07	SU02	47.36	-85.62	1.5	-8.60	-66.7	1.4	53.1	7.9

Lake	Cruise ID	Date	Station	Latitude	Longitude	Depth (m)	$\delta^{18}O$ (‰SMOW)	$\delta^{2}H$ (‰SMOW)	T (°C)	EC (µS/cm)	pH
Superior	SU0711	16/04/07	SU02	47.36	-85.62	74.8	-8.66	-66.8	1.4	53.3	8.0
Superior	SU0711	16/04/07	SU02	47.36	-85.62	139.4	-8.65	-67.2	2.5	55.3	7.9
Superior	SU0711	16/04/07	SU02	47.36	-85.62	148.1	-8.63	-66.8	2.5	55.3	7.9
Superior	SU0711	16/04/07	SU03	46.89	-85.85	1.0	-8.61	-66.6	1.3	52.9	7.9
Superior	SU0711	16/04/07	SU03	46.89	-85.85	72.8	-8.74	-66.8	1.4	53.2	8.0
Superior	SU0711	16/04/07	SU03	46.89	-85.85	137.1	-8.64	-66.8	1.8	54.0	8.0
Superior	SU0711	16/04/07	SU03	46.89	-85.85	145.6	-8.58	-66.8	1.9	54.1	8.0
Superior	SU0711	16/04/07	SU04	47.26	-86.35	1.7	-8.61	-67.4	1.7	53.6	7.9
Superior	SU0711	16/04/07	SU04	47.26	-86.35	71.1	-8.53	-67.4	1.7	53.8	8.0
Superior	SU0711	16/04/07	SU04	47.26	-86.35	132.4	-8.52	-67.2	1.9	54.3	8.0
Superior	SU0711	16/04/07	SU04	47.26	-86.35	141.0	-8.47	-67.0	2.0	54.4	8.0
Superior	SU0711	16/04/07	SU05	46.77	-86.56	1.7	-8.64	-66.7	1.5	53.2	8.0
Superior	SU0711	16/04/07	SU05	46.77	-86.56	87.0	-8.58	-66.5	1.6	53.5	8.0
Superior	SU0711	16/04/07	SU05	46.77	-86.56	164.0	-8.49	-67.4	1.7	53.8	8.0
Superior	SU0711	16/04/07	SU05	46.77	-86.56	172.5	-8.49	-67.0	1.8	53.9	8.0
Superior	SU0711	17/04/07	SU06	48.56	-86.38	1.6	-8.63	-67.0	1.0	52.6	8.0
Superior	SU0711	17/04/07	SU06	48.56	-86.38	82.1	-8.65	-67.3	1.0	52.9	8.0
Superior	SU0711	17/04/07	SU06	48.56	-86.38	154.4	-8.55	-67.1	2.0	54.4	8.0
Superior	SU0711	17/04/07	SU06	48.56	-86.38	163.5	-8.60	-66.9	2.5	55.7	8.0
Superior	SU0711	17/04/07	SU07	48.07	-86.59	1.5	-8.60	-67.0	1.4	53.2	8.0
Superior	SU0711	17/04/07	SU07	48.07	-86.59	97.8	-8.52	-67.1	1.5	53.6	8.0
Superior	SU0711	17/04/07	SU07	48.07	-86.59	185.9	-8.55	-67.1	2.7	55.7	8.0
Superior	SU0711	17/04/07	SU07	48.07	-86.59	194.5	-8.55	-67.1	2.8	55.7	8.0
Superior	SU0711	16/04/07	SU08M	47.61	-86.82	1.5	-8.62	-66.9	2.0	54.1	8.0
Superior	SU0711	16/04/07	SU08M	47.61	-86.82	99.9	-8.53	-66.6	2.0	54.4	8.1
Superior	SU0711	16/04/07	SU08M	47.61	-86.82	200.2	-8.51	-66.8	2.5	55.3	8.0

Lake	Cruise ID	Date	Station	Latitude	Longitude	Depth (m)	$\delta^{18}O$ (‰SMOW)	$\delta^{2}H$ (‰SMOW)	T (°C)	EC ($\mu S/cm$)	pH
Superior	SU0711	16/04/07	SU08M	47.61	-86.82	288.2	-8.67	-66.6	3.3	56.6	7.9
Superior	SU0711	17/04/07	SU09	48.44	-87.09	1.5	-8.56	-67.0	1.2	52.9	8.0
Superior	SU0711	17/04/07	SU09	48.44	-87.09	117.2	-8.56	-67.2	1.5	53.6	8.1
Superior	SU0711	17/04/07	SU09	48.44	-87.09	224.3	-8.57	-67.1	3.2	56.5	8.0
Superior	SU0711	17/04/07	SU09	48.44	-87.09	232.2	-8.69	-67.2	3.2	56.5	8.0
Superior	SU0711	16/04/07	SU10	47.51	-87.55	1.5	-8.55	-66.8	1.8	53.9	7.9
Superior	SU0711	16/04/07	SU10	47.51	-87.55	76.1	-8.60	-66.8	1.8	54.0	8.0
Superior	SU0711	16/04/07	SU10	47.51	-87.55	142.1	-8.54	-67.5	2.7	55.6	7.9
Superior	SU0711	16/04/07	SU10	47.51	-87.55	150.0	-8.58	-67.4	2.7	55.7	8.0
Superior	SU0711	17/04/07	SU11	48.34	-87.83	3.0	-8.62	-65.7	1.4	53.2	8.0
Superior	SU0711	17/04/07	SU11	48.34	-87.83	111.1	-8.66	-67.2	1.4	53.5	8.0
Superior	SU0711	17/04/07	SU11	48.34	-87.83	212.3	-8.62	-66.8	3.3	56.7	7.9
Superior	SU0711	17/04/07	SU11	48.34	-87.83	220.3	-8.50	-66.9	3.3	56.7	7.9
Superior	SU0711	17/04/07	SU12	47.86	-88.04	1.5	-8.72	-65.3	1.3	52.9	8.0
Superior	SU0711	17/04/07	SU12	47.86	-88.04	116.0	-8.57	-64.6	1.3	53.2	8.0
Superior	SU0711	17/04/07	SU12	47.86	-88.04	222.1	-8.63	-65.4	2.9	56.1	8.0
Superior	SU0711	17/04/07	SU12	47.86	-88.04	230.7	-8.60	-65.4	3.0	56.1	8.0
Superior	SU0711	17/04/07	SU13	48.23	-88.55	2.9	-8.49	-64.9	0.9	52.6	8.0
Superior	SU0711	17/04/07	SU13	48.23	-88.55	72.3	-8.59	-65.4	0.9	52.8	8.0
Superior	SU0711	17/04/07	SU13	48.23	-88.55	134.9	-8.69	-65.6	2.5	55.4	7.9
Superior	SU0711	17/04/07	SU13	48.23	-88.55	142.8	-8.68	-65.8	2.6	55.5	7.9
Superior	SU0711	18/04/07	SU14	47.74	-88.74	1.5	-8.63	-65.7	1.2	52.8	8.0
Superior	SU0711	18/04/07	SU14	47.74	-88.74	116.6	-8.55	-65.0	1.3	53.2	8.0
Superior	SU0711	18/04/07	SU14	47.74	-88.74	223.5	-8.57	-65.5	2.8	55.8	7.9
Superior	SU0711	18/04/07	SU14	47.74	-88.74	232.2	-8.67	-65.5	2.8	55.9	7.9
Superior	SU0711	17/04/07	SU15	48.08	-89.25	2.1	-8.64	-66.3	1.0	52.7	7.9

Lake	Cruise ID	Date	Station	Latitude	Longitude	Depth (m)	$\delta^{18}O$ (‰SMOW)	$\delta^{2}H$ (‰SMOW)	T (°C)	EC (µS/cm)	pH
Superior	SU0711	17/04/07	SU15	48.08	-89.25	111.7	-8.79	-66.0	1.0	52.9	8.0
Superior	SU0711	17/04/07	SU15	48.08	-89.25	213.5	-8.54	-66.0	2.6	55.6	7.9
Superior	SU0711	17/04/07	SU15	48.08	-89.25	221.5	-8.68	-65.3	2.6	55.6	7.9
Superior	SU0711	18/04/07	SU16	47.62	-89.46	2.6	-8.68	-65.1	1.4	53.2	8.1
Superior	SU0711	18/04/07	SU16	47.62	-89.46	87.3	-8.60	-65.4	1.4	53.5	8.1
Superior	SU0711	18/04/07	SU16	47.62	-89.46	165.0	-8.65	-65.6	3.2	56.7	7.9
Superior	SU0711	18/04/07	SU16	47.62	-89.46	173.7	-8.54	-66.4	3.2	56.7	7.9
Superior	SU0711	18/04/07	SU17M	47.16	-89.66	2.7	-8.54	-65.4	1.4	53.4	8.1
Superior	SU0711	18/04/07	SU17M	47.16	-89.66	50.0	-8.63	-65.5	1.4	53.5	8.0
Superior	SU0711	18/04/07	SU17M	47.16	-89.66	99.9	-8.59	-64.9	1.4	53.5	8.0
Superior	SU0711	18/04/07	SU17M	47.16	-89.66	197.0	-8.67	-65.4	3.2	56.6	7.9
Superior	SU0711	18/04/07	SU18	47.51	-90.15	2.5	-8.55	-65.5	1.1	52.8	8.0
Superior	SU0711	18/04/07	SU18	47.51	-90.15	75.5	-8.53	-65.8	1.1	53.0	8.1
Superior	SU0711	18/04/07	SU18	47.51	-90.15	141.1	-8.59	-65.7	2.8	55.8	7.9
Superior	SU0711	18/04/07	SU18	47.51	-90.15	150.0	-8.62	-65.1	2.8	55.9	7.9
Superior	SU0711	18/04/07	SU19	47.37	-90.85	1.6	-8.56	-66.2	1.2	53.1	8.0
Superior	SU0711	18/04/07	SU19	47.37	-90.85	91.2	-8.56	-65.2	1.3	53.3	8.0
Superior	SU0711	18/04/07	SU19	47.37	-90.85	172.2	-8.62	-65.8	2.8	56.0	7.9
Superior	SU0711	18/04/07	SU19	47.37	-90.85	180.2	-8.49	-65.9	2.9	56.2	7.9
Superior	SU0711	16/04/07	SUFO	47.42	-87.58	1.2	-8.54	-65.4	1.7	53.8	7.9
Superior	SU0711	16/04/07	SUFO	47.42	-87.58	29.4	-8.56	-65.9	1.7	54.0	8.1
Superior	SU0711	16/04/07	SUFO	47.42	-87.58	48.2	-8.51	-65.8	1.8	54.1	8.1
Superior	SU0711	16/04/07	SUFO	47.42	-87.58	56.3	-8.53	-66.0	1.8	54.3	8.1

Lake	Cruise ID	Station	Date	Latitude	Longitude	Depth (m)	$\delta^{18}O$ (‰SMOW)	$\delta^{2}H$ (‰SMOW)	T (°C)	EC (µS/cm)	pH
Erie	ER0721	ER09	09/08/07	42.54	-79.62	1.7	-6.47	-47.2	24.2	277.4	9.6
Erie	ER0721	ER09	09/08/07	42.54	-79.62	4.9	-6.42	-47.0	24.1	277.5	9.6
Erie	ER0721	ER09	09/08/07	42.54	-79.62	48.1	-6.56	-47.0	5.2	177.3	8.8
Erie	ER0721	ER10	09/08/07	42.68	-79.69	1.6	-6.44	-47.2	24.0	276.3	9.6
Erie	ER0721	ER10	09/08/07	42.68	-79.69	27.5	-6.53	-47.5	6.3	184.7	8.8
Erie	ER0721	ER10	09/08/07	42.68	-79.69	32.1	-6.53	-47.4	6.1	183.2	8.9
Erie	ER0721	ER15M	09/08/07	42.52	-79.89	1.6	-6.43	-48.5	24.2	277.3	9.6
Erie	ER0721	ER15M	09/08/07	42.52	-79.89	25.3	-6.53	-47.2	4.4	170.8	8.9
Erie	ER0721	ER15M	09/08/07	42.52	-79.89	61.4	-6.55	-47.3	4.3	171.7	8.9
Erie	ER0721	ER30	08/08/07	42.43	-81.21	1.8	-6.80	-44.6	24.2	272.4	9.6
Erie	ER0721	ER30	08/08/07	42.43	-81.21	5.6	-6.75	-46.6	23.7	269.8	9.6
Erie	ER0721	ER30	08/08/07	42.43	-81.21	20.0	-6.57	-49.2	13.1	218.8	8.4
Erie	ER0721	ER31	08/08/07	42.25	-81.11	1.7	-6.63	-47.7	24.2	275.6	9.7
Erie	ER0721	ER31	08/08/07	42.25	-81.11	7.1	-6.61	-47.9	23.7	272.2	9.7
Erie	ER0721	ER31	08/08/07	42.25	-81.11	21.1	-6.48	-47.7	11.3	212.8	8.3
Erie	ER0721	ER32	08/08/07	42.08	-81.01	1.7	-6.56	-48.0	24.7	278.6	9.7
Erie	ER0721	ER32	08/08/07	42.08	-81.01	7.0	-6.57	-48.0	23.9	273.6	9.7
Erie	ER0721	ER32	08/08/07	42.08	-81.01	21.6	-6.64	-47.4	12.3	219.2	8.4
Erie	ER0721	ER36	08/08/07	41.94	-81.48	1.6	-6.60	-47.1	24.5	278.6	9.6
Erie	ER0721	ER36	08/08/07	41.94	-81.48	4.9	-6.61	-47.8	24.4	277.6	9.6
Erie	ER0721	ER36	08/08/07	41.94	-81.48	22.1	-6.56	-47.5	11.5	210.1	8.4
Erie	ER0721	ER37	08/08/07	42.11	-81.58	1.9	-6.67	-48.3	24.8	279.1	9.7
Erie	ER0721	ER37	08/08/07	42.11	-81.58	7.0	-6.72	-47.9	24.1	274.6	9.6
Erie	ER0721	ER37	08/08/07	42.11	-81.58	23.0	-6.61	-48.0	11.2	208.9	8.4
Erie	ER0721	ER38	08/08/07	42.28	-81.67	1.9	-6.77	-48.2	23.8	271.3	9.6
Erie	ER0721	ER38	08/08/07	42.28	-81.67	17.6	-6.52	-47.6	11.0	208.0	8.3

Lake	Cruise ID	Station	Date	Latitude	Longitude	Depth (m)	$\delta^{18}O$ (‰SMOW)	$\delta^{2}H$ (‰SMOW)	T (°C)	EC (µS/cm)	pH
Erie	ER0721	ER38	08/08/07	42.28	-81.67	21.1	-6.51	-47.3	10.9	207.5	8.4
Erie	ER0721	ER42	08/08/07	41.97	-82.04	1.6	-6.47	-48.0	24.1	274.3	9.6
Erie	ER0721	ER42	08/08/07	41.97	-82.04	19.2	-6.53	-47.6	11.5	208.7	8.2
Erie	ER0721	ER42	08/08/07	41.97	-82.04	21.4	-6.55	-47.5	11.5	208.7	8.2
Erie	ER0721	ER43	08/08/07	41.79	-81.95	1.5	-6.53	-46.6	24.2	279.2	9.6
Erie	ER0721	ER43	08/08/07	41.79	-81.95	8.5	-6.55	-47.9	24.2	279.1	9.6
Erie	ER0721	ER43	08/08/07	41.79	-81.95	20.9	-6.49	-46.7	10.8	204.9	8.3
Erie	ER0721	ER58	08/08/07	41.69	-82.93	1.6	-6.61	-48.8	25.6	250.9	9.6
Erie	ER0721	ER58	08/08/07	41.69	-82.93	4.6	-6.57	-47.8	25.6	250.9	9.5
Erie	ER0721	ER58	08/08/07	41.69	-82.93	8.5	-6.55	-48.7	25.0	255.6	9.2
Erie	ER0721	ER59	07/08/07	41.73	-83.15	1.8	-6.51	-48.3	25.7	250.0	9.6
Erie	ER0721	ER59	07/08/07	41.73	-83.15	4.0	-6.54	-48.5	25.7	249.9	9.5
Erie	ER0721	ER59	07/08/07	41.73	-83.15	7.1	-6.63	-48.6	25.1	248.0	9.1
Erie	ER0721	ER60	07/08/07	41.89	-83.20	1.8	-6.88	-50.5	26.1	226.8	9.7
Erie	ER0721	ER60	07/08/07	41.89	-83.20	4.1	-6.92	-50.5	26.1	226.8	9.7
Erie	ER0721	ER60	07/08/07	41.89	-83.20	7.6	-6.91	-51.0	25.4	225.5	9.3
Erie	ER0721	ER61	07/08/07	41.95	-83.05	1.9	-6.90	-50.9	25.4	218.5	9.4
Erie	ER0721	ER61	07/08/07	41.95	-83.05	4.5	-6.96	-51.1	25.3	218.8	9.3
Erie	ER0721	ER61	07/08/07	41.95	-83.05	8.1	-6.86	-50.8	24.8	221.9	9.1
Erie	ER0721	ER63	09/08/07	42.42	-79.80	1.8	-6.37	-47.7	24.3	278.0	9.6
Erie	ER0721	ER63	09/08/07	42.42	-79.80	34.6	-6.48	-47.0	5.4	177.2	8.8
Erie	ER0721	ER63	09/08/07	42.42	-79.80	43.9	-6.45	-47.6	5.3	177.5	8.8
Erie	ER0721	ER73	08/08/07	41.98	-81.76	1.7	-6.54	-49.4	24.3	277.0	9.7
Erie	ER0721	ER73	08/08/07	41.98	-81.76	10.1	-6.50	-49.3	24.0	276.4	9.6
Erie	ER0721	ER73	08/08/07	41.98	-81.76	23.1	-6.52	-49.3	10.9	205.0	8.3
Erie	ER0721	ER78M	08/08/07	42.12	-81.25	1.7	-6.56	-49.6	24.2	274.9	9.7

Lake	Cruise ID	Station	Date	Latitude	Longitude	Depth (m)	$\delta^{18}O$ (‰SMOW)	$\delta^{2}H$ (‰SMOW)	T (°C)	EC (µS/cm)	pH
Erie	ER0721	ER78M	08/08/07	42.12	-81.25	5.3	-6.47	-49.2	24.2	274.8	9.7
Erie	ER0721	ER78M	08/08/07	42.12	-81.25	22.2	-6.43	-49.1	11.2	211.1	8.5
Erie	ER0721	ER91M	08/08/07	41.84	-82.92	1.9	-6.65	-51.6	25.2	227.7	9.5
Erie	ER0721	ER91M	08/08/07	41.84	-82.92	5.0	-6.72	-52.3	25.2	227.9	9.5
Erie	ER0721	ER91M	08/08/07	41.84	-82.92	9.1	-6.75	-51.8	25.1	230.7	9.3
Erie	ER0721	ER92	08/08/07	41.95	-82.69	1.7	-6.85	-52.0	25.0	222.9	9.6
Erie	ER0721	ER92	08/08/07	41.95	-82.69	5.0	-6.83	-52.5	25.0	223.0	9.6
Erie	ER0721	ER92	08/08/07	41.95	-82.69	9.8	-6.90	-52.2	24.5	227.7	9.2
Erie	ER0721	ERFO	09/08/07	42.42	-79.58	1.6	-6.40	-48.8	24.4	280.1	9.6
Erie	ER0721	ERFO	09/08/07	42.42	-79.58	25.0	-6.58	-49.4	5.8	182.0	8.7
Erie	ER0721	ERFO	09/08/07	42.42	-79.58	30.5	-6.48	-49.3	5.7	182.2	8.7
Huron	HU0721	HU06	07/08/07	43.47	-82.00	1.9	-7.18	-52.9	22.0	201.2	9.3
Huron	HU0721	HU06	07/08/07	43.47	-82.00	40.5	-7.02	-52.1	5.8	132.7	9.0
Huron	HU0721	HU06	07/08/07	43.47	-82.00	49.6	-7.04	-53.4	4.9	129.6	8.9
Huron	HU0721	HU09	06/08/07	43.63	-82.22	1.8	-6.97	-53.0	21.7	201.6	9.3
Huron	HU0721	HU09	06/08/07	43.63	-82.22	38.9	-7.03	-53.1	6.2	133.0	9.3
Huron	HU0721	HU09	06/08/07	43.63	-82.22	56.6	-7.08	-53.4	4.7	128.4	8.9
Huron	HU0721	HU12	06/08/07	43.89	-82.06	1.7	-7.00	-52.9	21.8	201.7	9.3
Huron	HU0721	HU12	06/08/07	43.89	-82.06	57.1	-7.06	-54.0	4.6	127.4	8.9
Huron	HU0721	HU12	06/08/07	43.89	-82.06	84.7	-7.12	-51.5	4.4	127.8	8.9
Huron	HU0721	HU15M	06/08/07	44.00	-82.35	1.7	-7.04	-52.4	21.7	201.4	9.4
Huron	HU0721	HU15M	06/08/07	44.00	-82.35	34.2	-7.19	-53.4	5.6	130.7	9.3
Huron	HU0721	HU15M	06/08/07	44.00	-82.35	64.4	-7.00	-53.5	4.4	127.8	8.9
Huron	HU0721	HU27	06/08/07	44.20	-82.50	1.7	-7.04	-53.2	20.1	188.8	9.3
Huron	HU0721	HU27	06/08/07	44.20	-82.50	36.2	-7.08	-53.2	5.6	130.7	9.0
Huron	HU0721	HU27	06/08/07	44.20	-82.50	52.7	-7.12	-52.8	5.3	129.9	9.0

Lake	Cruise ID	Station	Date	Latitude	Longitude	Depth (m)	$\delta^{18}O$ (‰ SMOW)	$\delta^{2}H$ (‰ SMOW)	T (°C)	EC (µS/cm)	pH
Huron	HU0721	HU32	06/08/07	44.45	-82.34	2.2	-7.09	-53.7	20.5	187.4	9.2
Huron	HU0721	HU32	06/08/07	44.45	-82.34	55.0	-7.05	-52.9	4.2	125.9	8.9
Huron	HU0721	HU32	06/08/07	44.45	-82.34	81.5	-7.16	-53.7	4.1	126.1	8.9
Huron	HU0721	HU37	05/08/07	44.76	-82.78	2.3	-7.07	-53.7	19.8	185.3	9.2
Huron	HU0721	HU37	05/08/07	44.76	-82.78	48.6	-7.09	-53.4	4.5	126.8	8.9
Huron	HU0721	HU37	05/08/07	44.76	-82.78	71.9	-7.01	-53.6	4.4	127.0	8.8
Huron	HU0721	HU38	06/08/07	44.74	-82.06	2.7	-7.11	-53.3	20.7	191.7	8.9
Huron	HU0721	HU38	06/08/07	44.74	-82.06	85.1	-7.05	-53.7	3.8	123.5	5.9
Huron	HU0721	HU38	06/08/07	44.74	-82.06	132.6	-7.00	-54.0	3.8	124.0	2.7
Huron	HU0721	HU45M	05/08/07	45.14	-82.98	1.9	-7.18	-54.9	19.5	181.2	9.3
Huron	HU0721	HU45M	05/08/07	45.14	-82.98	50.0	-7.08	-53.6	4.0	124.6	8.9
Huron	HU0721	HU45M	05/08/07	45.14	-82.98	95.6	-7.03	-53.8	4.0	125.6	8.8
Huron	HU0721	HU48	05/08/07	45.28	-82.45	1.9	-7.08	-54.6	19.3	182.5	9.2
Huron	HU0721	HU48	05/08/07	45.28	-82.45	68.3	-7.06	-53.0	3.9	123.8	8.9
Huron	HU0721	HU48	05/08/07	45.28	-82.45	108.2	-7.13	-53.5	3.8	124.4	8.9
Huron	HU0721	HU53	05/08/07	45.45	-82.92	1.9	-7.16	-53.8	17.9	175.6	9.2
Huron	HU0721	HU53	05/08/07	45.45	-82.92	60.0	-7.09	-53.2	4.1	124.5	8.9
Huron	HU0721	HU53	05/08/07	45.45	-82.92	90.0	-7.09	-53.6	3.9	124.6	8.9
Huron	HU0721	HU54M	05/08/07	45.52	-83.42	2.0	-7.18	-54.0	19.1	185.0	9.3
Huron	HU0721	HU54M	05/08/07	45.52	-83.42	50.1	-7.29	-53.5	4.0	122.9	8.9
Huron	HU0721	HU54M	05/08/07	45.52	-83.42	122.5	-7.15	-53.6	3.9	123.6	8.9
Huron	HU0721	HU61	05/08/07	45.75	-83.92	2.1	-7.10	-53.1	19.7	187.0	9.2
Huron	HU0721	HU61	05/08/07	45.75	-83.92	70.0	-7.18	-53.5	3.9	123.5	8.8
Huron	HU0721	HU61	05/08/07	45.75	-83.92	115.5	-7.11	-53.6	3.9	124.0	8.8
Huron	HU0721	HU93	06/08/07	44.10	-82.12	1.6	-7.06	-52.6	21.4	198.2	9.3
Huron	HU0721	HU93	06/08/07	44.10	-82.12	58.9	-7.12	-53.2	4.5	127.7	9.0

Lake	Cruise ID	Station	Date	Latitude	Longitude	Depth (m)	$\delta^{18}O$ (‰SMOW)	$\delta^{2}H$ (‰SMOW)	T (°C)	EC (µS/cm)	pH
Huron	HU0721	HU93	06/08/07	44.10	-82.12	86.3	-7.12	-53.5	4.2	128.1	8.9
Huron	HU0721	HUFO	06/08/07	44.08	-82.75	1.7	-7.14	-53.2	17.2	179.4	9.3
Huron	HU0721	HUFO	06/08/07	44.08	-82.75	26.8	-7.11	-53.9	5.8	131.8	9.0
Huron	HU0721	HUFO	06/08/07	44.08	-82.75	34.9	-7.06	-53.3	5.8	132.3	9.0
Michigan	MI0721	MI11	02/08/07	42.38	-87.00	1.8	-5.81	-43.3	24.7	291.5	9.3
Michigan	MI0721	MI11	02/08/07	42.38	-87.00	72.2	-5.90	-43.4	4.3	174.9	8.9
Michigan	MI0721	MI11	02/08/07	42.38	-87.00	124.0	-5.78	-43.2	3.9	174.9	8.8
Michigan	MI0721	MI17	01/08/07	42.73	-87.42	1.8	-5.86	-43.3	22.5	275.6	9.3
Michigan	MI0721	MI17	01/08/07	42.73	-87.42	65.0	-5.76	-43.6	4.2	175.0	8.8
Michigan	MI0721	MI17	01/08/07	42.73	-87.42	97.4	-5.76	-43.3	4.2	175.9	8.8
Michigan	MI0721	MI18M	01/08/07	42.73	-87.00	1.6	-5.75	-43.3	23.5	283.0	9.3
Michigan	MI0721	MI18M	01/08/07	42.73	-87.00	100.0	-5.76	-43.6	4.0	174.2	8.9
Michigan	MI0721	MI18M	01/08/07	42.73	-87.00	156.0	-5.82	-44.1	3.8	175.4	8.8
Michigan	MI0721	MI19	02/08/07	43.06	-86.65	1.9	-5.79	-43.9	23.5	282.6	9.3
Michigan	MI0721	MI19	02/08/07	43.06	-86.65	58.9	-5.78	-44.2	4.3	174.8	8.9
Michigan	MI0721	MI19	02/08/07	43.06	-86.65	88.1	-5.90	-43.7	4.2	175.2	8.8
Michigan	MI0721	MI23	02/08/07	43.13	-87.00	1.7	-5.88	-43.5	22.5	274.6	9.3
Michigan	MI0721	MI23	02/08/07	43.13	-87.00	57.2	-5.89	-44.4	4.4	175.5	8.9
Michigan	MI0721	MI23	02/08/07	43.13	-87.00	88.9	-5.81	-44.3	4.2	176.0	8.9
Michigan	MI0721	MI27M	02/08/07	43.60	-86.92	1.9	-5.94	-44.9	22.5	274.7	9.3
Michigan	MI0721	MI27M	02/08/07	43.60	-86.92	49.9	-5.78	-43.9	4.4	175.1	8.9
Michigan	MI0721	MI27M	02/08/07	43.60	-86.92	101.8	-5.78	-43.8	4.0	174.2	8.9
Michigan	MI0721	MI32	03/08/07	44.14	-87.23	2.0	-5.81	-44.7	21.8	268.9	9.3
Michigan	MI0721	MI32	03/08/07	44.14	-87.23	95.0	-5.77	-44.7	3.9	172.4	9.0
Michigan	MI0721	MI32	03/08/07	44.14	-87.23	160.0	-5.83	-44.7	3.8	172.7	8.9
Michigan	MI0721	MI34	03/08/07	44.09	-86.77	1.9	-5.78	-44.8	21.7	271.4	9.4

Lake	Cruise ID	Station	Date	Latitude	Longitude	Depth (m)	$\delta^{18}O$ (‰SMOW)	$\delta^{2}H$ (‰SMOW)	T (°C)	EC (µS/cm)	pH
Michigan	MI0721	MI34	03/08/07	44.09	-86.77	85.0	-5.85	-44.4	4.1	173.5	9.0
Michigan	MI0721	MI34	03/08/07	44.09	-86.77	154.5	-5.85	-44.1	3.8	173.1	8.9
Michigan	MI0721	MI40	03/08/07	44.76	-86.97	1.7	-6.02	-44.5	21.5	267.4	9.4
Michigan	MI0721	MI40	03/08/07	44.76	-86.97	100.0	-5.89	-44.0	4.0	173.1	9.0
Michigan	MI0721	MI40	03/08/07	44.76	-86.97	165.1	-5.86	-44.6	3.7	173.0	9.0
Michigan	MI0721	MI41M	03/08/07	44.74	-86.72	1.8	-5.89	-44.4	21.3	267.6	9.4
Michigan	MI0721	MI41M	03/08/07	44.74	-86.72	100.1	-5.81	-44.3	4.1	173.4	9.0
Michigan	MI0721	MI41M	03/08/07	44.74	-86.72	256.7	-5.74	-44.4	3.6	172.3	9.0
Michigan	MI0721	MI47	04/08/07	45.18	-86.38	2.0	-5.94	-45.7	20.9	263.3	9.5
Michigan	MI0721	MI47	04/08/07	45.18	-86.38	110.0	-5.83	-45.0	3.9	172.8	9.0
Michigan	MI0721	MI47	04/08/07	45.18	-86.38	187.5	-5.94	-44.1	3.7	173.0	8.9
Michigan	MI0721	MIFO	03/08/07	44.75	-87.08	1.7	-5.85	-44.8	20.8	263.2	9.4
Michigan	MI0721	MIFO	03/08/07	44.75	-87.08	75.4	-5.80	-44.4	4.1	173.6	9.0
Michigan	MI0721	MIFO	03/08/07	44.75	-87.08	115.7	-5.92	-44.6	3.9	173.5	9.0
Ontario	ON0721	ON12	10/08/07	43.50	-79.35	1.8	-6.37	-48.6	21.2	281.7	9.8
Ontario	ON0721	ON12	10/08/07	43.50	-79.35	66.0	-6.42	-49.0	3.9	182.5	9.1
Ontario	ON0721	ON12	10/08/07	43.50	-79.35	102.6	-6.50	-49.2	3.8	183.5	9.0
Ontario	ON0721	ON25	10/08/07	43.52	-79.08	1.9	-6.48	-49.1	23.4	289.5	9.7
Ontario	ON0721	ON25	10/08/07	43.52	-79.08	78.0	-6.45	-49.2	3.9	182.2	9.1
Ontario	ON0721	ON25	10/08/07	43.52	-79.08	134.2	-6.56	-49.2	3.8	182.6	9.1
Ontario	ON0721	ON33M	11/08/07	43.60	-78.80	1.7	-6.48	-48.6	22.2	281.0	9.8
Ontario	ON0721	ON33M	11/08/07	43.60	-78.80	50.1	-6.57	-49.2	4.1	182.7	9.1
Ontario	ON0721	ON33M	11/08/07	43.60	-78.80	136.5	-6.58	-49.0	3.8	182.2	9.1
Ontario	ON0721	ON41	11/08/07	43.72	-78.03	1.7	-6.50	-48.5	22.9	283.7	9.8
Ontario	ON0721	ON41	11/08/07	43.72	-78.03	76.3	-6.58	-49.1	3.9	182.3	9.1
Ontario	ON0721	ON41	11/08/07	43.72	-78.03	127.8	-6.47	-48.8	3.8	182.9	9.1

Lake	Cruise ID	Station	Date	Latitude	Longitude	Depth (m)	$\delta^{18}O$ (‰SMOW)	$\delta^{2}H$ (‰SMOW)	T (°C)	EC (µS/cm)	pH
Ontario	ON0721	ON49	11/08/07	43.77	-77.44	1.7	-6.47	-49.2	22.7	283.8	9.9
Ontario	ON0721	ON49	11/08/07	43.77	-77.44	34.9	-6.54	-49.6	5.5	193.0	8.9
Ontario	ON0721	ON49	11/08/07	43.77	-77.44	48.0	-6.62	-49.7	5.5	193.6	8.9
Ontario	ON0721	ON55M	12/08/07	43.44	-77.44	1.5	-6.32	-47.9	24.3	292.3	9.9
Ontario	ON0721	ON55M	12/08/07	43.44	-77.44	100.2	-6.56	-48.8	3.9	182.3	9.1
Ontario	ON0721	ON55M	12/08/07	43.44	-77.44	190.5	-6.48	-49.1	3.7	182.1	9.1
Ontario	ON0721	ON60	11/08/07	43.58	-77.20	1.6	-6.45	-48.6	23.9	288.9	9.8
Ontario	ON0721	ON60	11/08/07	43.58	-77.20	90.1	-6.56	-49.2	3.9	182.8	9.1
Ontario	ON0721	ON60	11/08/07	43.58	-77.20	149.3	-6.57	-49.1	3.8	183.3	9.1
Ontario	ON0721	ON63	11/08/07	43.73	-77.02	2.0	-6.48	-48.5	23.5	285.3	9.8
Ontario	ON0721	ON63	11/08/07	43.73	-77.02	55.2	-6.65	-49.5	4.2	186.3	9.0
Ontario	ON0721	ON63	11/08/07	43.73	-77.02	85.4	-6.61	-49.1	4.1	186.8	9.0
Ontario	ON0721	ONFO	13/08/07	43.42	-77.92	2.3	-6.45	-48.2	23.3	284.8	9.8
Ontario	ON0721	ONFO	13/08/07	43.42	-77.92	57.7	-6.53	-48.9	4.0	183.9	8.9
Ontario	ON0721	ONFO	13/08/07	43.42	-77.92	79.6	-6.55	-49.0	4.0	184.9	8.9
Superior	SU0721	SU01M	18/08/07	46.99	-85.16	1.4	-8.58	-65.6	14.3	77.5	9.3
Superior	SU0721	SU01M	18/08/07	46.99	-85.16	49.9	-8.60	-65.9	4.9	60.2	8.8
Superior	SU0721	SU01M	18/08/07	46.99	-85.16	91.6	-8.64	-65.6	4.0	59.1	8.8
Superior	SU0721	SU02	18/08/07	47.34	-85.62	1.7	-8.63	-65.1	13.0	74.3	9.2
Superior	SU0721	SU02	18/08/07	47.34	-85.62	90.0	-8.59	-65.9	3.9	58.1	8.8
Superior	SU0721	SU02	18/08/07	47.34	-85.62	147.3	-8.66	-65.6	3.8	58.3	8.8
Superior	SU0721	SU03	24/08/07	46.89	-85.85	1.5	-8.72	-65.0	17.3	83.3	9.4
Superior	SU0721	SU03	24/08/07	46.89	-85.85	91.0	-8.56	-65.3	4.0	58.5	9.0
Superior	SU0721	SU03	24/08/07	46.89	-85.85	146.0	-8.61	-64.6	3.9	58.6	8.9
Superior	SU0721	SU04	18/08/07	47.26	-86.35	1.7	-8.65	-64.6	13.8	75.9	9.2
Superior	SU0721	SU04	18/08/07	47.26	-86.35	80.0	-8.62	-65.3	4.2	58.5	8.9

Lake	Cruise ID	Station	Date	Latitude	Longitude	Depth (m)	$\delta^{18}O$ (‰SMOW)	$\delta^{2}H$ (‰SMOW)	T (°C)	EC (µS/cm)	pH
Superior	SU0721	SU04	18/08/07	47.26	-86.35	140.9	-8.61	-65.4	3.9	58.4	8.8
Superior	SU0721	SU05	24/08/07	46.77	-86.55	1.6	-8.65	-64.4	17.9	84.7	9.4
Superior	SU0721	SU05	24/08/07	46.77	-86.55	95.2	-8.55	-64.7	3.9	58.2	8.9
Superior	SU0721	SU05	24/08/07	46.77	-86.55	145.7	-8.67	-64.8	3.7	58.3	8.9
Superior	SU0721	SU06	19/08/07	48.56	-86.38	1.5	-8.64	-64.9	15.2	79.1	9.4
Superior	SU0721	SU06	19/08/07	48.56	-86.38	90.1	-8.69	-64.9	4.1	58.5	8.9
Superior	SU0721	SU06	19/08/07	48.56	-86.38	163.8	-8.74	-64.9	3.8	60.5	8.9
Superior	SU0721	SU07	19/08/07	48.07	-86.59	1.6	-8.71	-65.1	12.4	73.1	9.2
Superior	SU0721	SU07	19/08/07	48.07	-86.59	110.4	-8.65	-65.0	4.0	58.0	8.5
Superior	SU0721	SU07	19/08/07	48.07	-86.59	194.8	-8.59	-64.8	3.7	57.8	8.0
Superior	SU0721	SU08M	19/08/07	47.61	-86.82	1.7	-8.61	-65.1	13.3	75.4	9.3
Superior	SU0721	SU08M	19/08/07	47.61	-86.82	100.2	-8.60	-64.8	4.1	58.0	8.9
Superior	SU0721	SU08M	19/08/07	47.61	-86.82	290.0	-8.57	-64.7	3.6	57.5	8.8
Superior	SU0721	SU09	19/08/07	48.44	-87.10	1.4	-8.74	-65.1	13.2	74.6	9.3
Superior	SU0721	SU09	19/08/07	48.44	-87.10	124.9	-8.61	-65.0	3.9	57.9	8.9
Superior	SU0721	SU09	19/08/07	48.44	-87.10	229.6	-8.63	-64.8	3.7	58.0	8.9
Superior	SU0721	SU10	23/08/07	47.51	-87.55	1.7	-8.68	-65.0	16.9	82.5	9.4
Superior	SU0721	SU10	23/08/07	47.51	-87.55	84.7	-8.62	-64.8	4.2	58.8	8.9
Superior	SU0721	SU10	23/08/07	47.51	-87.55	149.3	-8.65	-64.9	3.8	58.7	8.9
Superior	SU0721	SU11	19/08/07	48.34	-87.82	1.5	-8.75	-64.9	12.4	73.4	9.3
Superior	SU0721	SU11	19/08/07	48.34	-87.82	124.8	-8.65	-64.8	3.9	58.0	8.9
Superior	SU0721	SU11	19/08/07	48.34	-87.82	221.1	-8.63	-65.1	3.7	58.0	8.9
Superior	SU0721	SU12	23/08/07	47.86	-88.04	1.4	-8.73	-64.7	13.4	75.4	9.4
Superior	SU0721	SU12	23/08/07	47.86	-88.04	129.9	-8.64	-64.9	3.9	58.1	9.0
Superior	SU0721	SU12	23/08/07	47.86	-88.04	230.0	-8.70	-64.8	3.7	58.1	8.9
Superior	SU0721	SU13	19/08/07	48.23	-88.55	1.5	-8.77	-64.9	14.8	78.8	9.3

Lake	Cruise ID	Station	Date	Latitude	Longitude	Depth (m)	$\delta^{18}O$ (‰SMOW)	$\delta^{2}H$ (‰SMOW)	T (°C)	EC (µS/cm)	pH
Superior	SU0721	SU13	19/08/07	48.23	-88.55	88.0	-8.72	-65.1	4.0	58.6	8.9
Superior	SU0721	SU13	19/08/07	48.23	-88.55	143.7	-8.62	-64.8	3.8	58.7	8.8
Superior	SU0721	SU14	23/08/07	47.74	-88.74	1.3	-8.71	-64.9	13.3	75.0	9.4
Superior	SU0721	SU14	23/08/07	47.74	-88.74	124.7	-8.68	-65.2	3.9	58.0	8.9
Superior	SU0721	SU14	23/08/07	47.74	-88.74	231.4	-8.73	-65.3	3.7	58.0	8.9
Superior	SU0721	SU15	20/08/07	48.08	-89.25	1.6	-8.82	-65.5	14.3	79.2	9.3
Superior	SU0721	SU15	20/08/07	48.08	-89.25	127.8	-8.70	-65.1	3.9	58.3	8.9
Superior	SU0721	SU15	20/08/07	48.08	-89.25	226.7	-8.68	-64.7	3.7	58.3	8.8
Superior	SU0721	SU16	20/08/07	47.62	-89.46	1.8	-8.71	-65.2	13.5	75.5	9.4
Superior	SU0721	SU16	20/08/07	47.62	-89.46	102.2	-8.64	-64.9	4.0	58.2	9.0
Superior	SU0721	SU16	20/08/07	47.62	-89.46	173.7	-8.66	-65.1	3.8	58.3	8.9
Superior	SU0721	SU17M	23/08/07	47.17	-89.66	1.6	-8.70	-65.2	13.3	75.7	9.4
Superior	SU0721	SU17M	23/08/07	47.17	-89.66	100.2	-8.64	-65.2	4.0	58.3	8.9
Superior	SU0721	SU17M	23/08/07	47.17	-89.66	195.7	-8.66	-65.3	3.7	58.2	8.8
Superior	SU0721	SU18	20/08/07	47.51	-90.15	2.9	-8.71	-64.9	12.3	73.2	9.3
Superior	SU0721	SU18	20/08/07	47.51	-90.15	84.8	-8.71	-65.0	3.9	58.3	8.8
Superior	SU0721	SU18	20/08/07	47.51	-90.15	150.4	-8.59	-65.0	3.8	58.4	8.7
Superior	SU0721	SU19	20/08/07	47.37	-90.85	3.0	-8.72	-65.2	14.3	77.8	9.4
Superior	SU0721	SU19	20/08/07	47.37	-90.85	100.3	-8.55	-64.8	3.9	58.2	8.9
Superior	SU0721	SU19	20/08/07	47.37	-90.85	180.3	-8.62	-65.0	3.7	58.3	8.9
Superior	SU0721	SUFO	08/23/07	47.42	-87.58	1.1	-8.69	-65.1	15.6	79.9	9.3
Superior	SU0721	SUFO	08/23/07	47.42	-87.58	50.1	-8.59	-65.2	4.7	60.0	8.9
Superior	SU0721	SUFO	08/23/07	47.42	-87.58	82.8	-8.59	-65.3	4.4	60.0	8.9

Appendix B:
Contour plots – $\delta^{18}O$ in H_2O

In order, plots shown are:
- Lake Superior: Spring
- Lake Superior: Summer
- Lake Huron: Spring
- Lake Huron: Summer
- Lake Michigan: Spring
- Lake Michigan: Summer
- Lake Erie: Spring
- Lake Erie: Summer
- Lake Ontario: Spring
- Lake Ontario: Summer

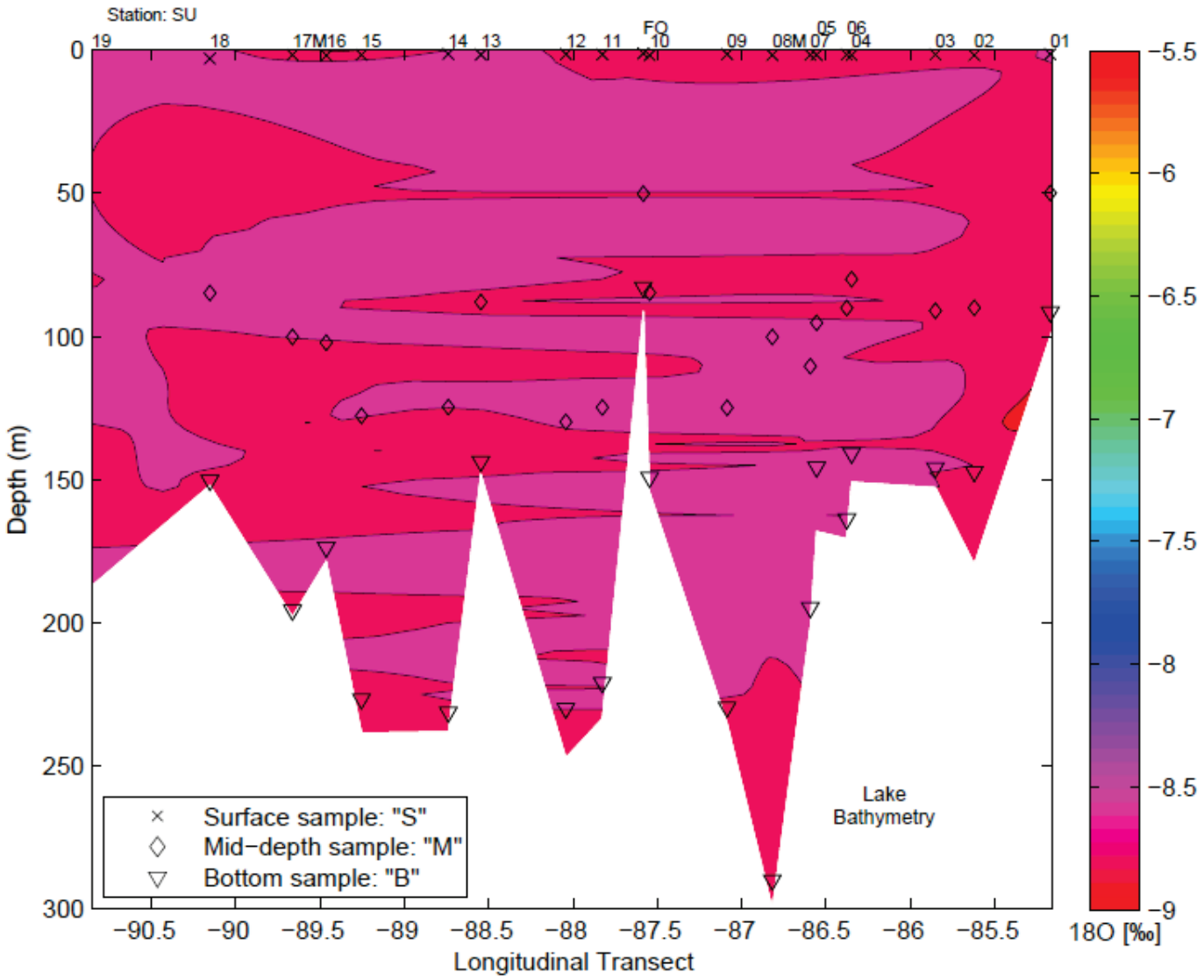
Station: SU
19
18
17M
16
15
14
13
12
11
FQ
10
09
08M
07
05
06
04
03
02
01
0
50
100
150
200
250
300
Depth (m)
−90.5
−90
−89.5
−89
−88.5
−88
−87.5
−87
−86.5
−86
−85.5
Longitudinal Transect
Surface sample: "S"
Mid−depth sample: "M"
Bottom sample: "B"
Lake
Bathymetry
−5.5
−6
−6.5
−7
−7.5
−8
−8.5
−9
18O [‰]

187

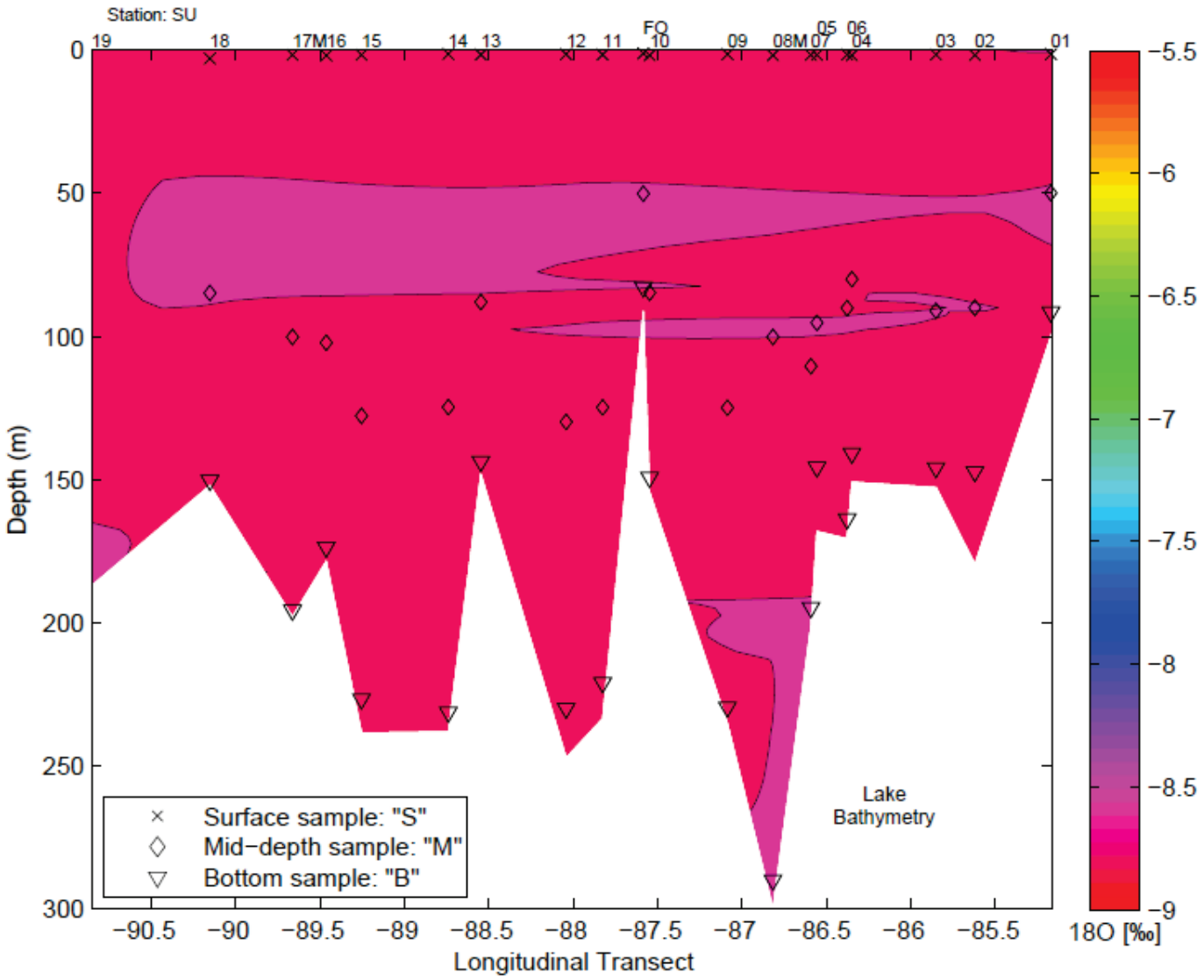
Station: SU
19
18
17M
16
15
14
13
12
11
FQ
10
09
08M
07
05
06
04
03
02
01
0
50
100
150
200
250
300
Depth (m)
−90.5
−90
−89.5
−89
−88.5
−88
−87.5
−87
−86.5
−86
−85.5
Longitudinal Transect
Surface sample: "S"
Mid−depth sample: "M"
Bottom sample: "B"
Lake
Bathymetry
−5.5
−6
−6.5
−7
−7.5
−8
−8.5
−9
18O [‰]

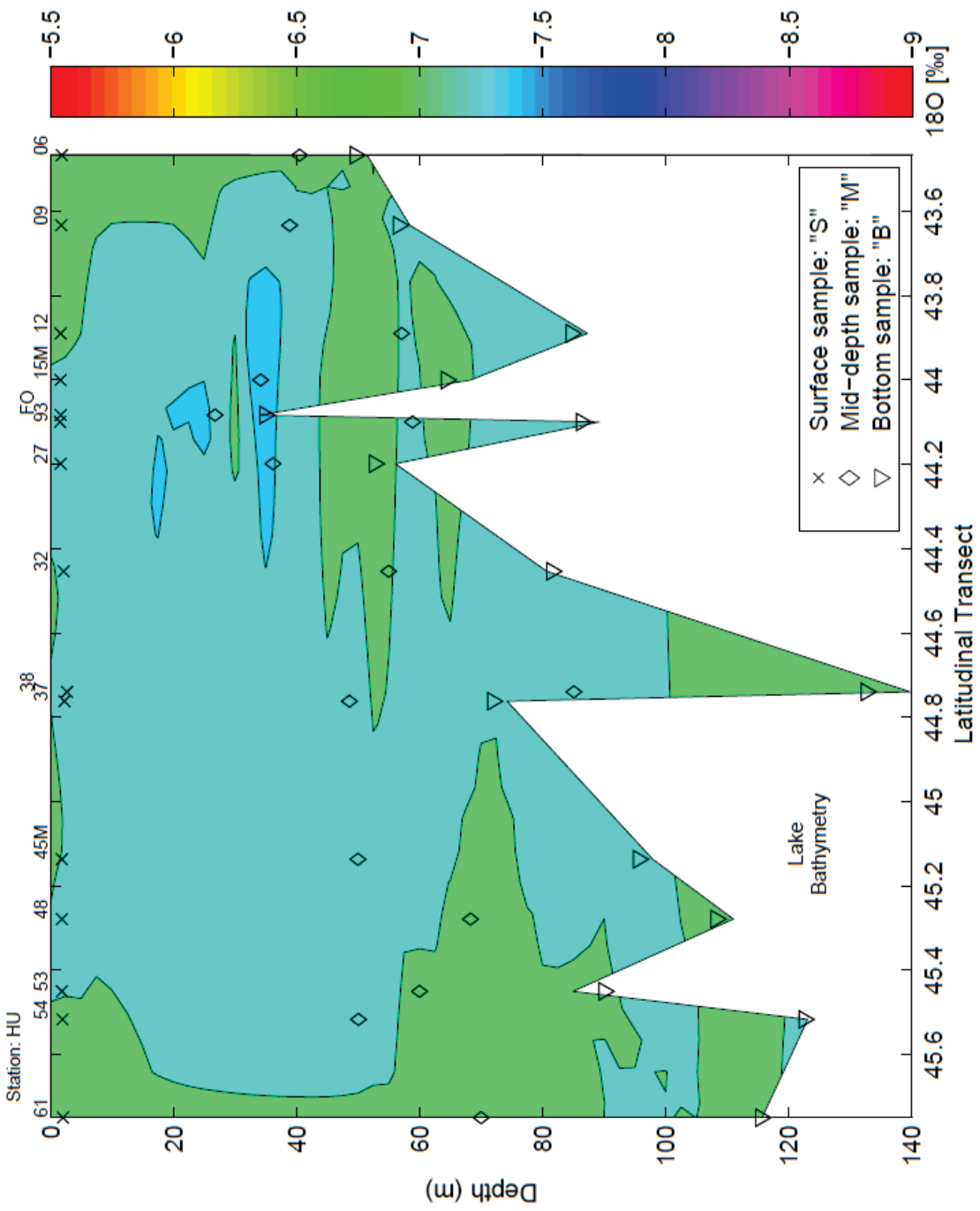
Station: HU
61
54
53
48
45M
38
37
32
27
93
FO
15M
12
09
06
Depth (m)
0
20
40
60
80
100
120
140
Lake
Bathymetry
Surface sample: "S"
Mid−depth sample: "M"
Bottom sample: "B"
45.6
45.4
45.2
45
44.8
44.6
44.4
44.2
44
43.8
43.6
Latitudinal Transect
−5.5
−6
−6.5
−7
−7.5
−8
−8.5
−9
18O [‰]

189

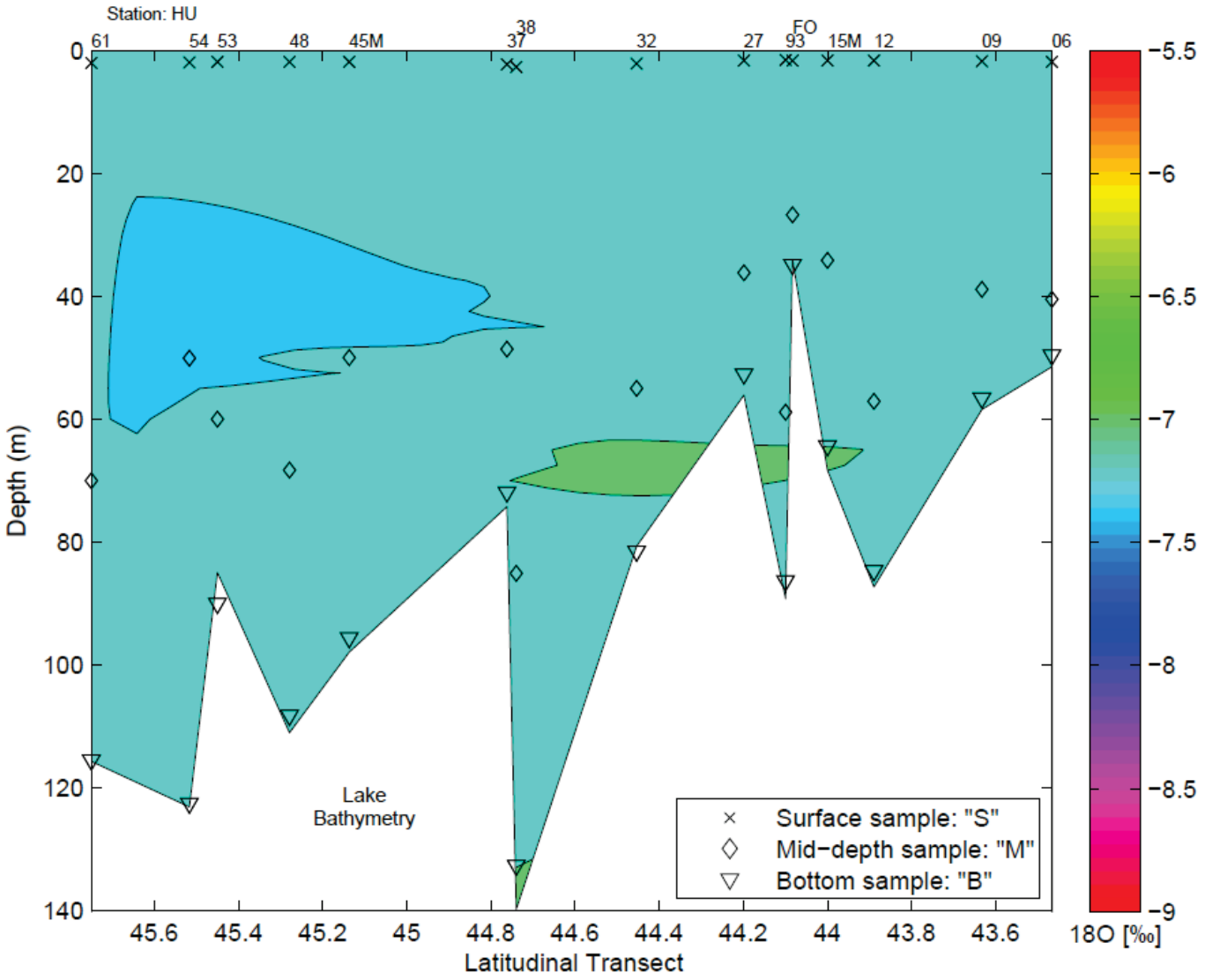
Station: HU
61
54
53
48
45M
38
37
32
FO
27
93
15M
12
09
06
0
20
40
60
80
100
120
140
Depth (m)
45.6
45.4
45.2
45
44.8
44.6
44.4
44.2
44
43.8
43.6
Latitudinal Transect
Lake
Bathymetry
Surface sample: "S"
Mid−depth sample: "M"
Bottom sample: "B"
−5.5
−6
−6.5
−7
−7.5
−8
−8.5
−9
18O [‰]

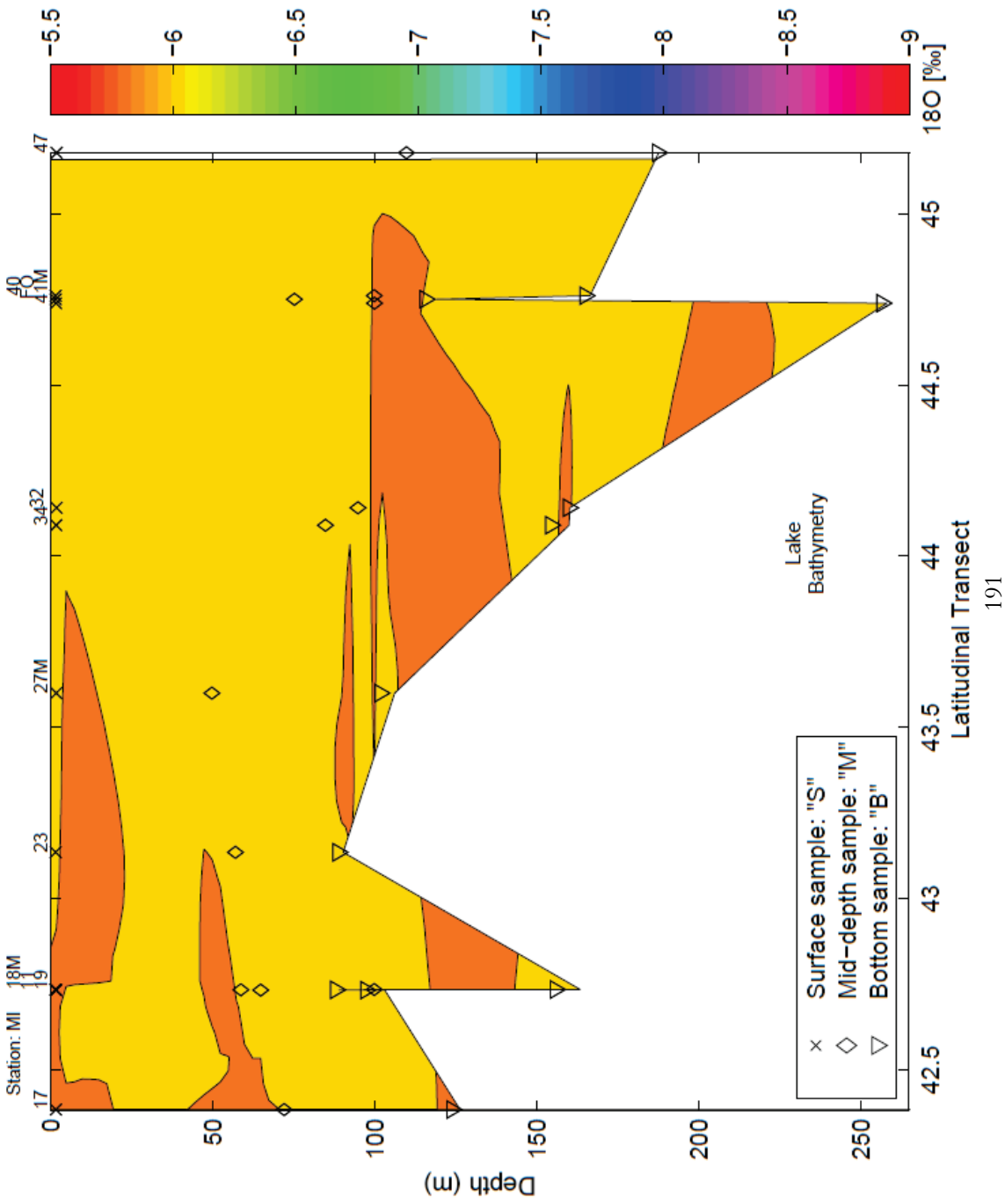
Station: MI
17
18M
19
23
27M
32
34
40
41M
47
0
50
100
150
200
250
Depth (m)
42.5
43
43.5
44
44.5
45
Latitudinal Transect
Lake
Bathymetry
Surface sample: "S"
Mid−depth sample: "M"
Bottom sample: "B"
−5.5
−6
−6.5
−7
−7.5
−8
−8.5
−9
18O [‰]

191

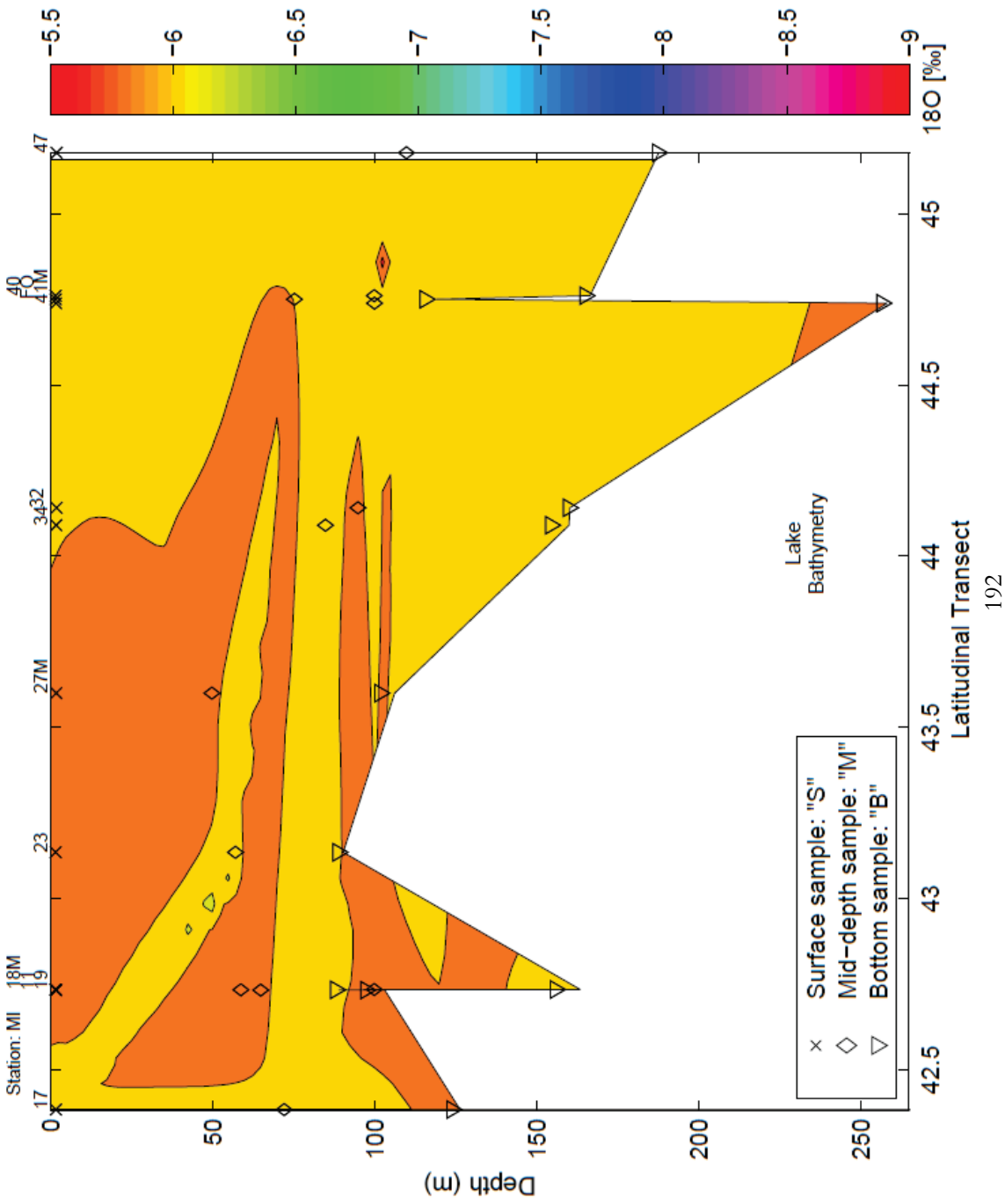
Station: MI
17
18M
19
23
27M
32
34
40
41M
47
0
50
100
150
200
250
Depth (m)
42.5
43
43.5
44
44.5
45
Latitudinal Transect
Lake
Bathymetry
Surface sample: "S"
Mid−depth sample: "M"
Bottom sample: "B"
−5.5
−6
−6.5
−7
−7.5
−8
−8.5
−9
18O [‰]

192

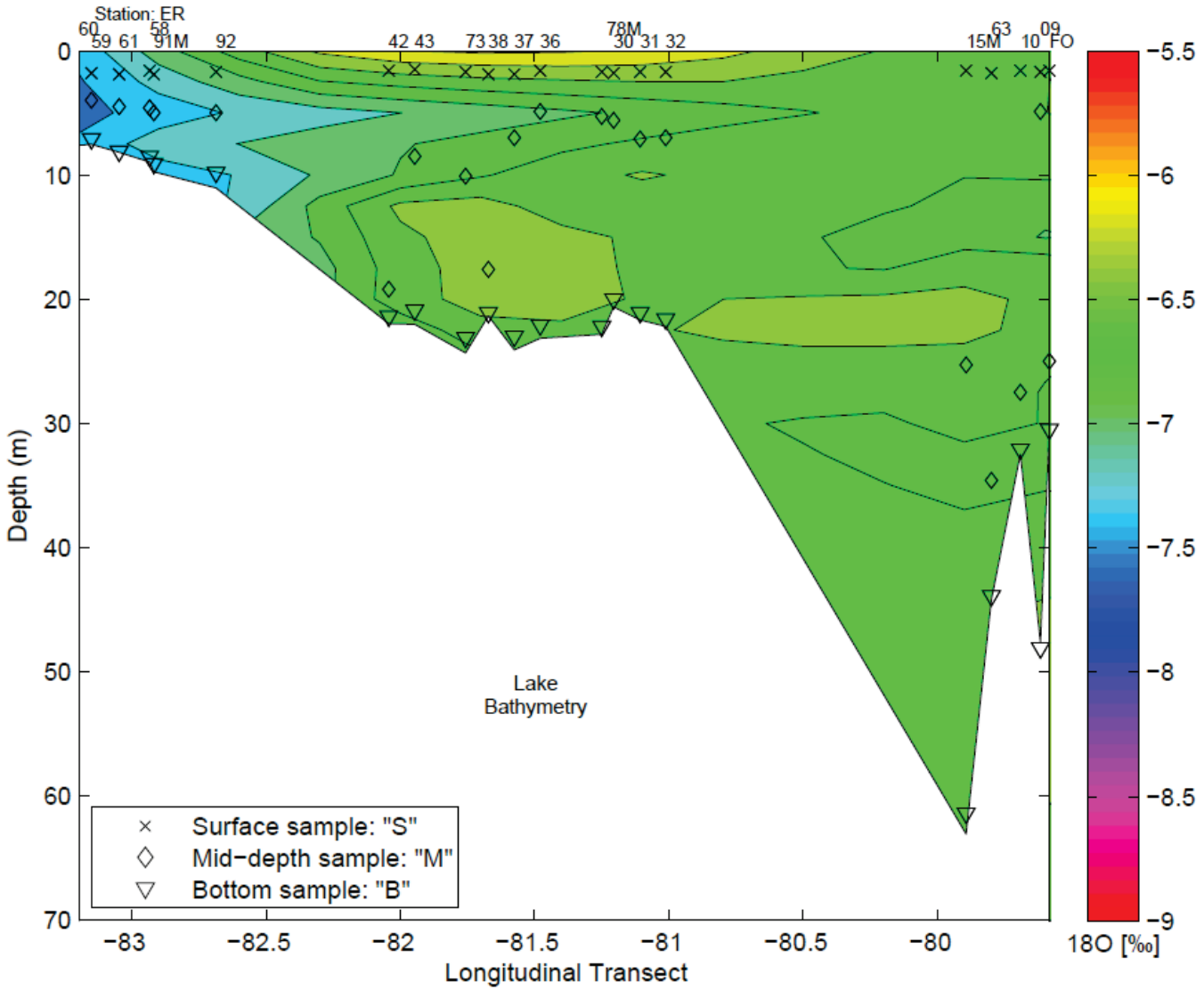
Station: ER
60
59 61
58
91M
92
42 43
73 38 37 36
78M
30 31 32
63
15M
09
10 FO
Depth (m)
0
10
20
30
40
50
60
70
Lake
Bathymetry
Surface sample: "S"
Mid−depth sample: "M"
Bottom sample: "B"
−83
−82.5
−82
−81.5
−81
−80.5
−80
Longitudinal Transect
−5.5
−6
−6.5
−7
−7.5
−8
−8.5
−9
18O [‰]

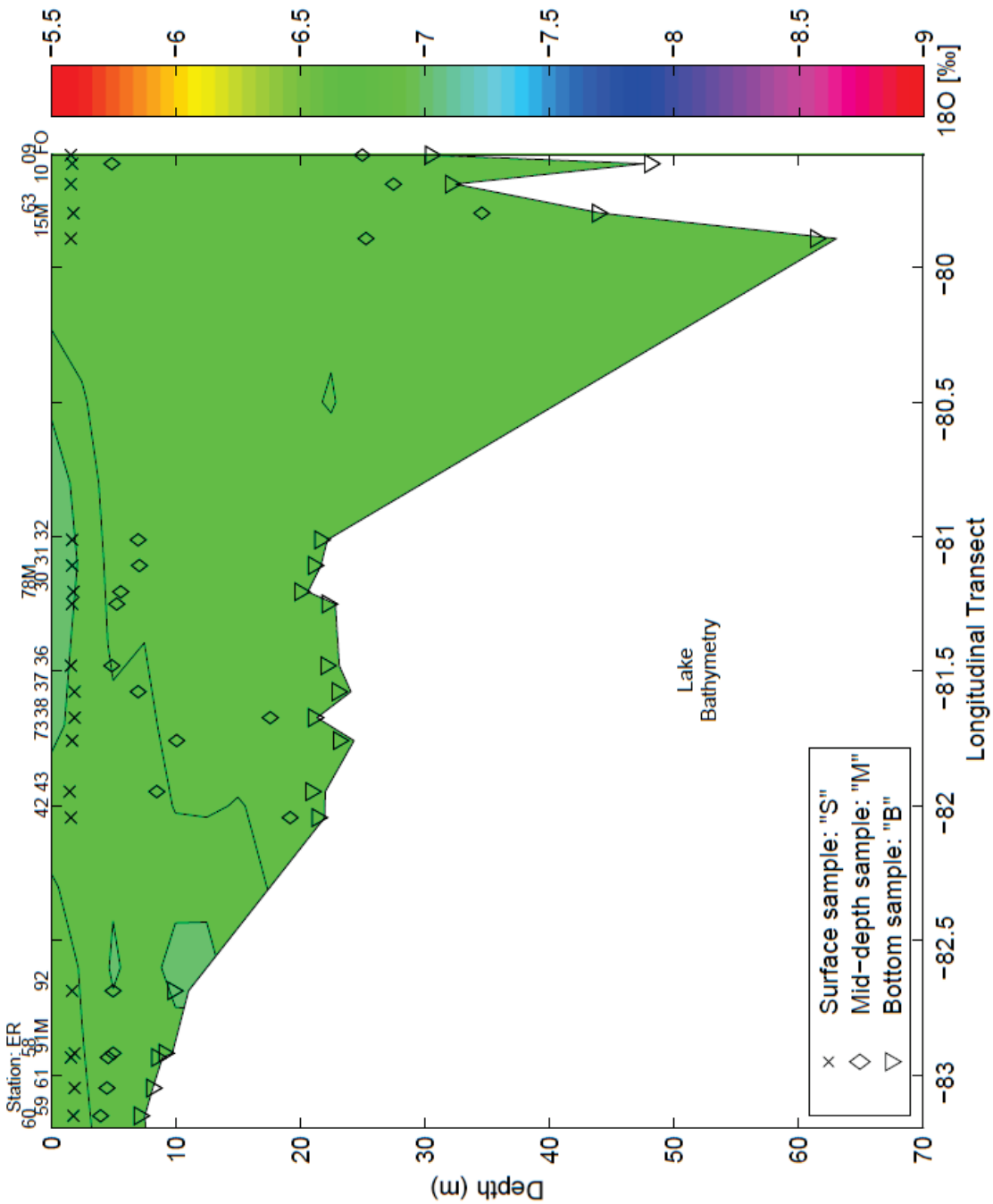
Station: ER
60 59 61 58 91M 92 42 43 73 38 37 36 78M 30 31 32 63 15M 10 09 FO
0
10
20
30
40
50
60
70
Depth (m)
−83
−82.5
−82
−81.5
−81
−80.5
−80
Longitudinal Transect
Surface sample: "S"
Mid−depth sample: "M"
Bottom sample: "B"
Lake
Bathymetry
−5.5
−6
−6.5
−7
−7.5
−8
−8.5
−9
18O [‰]

194

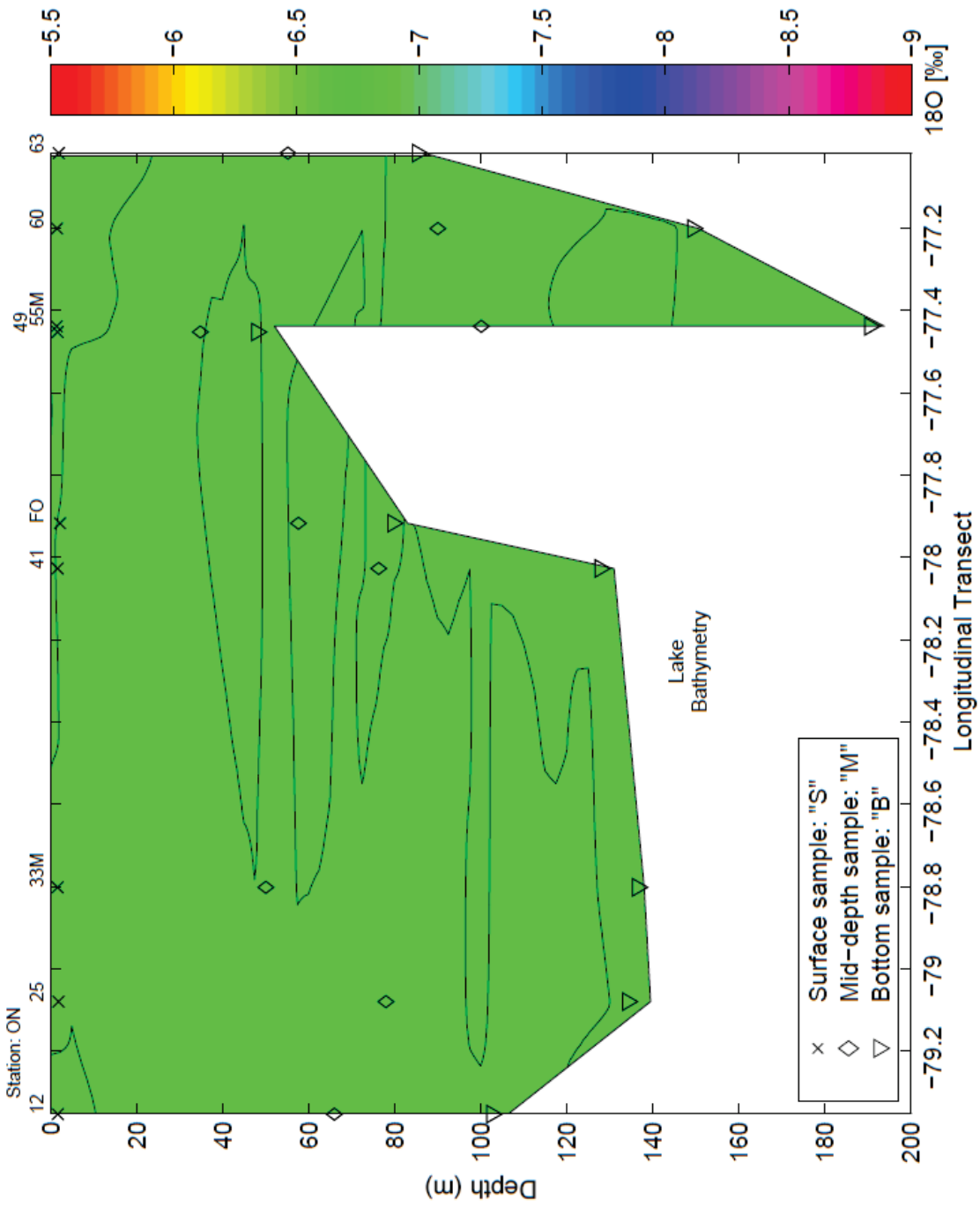
Station: ON
12
25
33M
41 FO
49
55M
60
63
Depth (m)
0
20
40
60
80
100
120
140
160
180
200
-79.2
-79
-78.8
-78.6
-78.4
-78.2
-78
-77.8
-77.6
-77.4
-77.2
Longitudinal Transect
Lake
Bathymetry
Surface sample: "S"
Mid-depth sample: "M"
Bottom sample: "B"
-5.5
-6
-6.5
-7
-7.5
-8
-8.5
-9
18O [‰]

195

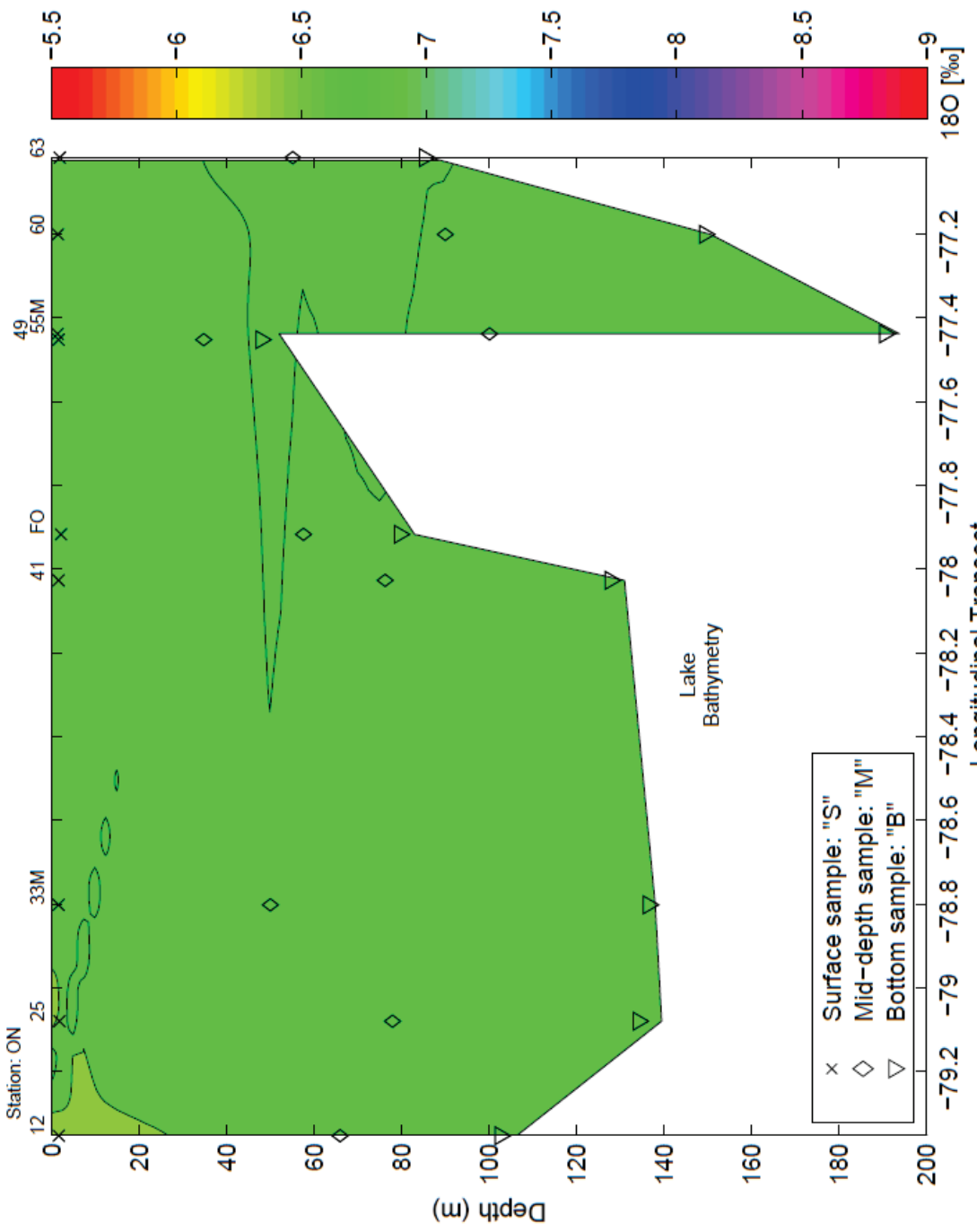
Station: ON
12
25
33M
41
FO
49
55M
60
63
Depth (m)
0
20
40
60
80
100
120
140
160
180
200
-79.2
-79
-78.8
-78.6
-78.4
-78.2
-78
-77.8
-77.6
-77.4
-77.2
Longitudinal Transect
Surface sample: "S"
Mid-depth sample: "M"
Bottom sample: "B"
Lake
Bathymetry
-5.5
-6
-6.5
-7
-7.5
-8
-8.5
-9
18O [‰]

196

Appendix C:
Contour plots – Temperature

In order, plots shown are:
- Lake Superior: Spring
- Lake Superior: Summer
- Lake Huron: Spring
- Lake Huron: Summer
- Lake Michigan: Spring
- Lake Michigan: Summer
- Lake Erie: Spring
- Lake Erie: Summer
- Lake Ontario: Spring
- Lake Ontario: Summer

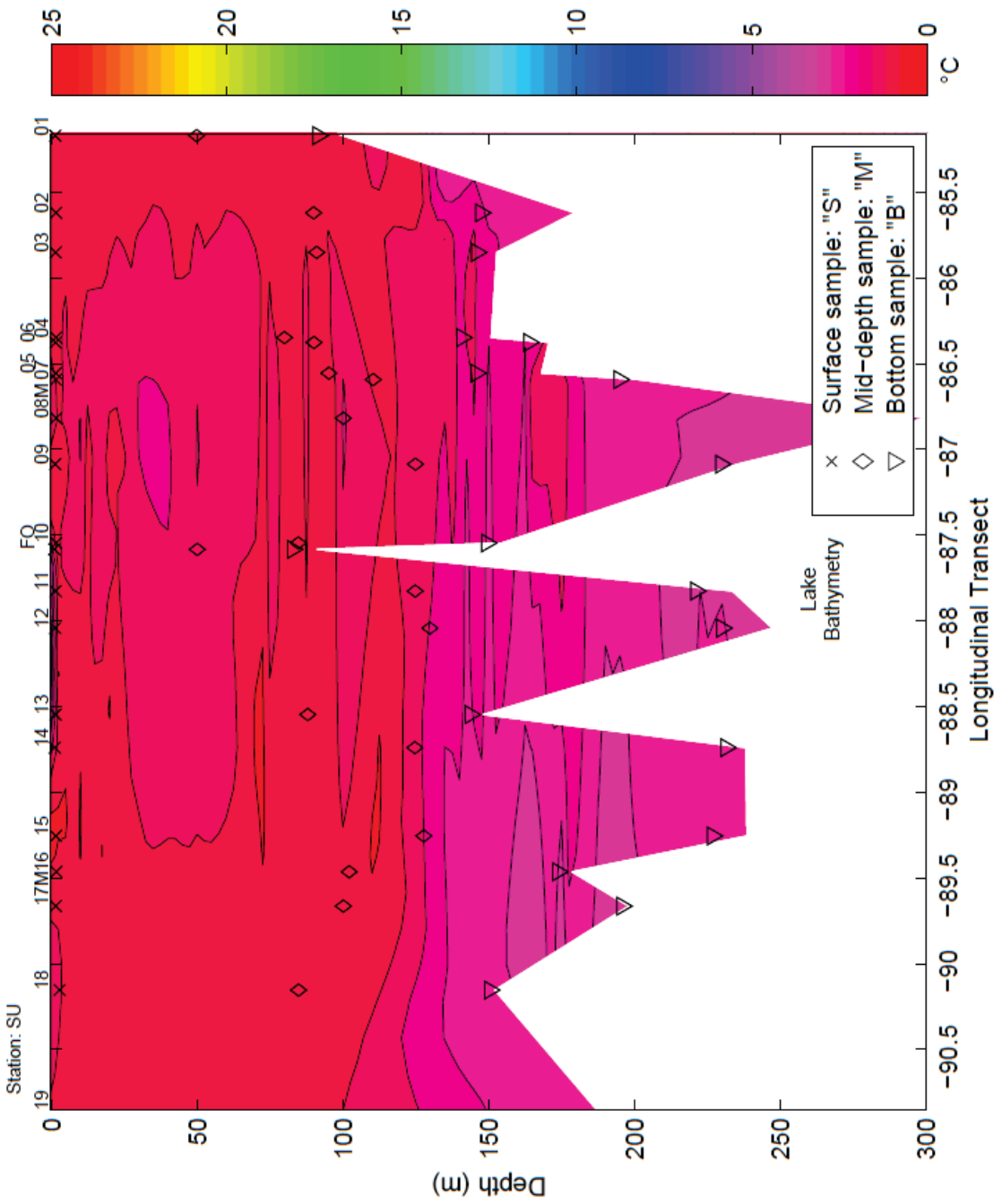
Station: SU
01
02
03
04
05
06
07
08M
09
FQ
10
11
12
13
14
15
17M16
18
19
Depth (m)
0
50
100
150
200
250
300
Lake
Bathymetry
Surface sample: "S"
Mid−depth sample: "M"
Bottom sample: "B"
−90.5
−90
−89.5
−89
−88.5
−88
−87.5
−87
−86.5
−86
−85.5
Longitudinal Transect
25
20
15
10
5
0
°C

198

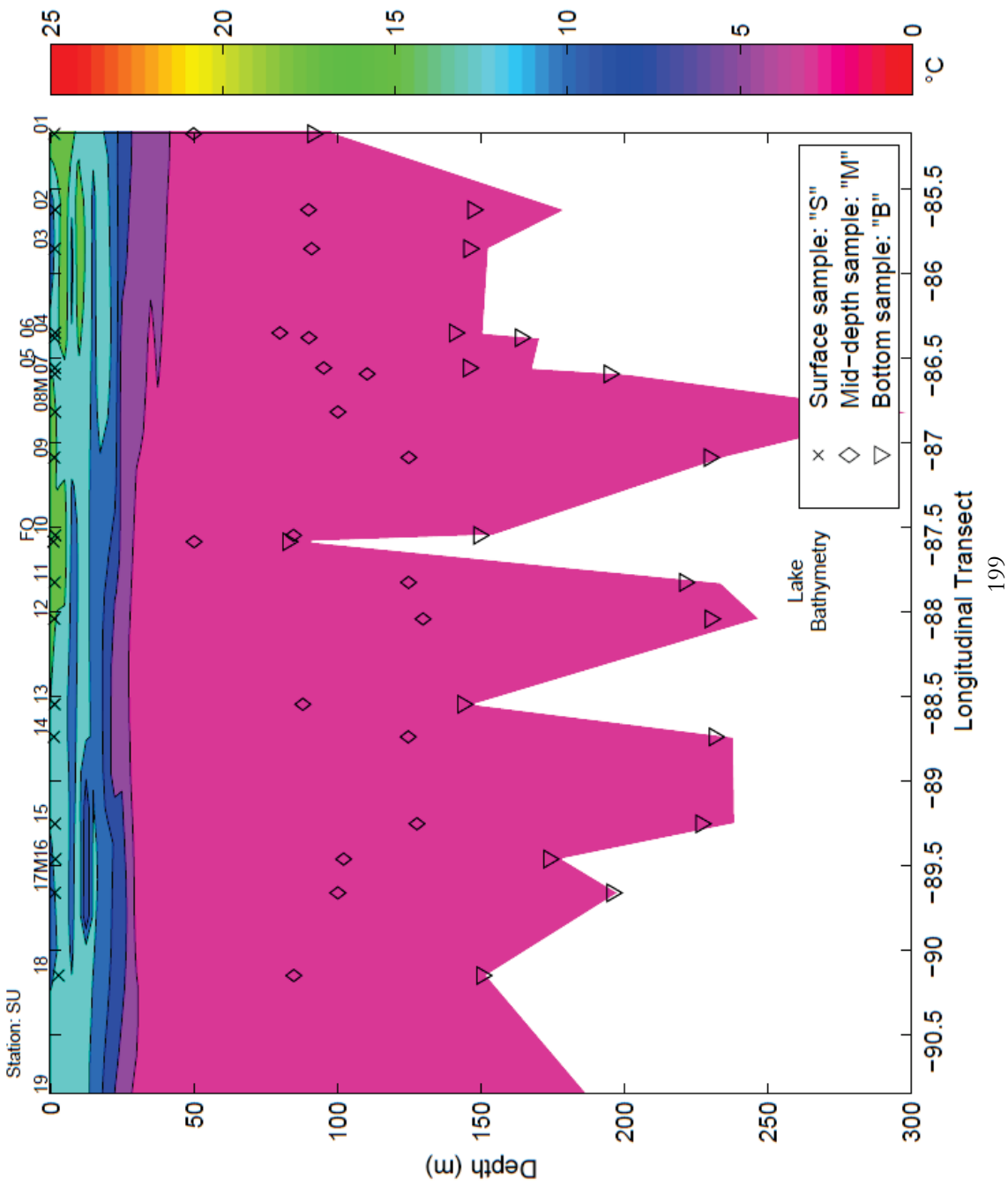
Station: SU
01
02
03
04
05
06
07
08M
09
10
FQ
11
12
13
14
15
16M17
18
19
0
50
100
150
200
250
300
Depth (m)
−90.5
−90
−89.5
−89
−88.5
−88
−87.5
−87
−86.5
−86
−85.5
Longitudinal Transect
Surface sample: "S"
Mid−depth sample: "M"
Bottom sample: "B"
Lake
Bathymetry
25
20
15
10
5
0
°C

199

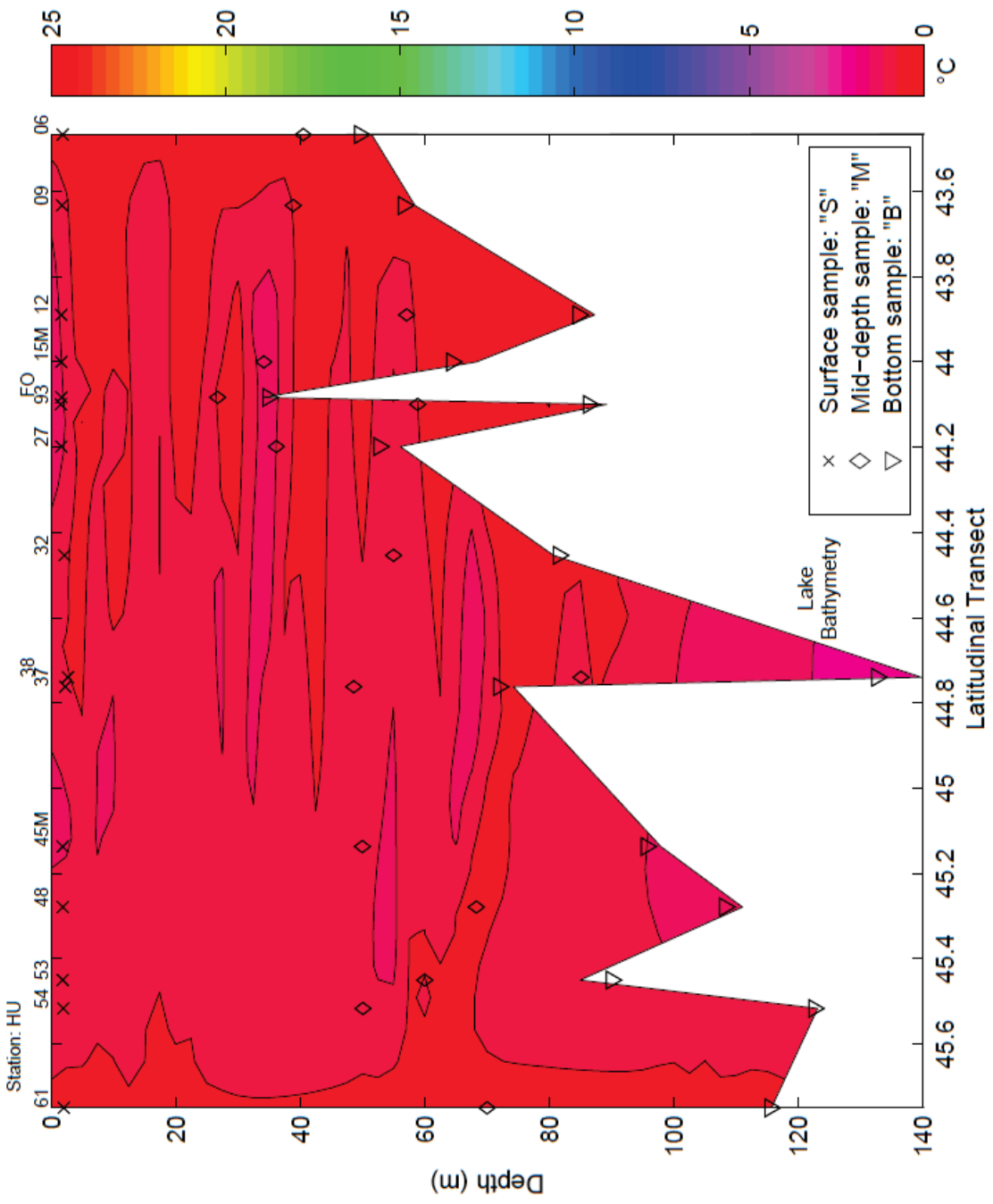
Station: HU
61
54
53
48
45M
38
37
32
27
FO
93
15M
12
09
06
Depth (m)
0
20
40
60
80
100
120
140
45.6
45.4
45.2
45
44.8
44.6
44.4
44.2
44
43.8
43.6
Latitudinal Transect
Lake
Bathymetry
Surface sample: "S"
Mid−depth sample: "M"
Bottom sample: "B"
25
20
15
10
5
0
°C

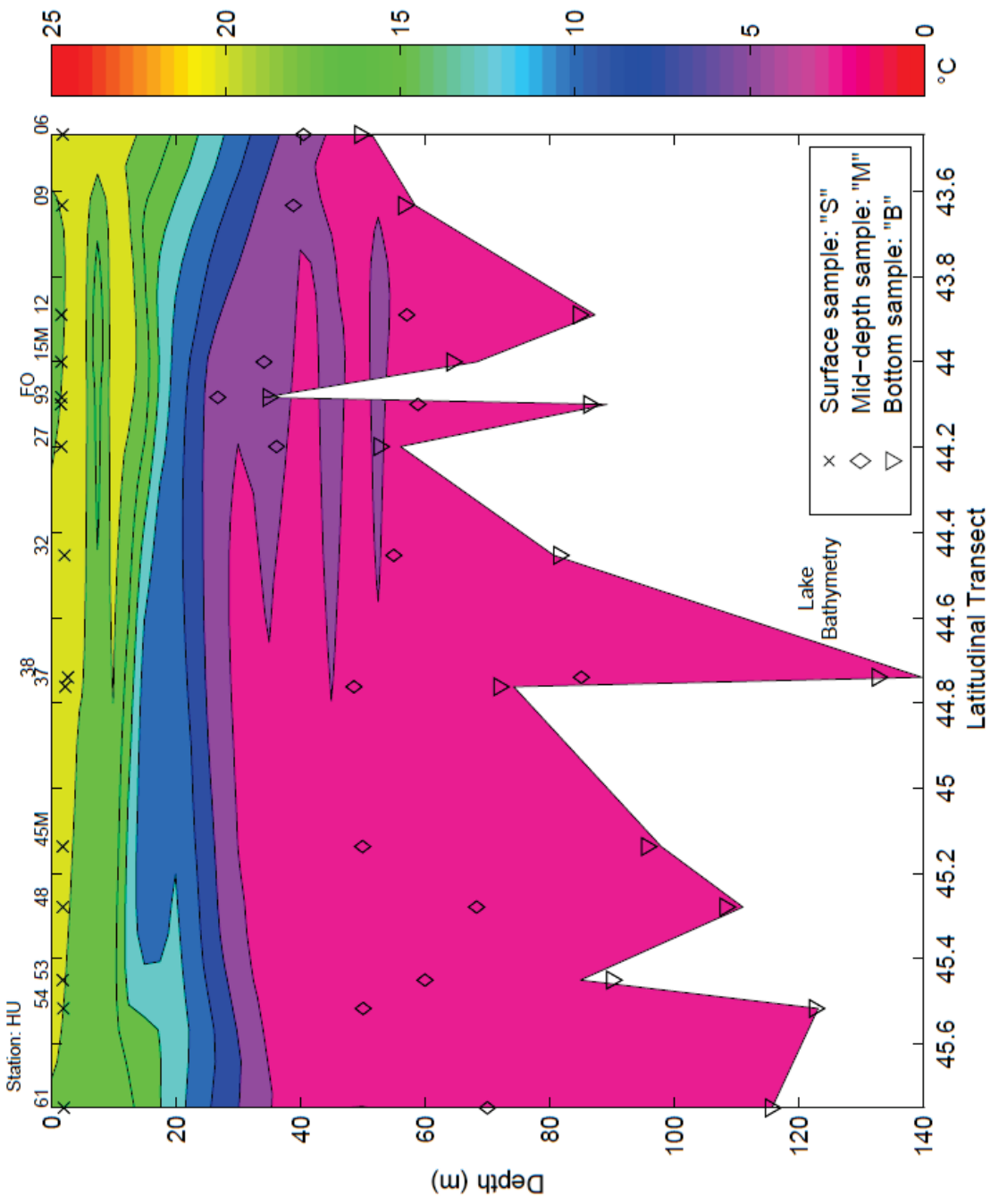
Station: HU
61
54
53
48
45M
38
37
32
27
93
FO
15M
12
09
06
Depth (m)
0
20
40
60
80
100
120
140
45.6
45.4
45.2
45
44.8
44.6
44.4
44.2
44
43.8
43.6
Latitudinal Transect
Lake
Bathymetry
Surface sample: "S"
Mid−depth sample: "M"
Bottom sample: "B"
25
20
15
10
5
0
°C

201

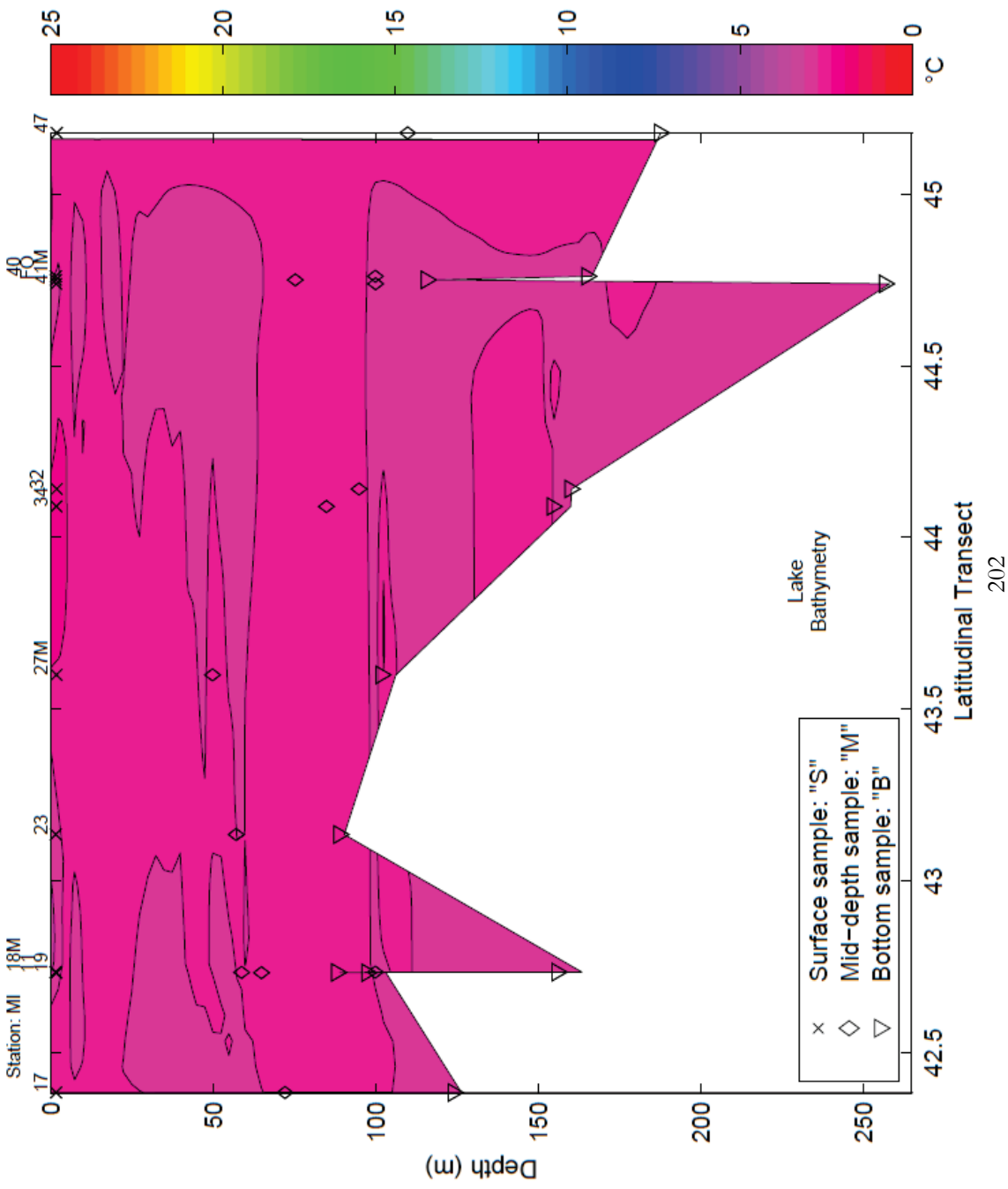
Station: MI
17
18M
19
23
27M
32
34
40
41M
47
0
50
100
150
200
250
Depth (m)
42.5
43
43.5
44
44.5
45
Latitudinal Transect
Surface sample: "S"
Mid−depth sample: "M"
Bottom sample: "B"
Lake
Bathymetry
25
20
15
10
5
0
°C

202

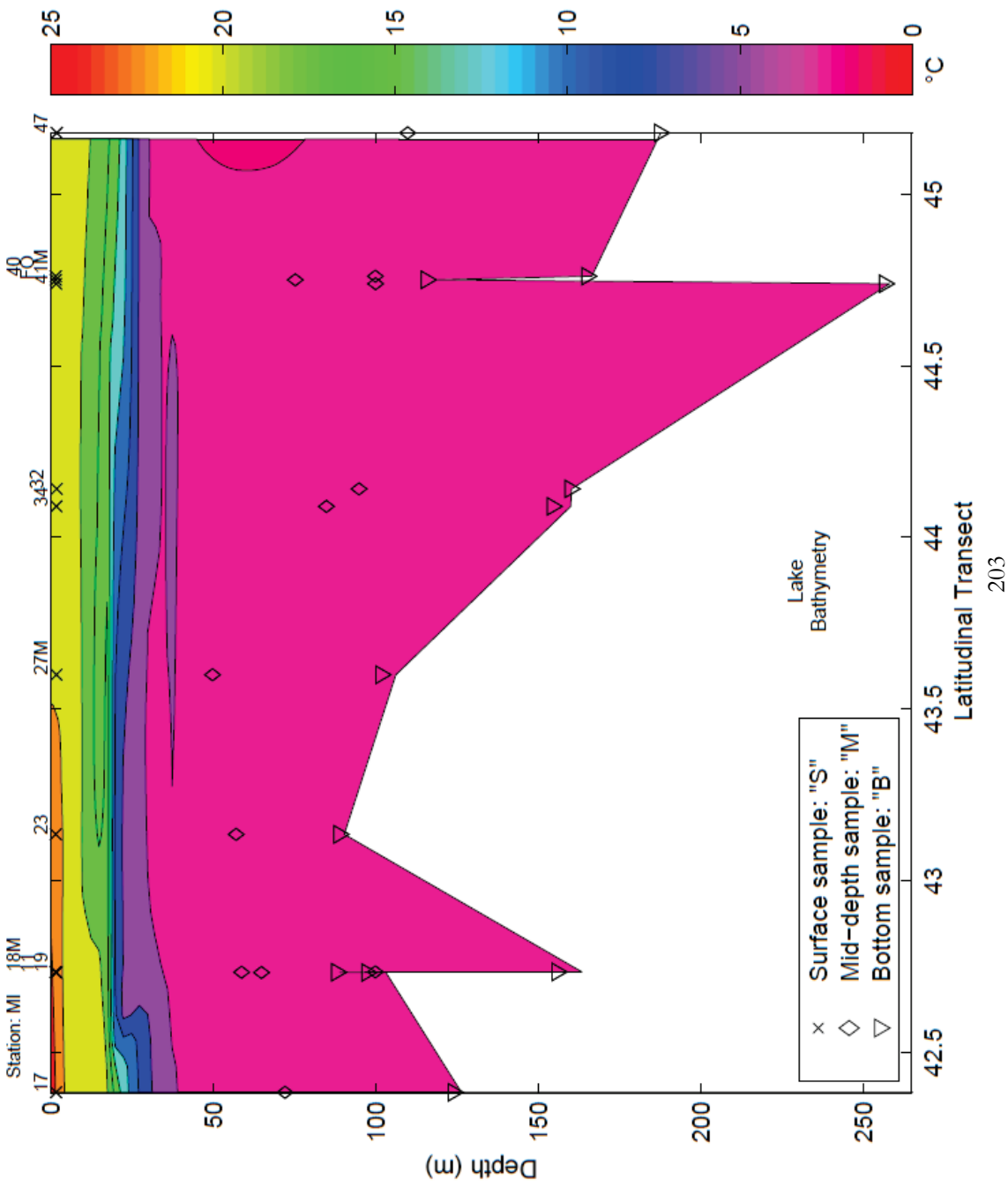
Station: MI
17
18M
19
23
27M
32
34
40
41M
47
0
50
100
150
200
250
Depth (m)
42.5
43
43.5
44
44.5
45
Latitudinal Transect
Surface sample: "S"
Mid-depth sample: "M"
Bottom sample: "B"
Lake
Bathymetry
25
20
15
10
5
0
°C

203

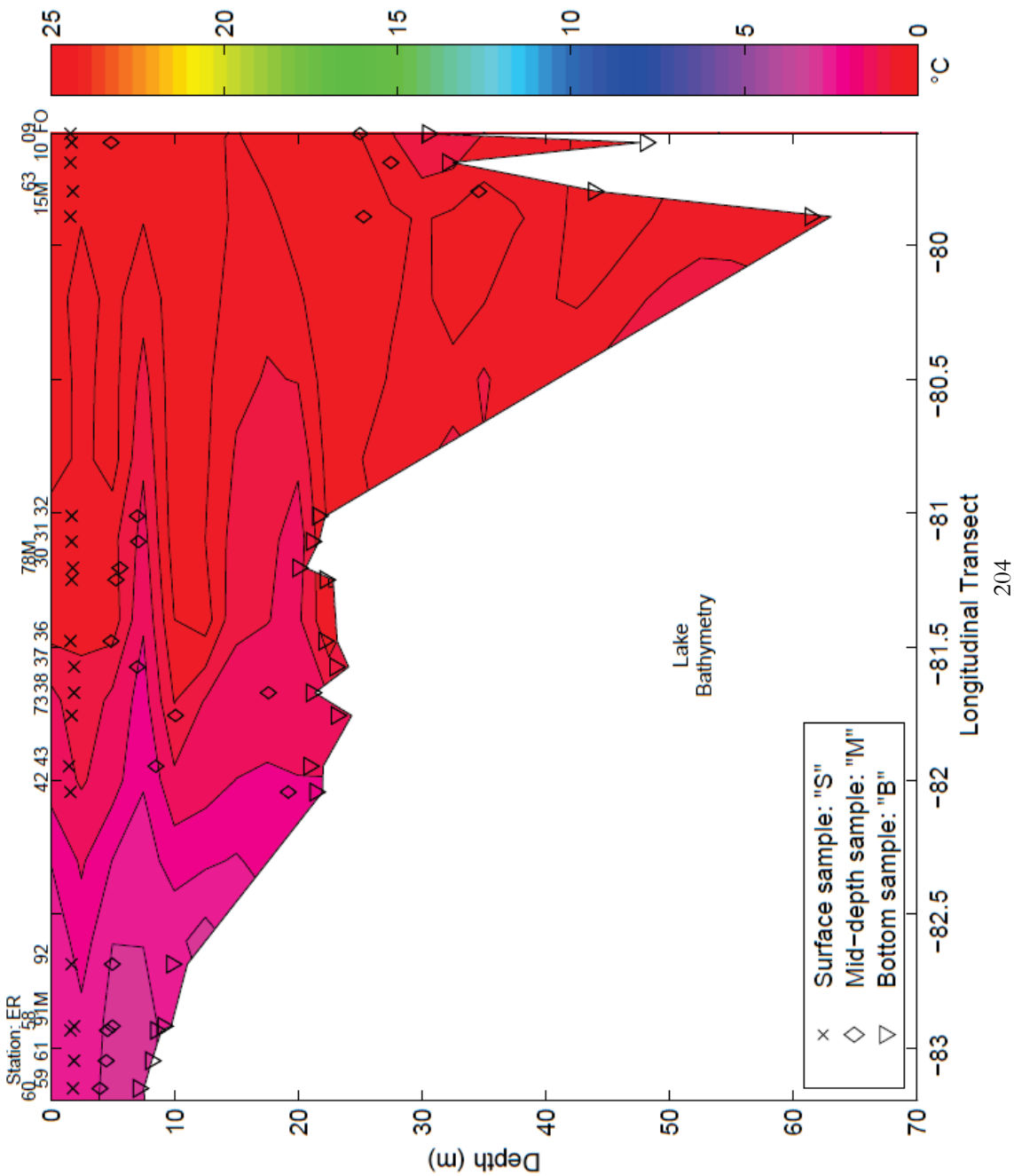
Station: ER
60 59 61 58 91M 92 42 43 73 38 37 36 78M 30 31 32 63 15M 10 09 FO
Surface sample: "S"
Mid-depth sample: "M"
Bottom sample: "B"
Lake
Bathymetry
Depth (m)
Longitudinal Transect
°C

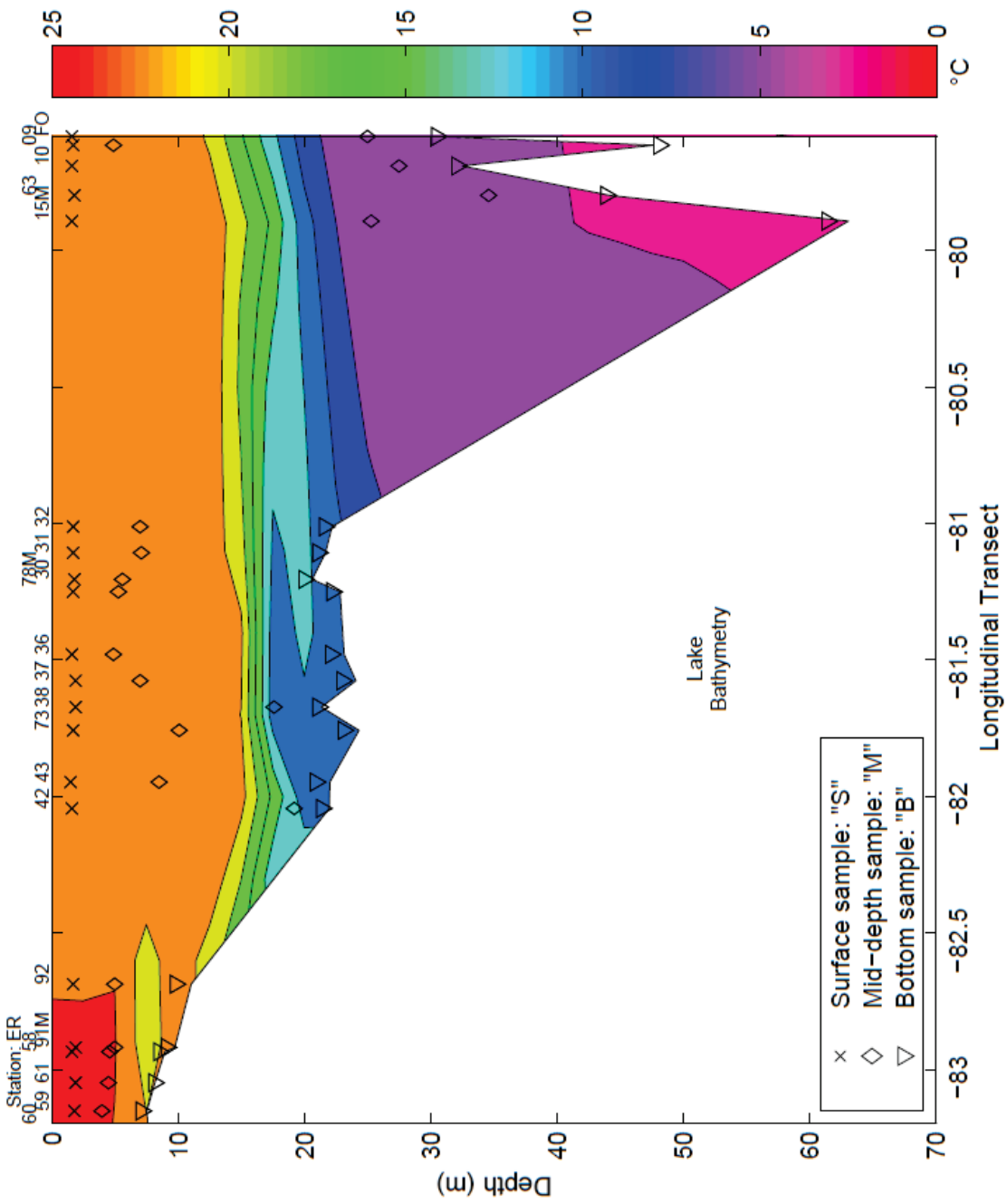
Station: ER
60 59 61 58 91M 92 42 43 73 38 37 36 78M 30 31 32 63 15M 10 09 PO
Depth (m)
0 10 20 30 40 50 60 70
−83 −82.5 −82 −81.5 −81 −80.5 −80
Longitudinal Transect
Lake
Bathymetry
Surface sample: "S"
Mid−depth sample: "M"
Bottom sample: "B"
°C
0 5 10 15 20 25

205

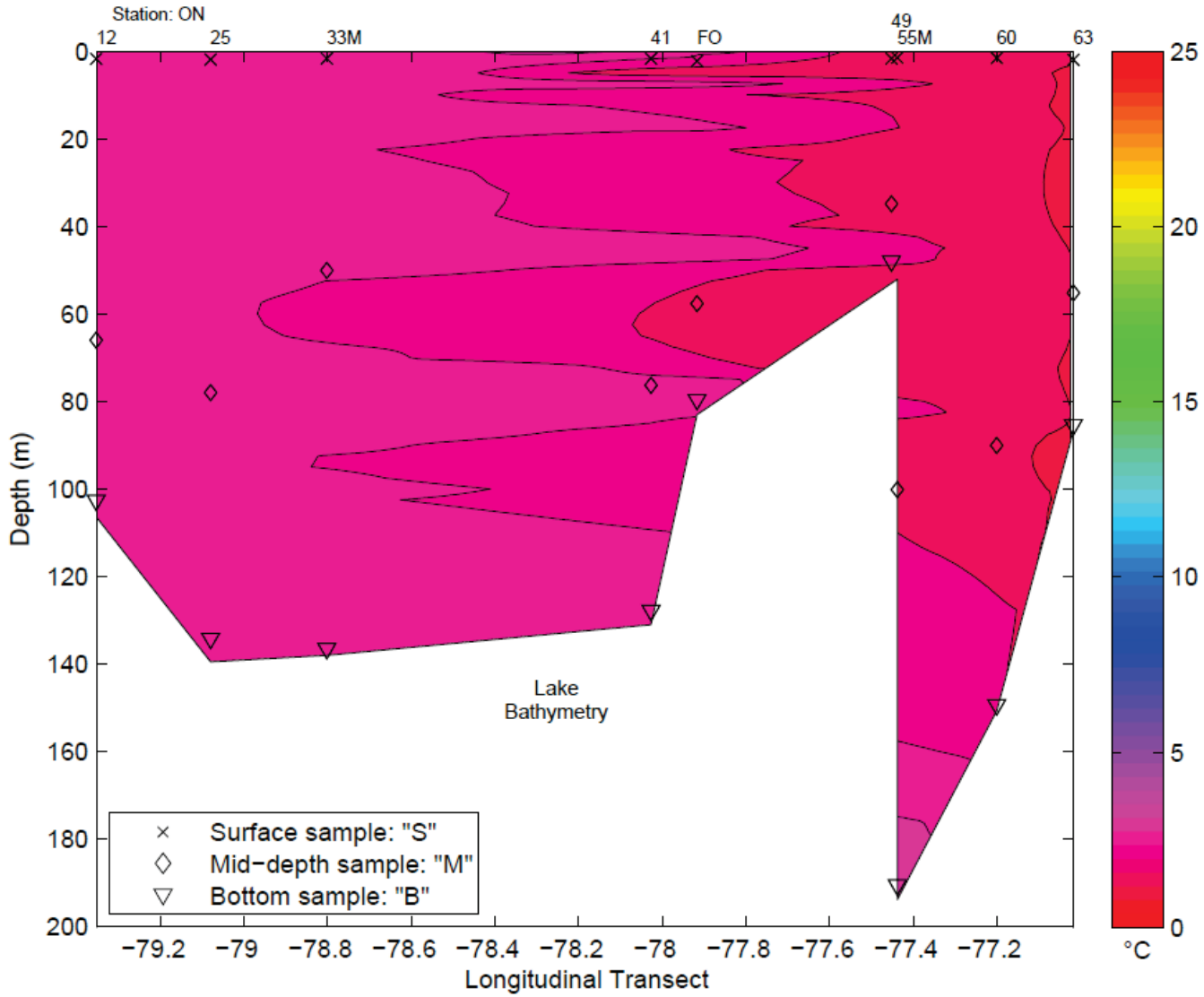
Station: ON
12
25
33M
41
FO
49
55M
60
63
Depth (m)
0
20
40
60
80
100
120
140
160
180
200
Lake
Bathymetry
Surface sample: "S"
Mid−depth sample: "M"
Bottom sample: "B"
−79.2
−79
−78.8
−78.6
−78.4
−78.2
−78
−77.8
−77.6
−77.4
−77.2
Longitudinal Transect
25
20
15
10
5
0
°C

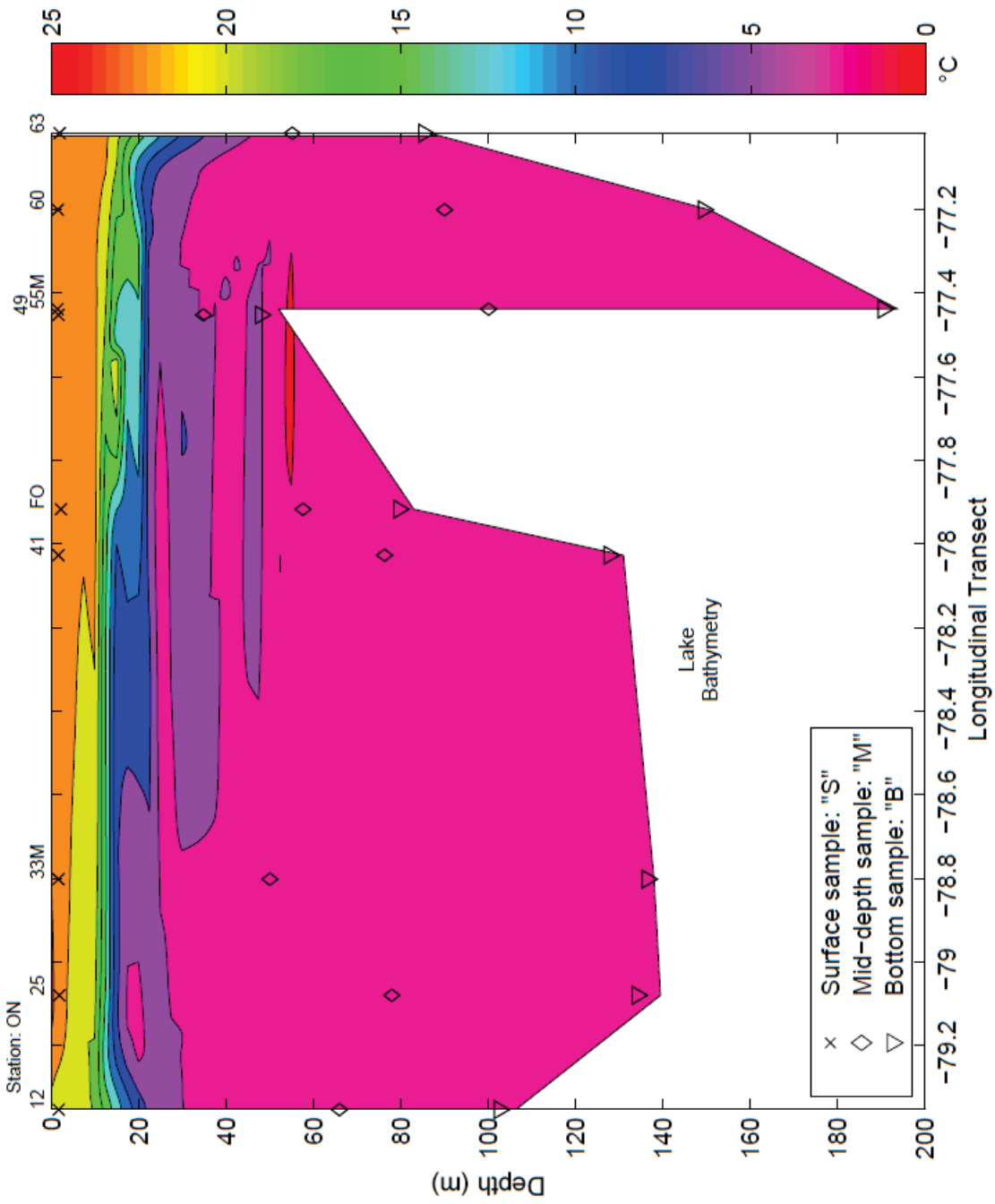
Station: ON
12
25
33M
41
FO
49
55M
60
63
Depth (m)
0
20
40
60
80
100
120
140
160
180
200
-79.2
-79
-78.8
-78.6
-78.4
-78.2
-78
-77.8
-77.6
-77.4
-77.2
Longitudinal Transect
Lake
Bathymetry
Surface sample: "S"
Mid-depth sample: "M"
Bottom sample: "B"
25
20
15
10
5
0
°C

207

Appendix D:

Contour plots – Chloride concentration

In order, plots shown are:
- Lake Superior: Spring
- Lake Superior: Summer
- Lake Huron: Spring
- Lake Huron: Summer
- Lake Michigan: Spring
- Lake Michigan: Summer
- Lake Erie: Spring
- Lake Erie: Summer
- Lake Ontario: Spring
- Lake Ontario: Summer

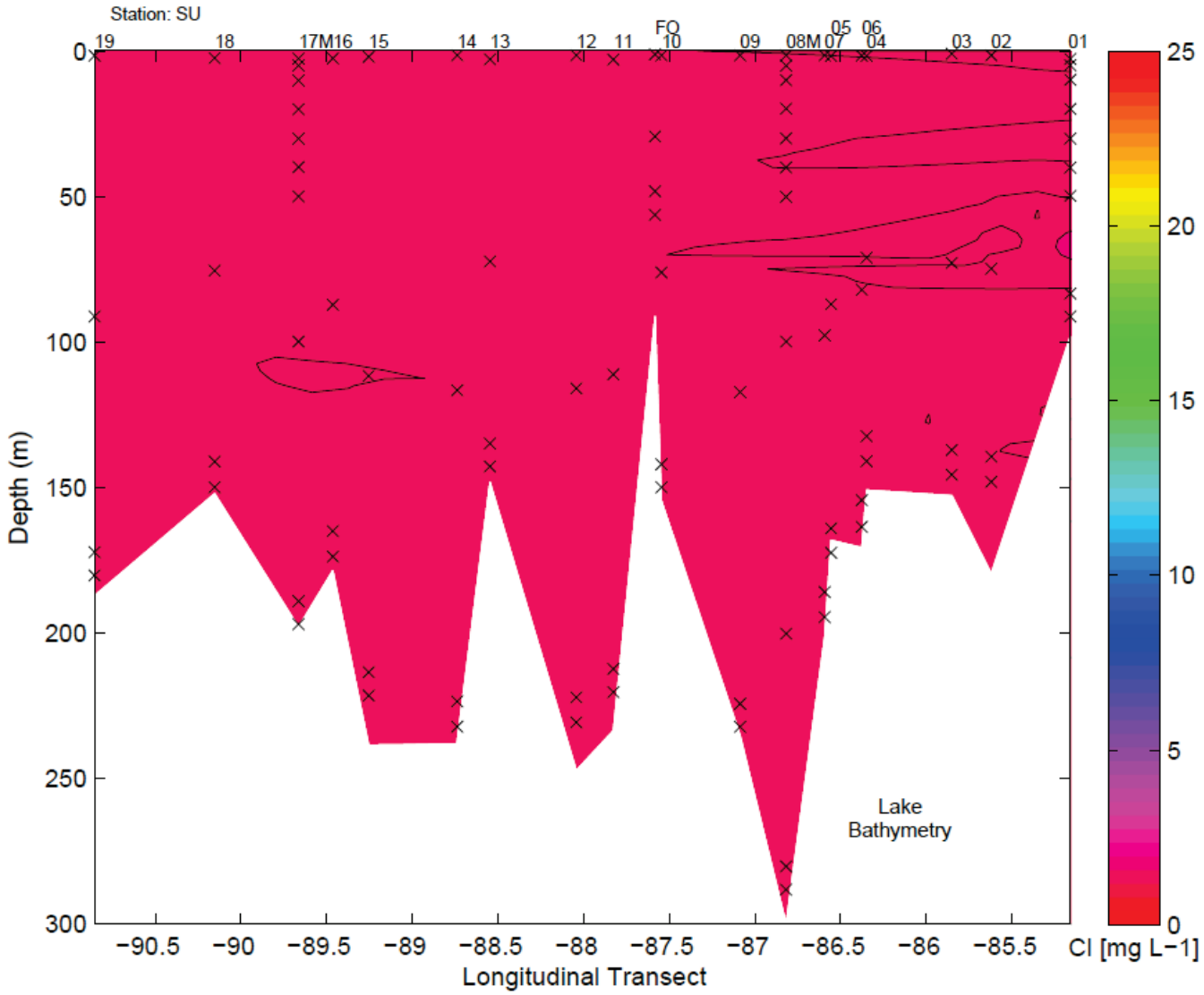
Station: SU
19
18
17M
16
15
14
13
12
11
FQ
10
09
08M
05
06
07
04
03
02
01
0
50
100
150
200
250
300
Depth (m)
−90.5
−90
−89.5
−89
−88.5
−88
−87.5
−87
−86.5
−86
−85.5
Longitudinal Transect
Lake
Bathymetry
25
20
15
10
5
0
Cl [mg L−1]

209

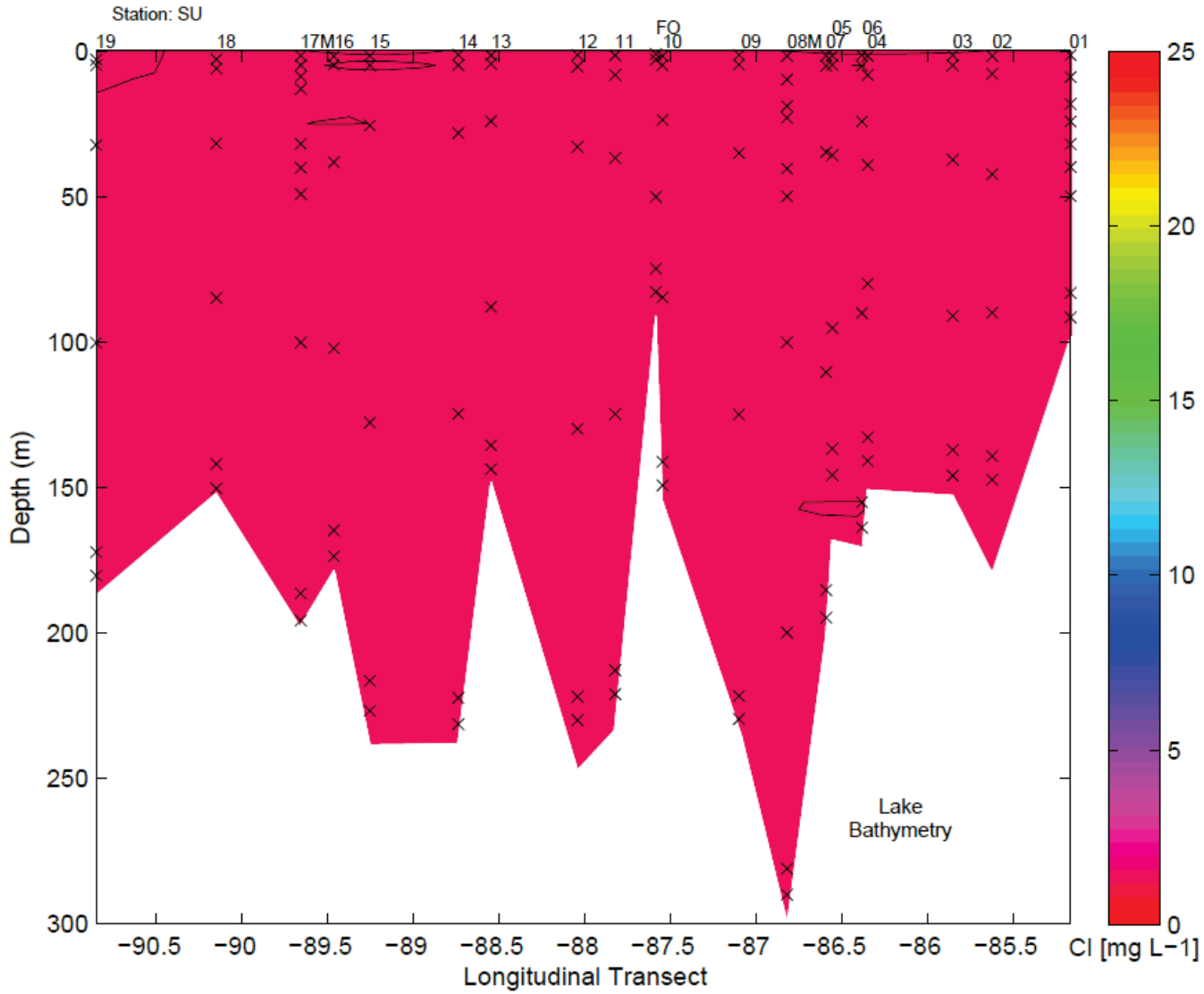
Station: SU
19
18
17M
16
15
14
13
12
11
FQ
10
09
08M
07
05
06
04
03
02
01
0
50
100
150
200
250
300
Depth (m)
−90.5
−90
−89.5
−89
−88.5
−88
−87.5
−87
−86.5
−86
−85.5
Longitudinal Transect
Lake
Bathymetry
25
20
15
10
5
0
Cl [mg L−1]

210

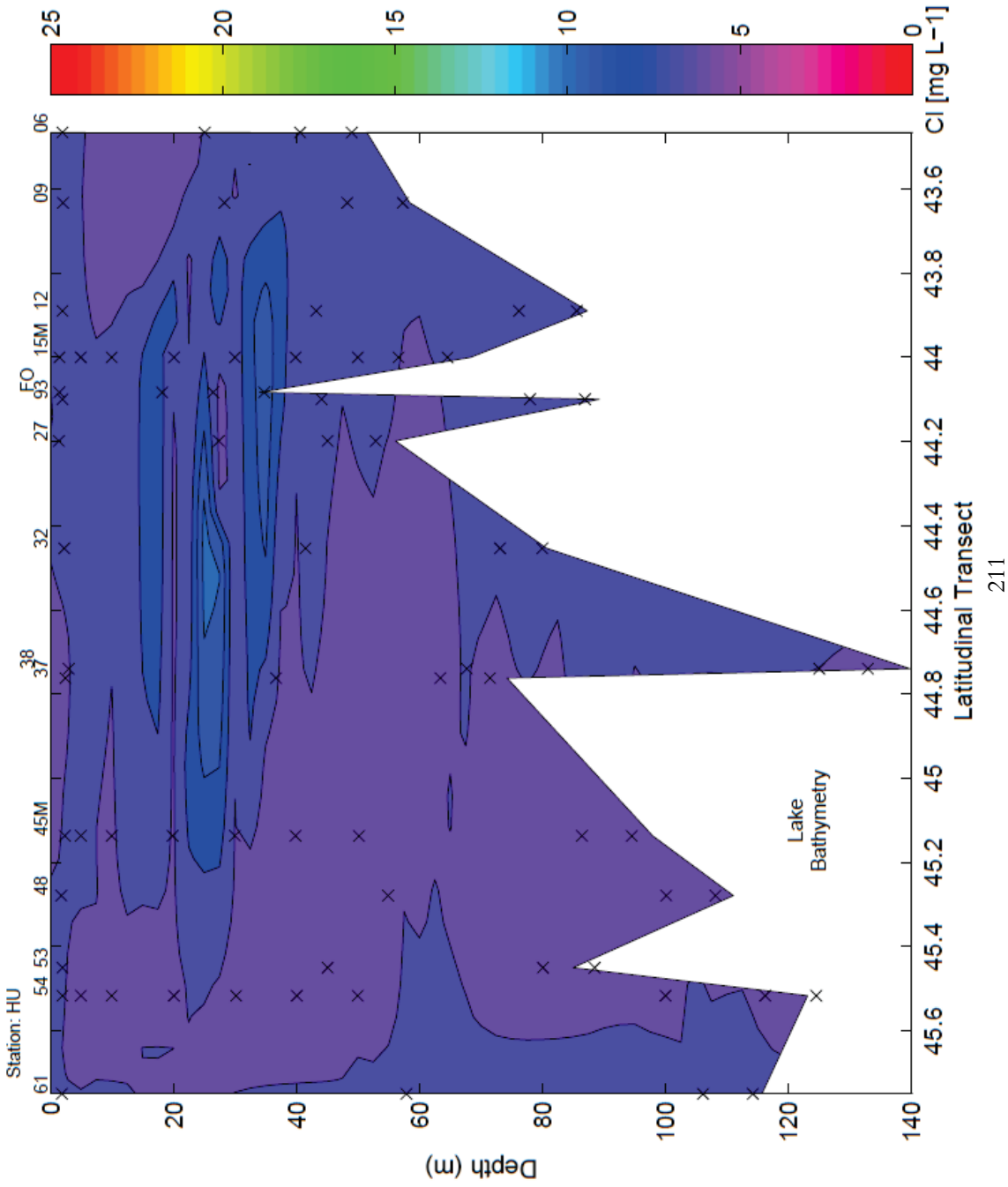
Cl [mg L−1]
25
20
15
10
5
0
Depth (m)
0
20
40
60
80
100
120
140
Latitudinal Transect
45.6
45.4
45.2
45
44.8
44.6
44.4
44.2
44
43.8
43.6
Station: HU
61
54
53
48
45M
38
37
32
27
93
FO
15M
12
09
06
Lake
Bathymetry

211

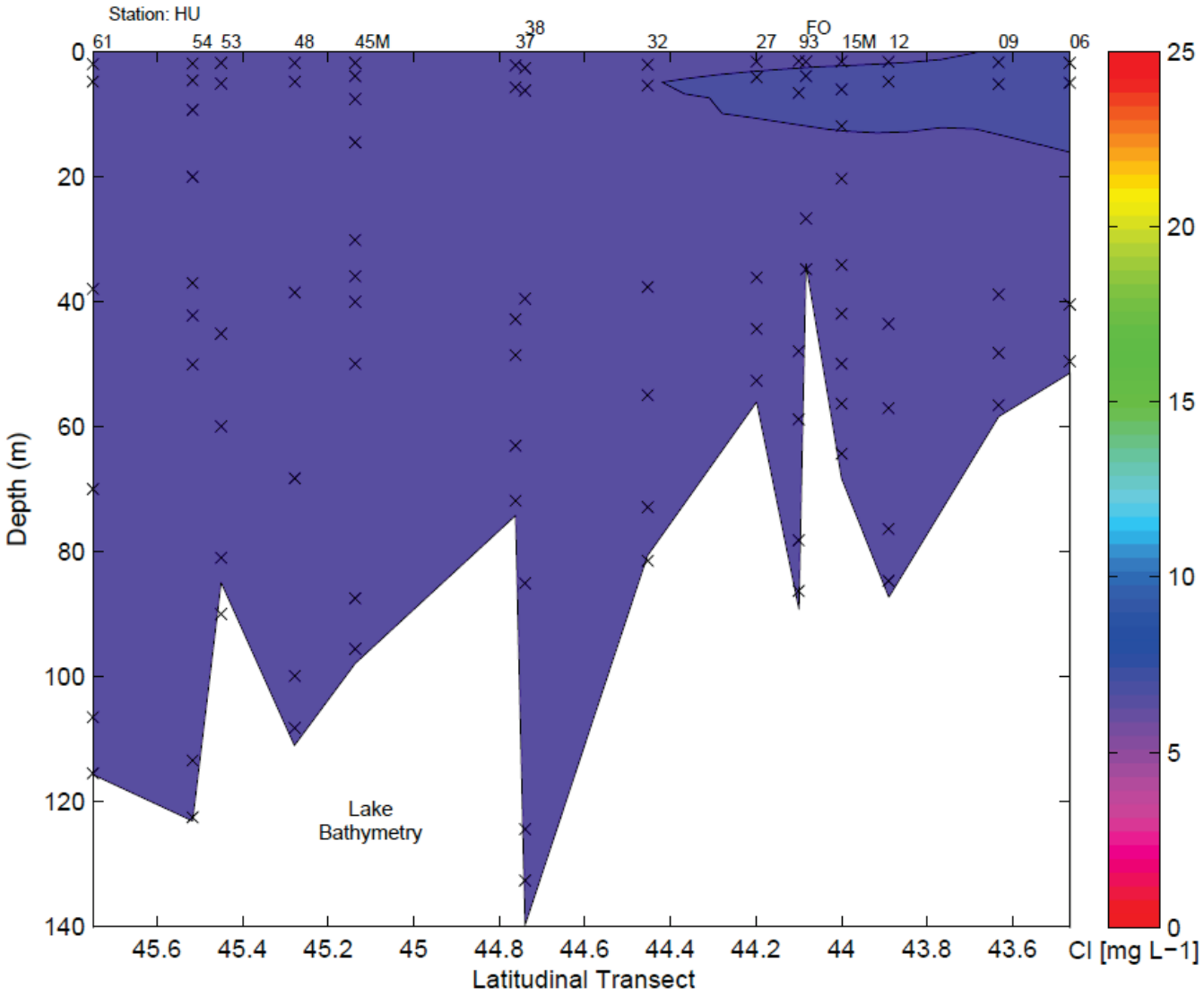
Station: HU
61
54
53
48
45M
38
37
32
FO
27
93
15M
12
09
06
0
20
40
60
80
100
120
140
Depth (m)
Lake
Bathymetry
45.6
45.4
45.2
45
44.8
44.6
44.4
44.2
44
43.8
43.6
Latitudinal Transect
25
20
15
10
5
0
Cl [mg L−1]

212

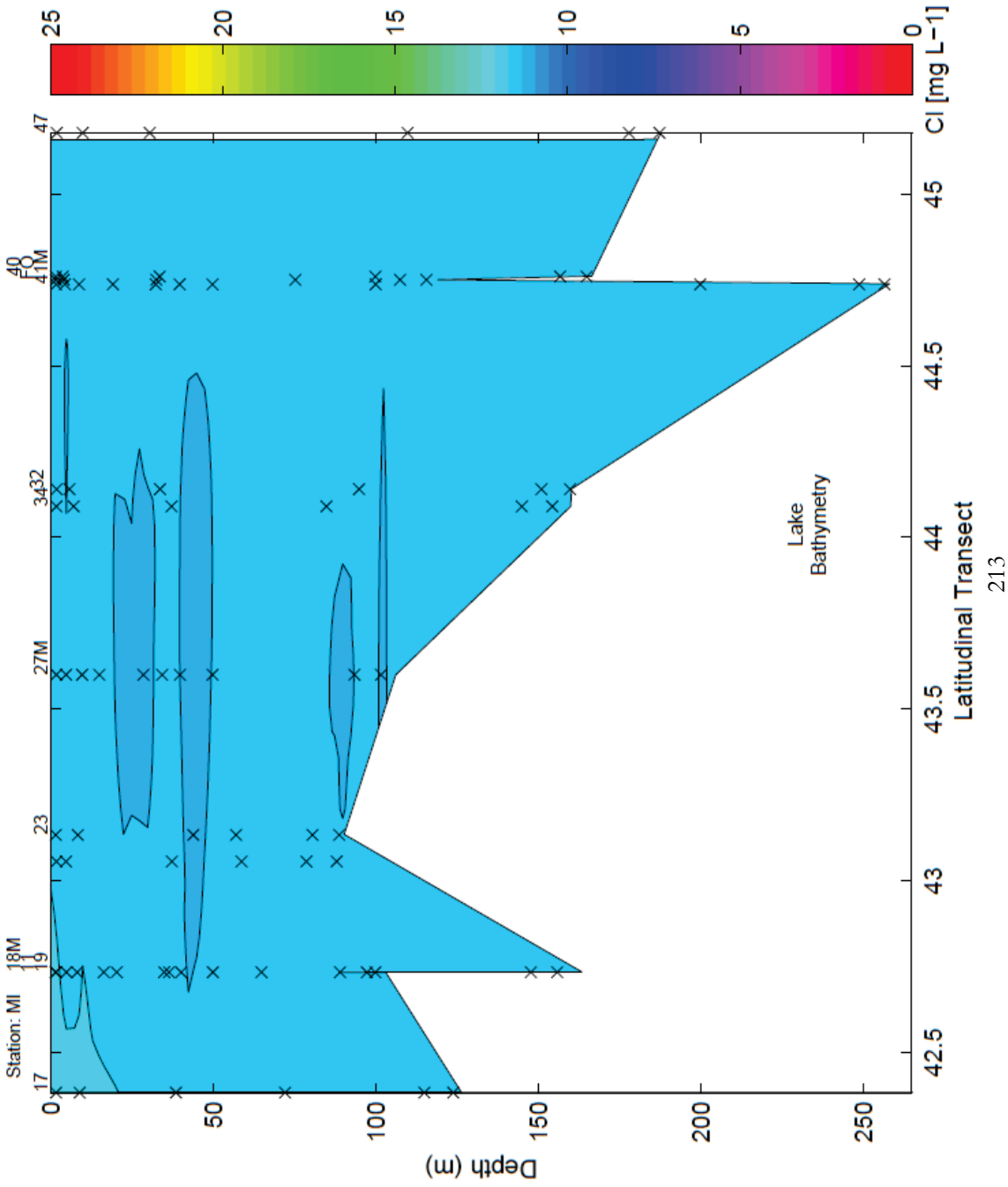
Cl [mg L−1]
25
20
15
10
5
0
Depth (m)
0
50
100
150
200
250
Latitudinal Transect
42.5
43
43.5
44
44.5
45
Lake
Bathymetry
Station: MI
17
19
18M
23
27M
32
34
40
41M
47

213

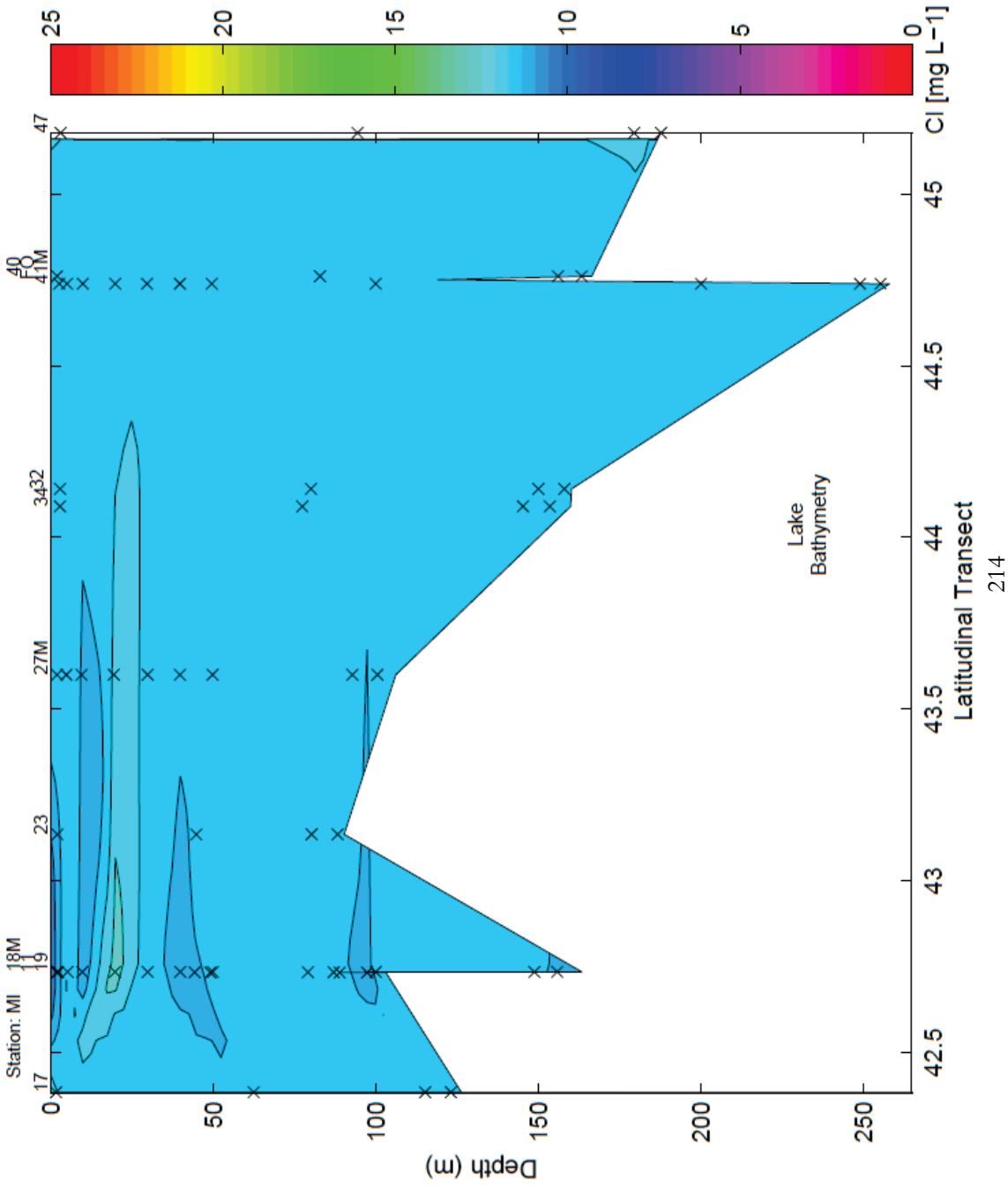
Cl [mg L−1]
25
20
15
10
5
0
Depth (m)
0
50
100
150
200
250
Latitudinal Transect
42.5
43
43.5
44
44.5
45
Lake
Bathymetry
Station: MI
17
18M
19
23
27M
32
34
40
41M
47

214

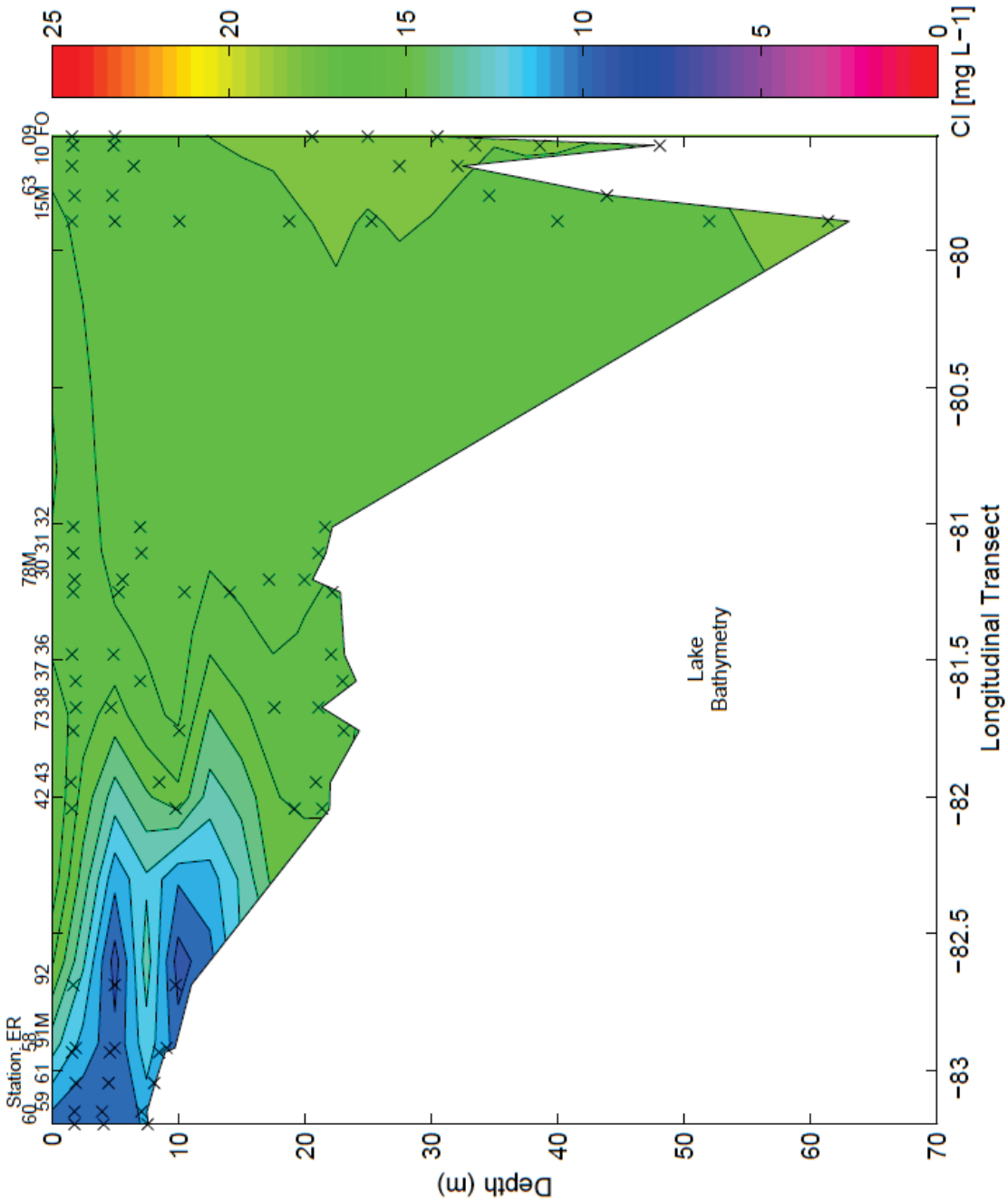
Cl [mg L−1]
25
20
15
10
5
0
Depth (m)
0
10
20
30
40
50
60
70
−83
−82.5
−82
−81.5
−81
−80.5
−80
Longitudinal Transect
Lake
Bathymetry
Station: ER
59 61 60 91M 58 92 42 43 73 38 37 36 78M 30 31 32 15M 63 10 09 FO

215

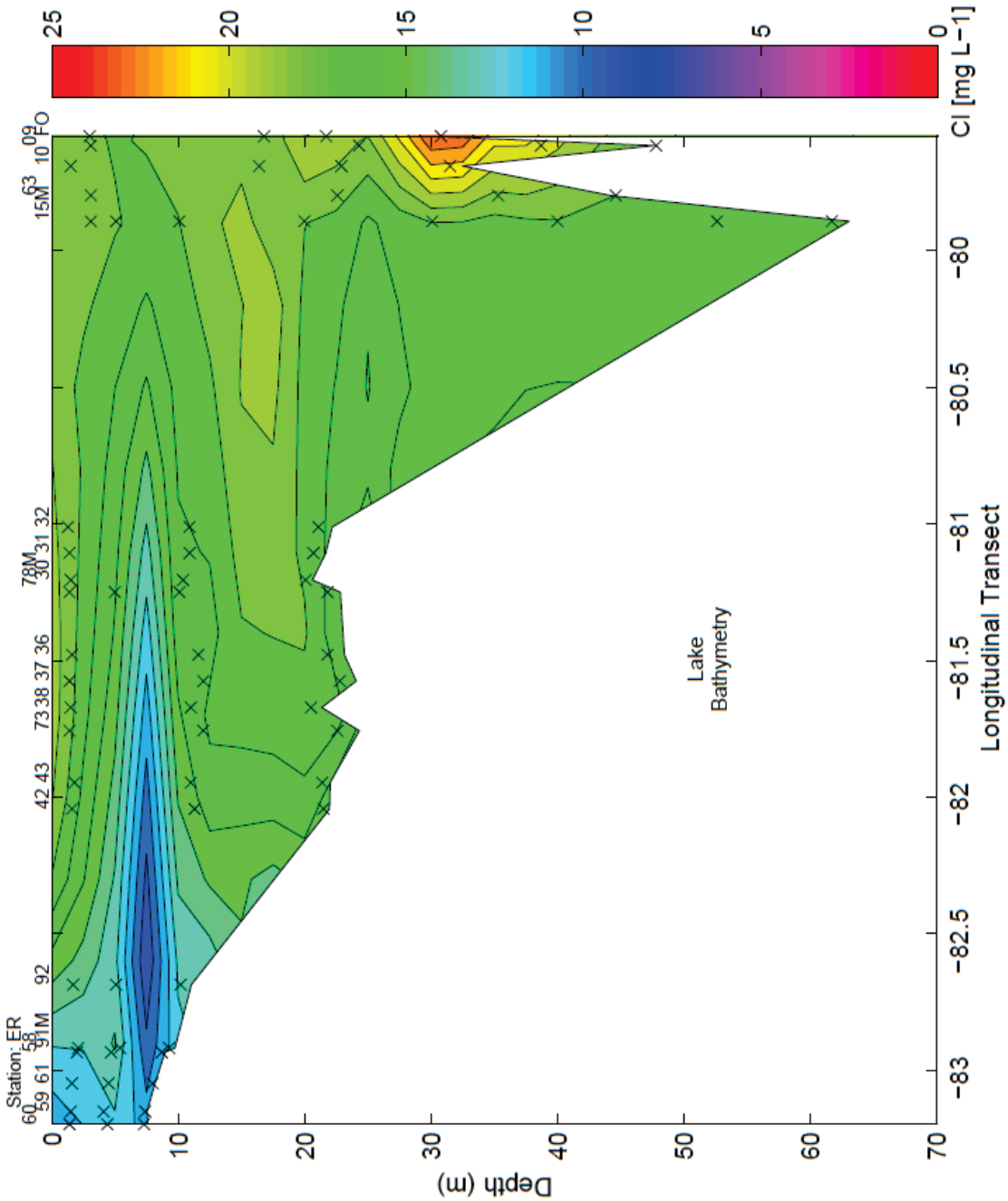
Cl [mg L−1]
25
20
15
10
5
0
Depth (m)
0
10
20
30
40
50
60
70
−83
−82.5
−82
−81.5
−81
−80.5
−80
Longitudinal Transect
Lake
Bathymetry
Station: ER
60 59 61 58 91M 92 42 43 73 38 37 36 78M 30 31 32 63 15M 10 09 FO

216

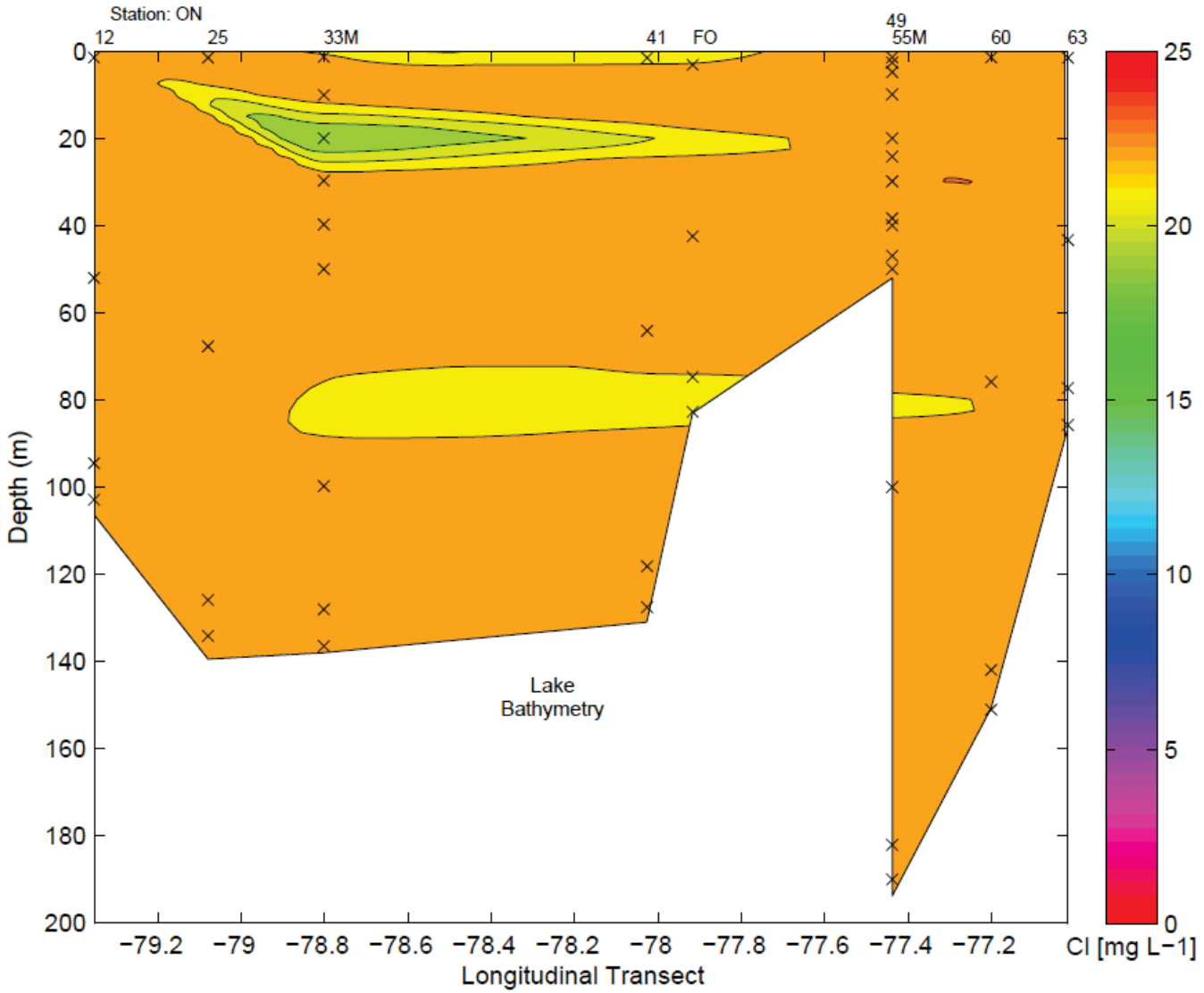
Station: ON
12
25
33M
41
FO
49
55M
60
63
0
20
40
60
80
100
120
140
160
180
200
Depth (m)
Lake
Bathymetry
−79.2
−79
−78.8
−78.6
−78.4
−78.2
−78
−77.8
−77.6
−77.4
−77.2
Longitudinal Transect
25
20
15
10
5
0
Cl [mg L−1]

217

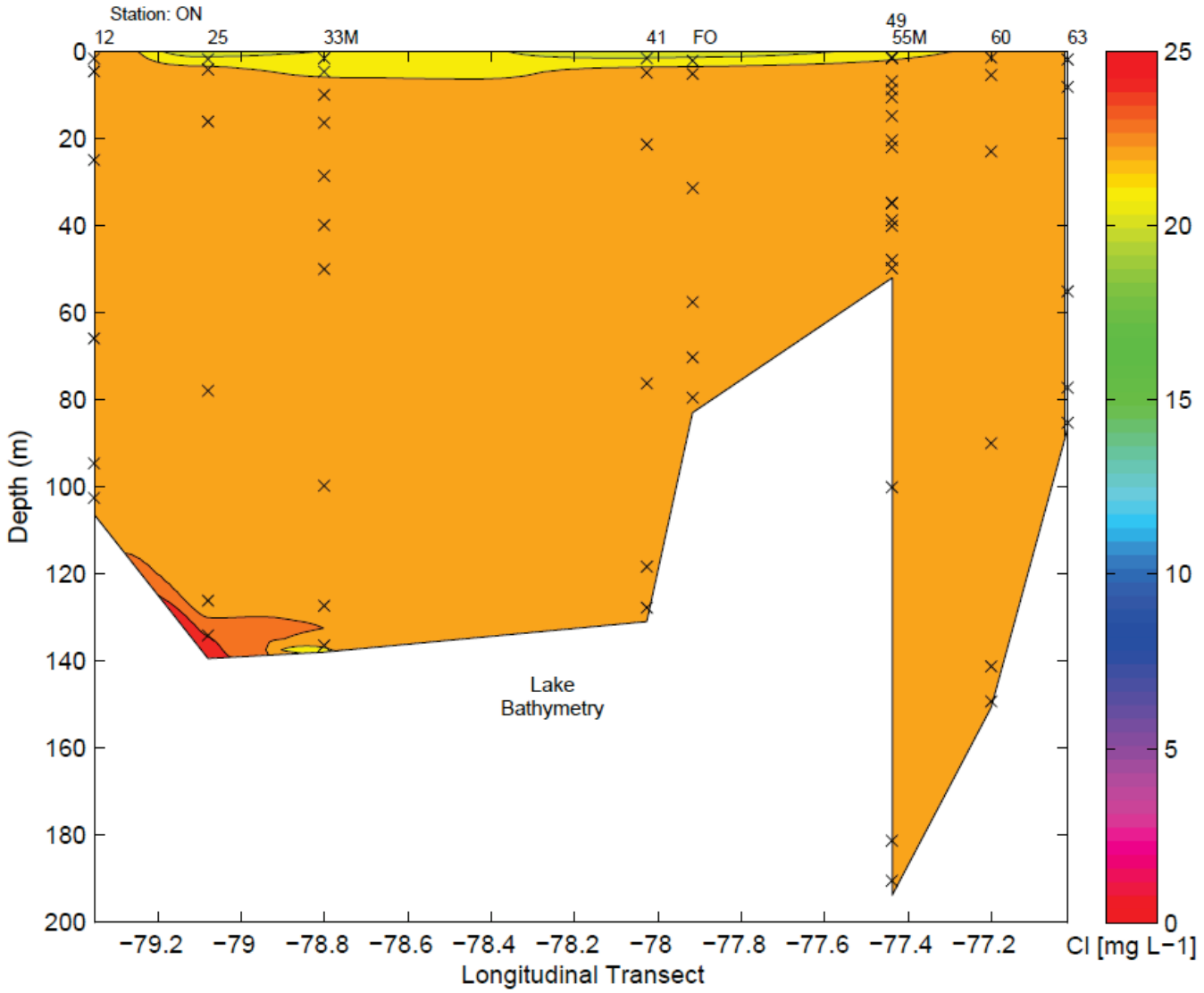
Station: ON
12
25
33M
41
FO
49
55M
60
63
Depth (m)
0
20
40
60
80
100
120
140
160
180
200
Lake
Bathymetry
−79.2
−79
−78.8
−78.6
−78.4
−78.2
−78
−77.8
−77.6
−77.4
−77.2
Longitudinal Transect
25
20
15
10
5
0
Cl [mg L−1]

218

Appendix E:
Contour plots – Density

In order, plots shown are:
- Lake Superior: Spring
- Lake Superior: Summer
- Lake Huron: Spring
- Lake Huron: Summer
- Lake Michigan: Spring
- Lake Michigan: Summer
- Lake Erie: Spring
- Lake Erie: Summer
- Lake Ontario: Spring
- Lake Ontario: Summer

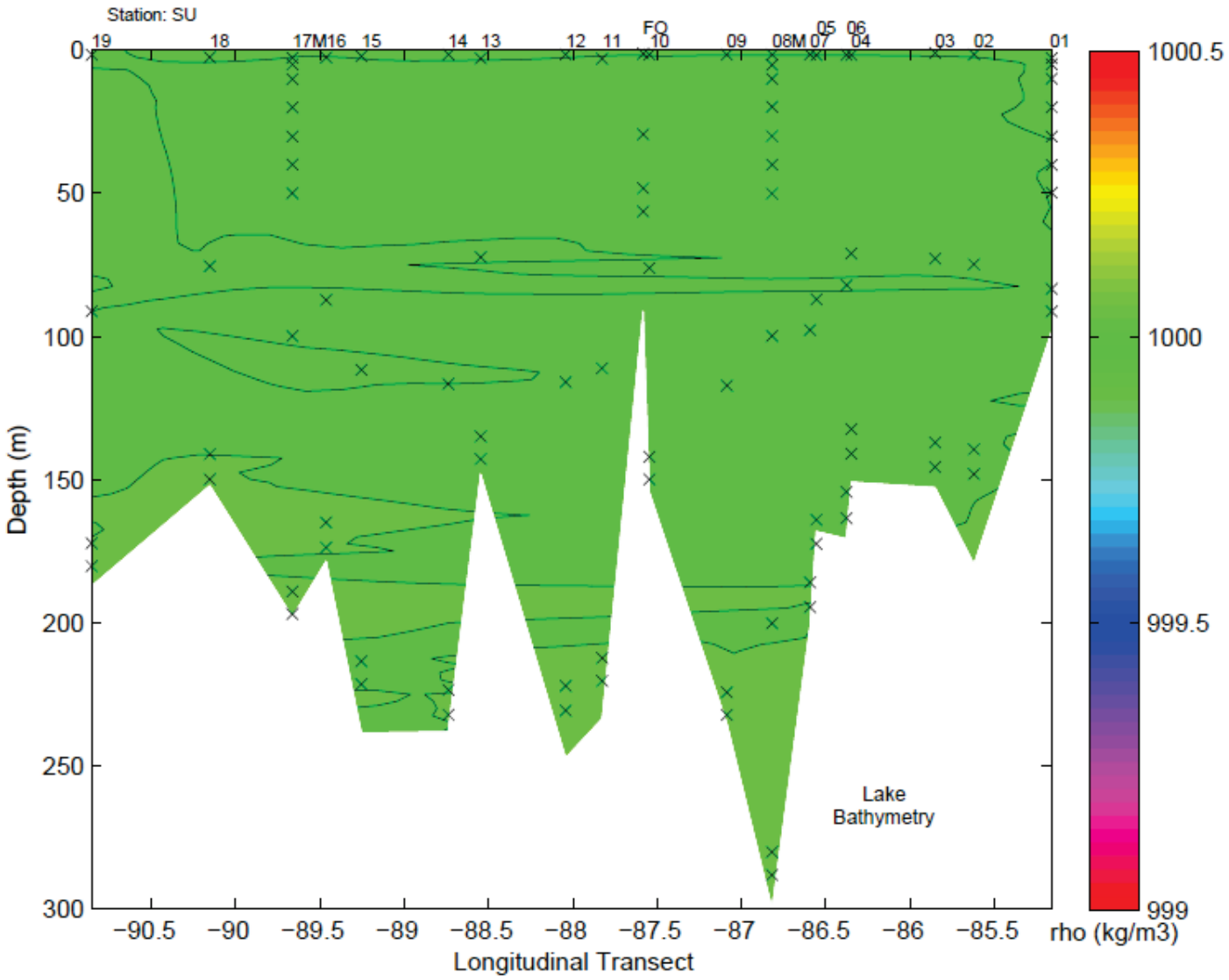
Station: SU
19
18
17M
16
15
14
13
12
11
FQ
10
09
08M
07
05
06
04
03
02
01
0
50
100
150
200
250
300
Depth (m)
−90.5
−90
−89.5
−89
−88.5
−88
−87.5
−87
−86.5
−86
−85.5
Longitudinal Transect
Lake
Bathymetry
1000.5
1000
999.5
999
rho (kg/m3)

220

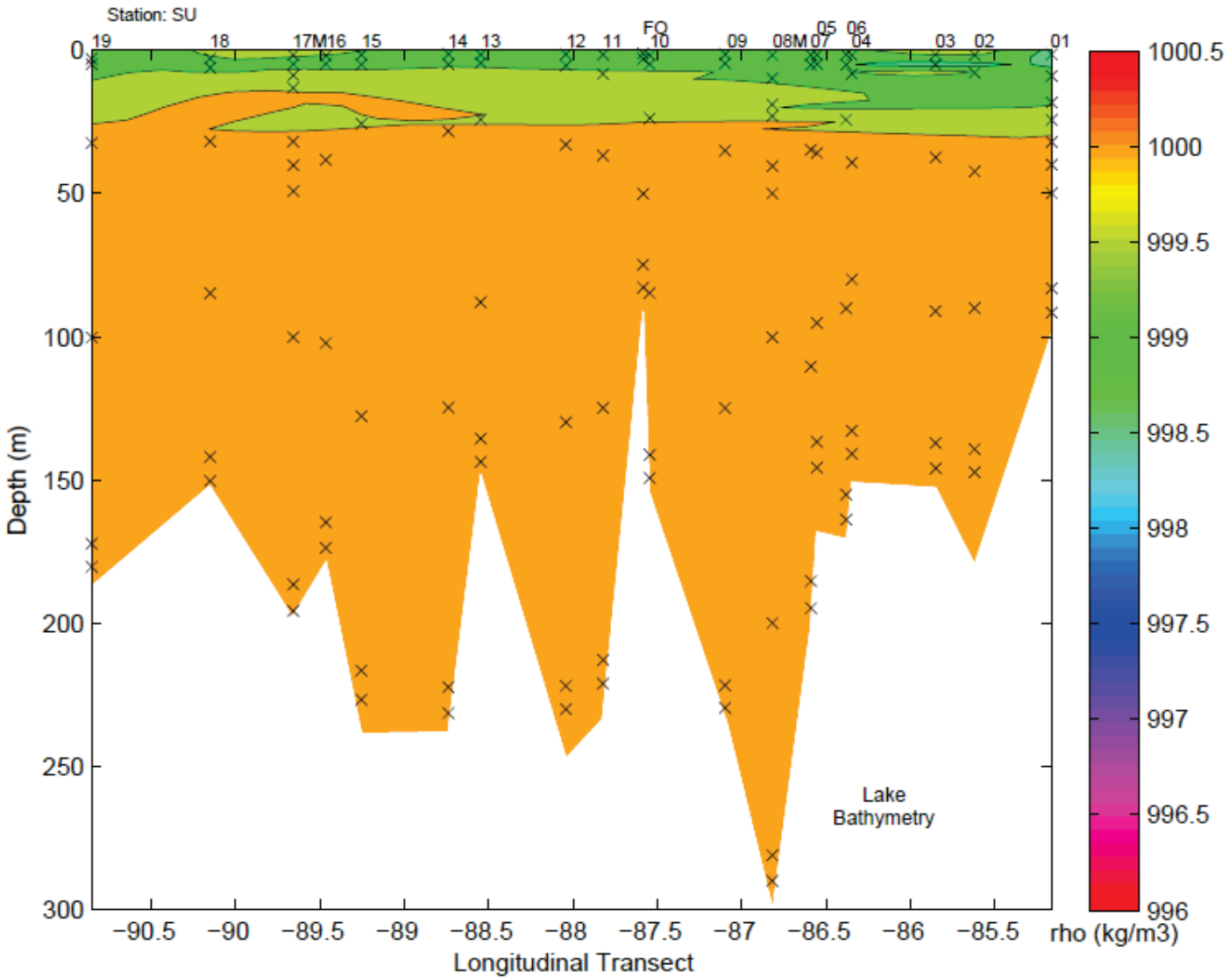
Station: SU
19
18
17M
16
15
14
13
12
11
FQ
10
09
08M
07
05
06
04
03
02
01
0
50
100
150
200
250
300
Depth (m)
−90.5
−90
−89.5
−89
−88.5
−88
−87.5
−87
−86.5
−86
−85.5
Longitudinal Transect
Lake
Bathymetry
1000.5
1000
999.5
999
998.5
998
997.5
997
996.5
996
rho (kg/m3)

221

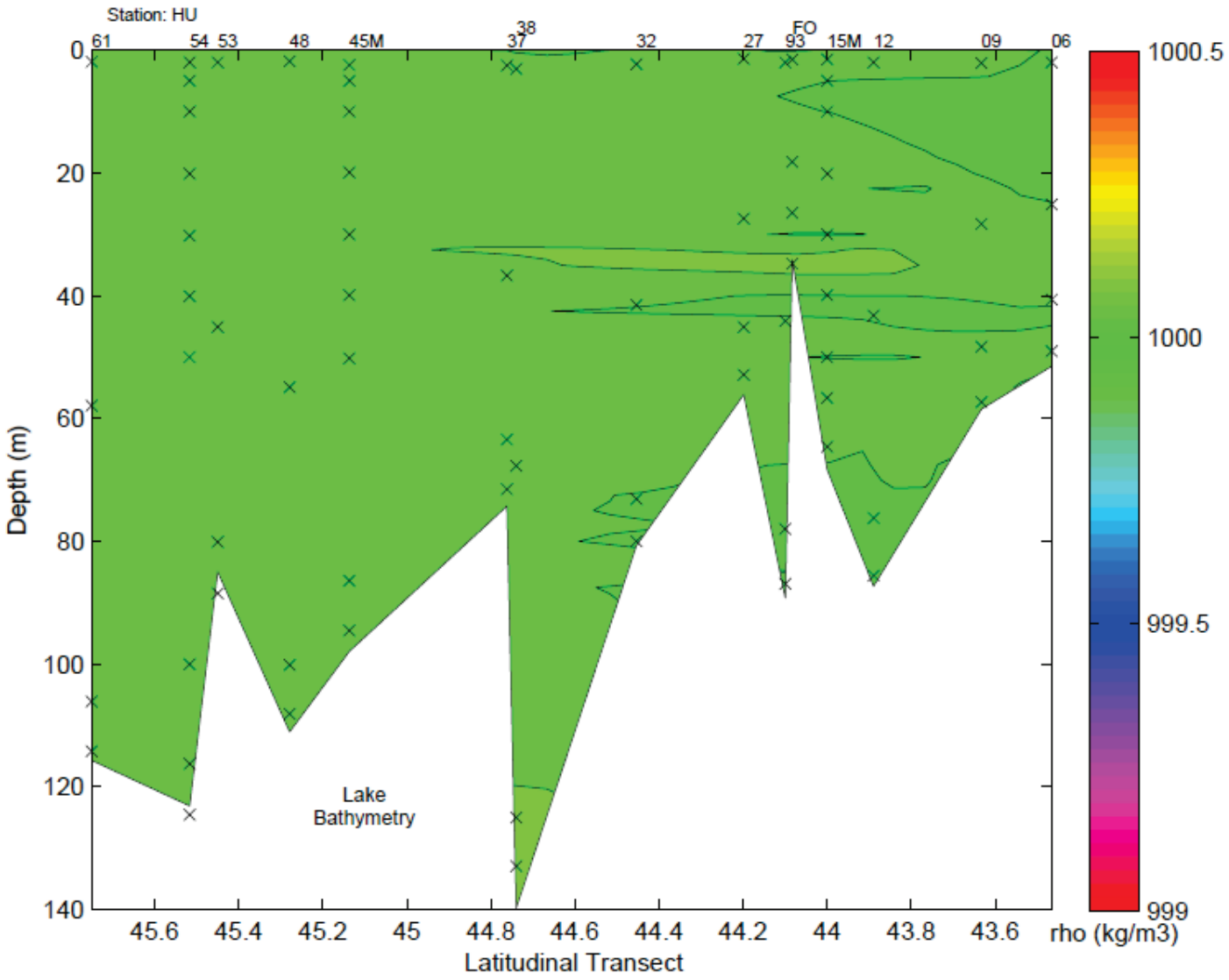
Station: HU
61
54
53
48
45M
38
37
32
FO
27
93
15M
12
09
06
0
20
40
60
80
100
120
140
Depth (m)
Lake
Bathymetry
45.6
45.4
45.2
45
44.8
44.6
44.4
44.2
44
43.8
43.6
Latitudinal Transect
1000.5
1000
999.5
999
rho (kg/m3)

222

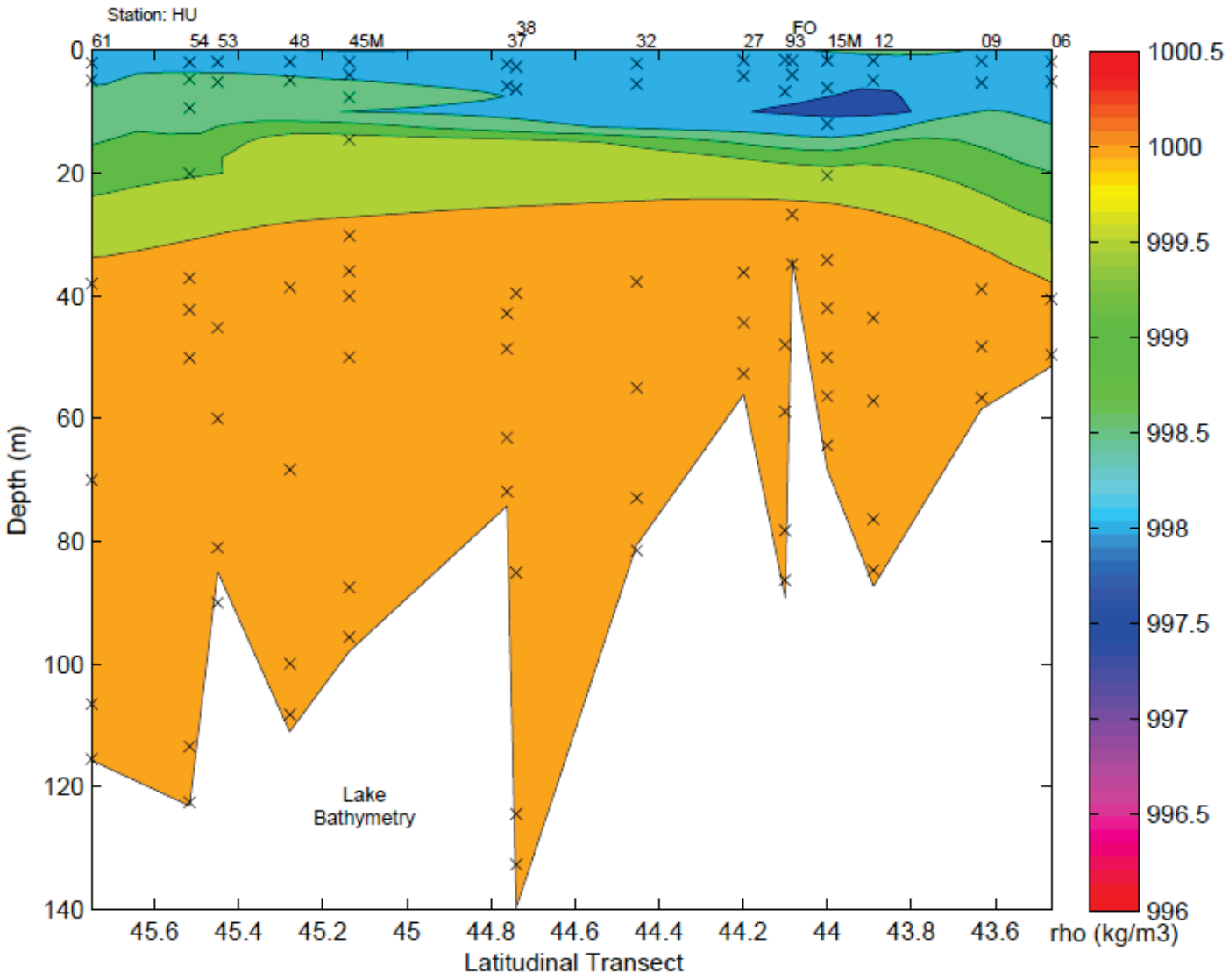
Station: HU
61
54
53
48
45M
38
37
32
FO
27
93
15M
12
09
06
0
20
40
60
80
100
120
140
Depth (m)
Lake
Bathymetry
45.6
45.4
45.2
45
44.8
44.6
44.4
44.2
44
43.8
43.6
Latitudinal Transect
1000.5
1000
999.5
999
998.5
998
997.5
997
996.5
996
rho (kg/m3)

223

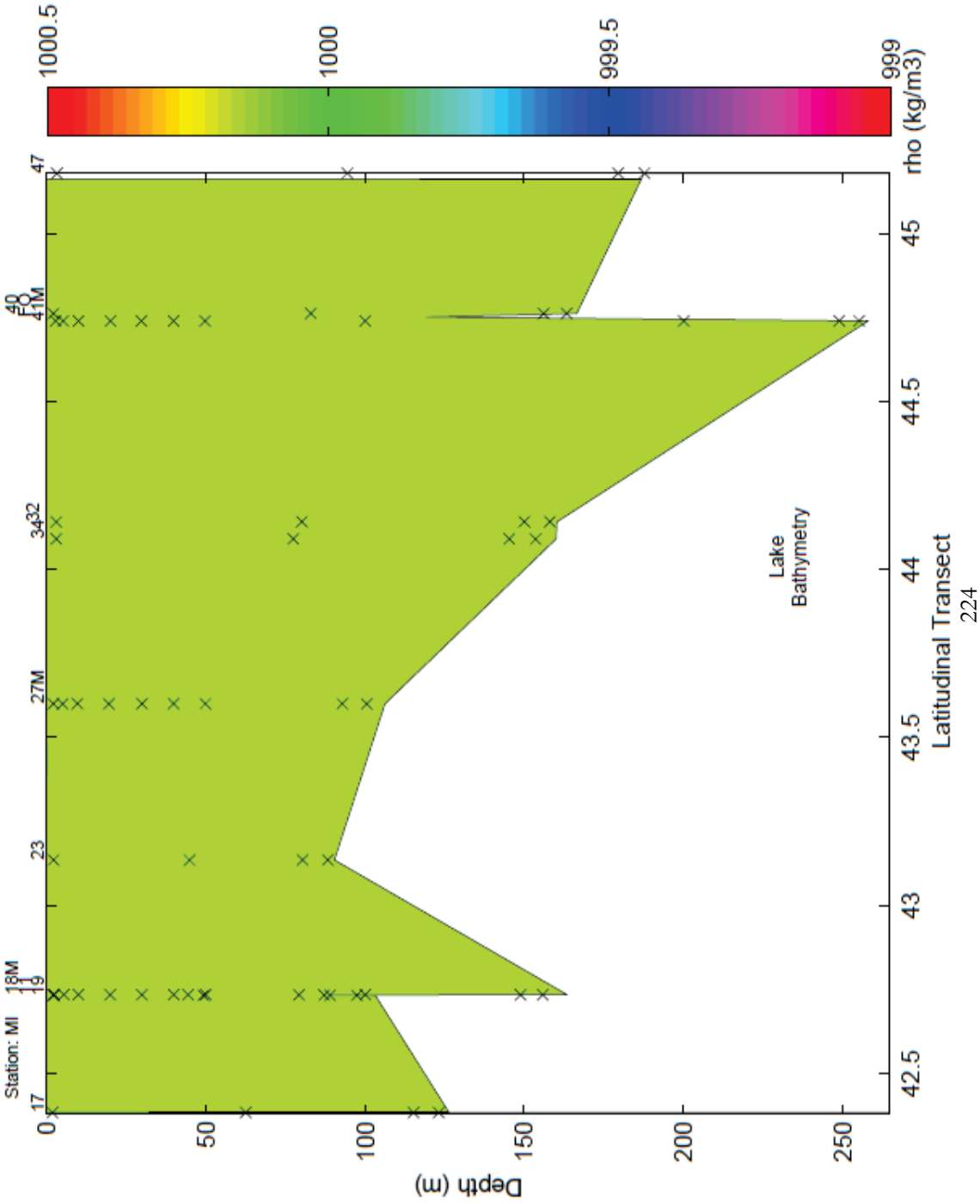
1000.5
1000
999.5
999
rho (kg/m3)
47
40
F0
41M
34
32
27M
23
18M
19
17
Station: MI
0
50
100
150
200
250
Depth (m)
42.5
43
43.5
44
44.5
45
Latitudinal Transect
224
Lake
Bathymetry

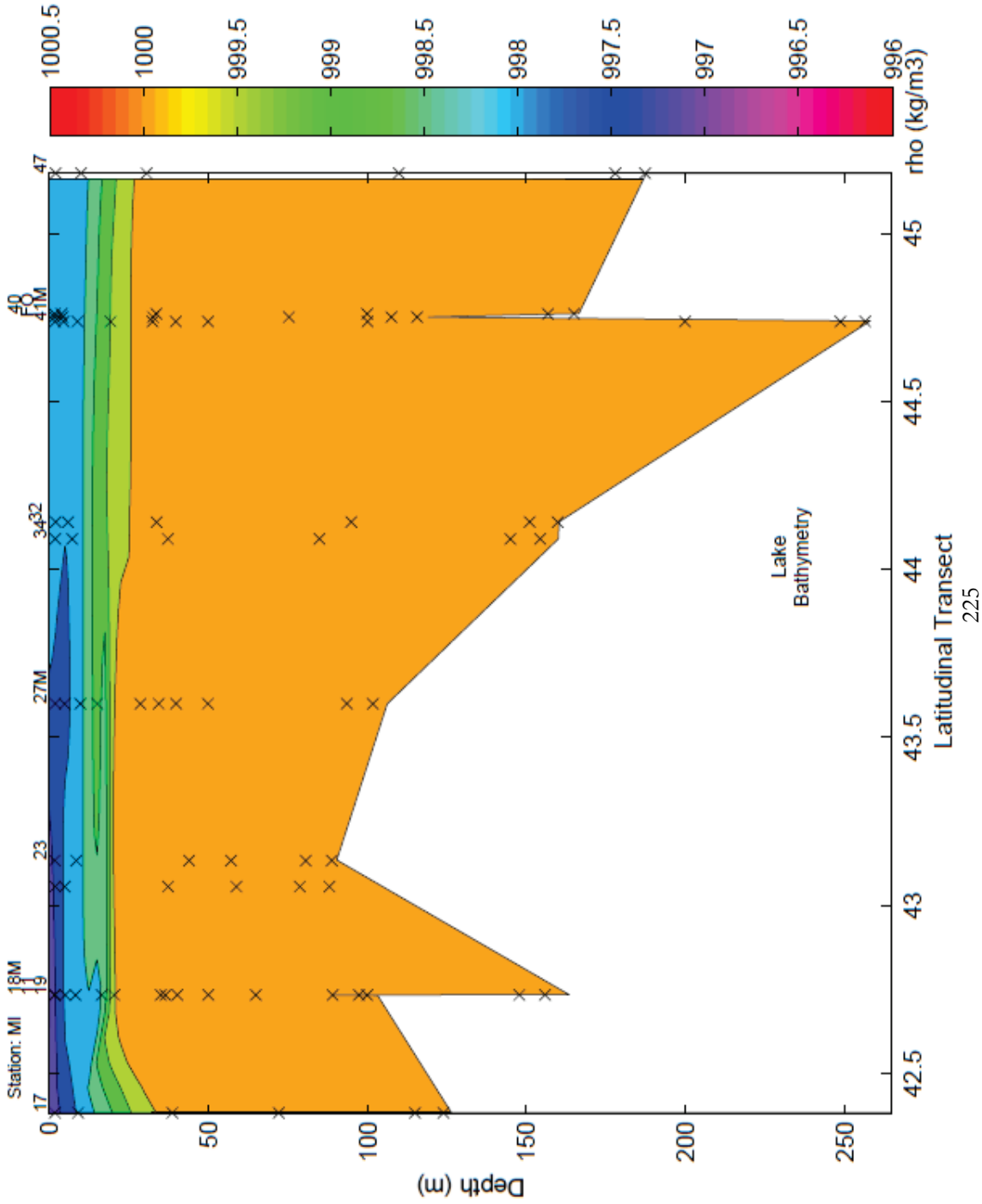
rho (kg/m3)
1000.5
1000
999.5
999
998.5
998
997.5
997
996.5
996
Station: MI
17
18M
19
23
27M
32
34
40
41M
47
Depth (m)
0
50
100
150
200
250
42.5
43
43.5
44
44.5
45
Latitudinal Transect
225
Lake
Bathymetry

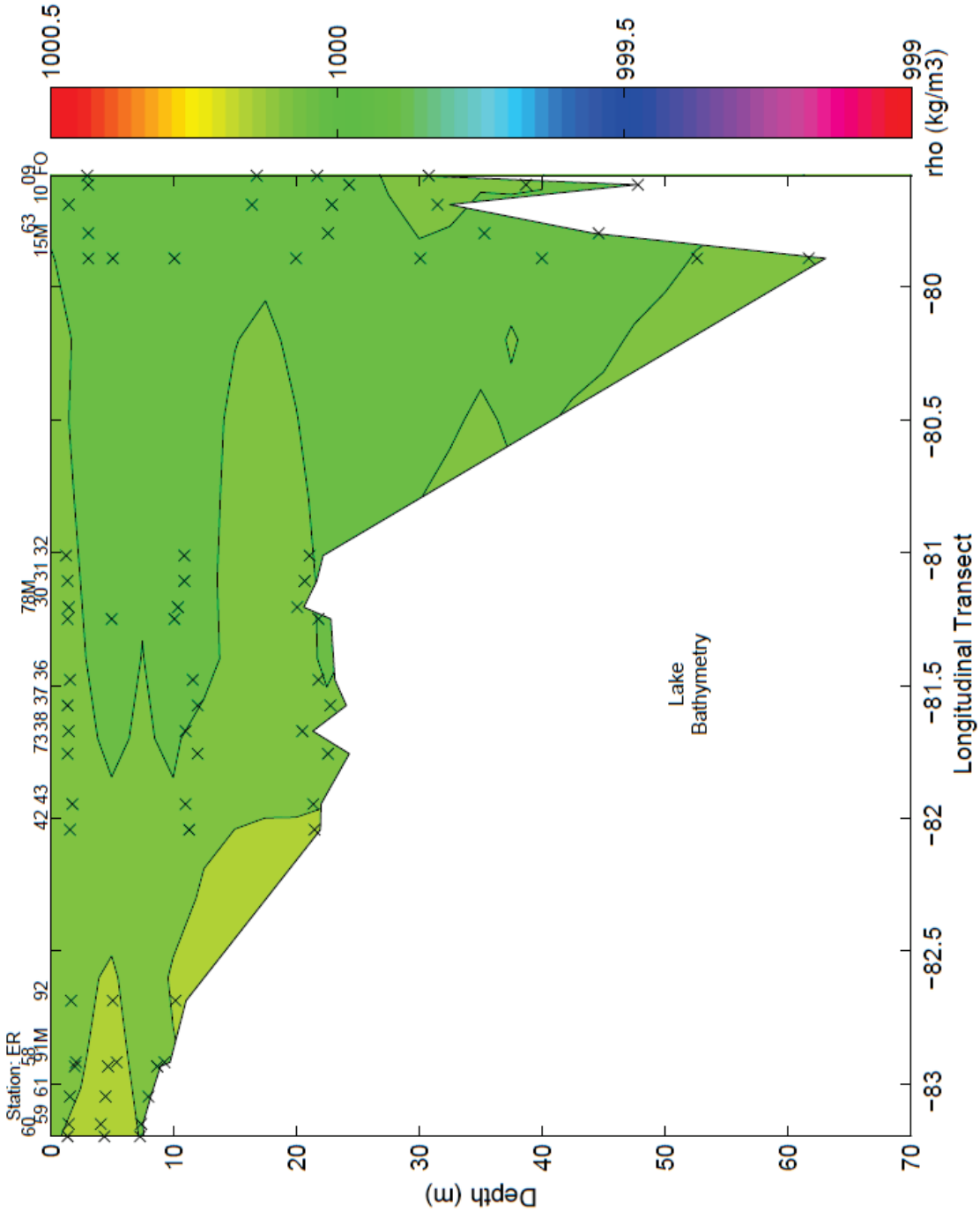
1000.5
1000
999.5
999
rho (kg/m3)
Station: ER
60 59 61 58 91M 92 42 43 73 38 37 36 78M 30 31 32 63 15M 10 09 FO
0
10
20
30
40
50
60
70
Depth (m)
-83
-82.5
-82
-81.5
-81
-80.5
-80
Longitudinal Transect
Lake
Bathymetry

226

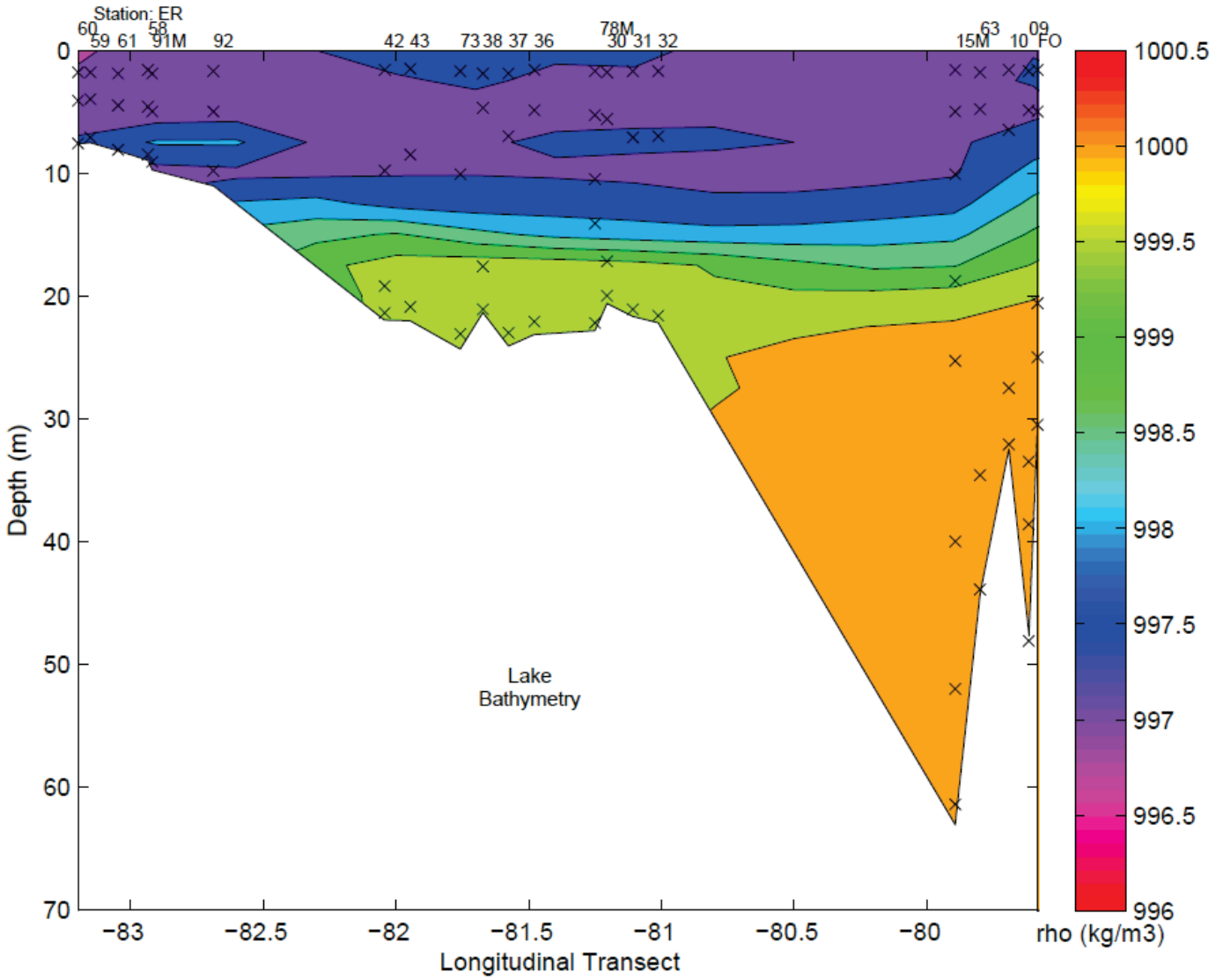
Station: ER
60
59 61
58
91M
92
42 43
73 38 37 36
78M
30 31 32
63
15M
09
10
FO
Depth (m)
0
10
20
30
40
50
60
70
Lake
Bathymetry
−83
−82.5
−82
−81.5
−81
−80.5
−80
Longitudinal Transect
1000.5
1000
999.5
999
998.5
998
997.5
997
996.5
996
rho (kg/m3)

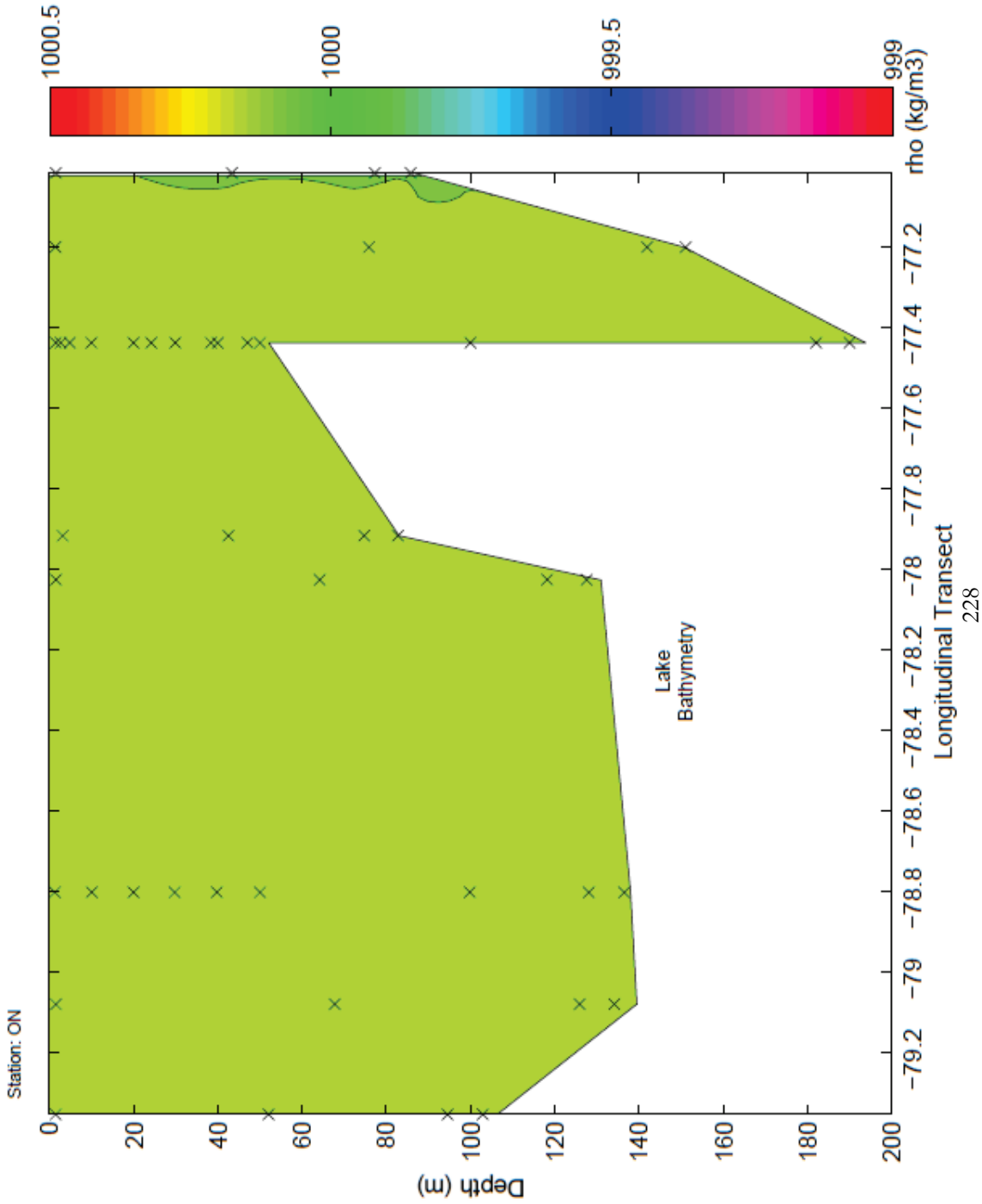
Station: ON
Depth (m)
0
20
40
60
80
100
120
140
160
180
200
Lake
Bathymetry
-79.2
-79
-78.8
-78.6
-78.4
-78.2
-78
-77.8
-77.6
-77.4
-77.2
Longitudinal Transect
228
rho (kg/m3)
1000.5
1000
999.5
999

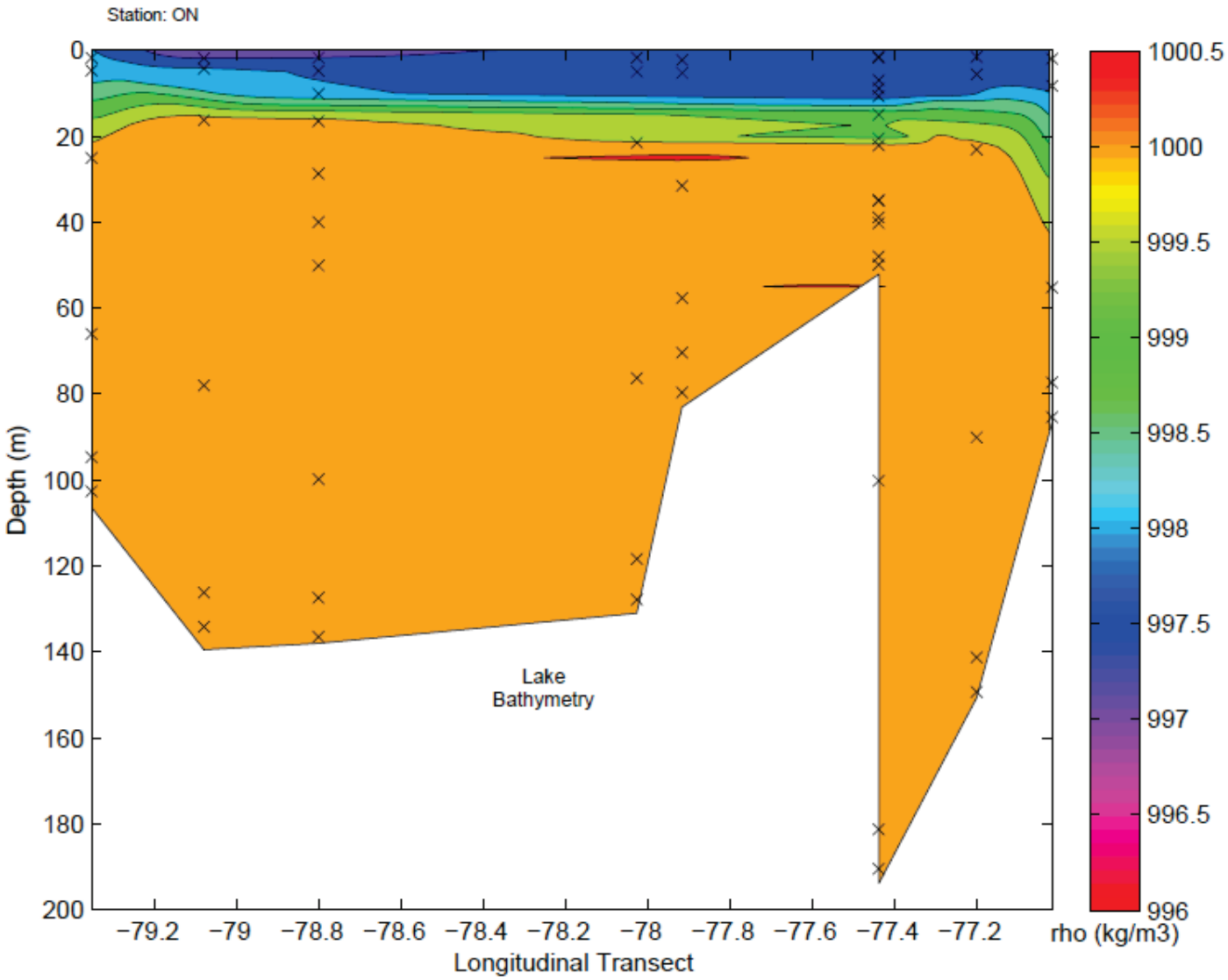
Station: ON
Depth (m)
0
20
40
60
80
100
120
140
160
180
200
Lake
Bathymetry
−79.2
−79
−78.8
−78.6
−78.4
−78.2
−78
−77.8
−77.6
−77.4
−77.2
Longitudinal Transect
1000.5
1000
999.5
999
998.5
998
997.5
997
996.5
996
rho (kg/m3)